

2018

EFFECT OF NON-ALCOHOLIC FATTY LIVER DISEASE (NAFLD) ON HEPATIC DRUG METABOLISM ENZYMES IN HUMAN

Rohitash Jamwal
University of Rhode Island, rohitash@my.uri.edu

Follow this and additional works at: https://digitalcommons.uri.edu/oa_diss

Terms of Use

All rights reserved under copyright.

Recommended Citation

Jamwal, Rohitash, "EFFECT OF NON-ALCOHOLIC FATTY LIVER DISEASE (NAFLD) ON HEPATIC DRUG METABOLISM ENZYMES IN HUMAN" (2018). *Open Access Dissertations*. Paper 811.
https://digitalcommons.uri.edu/oa_diss/811

This Dissertation is brought to you by the University of Rhode Island. It has been accepted for inclusion in Open Access Dissertations by an authorized administrator of DigitalCommons@URI. For more information, please contact digitalcommons-group@uri.edu. For permission to reuse copyrighted content, contact the author directly.

EFFECT OF NON-ALCOHOLIC FATTY LIVER DISEASE (NAFLD) ON HEPATIC
DRUG METABOLISM ENZYMES IN HUMAN

BY

ROHITASH JAMWAL

A DISSERTATION SUBMITTED IN PARTIAL FULFILLMENT OF THE

REQUIREMENTS FOR THE DEGREE OF

DOCTOR OF PHILOSOPHY

IN

PHARMACEUTICAL SCIENCES

UNIVERSITY OF RHODE ISLAND

2018

DOCTOR OF PHILOSOPHY DISSERTATION

OF

ROHITASH JAMWAL

APPROVED:

Dissertation Committee

Major Professor: Fatemeh Akhlaghi

Navindra Seeram

Ingrid Lofgren

Nasser H. Zawia
DEAN OF GRADUATE SCHOOL

UNIVERSITY OF RHODE ISLAND

2018

ABSTRACT

Significant changes in dietary habits have led to a rampant increase in metabolic disorders. Non-alcoholic fatty liver disease (NAFLD) is one such disorder characterized by the excess buildup of fat in hepatocytes of people who drink little or no alcohol. If not managed, NAFL (simple steatosis) progress into nonalcoholic steatohepatitis (NASH) and further deteriorate to cirrhosis leading to severe illness or even death. Drug disposition proteins (enzymes and transporters) in liver control the systemic exposure of drugs and xenobiotics in human and drive the efficacy as well as adverse events in the body. Therefore, it is critical to address the effect of NAFLD on the abundance of these proteins. A variation would result in an altered pharmacokinetic and/or pharmacodynamic profile of substrate drugs in patients with NAFLD. Most studies were performed in preclinical species (rat, mice) and only a few reports are available in human. The primary objective of this doctoral project was to investigate the effect of NALFD on the abundance of hepatic drug disposition proteins (DDP) in a human liver-bank. The levels of proteins were determined using an LC-MS/MS based label-free, global proteomics method. In addition, CYP3A4 enzyme kinetics parameters were determined using midazolam as a probe substrate. Considerable changes in the protein expression and activity of CYP3A4 and CYP1A2 were found in NAFL and NASH. Only marginal alterations were observed for other cytochrome P450 enzymes in this study. Levels of uridine 5'-diphosphoglucuronosyltransferases (UGT) and sulfotransferases (SULT) in NAFLD were mostly unaltered. Dysregulation of mitochondrial proteins involved in lipid metabolism (ACADSB, ACSM3/5, CPS1) was also observed. A significant downregulation of CYP3A4 protein and activity but not mRNA in NAFLD was observed suggesting that post-

transcriptional changes may play a more significant role in the observed phenotypic perturbations for the isoform. Overall, enzyme kinetics and quantitative protein abundance data from this project will be important in the development of physiologically based pharmacokinetic (PBPK) models for prediction of drug disposition in the NAFLD population

ACKNOWLEDGMENTS

First and foremost, I would like to thank and extend my gratitude to my doctoral research advisor, Prof. Fatemeh Akhlaghi. Through this journey of completing my dissertation, she has supported and contributed to my development and growth as a researcher and a person. I am especially indebted to you for believing in me and giving me an opportunity to be a part of your lab. Thank you, Dr. Akhlaghi.

I thank my committee member Professors Navindra Seeram and Ingrid Lofgren for their continuous support throughout this process. I also want to acknowledge Prof. Sara Rosenbaum and others who guided and supported me. I would be amiss not to thank Kathleen Hayes for help throughout this journey.

I am grateful to my colleagues and friends without whom I couldn't have made it this far. Sravani, thank you for your friendship and support. Ben, couldn't have done this dissertation work without you. Armin, Anitha, and Ghadah thank you for your timely and open feedback. I also thank my past lab members Enoch, Mwlod, Abdullah. Thank you to Ankit, Amrita, Rupal, Rohit, Nikhil, Swati, Zara, Francesca, Bonita, Sumanta, Manoj, Jayam, Udai, Kedar and Akshara for encouragement and friendship. I thank Carol, Tony, Dave, and Tonya for making me feel at home all these years. I thank my industry mentors; Peter Jackson (Amyris Inc.), Daniel Tatosian (Merck & Co.). I am grateful to everyone else with whom I have had the pleasure to work all these years.

Lastly, nobody has been more significant in this pursuit than my family. Thank you for your love, patience and continual support in the quest of my dreams. Thank you!

PREFACE

This dissertation was prepared according to the University of Rhode Island Thesis/Dissertation Process: From Proposal to Defense standards for the manuscript format. This dissertation consists of five manuscripts that have been combined to satisfy the requirements of the Department of Biomedical and Pharmaceutical Sciences, College of Pharmacy, University of Rhode Island. Two of the manuscript have already been published while three others would be submitted in future.

Manuscript I: Nonalcoholic fatty liver disease and hepatic drug metabolism enzymes and transporters.

This manuscript reviews the current literature on alterations in drug metabolism enzymes in NAFLD with focus on human studies. The work has been prepared as a research article for submission to Drug Metabolism Reviews, Taylor & Francis Online.

Manuscript II: Multiplex and Label-Free Relative Quantification Approach for Studying Protein Abundance of Drug Metabolizing Enzymes in Human Liver Microsomes Using SWATH-MS.

This manuscript described the development of a mass spectrometry-based method for simultaneous quantification of CYP450 enzymes in human liver microsomes. The protein abundance was further correlated with mRNA and activity. It was found that for most CYP enzymes, protein levels correlated stronger with activity than the mRNA. The work was published in the Journal of Proteome Research, 2017 Nov 3;16(11):4134-4143. PMID 28944677

Manuscript III: Nonalcoholic fatty liver disease and diabetes is associated with decreased CYP3A4 protein expression and activity in human liver

This work determined the effect of NAFLD and diabetes on the enzyme kinetic parameters and protein abundance of CYP3A4, one of the most important drug metabolism enzymes. A PBPK model was developed for NAFLD population with study generated in vitro kinetics and protein expression data. The results suggested an almost two-fold decrease in CYP3A4 activity and protein expression but not mRNA suggesting the involvement of post-transcriptional alterations. The manuscript published as a research article in *Molecular Pharmaceutics*, 2018 June 11; PMID 29792708

Manuscript IV: Effect of non-alcoholic fatty liver disease (NAFLD) on the protein abundance and activity of hepatic drug metabolizing enzymes in human.

This manuscript determined the effect of NAFLD on the protein abundance of major drug disposition proteins in the human liver. The results suggest downregulation of CYP1A2 and CYP3A4 activity while the levels of other CYP450 and drug metabolizing enzymes were similar. This manuscript has been prepared as a research article for submission to the *Journal of Pharmacology and Experimental Therapeutics*, ASPET Publications

Manuscript V: SWATH-MS based method for simultaneous relative quantification of 25 clinically important drug transporters in human liver.

This manuscript describes the development of a SWATH-MS based method for quantification of human xenobiotic transporters. The manuscript has been prepared as a research article for submission to the *Journal of Proteomics*, Elsevier

Other manuscripts authored during PhD program but not included in the dissertation

Rohitash Jamwal, Ariel R Topletz, Bharat Ramratnam, Fatemeh Akhlaghi F. **Ultra-high-performance liquid chromatography tandem mass-spectrometry for simple and simultaneous quantification of cannabinoids.** J Chromatogr B Analyt Technol Biomed Life Sci. 2017 Mar 24;1048:10-18. PMID: 28192758

This project aimed to develop and validate a LC-MS/MS based method for simultaneous quantification of cannabinoids in human plasma.

TABLE OF CONTENTS

ABSTRACT	ii
ACKNOWLEDGMENTS	iv
PREFACE.....	v
TABLE OF CONTENTS.....	viii
LIST OF TABLES.....	ix
LIST OF FIGURES.....	x
MANUSCRIPT I.....	1
MANUSCRIPT II.....	41
MANUSCRIPT III.....	97
MANUSCRIPT IV.....	160
MANUSCRIPT V.....	211

LIST OF TABLES

Table I-1: Therapeutic agents currently being developed for treatment of NAFLD.....	38
Table I-2: Altered expression and activity levels of CYP450 enzymes in NAFLD.....	39
Table I-3: Hepatic blood flow changes in different stages of NAFLD.....	40
Table II-1: Brief demographic summary of donors.....	71
Table II-2 Correlation between protein levels and activity, mRNA and activity, mRNA and protein.....	72
Table III-1: Overview of Caucasian donor demographics.....	136
Table III-2: Effect of nonalcoholic fatty liver disease on midazolam enzyme kinetics....	137
Table III-3: Effect of nonalcoholic fatty liver disease on protein abundance.....	138
Table III-4: Effect of diabetes and NAFLD on CYP3A4 activity, protein and mRNA expression, and relevant proteins and transcription factors.....	139
Table IV-1: Demographic characteristics of control, NAFL and NASH groups.....	200
Table IV-2: Effect of NAFLD on the expression of major CYP450 enzymes and auxiliary proteins.....	201
Table IV-3: Effect of NAFLD on the expression of major UGT and SULT enzymes.....	202
Table IV-4: Effect of NAFLD on the expression of NAFLD specific marker proteins....	203
Table V-1: Donor demographics data for transporter quantification.....	243
Table V-2: Gender-specific expression levels of hepatic efflux transporters.....	244
Table V-3: Gender-specific expression levels of hepatic efflux/uptake transporters.....	245
Table V-4: Gender-specific expression levels of hepatic uptake transporters.....	246

LIST OF FIGURES

Figure I-1: Hematoxylin and Eosin staining of liver samples.....	35
Figure I-2: Effect of altered CYP3A4 on systemic midazolam exposure.....	36
Figure I-3: Graphical illustration of the advantage of SWATH-MS over traditional MRM based quantification method.....	37
Figure II-1: Identified proteins and peptides at 1% false discovery rate (FDR).....	74
Figure II-2 (a-l): Correlation plots for relative protein expression and enzyme activity...	75
Figure II-3 (a-l): Correlation plots for mRNA and enzyme activity.....	76
Figure II-4 (a-j): Correlation plots for mRNA and protein expression.....	77
Figure III-1: Histological staining of liver sections.....	142
Figure III-2: Effect of nonalcoholic fatty liver disease on CYP3A4 activity.....	143
Figure III-3: Effect of nonalcoholic fatty liver disease on protein expression.....	144
Figure III-4: Effect of nonalcoholic fatty liver disease on relative mRNA expression...	145
Figure III-5: Effect of different grades of steatosis.....	146
Figure III-6: SimCYP predicted plasma concentration of midazolam in virtual Caucasian population indicating a higher concentration and longer sedation time with respect to disease state.....	147
Figure IV-1: Effect of NAFLD on protein expression of various CYP450 proteins.....	194
Figure IV-2: Effect of NAFLD on functional activity of various CYP450 proteins.....	195
Figure IV-3: Effect of NAFLD on protein expression of UGT proteins.....	196
Figure IV-4: Effect of NAFLD on protein expression of SULT proteins.....	197
Figure IV-5: Correlation of protein expression and activity of CYP enzymes.....	198

Figure IV-6: Effect of NAFLD on protein expression of some marker proteins in NAFLD.....	199
Figure V-1: Gender difference on membrane protein abundance and ATP1A4 membrane protein marker.....	250
Figure V-2 (a-c): Effect of gender on hepatic (a) efflux, (b) efflux (MRPs), and (c) efflux/uptake transporters.....	251
Figure V-3: Effect of gender on hepatic uptake transporters.....	252

MANUSCRIPT I

This manuscript has been prepared as a research article for submission to *Drug Metabolism Reviews*, Taylor & Francis Online

Nonalcoholic fatty liver disease (NAFLD) and hepatic drug disposition proteins of clinical importance

Rohitash Jamwal, Fatemeh Akhlaghi*

Department of Biomedical and Pharmaceutical Sciences, University of Rhode Island,
Kingston, 02881, RI, USA

Author for correspondence:

*Fatemeh Akhlaghi, Ph.D., PharmD

Clinical Pharmacokinetics Research Laboratory, Department of Biomedical and Pharmaceutical Sciences, University of Rhode Island, 495A College of Pharmacy, 7 Greenhouse Road, Kingston, RI 02881, United States.

Email address: fatemeh@uri.edu

Word count including tables, references and figure captions: 8713

Abstract

Significant lifestyle and diet changes in last few decades have led to a rampant increase in metabolic diseases in human. Nonalcoholic fatty liver disease (NAFLD) is characterized by the excessive buildup of fats in the liver. The disease can range from simple steatosis (fat accumulation) to nonalcoholic steatohepatitis (NASH) which represents a severe form of NAFLD and is accompanied with inflammation, fibrosis and hepatocyte damage in addition to significant steatosis. Hepatic proteins involved in metabolism (enzymes) and uptake/efflux (transporters) of xenobiotics are collectively known as drug disposition proteins (DDPs). While the expression of DDPs is well studied in healthy volunteers, our understanding of the alterations of these proteins in NAFLD is limited. Much of the existing knowledge on the subject is derived from pre-clinical species, and clinical translation of these findings is poor. The effect of NAFLD on these proteins in human is debatable and currently lacks a consensus among different reports. Global label-free, mass-spectrometry-based quantitative proteomics is a promising tool to study the changes associated with NAFLD without the need for protein-specific targeted quantification. Protein expression is important in vitro physiological parameter controlling the pharmacokinetics. The last decade has also seen a rise in the use of physiologically based pharmacokinetic (PBPK) modeling for prediction of drug pharmacokinetics in special populations. Here, we present a review of current literature on the alterations in human hepatic DDPs in NAFLD.

Keywords: NAFLD, NASH, Cytochrome P450, LC-MS/MS, Proteomics, PBPK

Introduction

Substantial changes in the dietary habits of our generation are fueling an epidemic of various metabolic disorders. Nonalcoholic fatty acid liver disease (NAFLD) is one such metabolic syndrome which is rising at an alarming rate (Ahmed 2015; Mikolasevic et al. 2016). The prevalence of NAFLD is higher in patients with diabetes, obesity, hyperlipemia, hypertension and hypertriglyceridemia (Lonardo et al. 2016; Younossi, Koenig, et al. 2016). NAFLD is characterized by the presence of greater than 5% of hepatic fat in people without significant alcohol intake (<20 g per day for women, <30 g per day for men) (Chalasani et al. 2012; Leoni et al. 2018). Fat-accumulation in hepatocytes is triggered by various mechanisms which include the increased hepatic uptake of circulating fatty acids, increased hepatic *de novo* fatty acid synthesis, decreased hepatic beta-oxidation and decreased hepatic lipid export (Geisler and Renquist 2017). The disease is characterized by the accumulation of free fatty acids and triglycerides in the hepatocytes, and severity ranges from benign steatosis to nonalcoholic steatohepatitis (figure 1) (McCullough 2006). NASH, characterized by significant lobular inflammation, hepatic fibrosis, and hepatocyte necrosis, can progress to life-threatening liver cirrhosis and hepatocellular carcinoma (HCC) (Farrell and Larter 2006).

Pathogenesis, epidemiology and risk factors

The current “multiple hit” theory for the pathogenesis of NAFLD proposes first hit as the accumulation of lipid droplets (triglycerides) in >5% of liver hepatocytes (Takaki et al. 2014). A successive second hit characterized by excessive free radical and pro-inflammatory cytokine formation leading to inflammation, necrosis and consequently, fibrosis (Takaki et al. 2014). A number of histologic scoring systems have been introduced

in the past decade for diagnostic evaluation of different stages of NAFLD (Brunt E. M. et al. 1999; Kleiner et al. 2005; Bedossa et al. 2012). Pathologists commonly differentiate different stages of NAFLD using semi-quantitative evaluation based on steatosis, lobular inflammation, hepatocellular ballooning, and/or fibrosis (Brunt E. M. 2016). Liver biopsy is the gold standard for the diagnosis of NAFLD but ethical, and feasibility constraints limit the direct assessment of its prevalence. The global prevalence of NAFLD diagnosed by imaging was estimated to be 25.2%, and it was >30% in the Middle East and South America (Chalasani et al. 2018). The lowest prevalence of NAFLD was reported from Africa (13.5%). The prevalence of NAFLD diagnosed with ultrasonography was 24.13%. The overall prevalence of nonalcoholic steatohepatitis (NASH) in general populations is estimated to be between 1.5-6.5% (Chalasani et al. 2018). In the USA, NAFLD is also associated with significant economic (~\$103 billion) and clinical burden (~64 million people projected to have NAFLD) (Younossi, Blissett, et al. 2016). Ethnic differences exist in the prevalence of NAFLD and Hispanics are more susceptible to the disease as compared to Caucasians and Afro-Americans (Kalia and Gaglio 2016). The disease was initially thought to be present only in obese adults; however recent studies have shown its prevalence in people with normal BMI as well as children (Margariti et al. 2012; Anderson et al. 2015; Bush et al. 2017). Certain genetic factors are also responsible for predisposition of carriers to NAFLD. PNLA3 (Patatin-like phospholipase domain-containing protein 3) is a multifunctional enzyme involved in the hydrolysis of triacylglycerol (TAG) in the liver, and rs738409 variant is the strongest genetic risk factor for NAFLD (Romeo et al. 2008). Recent genome-wide association studies (GWAS) have identified increased NAFLD susceptibility in variants of TM6SF2 (rs58542926; transmembrane 6 superfamily member

2), *GCKR* (rs780094, Glucokinase regulator), *NCAN* (rs2228603, Neurocan), *LYPLAL1* (rs12137855, Lysophospholipase-like 1) (Sookoian and Pirola 2017; Sliz et al. 2018). The association of rs641738 variant of *MBOAT7-TMC4* locus (membrane bound O-acyltransferase domain-containing 7, transmembrane channel-like 4) is controversial and inconclusive (Mancina et al. 2016; Sookoian et al. 2018).

Physical findings show that patients with NAFLD often have obesity and hepatomegaly (enlarged liver) due to fat infiltration of the liver. NAFLD patients show mild or moderate elevations in the aspartate aminotransferase (AST) and alanine aminotransferase (ALT), although normal aminotransferase levels do not exclude NAFLD. When elevated, the AST and ALT are typically 2 to 5 times the upper limit of normal with an AST to ALT ratio of less than one (>1.5 for alcoholic liver disease) (Sattar et al. 2014). Alkaline phosphatase may also be elevated 2-3 times the upper limit of normal and patients may have an elevated serum ferritin concentration or transferrin saturation. Decreased hepatic attenuation on computed tomography (CT) and an increased fat signal on magnetic resonance imaging (MRI) are generally evident in radiographic findings (Decarie et al. 2011).

Classification systems for NAFLD

NAFLD is a complex disease and differentiating definite NASH from NAFL can be equally complicated for basic researchers as well as for pathologists. The gray zone of distinction between NAFL and NASH is precarious, and diagnosis often varies dramatically among pathologists due to the heterogenous histopathologic spectrum of NAFLD and its progression over time (Younossi et al. 2011). Controversy exists over the

use of these classifications has led to misuse of scoring systems (Kleiner et al. 2005; Angulo Paul 2011; Brunt Elizabeth M. et al. 2011). The categorical nature of the histopathological scoring system adds to the discrepancies in the diagnosis of the type of NAFLD. Since the categories are not well-defined, it eventually leads to varying interpretations and conclusions from researchers and pathologists (Brunt E. M. 2016). Additive nature of recent scoring systems (NAS or SAF) deconvolutes the contribution of each histologic lesion. Interestingly, NAS scoring system was not designed to be used as a diagnostic tool for determination of NASH versus NAFL (Kleiner et al. 2005; Brunt Elizabeth M. et al. 2011). It was intended to evaluate the changes in histological lesions (steatosis, inflammation, hepatocyte ballooning, fibrosis) that can occur over time (Angulo P. 2011). Fatty liver inhibition of progression (FLIP) algorithm was proposed to improve the consistency in the diagnosis of NASH in adults and takes into account fibrosis along with steatosis and activity score (inflammation, ballooning) (Younossi et al. 2011). The use of different classification systems may, therefore, contribute to significant variability seen in the literature on the subject. Surgical hepatitis and potential differences between the biopsy site (right or left lobe) also confound the diagnosis of histologic lesions and subsequently the proper classification of disease (Brunt E. M. 2016).

Treatment strategies to manage NAFLD

Hepatic pathological conditions have been known to impact the abundance of DMEs and transporters in the liver, leading to altered drug profiles and often to side-effects (Gandhi et al. 2012). Despite the widespread prevalence of NAFLD/NASH, currently, there are no pharmacological therapies available for its treatment and involves the management of associated conditions including obesity, diabetes and hyperlipidemia (Takei 2013; Barb et

al. 2016; Sumida et al. 2016). Weight loss is usually the first and most common intervention recommended for any metabolic syndrome (Marchesini et al. 2016). Similarly, lifestyle modifications through exercise and dietary restriction are considered vital in the management of NAFLD (Vilar-Gomez et al. 2015). Patients with the disease are advised to avoid intake of positive calorie foods like soda and sweetened drink which are rich in simple carbohydrates which are readily absorbed (Zivkovic et al. 2007). Patients are also asked/recommended to avoid diets rich in cholesterol, fructose and other saturated fats which are often linked with progression of NAFLD (Musso et al. 2009; Abdelmalek et al. 2010).

Interestingly, consumption of fructose-sweetened and non-glucose sweetened beverages has been associated with elevated insulin resistance and an increase in visceral adiposity and lipids in overweight and obese humans (Stanhope et al. 2009). Ryan et al. found that the Mediterranean diet improved insulin sensitivity and reduced hepatic steatosis in NAFLD patients with insulin-resistance (Ryan et al. 2013). A considerable effort is currently underway in the development of therapeutic agents for the treatment of NAFLD, and multiple molecular pathways are now being targeted for drug development (Perazzo and Dufour 2017). Pioglitazone, vitamin E and, GLP-1 and SGLT2 inhibitors have shown some efficacy in NASH. New therapies in development target one or more of the following pathways; a) hepatic fat accumulation and insulin resistance, b) oxidative stress, inflammation and apoptosis, and c) hepatic fibrosis (Sumida and Yoneda 2018). An overview of some of the therapeutic agents in clinical development is given in table 1. Leoni et al. recently published a review analyzing the current guidelines in the diagnosis of NAFLD as well as the areas of therapeutic focus.

Drug metabolism enzymes and NAFLD

Human liver, facilitated by several drug metabolizing enzymes (DMEs), is the primary organ responsible for the elimination of xenobiotics and endogenous compounds. DMEs are responsible for the metabolism of diverse chemicals which include xenobiotics like drugs, pesticides and endogenous substrates like steroids and bile acids (Zanger and Schwab 2013). DMEs are broadly classified into phase I enzymes which are mostly oxidative, reductive or hydrolytic; and phase II enzymes which are conjugative. Major proteins involved in oxidative biotransformation belongs to cytochrome P450 (CYP450s), flavin-monooxygenases (FMOs), monoamine oxidases (MAOs), alcohol and aldehyde dehydrogenases, and aldehyde and xanthine oxidase (Appendix: Drug Metabolizing Enzymes and Biotransformation Reactions 2012). Aldo-keto reductases (AKRs), azo- and nitro-reductases constitute reductive enzymes involved in metabolism whereas epoxide hydrolases, esterases, and peptidases are responsible for the bulk of hydrolysis reactions in the liver (Appendix: Drug Metabolizing Enzymes and Biotransformation Reactions 2012).

Cytochrome P450 superfamily enzymes are involved in the majority of reductive reactions and are reported to be responsible for the metabolism of ~70-80% of all the available drugs in the market (Zanger and Schwab 2013). Conjugation reactions in the liver are carried out by uridine diphosphate-glucuronosyltransferases (UGTs), sulfotransferases (SULTs), N-acetyltransferases (NATs), glutathione S-transferases (GSTs), amino acid conjugation enzymes and methyltransferases (Jancova et al. 2010; Appendix: Drug Metabolizing Enzymes and Biotransformation Reactions 2012). Majority of studies evaluating the effect of NAFLD on drug disposition proteins draw their conclusions from studies performed in preclinical animal models. A careful interrogation often suggests a

complex and heterogeneous alteration in drug metabolizing enzymes and transporters in human. Such discrepancies are partly due to species differences and lack of animal models which accurately reflect the complexity and pathophysiology of human disease.

Studies in preclinical species

Preclinical species have played a key role in our understanding of NAFLD (Santhekadur et al. 2018). Genetic as well as dietary animal models have been developed to understand the disease. Common genetic mice models of NAFLD include leptin-deficient (ob/ob), leptin receptor-deficient (db/db) and low-density lipoprotein deficient mice. Even though low leptin levels are not observed in human NAFLD, leptin-deficient mice (ob/ob) represents obesity, hyperlipidemia and insulin resistance, steatosis but without fibrosis (Trak-Smayra et al. 2011; Canet et al. 2014).

However, fibrosis can be induced in leptin receptor-deficient mice (db/db) from external stimuli. Low-density lipoprotein receptor-deficient mice (LDLR) exhibit a pathology similar to db/db mice and can develop fibrosis. But not all studies in mice models are consistent among different models, the results have shown to vary according to the diet and species. (Kim et al. 2004; Yoshinari et al. 2006; Fisher et al. 2008). Dietary models are developed using methionine and choline-deficient (MCD) and hypercaloric diets (Stephenson et al. 2018). MCD models exhibit steatosis, inflammation, fibrosis similar to human disease but significantly differ in metabolic phenotype of the disease. MCD-fed mice show increased insulin sensitivity, significant weight loss, and low blood glucose.

Similarly, hypercaloric diet (Western-like diet) model show steatosis, inflammation, fibrosis but take a significant time for disease induction. DIAMOND (diet-

induced animal model of alcoholic fatty liver disease) and STAM (Stelic Animal Model) models are proposed to exhibit considerable similarity with human NAFLD in pathology and phenotype (Fujii et al. 2013; Asgharpour et al. 2016). Both the models gain weight and develop insulin resistance, steatosis, fibrosis, and hepatocellular carcinoma. Dietrich et al. have extensively discussed the pros and cons of different animal models of NAFLD (Dietrich et al. 2017).

Given the complexity of human disease, no single animal model to date fully recapitulates the human disease state (Dietrich et al. 2017). The failure of some compounds which showed a significant promise in preclinical studies has raised a concern about the inadequacies of animal models for the disease. ASP9831, a potent PDE4 inhibitor was being developed by Astellas Pharma to modulate cyclic adenosine monophosphate activity. Compared to placebo, ASP9831 drug failed to improve the biochemical parameters associated with NASH in a 12-week phase-II clinical trial (Ratziu et al. 2014). Similarly, resveratrol was unable to improve hepatic steatosis and insulin sensitivity at pharmacological doses in an 8-week study (Chachay et al. 2014).

Studies in human

Disease-mediated changes have been known to impact the abundance of drug disposition proteins in the liver, hence leading to altered drug profiles (Merrell and Cherrington 2011; Gandhi et al. 2012; Cobbina and Akhlaghi 2017; Evers et al. 2018). Theoretically, an alteration in DDPs could lead to undesirable pharmacokinetic and pharmacodynamic outcomes (figure 2). Clinical studies in NAFLD are currently limited but are critical to understanding the implication of altered drug metabolizing enzyme

profile on therapeutic result in the disease state. Current literature on studies with human tissue is confounding with reports of increase, decrease or non-significant change in the activity, protein, and/or mRNA levels of clinically relevant hepatic cytochrome P450 enzymes (*table 2*). Genome-wide studies (GWAS) in NAFLD patients found no significant changes in ADME proteins between normal and steatotic livers at mRNA expression level (Greco et al. 2008; Lake et al. 2011). However, mRNA-based studies do not account for the potential contribution of post-transcriptional and post-translational changes relevant to protein expression or enzyme activity. A comprehensive table of alteration in drug metabolism enzyme expression or activity is given in table 1. In general, a decrease in CYP3A4 and CYP2E1 activity appears to be dominant in the studies in subjects and human tissue (Merrell and Cherrington 2011; Woolsey et al. 2015; Cobbina and Akhlaghi 2017). Even though the effect of NAFLD on CYP450s has been extensively studied in vitro, our understanding of the disease associated impact on other DMEs is limited due to the scarcity of studies. Similar to CYP450s, differential regulation appears to be at play for other DMEs including UGT and SULTs in human NAFLD. Studies in human tissue found the minimal effect of NAFLD on UGT enzymes while a significant alteration was reported in hepatic sulfotransferase expression and activity (Hardwick et al. 2013). NASH mediated upregulation of UGT1A9, 2B10, and 3A1 mRNA was reported in human liver (Hardwick et al. 2013). It was also noteworthy that the protein expression of UGT1A9 and 1A6 decreased in NASH (Hardwick et al. 2013). Elevated SULT1C4 mRNA was seen in NASH whereas SULT1A1 and 2A1 protein levels were lower in disease samples compared to control samples (Hardwick et al. 2013).

Label-free mass spectrometry-based proteomics

Traditionally, the level of expression is determined using Western blotting, but last decade has seen a rise in mass-spectrometry-based methods for quantification of proteins. Omics technologies have been used extensively in the quest to identify novel biomarkers for NAFLD (Pirola and Sookoian 2018). Targeted proteomics (SRSM, MRM) based approaches have also proven to be useful in quantification of DDPs. While the targeted quantification represents the most robust method of choice for absolute quantification, cost and significant time for optimization of mass spectrometer conditions for each targeted peptide limit its application to a few target proteins.

In contrast, label-free quantification or more commonly known as LFQ has emerged recently as an alternative approach for comparative analysis of protein expression across different samples owing to fast and low-cost of this technique (Wong and Cagney 2010). LFQ approaches are relatively inexpensive as compared to targeted MRM methods as there is no need to synthesize unique peptides for each protein and isotopically labeled isoforms of this peptide as the internal standard. Accurate and robust quantification with LFQ approaches is intricate, and different strategies for extracting quantitative data from LFQ analysis has been developed (Wong and Cagney 2010). A comprehensive cost comparison of various mass spectrometry-based techniques reported significant cost savings with label-free based quantitative proteomics (Al Feteisi et al. 2015).

Studies have shown that protein expression is a better surrogate than mRNA for prediction of functional activity of cytochrome P450 enzymes. Data-dependent (DDA) and data independent analysis (DIA) are two common data collection modes in shotgun proteomics. In DDA mode, most abundant ion species from a precursor scan (MS1) at a

given retention time are selectively selected for fragmentation (MS/MS). Alternatively, the precursors are selected in a specific m/z range and are fragmented without any prioritization to their relative abundance. This approach offers a more comprehensive and complete analysis of samples than traditional DDA. SWATH-MS (sequential window acquisition of all theoretical mass spectra) is one such DIA technique that provides an alternative to DDA and targeted approaches for protein estimation (Gillet et al. 2012). As mentioned previously, SWATH is a DIA technique in which all the precursors within a predefined m/z are fragmented, and product ions of these precursors are recorded as a digital repository (Rosenberger et al. 2014). However, coeluting precursors and fragments at any given RT in DIA data make it difficult to select the correct peak without a robust spectral library. Therefore, a reference spectral library is often used for DIA and data are further deconvoluted and extracted using software like OpenSWATH, SWATH 2.0 and Skyline (Navarro et al. 2016). A significant advantage of SWATH-MS over the other mass spectrometry methods is related to the ability to perform retrospective mining of the data. The targeted protein extraction can be improved by expanding the coverage of reference spectral library and re-mining the DIA data. For instance, if the researcher comes up with a new hypothesis in the future, SWATH-MS data would allow interrogation of the existing data for additional protein/s of interest without the need for sample digestion or data reacquisition (figure 3). Such a strategy offers a tremendous benefit concerning the saving of sample, time and money.

Absolute protein concentrations are vital to simulate drug exposure using physiologically based pharmacokinetic (PBPK) models. However, despite all the advantages, DIA approaches are relative, and hence absolute protein concentration levels

can't be determined using techniques like SWATH-MS. Alternatively, a spike in standard or targeted approach for a protein of interest would be needed to determine the protein levels. Global proteomics using DDA data and “total protein approach (TPA)” can be instead used to estimate protein concentrations. TPA is widely accepted and delivers protein concentrations without the need for the isotope-labeled spike in reference peptides (Wisniewski et al. 2014). TPA assumes that a protein's abundance within a cell as a fraction of total protein is approximately the same as the proportion of its MS signal to the total MS signal of the cell.

$$Protein\ abundance = \frac{MS\ signal}{Total\ MS\ signal} \sim \frac{Protein\ mass}{Total\ protein\ mass}$$

The absolute protein concentration (p), expressed as mol/g of total protein can further be calculated using equation 2 (Wisniewski and Mann 2016). $MW(p)$ is the molar mass of protein.

$$p = \frac{MS\ signal(p)}{Total\ MS\ signal \times MW(p)}$$

Physiologically based pharmacokinetic (PBPK) model

While there is a significant amount of literature available for the levels of these proteins in healthy people, little is known about how NAFLD changes the concentration of these enzymes in the human liver. The information is essential to determine the influence of the disease on the drug disposition, but clinical studies in NAFLD subjects are limited. The use of physiologically based pharmacokinetic models for prediction of pharmacokinetic and drug metabolism in populations which present clinical challenges is

increasing in popularity (Sager et al. 2015). PBPK modeling is a bottom-up simulation approach which takes in account multiple parameters specific to the drug, physiology of the species (different organs represented as compartments) and an understanding of the pharmacokinetic properties of the drug of interest (Zhuang and Lu 2016). System or dependent population parameters which are essential for prediction of exposure and include hepatic blood flow and enzyme or transporter abundance among others. Drug-dependent parameters are derived from physicochemical properties of the molecules and rest are determined from in vitro studies (protein binding, metabolism, enzyme kinetics, intrinsic clearance, etc.). An exhaustive list of different parameters required for building a PBPK model is discussed elsewhere (Zhuang and Lu 2016).

In vitro and in vivo parameters which accurately reflect the human disease are vital to predict and simulate in silico drug exposure. Some commercial PBPK platforms like GastroPlus (Simulation Plus Inc.), Simcyp (Certara L.P.) PKSIM (Bayer), CloePK (Evotec A.G.) are currently available. PBPK models for NAFLD are presently not available in different simulation platforms. A lack of sufficient in vitro and in vivo data is a significant hurdle in the development of PBPK models for NAFLD.

Hepatic blood flow is a critical parameter determining the rate of presentation of the drug for its metabolism in the liver. Hepatic portal vein (HPV) supplies 70% whereas hepatic artery (HA) is responsible for ~30% of the blood reaching the liver. HPV supplies liver with nutrients and xenobiotics (drugs) absorbed in the GI tract and HA is responsible for carrying oxygen. Fat-accumulation in hepatocytes was found to correlate with decreased HPV blood flow in NAFLD patients (Shigefuku et al. 2014). Hepatocyte ballooning associated with NASH cause sinusoidal distortion leading to reduced

intrasinusoidal volume and microvascular blood flow (Farrell et al. 2008). Impaired systemic circulation and modification of cellular membrane may also interrupt oxygen availability in NAFLD leading to hypoxia and accelerated lipid droplet formation (Anavi et al. 2017). Blood flow change in early fibrosis was attributed to outflow blockage in the liver sinusoidal area (Hirooka et al. 2015). The changes in hepatic blood flow during different stages of NAFLD is given in table 3 (Shigefuku et al. 2012).

Concluding remarks

The epidemic of NAFLD is upon us, and a widespread effort is currently underway to address different aspects of this multifaceted and complex metabolic disease. A lack of good preclinical models to recapitulate the spectrum of the disease remains a significant challenge and care should be taken when extrapolating results from preclinical species to human. Risk of alterations in the drug disposition proteins remains high in NAFLD due to significant structural and pathophysiological changes in the liver, the primary organ for drug disposition. PBPK has been used in recent past to simulate the exposure of various drugs in special populations. However, most of our understanding of these models comes from research done in healthy individuals, but little is known about the physiological as well as pharmacokinetic parameters of drugs in NAFLD. Moreover, after drug administration, there is also a need to understand how drug disposition proceeds in these disease/target populations. Two of the critical parameters governing the exposure include enzyme kinetics and expression of proteins involved in the disposition of the compound. There is also a need of predictive biomarkers for NAFLD to delineate NASH from NAFL in human and mass spectrometry-based proteomics may hold promise to fill this gap. In summary, it's of paramount importance to determine how disease alters the expression of

the proteins involved in the disposition of the drugs. Additionally, to improve translation ability and accuracy of simulation models, it is essential to understand how the pharmacokinetics and other physiological parameters change in NAFLD.

Acknowledgements

Authors acknowledge the support from National Institutes of Health [grant numbers R15-GM101599, UH3-TR000963] to Fatemeh Akhlaghi.

Declaration of interest statement

Authors have no conflict of interest to declare for this work.

References

- Abdelmalek MF, Suzuki A, Guy C, Unalp-Arida A, Colvin R, Johnson RJ, Diehl AM, Nonalcoholic Steatohepatitis Clinical Research N. 2010. Increased fructose consumption is associated with fibrosis severity in patients with nonalcoholic fatty liver disease. *Hepatology*. 51(6):1961-1971.
- Ahmed M. 2015. Non-alcoholic fatty liver disease in 2015. *World J Hepatol*. 7(11):1450-1459.
- Al Feteisi H, Achour B, Barber J, Rostami-Hodjegan A. 2015. Choice of LC-MS methods for the absolute quantification of drug-metabolizing enzymes and transporters in human tissue: a comparative cost analysis. *AAPS J*. 17(2):438-446.
- Anavi S, Madar Z, Tirosh O. 2017. Non-alcoholic fatty liver disease, to struggle with the strangle: Oxygen availability in fatty livers. *Redox Biol*. 13:386-392.
- Anderson EL, Howe LD, Jones HE, Higgins JP, Lawlor DA, Fraser A. 2015. The Prevalence of Non-Alcoholic Fatty Liver Disease in Children and Adolescents: A Systematic Review and Meta-Analysis. *PLoS One*. 10(10):e0140908.
- Angulo P. 2011. Diagnosing steatohepatitis and predicting liver-related mortality in patients with NAFLD: Two distinct concepts. *Hepatology*. 53(6):1792-1794.
- Angulo P. 2011. Diagnosing steatohepatitis and predicting liver-related mortality in patients with NAFLD: two distinct concepts. *Hepatology*. 53(6):1792-1794.
- Appendix: Drug Metabolizing Enzymes and Biotransformation Reactions. 2012. *ADME-Enabling Technologies in Drug Design and Development*. John Wiley & Sons, Inc.; p. 545-565.
- Armstrong MJ, Gaunt P, Aithal GP, Barton D, Hull D, Parker R, Hazlehurst JM, Guo K, team Lt, Abouda G et al. 2016. Liraglutide safety and efficacy in patients with non-

alcoholic steatohepatitis (LEAN): a multicentre, double-blind, randomised, placebo-controlled phase 2 study. *Lancet*. 387(10019):679-690.

Asgharpour A, Cazanave SC, Pacana T, Seneshaw M, Vincent R, Banini BA, Kumar DP, Daita K, Min HK, Mirshahi F et al. 2016. A diet-induced animal model of non-alcoholic fatty liver disease and hepatocellular cancer. *J Hepatol*. 65(3):579-588.

Baker SS, Baker RD, Liu W, Nowak NJ, Zhu L. 2010. Role of alcohol metabolism in non-alcoholic steatohepatitis. *PLoS One*. 5(3):e9570.

Barb D, Portillo-Sanchez P, Cusi K. 2016. Pharmacological management of nonalcoholic fatty liver disease. *Metabolism*. 65(8):1183-1195.

Bedossa P, Poitou C, Veyrie N, Bouillot JL, Basdevant A, Paradis V, Tordjman J, Clement K. 2012. Histopathological algorithm and scoring system for evaluation of liver lesions in morbidly obese patients. *Hepatology*. 56(5):1751-1759.

Bell LN, Temm CJ, Saxena R, Vuppalanchi R, Schauer P, Rabinovitz M, Krasinskas A, Chalasani N, Mattar SG. 2010. Bariatric surgery-induced weight loss reduces hepatic lipid peroxidation levels and affects hepatic cytochrome P-450 protein content. *Ann Surg*. 251(6):1041-1048.

Bergman A, Gonzalez SC, Tarabar S, Saxena A, Esler W, Amin N. 2018. Safety, tolerability, pharmacokinetics and pharmacodynamics of a liver-targeting ACC inhibitor (PF-05221304) following single and multiple oral doses. *Journal of Hepatology*. 68:S582.

Brunt EM. 2016. Nonalcoholic Fatty Liver Disease: Pros and Cons of Histologic Systems of Evaluation. *Int J Mol Sci*. 17(1).

Brunt EM, Janney CG, Di Bisceglie AM, Neuschwander-Tetri BA, Bacon BR. 1999. Nonalcoholic steatohepatitis: a proposal for grading and staging the histological lesions. *Am J Gastroenterol.* 94(9):2467-2474.

Brunt EM, Kleiner DE, Behling C, Contos MJ, Cummings OW, Ferrell LD, Torbenson MS, Yeh M. 2011. Misuse of scoring systems. *Hepatology.* 54(1):369-370.

Bush H, Golabi P, Younossi ZM. 2017. Pediatric Non-Alcoholic Fatty Liver Disease. *Children (Basel).* 4(6).

Canet MJ, Hardwick RN, Lake AD, Dzierlenga AL, Clarke JD, Cherrington NJ. 2014. Modeling human nonalcoholic steatohepatitis-associated changes in drug transporter expression using experimental rodent models. *Drug Metab Dispos.* 42(4):586-595.

Carlisle KM, Halliwell M, Read AE, Wells PN. 1992. Estimation of total hepatic blood flow by duplex ultrasound. *Gut.* 33(1):92-97.

Chachay VS, Macdonald GA, Martin JH, Whitehead JP, O'Moore-Sullivan TM, Lee P, Franklin M, Klein K, Taylor PJ, Ferguson M et al. 2014. Resveratrol does not benefit patients with nonalcoholic fatty liver disease. *Clin Gastroenterol Hepatol.* 12(12):2092-2103 e2091-2096.

Chalasani N, Gorski JC, Asghar MS, Asghar A, Foresman B, Hall SD, Crabb DW. 2003. Hepatic cytochrome P450 2E1 activity in nondiabetic patients with nonalcoholic steatohepatitis. *Hepatology.* 37(3):544-550.

Chalasani N, Younossi Z, Lavine JE, Charlton M, Cusi K, Rinella M, Harrison SA, Brunt EM, Sanyal AJ. 2018. The diagnosis and management of nonalcoholic fatty liver disease: Practice guidance from the American Association for the Study of Liver Diseases. *Hepatology.* 67(1):328-357.

Chalasani N, Younossi Z, Lavine JE, Diehl AM, Brunt EM, Cusi K, Charlton M, Sanyal AJ. 2012. The diagnosis and management of non-alcoholic fatty liver disease: practice Guideline by the American Association for the Study of Liver Diseases, American College of Gastroenterology, and the American Gastroenterological Association. *Hepatology*. 55(6):2005-2023.

Cobbina E, Akhlaghi F. 2017. Non-alcoholic fatty liver disease (NAFLD) - pathogenesis, classification, and effect on drug metabolizing enzymes and transporters. *Drug Metab Rev*. 49(2):197-211.

Colca JR, McDonald WG, Adams WJ. 2018. MSDC-0602K, a metabolic modulator directed at the core pathology of non-alcoholic steatohepatitis. *Expert Opin Investig Drugs*. 27(7):631-636.

Decarie PO, Lepanto L, Billiard JS, Olivie D, Murphy-Lavallee J, Kauffmann C, Tang A. 2011. Fatty liver deposition and sparing: a pictorial review. *Insights Imaging*. 2(5):533-538.

Dietrich CG, Rau M, Jahn D, Geier A. 2017. Changes in drug transport and metabolism and their clinical implications in non-alcoholic fatty liver disease. *Expert Opin Drug Metab Toxicol*. 13(6):625-640.

Donato MT, Jimenez N, Serralta A, Mir J, Castell JV, Gomez-Lechon MJ. 2007. Effects of steatosis on drug-metabolizing capability of primary human hepatocytes. *Toxicol In Vitro*. 21(2):271-276.

Donato MT, Lahoz A, Jimenez N, Perez G, Serralta A, Mir J, Castell JV, Gomez-Lechon MJ. 2006. Potential impact of steatosis on cytochrome P450 enzymes of human hepatocytes isolated from fatty liver grafts. *Drug Metab Dispos*. 34(9):1556-1562.

Emery MG, Fisher JM, Chien JY, Kharasch ED, Dellinger EP, Kowdley KV, Thummel KE. 2003. CYP2E1 activity before and after weight loss in morbidly obese subjects with nonalcoholic fatty liver disease. *Hepatology*. 38(2):428-435.

Evers R, Piquette-Miller M, Polli JW, Russel FGM, Sprowl JA, Tohyama K, Ware JA, de Wildt SN, Xie W, Brouwer KLR et al. 2018. Disease-Associated Changes in Drug Transporters May Impact the Pharmacokinetics and/or Toxicity of Drugs: A White Paper From the International Transporter Consortium. *Clin Pharmacol Ther*.

Farrell GC, Larter CZ. 2006. Nonalcoholic fatty liver disease: from steatosis to cirrhosis. *Hepatology*. 43(2 Suppl 1):S99-S112.

Farrell GC, Teoh NC, McCuskey RS. 2008. Hepatic microcirculation in fatty liver disease. *Anat Rec (Hoboken)*. 291(6):684-692.

Fisher CD, Jackson JP, Lickteig AJ, Augustine LM, Cherrington NJ. 2008. Drug metabolizing enzyme induction pathways in experimental non-alcoholic steatohepatitis. *Arch Toxicol*. 82(12):959-964.

Fisher CD, Lickteig AJ, Augustine LM, Ranger-Moore J, Jackson JP, Ferguson SS, Cherrington NJ. 2009. Hepatic cytochrome P450 enzyme alterations in humans with progressive stages of nonalcoholic fatty liver disease. *Drug Metab Dispos*. 37(10):2087-2094.

Friedman SL, Ratziu V, Harrison SA, Abdelmalek MF, Aithal GP, Caballeria J, Francque S, Farrell G, Kowdley KV, Craxi A et al. 2018. A randomized, placebo-controlled trial of cenicriviroc for treatment of nonalcoholic steatohepatitis with fibrosis. *Hepatology*. 67(5):1754-1767.

Fujii M, Shibazaki Y, Wakamatsu K, Honda Y, Kawauchi Y, Suzuki K, Arumugam S, Watanabe K, Ichida T, Asakura H et al. 2013. A murine model for non-alcoholic steatohepatitis showing evidence of association between diabetes and hepatocellular carcinoma. *Med Mol Morphol.* 46(3):141-152.

Gandhi A, Moorthy B, Ghose R. 2012. Drug disposition in pathophysiological conditions. *Curr Drug Metab.* 13(9):1327-1344.

Geisler CE, Renquist BJ. 2017. Hepatic lipid accumulation: cause and consequence of dysregulated glucoregulatory hormones. *J Endocrinol.* 234(1):R1-R21.

Gillet LC, Navarro P, Tate S, Rost H, Selevsek N, Reiter L, Bonner R, Aebersold R. 2012. Targeted data extraction of the MS/MS spectra generated by data-independent acquisition: a new concept for consistent and accurate proteome analysis. *Mol Cell Proteomics.* 11(6):O111 016717.

Greco D, Kotronen A, Westerbacka J, Puig O, Arkkila P, Kiviluoto T, Laitinen S, Kolak M, Fisher RM, Hamsten A et al. 2008. Gene expression in human NAFLD. *Am J Physiol Gastrointest Liver Physiol.* 294(5):G1281-1287.

Hardwick RN, Ferreira DW, More VR, Lake AD, Lu Z, Manautou JE, Slitt AL, Cherrington NJ. 2013. Altered UDP-glucuronosyltransferase and sulfotransferase expression and function during progressive stages of human nonalcoholic fatty liver disease. *Drug Metab Dispos.* 41(3):554-561.

Harrison S, Moussa S, Bashir M, Alkhouri N, Frias J, Baum S, Tetri B, Bansal M, Taub R. 2018. MGL-3196, a selective thyroid hormone receptor-beta agonist significantly decreases hepatic fat in NASH patients at 12 weeks, the primary endpoint in a 36 week serial liver biopsy study. *Journal of Hepatology.* 68:S38.

Harrison SA, Marri SR, Chalasani N, Kohli R, Aronstein W, Thompson GA, Irish W, Miles MV, Xanthakos SA, Lawitz E et al. 2016. Randomised clinical study: GR-MD-02, a galectin-3 inhibitor, vs. placebo in patients having non-alcoholic steatohepatitis with advanced fibrosis. *Aliment Pharmacol Ther.* 44(11-12):1183-1198.

Harrison SA, Rinella ME, Abdelmalek MF, Trotter JF, Paredes AH, Arnold HL, Kugelmas M, Bashir MR, Jaros MJ, Ling L et al. 2018. NGM282 for treatment of non-alcoholic steatohepatitis: a multicentre, randomised, double-blind, placebo-controlled, phase 2 trial. *Lancet.* 391(10126):1174-1185.

Hashmonai M, Schramek A, Better O. 1974. Causes of early obstruction of sub-cutaneous A-V fistulae for haemodialysis. *Vasc Surg.* 8(1):36-40.

HE Y, HAYNES WG, MEYERS CD, AMER A, ZHANG Y, MAHLING PC, MENDONZA AE, MA S, CHUTKOW W, BACHMAN ES. 2018. LIK066, a Dual SGLT1/2 Inhibitor, Reduces Weight and Improves Multiple Incretin Hormones in Clinical Proof-of-Concept Studies in Obese Patients With or Without Diabetes. *Diabetes.* 67(Supplement 1).

Hirooka M, Koizumi Y, Miyake T, Ochi H, Tokumoto Y, Tada F, Matsuura B, Abe M, Hiasa Y. 2015. Nonalcoholic fatty liver disease: portal hypertension due to outflow block in patients without cirrhosis. *Radiology.* 274(2):597-604.

Jamwal R, de la Monte SM, Ogasawara K, Adusumalli S, Barlock BB, Akhlaghi F. 2018. Nonalcoholic Fatty Liver Disease and Diabetes Are Associated with Decreased CYP3A4 Protein Expression and Activity in Human Liver. *Mol Pharm.* 15(7):2621-2632.

Jancova P, Anzenbacher P, Anzenbacherova E. 2010. Phase II drug metabolizing enzymes. *Biomed Pap Med Fac Univ Palacky Olomouc Czech Repub.* 154(2):103-116.

Kalia HS, Gaglio PJ. 2016. The Prevalence and Pathobiology of Nonalcoholic Fatty Liver Disease in Patients of Different Races or Ethnicities. *Clin Liver Dis.* 20(2):215-224.

Kim S, Sohn I, Ahn JI, Lee KH, Lee YS, Lee YS. 2004. Hepatic gene expression profiles in a long-term high-fat diet-induced obesity mouse model. *Gene.* 340(1):99-109.

Kleiner DE, Brunt EM, Van Natta M, Behling C, Contos MJ, Cummings OW, Ferrell LD, Liu YC, Torbenson MS, Unalp-Arida A et al. 2005. Design and validation of a histological scoring system for nonalcoholic fatty liver disease. *Hepatology.* 41(6):1313-1321.

Kohjima M, Enjoji M, Higuchi N, Kato M, Kotoh K, Yoshimoto T, Fujino T, Yada M, Yada R, Harada N et al. 2007. Re-evaluation of fatty acid metabolism-related gene expression in nonalcoholic fatty liver disease. *Int J Mol Med.* 20(3):351-358.

Kolwankar D, Vuppalanchi R, Ethell B, Jones DR, Wrighton SA, Hall SD, Chalasani N. 2007. Association between nonalcoholic hepatic steatosis and hepatic cytochrome P-450 3A activity. *Clin Gastroenterol Hepatol.* 5(3):388-393.

Lake AD, Novak P, Fisher CD, Jackson JP, Hardwick RN, Billheimer DD, Klimecki WT, Cherrington NJ. 2011. Analysis of global and absorption, distribution, metabolism, and elimination gene expression in the progressive stages of human nonalcoholic fatty liver disease. *Drug Metab Dispos.* 39(10):1954-1960.

Lawitz EJ, Coste A, Poordad F, Alkhoury N, Loo N, McColgan BJ, Tarrant JM, Nguyen T, Han L, Chung C et al. 2018. Acetyl-CoA Carboxylase Inhibitor GS-0976 for 12 Weeks Reduces Hepatic De Novo Lipogenesis and Steatosis in Patients With Nonalcoholic Steatohepatitis. *Clin Gastroenterol Hepatol.*

Leoni S, Tovoli F, Napoli L, Serio I, Ferri S, Bolondi L. 2018. Current guidelines for the management of non-alcoholic fatty liver disease: A systematic review with comparative analysis. *World J Gastroenterol.* 24(30):3361-3373.

Lonardo A, Byrne CD, Caldwell SH, Cortez-Pinto H, Targher G. 2016. Global epidemiology of nonalcoholic fatty liver disease: Meta-analytic assessment of prevalence, incidence, and outcomes. *Hepatology.* 64(4):1388-1389.

Loomba R, Lawitz E, Mantry PS, Jayakumar S, Caldwell SH, Arnold H, Diehl AM, Djedjos CS, Han L, Myers RP et al. 2017. The ASK1 inhibitor selonsertib in patients with nonalcoholic steatohepatitis: A randomized, phase 2 trial. *Hepatology.*

Mancina RM, Dongiovanni P, Petta S, Pingitore P, Meroni M, Rametta R, Boren J, Montalcini T, Pujia A, Wiklund O et al. 2016. The MBOAT7-TMC4 Variant rs641738 Increases Risk of Nonalcoholic Fatty Liver Disease in Individuals of European Descent. *Gastroenterology.* 150(5):1219-1230 e1216.

Marchesini G, Petta S, Dalle Grave R. 2016. Diet, weight loss, and liver health in nonalcoholic fatty liver disease: Pathophysiology, evidence, and practice. *Hepatology.* 63(6):2032-2043.

Margariti E, Deutsch M, Manolakopoulos S, Papatheodoridis GV. 2012. Non-alcoholic fatty liver disease may develop in individuals with normal body mass index. *Ann Gastroenterol.* 25(1):45-51.

McCullough AJ. 2006. Pathophysiology of nonalcoholic steatohepatitis. *J Clin Gastroenterol.* 40 Suppl 1:S17-29.

Merrell MD, Cherrington NJ. 2011. Drug metabolism alterations in nonalcoholic fatty liver disease. *Drug Metab Rev.* 43(3):317-334.

Mikolasevic I, Milic S, Turk Wensveen T, Grgic I, Jakopcic I, Stimac D, Wensveen F, Orlic L. 2016. Nonalcoholic fatty liver disease - A multisystem disease? *World J Gastroenterol.* 22(43):9488-9505.

Musso G, Gambino R, Pacini G, De Michieli F, Cassader M. 2009. Prolonged saturated fat-induced, glucose-dependent insulinotropic polypeptide elevation is associated with adipokine imbalance and liver injury in nonalcoholic steatohepatitis: dysregulated enteroadipocyte axis as a novel feature of fatty liver. *Am J Clin Nutr.* 89(2):558-567.

Nakamuta M, Kohjima M, Morizono S, Kotoh K, Yoshimoto T, Miyagi I, Enjoji M. 2005. Evaluation of fatty acid metabolism-related gene expression in nonalcoholic fatty liver disease. *Int J Mol Med.* 16(4):631-635.

Navarro P, Kuharev J, Gillet LC, Bernhardt OM, MacLean B, Rost HL, Tate SA, Tsou CC, Reiter L, Distler U et al. 2016. A multicenter study benchmarks software tools for label-free proteome quantification. *Nat Biotechnol.* 34(11):1130-1136.

Neuschwander-Tetri BA, Loomba R, Sanyal AJ, Lavine JE, Van Natta ML, Abdelmalek MF, Chalasani N, Dasarathy S, Diehl AM, Hameed B et al. 2015. Farnesoid X nuclear receptor ligand obeticholic acid for non-cirrhotic, non-alcoholic steatohepatitis (FLINT): a multicentre, randomised, placebo-controlled trial. *Lancet.* 385(9972):956-965.

Niemela O, Parkkila S, Juvonen RO, Viitala K, Gelboin HV, Pasanen M. 2000. Cytochromes P450 2A6, 2E1, and 3A and production of protein-aldehyde adducts in the liver of patients with alcoholic and non-alcoholic liver diseases. *J Hepatol.* 33(6):893-901.

Orellana M, Rodrigo R, Varela N, Araya J, Poniachik J, Csendes A, Smok G, Videla LA. 2006. Relationship between in vivo chlorzoxazone hydroxylation, hepatic cytochrome

P450 2E1 content and liver injury in obese non-alcoholic fatty liver disease patients. *Hepatol Res.* 34(1):57-63.

Perazzo H, Dufour JF. 2017. The therapeutic landscape of non-alcoholic steatohepatitis. *Liver Int.* 37(5):634-647.

Pirola CJ, Sookoian S. 2018. Multiomics biomarkers for the prediction of nonalcoholic fatty liver disease severity. *World J Gastroenterol.* 24(15):1601-1615.

Promptila N, Wittayalertrpanya S, Komolmit P. 2008. Hepatic cytochrome P450 2E1 activity in nonalcoholic fatty liver disease. *J Med Assoc Thai.* 91(5):733-738.

Ratziu V, Bedossa P, Francque SM, Larrey D, Aithal GP, Serfaty L, Voiculescu M, Preotescu L, Nevens F, De Ledinghen V et al. 2014. Lack of efficacy of an inhibitor of PDE4 in phase 1 and 2 trials of patients with nonalcoholic steatohepatitis. *Clin Gastroenterol Hepatol.* 12(10):1724-1730 e1725.

Ratziu V, Harrison SA, Francque S, Bedossa P, Leheret P, Serfaty L, Romero-Gomez M, Boursier J, Abdelmalek M, Caldwell S et al. 2016. Elafibranor, an Agonist of the Peroxisome Proliferator-Activated Receptor-alpha and -delta, Induces Resolution of Nonalcoholic Steatohepatitis Without Fibrosis Worsening. *Gastroenterology.* 150(5):1147-1159 e1145.

Romeo S, Kozlitina J, Xing C, Pertsemlidis A, Cox D, Pennacchio LA, Boerwinkle E, Cohen JC, Hobbs HH. 2008. Genetic variation in PNPLA3 confers susceptibility to nonalcoholic fatty liver disease. *Nat Genet.* 40(12):1461-1465.

Rosenberger G, Koh CC, Guo T, Rost HL, Kouvonen P, Collins BC, Heusel M, Liu Y, Caron E, Vichalkovski A et al. 2014. A repository of assays to quantify 10,000 human proteins by SWATH-MS. *Sci Data.* 1:140031.

Rubio A, Guruceaga E, Vazquez-Chantada M, Sandoval J, Martinez-Cruz LA, Segura V, Sevilla JL, Podhorski A, Corrales FJ, Torres L et al. 2007. Identification of a gene-pathway associated with non-alcoholic steatohepatitis. *J Hepatol.* 46(4):708-718.

Ryan MC, Itsiopoulos C, Thodis T, Ward G, Trost N, Hofferberth S, O'Dea K, Desmond PV, Johnson NA, Wilson AM. 2013. The Mediterranean diet improves hepatic steatosis and insulin sensitivity in individuals with non-alcoholic fatty liver disease. *J Hepatol.* 59(1):138-143.

Sager JE, Yu J, Ragueneau-Majlessi I, Isoherranen N. 2015. Physiologically Based Pharmacokinetic (PBPK) Modeling and Simulation Approaches: A Systematic Review of Published Models, Applications, and Model Verification. *Drug Metab Dispos.* 43(11):1823-1837.

Santhekadur PK, Kumar DP, Sanyal AJ. 2018. Preclinical models of non-alcoholic fatty liver disease. *J Hepatol.* 68(2):230-237.

Sanyal A, Charles ED, Neuschwander-Tetri B, Loomba R, Harrison S, Abdelmalek M, Lawitz E, Halegoua-DeMarzio D, Dong Y, Noviello S et al. 2017. BMS-986036 (pegylated FGF21) in patients with non-alcoholic steatohepatitis: a phase 2 study. *Journal of Hepatology.* 66(1):S89-S90.

Sattar N, Forrest E, Preiss D. 2014. Non-alcoholic fatty liver disease. *BMJ.* 349:g4596.

Shiffman M, Freilich B, Vuppalanchi R, Watt K, Burgess G, Morris M, Sheedy B, Schiff E. 2015. LP37 : A placebo-controlled, multicenter, double-blind, randomised trial of emricasan in subjects with non-alcoholic fatty liver disease (NAFLD) and raised transaminases. *Journal of Hepatology.* 62:S282.

Shigefuku R, Takahashi H, Kato M, Yoshida Y, Suetani K, Noguchi Y, Hatsugai M, Nakahara K, Ikeda H, Kobayashi M et al. 2014. Evaluation of hepatic tissue blood flow using xenon computed tomography with fibrosis progression in nonalcoholic fatty liver disease: comparison with chronic hepatitis C. *Int J Mol Sci.* 15(1):1026-1039.

Shigefuku R, Takahashi H, Kobayashi M, Ikeda H, Matsunaga K, Okuse C, Matsumoto N, Maeyama S, Sase S, Suzuki M et al. 2012. Pathophysiological analysis of nonalcoholic fatty liver disease by evaluation of fatty liver changes and blood flow using xenon computed tomography: can early-stage nonalcoholic steatohepatitis be distinguished from simple steatosis? *J Gastroenterol.* 47(11):1238-1247.

Sliz E, Sebert S, Wurtz P, Kangas AJ, Soinen P, Lehtimäki T, Kahonen M, Viikari J, Mannikko M, Ala-Korpela M et al. 2018. NAFLD risk alleles in PNPLA3, TM6SF2, GCKR and LYPLAL1 show divergent metabolic effects. *Hum Mol Genet.* 27(12):2214-2223.

Sookoian S, Flichman D, Garaycoechea ME, Gazzi C, Martino JS, Castano GO, Pirola CJ. 2018. Lack of evidence supporting a role of TMC4-rs641738 missense variant-MBOAT7-intergenic downstream variant-in the Susceptibility to Nonalcoholic Fatty Liver Disease. *Sci Rep.* 8(1):5097.

Sookoian S, Pirola CJ. 2017. Genetic predisposition in nonalcoholic fatty liver disease. *Clin Mol Hepatol.* 23(1):1-12.

Stanhope KL, Schwarz JM, Keim NL, Griffen SC, Bremer AA, Graham JL, Hatcher B, Cox CL, Dyachenko A, Zhang W et al. 2009. Consuming fructose-sweetened, not glucose-sweetened, beverages increases visceral adiposity and lipids and decreases insulin sensitivity in overweight/obese humans. *J Clin Invest.* 119(5):1322-1334.

Stepanova M, Hossain N, Afendy A, Perry K, Goodman ZD, Baranova A, Younossi Z. 2010. Hepatic gene expression of Caucasian and African-American patients with obesity-related non-alcoholic fatty liver disease. *Obes Surg.* 20(5):640-650.

Stephenson K, Kennedy L, Hargrove L, Demieville J, Thomson J, Alpini G, Francis H. 2018. Updates on Dietary Models of Nonalcoholic Fatty Liver Disease: Current Studies and Insights. *Gene Expr.* 18(1):5-17.

Sumida Y, Seko Y, Yoneda M, Japan Study Group of N. 2016. Novel antidiabetic medications for non-alcoholic fatty liver disease with type 2 diabetes mellitus. *Hepatol Res.*

Sumida Y, Yoneda M. 2018. Current and future pharmacological therapies for NAFLD/NASH. *J Gastroenterol.* 53(3):362-376.

Takaki A, Kawai D, Yamamoto K. 2014. Molecular mechanisms and new treatment strategies for non-alcoholic steatohepatitis (NASH). *Int J Mol Sci.* 15(5):7352-7379.

Takei Y. 2013. Treatment of non-alcoholic fatty liver disease. *J Gastroenterol Hepatol.* 28 Suppl 4:79-80.

Tiessen RG, Kennedy CA, Keller BT, Levin N, Acevedo L, Gedulin B, van Vliet AA, Dorenbaum A, Palmer M. 2018. Safety, tolerability and pharmacodynamics of apical sodium-dependent bile acid transporter inhibition with volixibat in healthy adults and patients with type 2 diabetes mellitus: a randomised placebo-controlled trial. *BMC Gastroenterol.* 18(1):3.

Trak-Smayra V, Paradis V, Massart J, Nasser S, Jebara V, Fromenty B. 2011. Pathology of the liver in obese and diabetic ob/ob and db/db mice fed a standard or high-calorie diet. *Int J Exp Pathol.* 92(6):413-421.

Tully DC, Rucker PV, Chianelli D, Williams J, Vidal A, Alper PB, Mutnick D, Bursulaya B, Schmeits J, Wu X et al. 2017. Discovery of Tropifexor (LJN452), a Highly Potent Non-bile Acid FXR Agonist for the Treatment of Cholestatic Liver Diseases and Nonalcoholic Steatohepatitis (NASH). *J Med Chem.* 60(24):9960-9973.

Vilar-Gomez E, Martinez-Perez Y, Calzadilla-Bertot L, Torres-Gonzalez A, Gra-Oramas B, Gonzalez-Fabian L, Friedman SL, Diago M, Romero-Gomez M. 2015. Weight Loss Through Lifestyle Modification Significantly Reduces Features of Nonalcoholic Steatohepatitis. *Gastroenterology.* 149(2):367-378 e365; quiz e314-365.

Weltman MD, Farrell GC, Hall P, Ingelman-Sundberg M, Liddle C. 1998. Hepatic cytochrome P450 2E1 is increased in patients with nonalcoholic steatohepatitis. *Hepatology.* 27(1):128-133.

Wisniewski JR, Hein MY, Cox J, Mann M. 2014. A "proteomic ruler" for protein copy number and concentration estimation without spike-in standards. *Mol Cell Proteomics.* 13(12):3497-3506.

Wisniewski JR, Mann M. 2016. A Proteomics Approach to the Protein Normalization Problem: Selection of Unvarying Proteins for MS-Based Proteomics and Western Blotting. *J Proteome Res.* 15(7):2321-2326.

Wong JW, Cagney G. 2010. An overview of label-free quantitation methods in proteomics by mass spectrometry. *Methods Mol Biol.* 604:273-283.

Woolsey SJ, Mansell SE, Kim RB, Tirona RG, Beaton MD. 2015. CYP3A Activity and Expression in Nonalcoholic Fatty Liver Disease. *Drug Metab Dispos.* 43(10):1484-1490.

Yoneda M, Endo H, Mawatari H, Nozaki Y, Fujita K, Akiyama T, Higurashi T, Uchiyama T, Yoneda K, Takahashi H et al. 2008. Gene expression profiling of non-alcoholic steatohepatitis using gene set enrichment analysis. *Hepatology Res.* 38(12):1204-1212.

Yoshinari K, Takagi S, Sugatani J, Miwa M. 2006. Changes in the expression of cytochromes P450 and nuclear receptors in the liver of genetically diabetic db/db mice. *Biol Pharm Bull.* 29(8):1634-1638.

Younossi ZM, Blissett D, Blissett R, Henry L, Stepanova M, Younossi Y, Racila A, Hunt S, Beckerman R. 2016. The economic and clinical burden of nonalcoholic fatty liver disease in the United States and Europe. *Hepatology.* 64(5):1577-1586.

Younossi ZM, Koenig AB, Abdelatif D, Fazel Y, Henry L, Wymer M. 2016. Global epidemiology of nonalcoholic fatty liver disease-Meta-analytic assessment of prevalence, incidence, and outcomes. *Hepatology.* 64(1):73-84.

Younossi ZM, Stepanova M, Rafiq N, Makhlof H, Younoszai Z, Agrawal R, Goodman Z. 2011. Pathologic criteria for nonalcoholic steatohepatitis: interprotocol agreement and ability to predict liver-related mortality. *Hepatology.* 53(6):1874-1882.

Zanger UM, Schwab M. 2013. Cytochrome P450 enzymes in drug metabolism: regulation of gene expression, enzyme activities, and impact of genetic variation. *Pharmacol Ther.* 138(1):103-141.

Zhuang X, Lu C. 2016. PBPK modeling and simulation in drug research and development. *Acta Pharm Sin B.* 6(5):430-440.

Zivkovic AM, German JB, Sanyal AJ. 2007. Comparative review of diets for the metabolic syndrome: implications for nonalcoholic fatty liver disease. *Am J Clin Nutr.* 86(2):285-300.

Figures and tables

Figure 1: Hematoxylin and Eosin staining of liver samples (A) Normal liver with uniform chord-like arrangements of hepatocytes, (B) Nonalcoholic fatty liver (NAFL) liver with lipid droplets, and (C) Nonalcoholic steatohepatitis (NASH) with significant hepatic steatosis and infiltration of lymphomononuclear inflammatory cells.

Figure 2: Effect of altered CYP3A4 on systemic midazolam exposure. The systemic exposure of a substrate may increase if the CYP450 responsible for its metabolism and clearance is reduced. The opposite is true when the expression is increase. The illustration shown here for CYP3A4 mediated midazolam (MDZ) in normal and altered states. 1'-OH-MDZ: 1-hydroxy midazolam.

Figure 3: Graphical illustration of the advantage of SWATH-MS over traditional MRM based quantification method. MRM, Multiple reaction monitoring; SWATH-MS, Sequential windowed analysis of all the theoretical mass spectra.

Table 1: Therapeutic agents currently being developed for treatment of NAFLD. ACC, Acetyl-CoA Carboxylase; AOC, amine oxidase, copper containing; ASK, Apoptosis signal-regulating kinase; FGF, fibroblast growth factor; FXR, Farnesoid X receptor; PPAR, peroxisome proliferator-activated receptors; mTOT, mitochondrial target of thiazolidinediones; SGLT, Sodium-dependent glucose cotransporter; GLP, Glucagon-like peptide; ASBT, apical sodium–bile acid transporter; ASK, apoptosis signal-regulating kinase; THB, thyroid hormone receptor

Table 2: Altered expression and activity levels of CYP450 enzymes in NAFLD. CYP, cytochrome P450; NASH: Nonalcoholic steatohepatitis

Table 3: Hepatic blood flow changes in different stages of NAFLD. Liver blood flow in the disease state were studied using xenon computed tomography. THBF: Total hepatic blood flow; PVBF: Portal vein blood flow; HABF: Hepatic artery blood flow

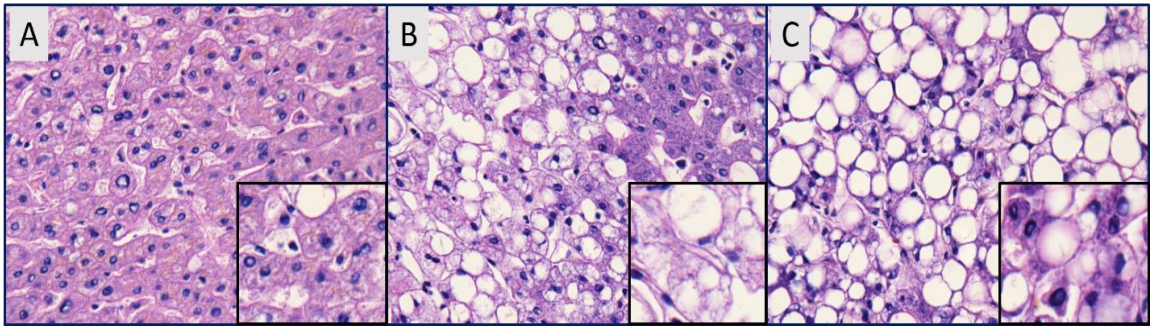


Figure 1: Hematoxylin and Eosin staining of liver samples. (A) Normal liver with uniform chord-like arrangements of hepatocytes, (B) Nonalcoholic fatty liver (NAFL) liver with lipid droplets, and (C) Nonalcoholic steatohepatitis (NASH) with significant hepatic steatosis and infiltration of lymphomononuclear inflammatory cells.

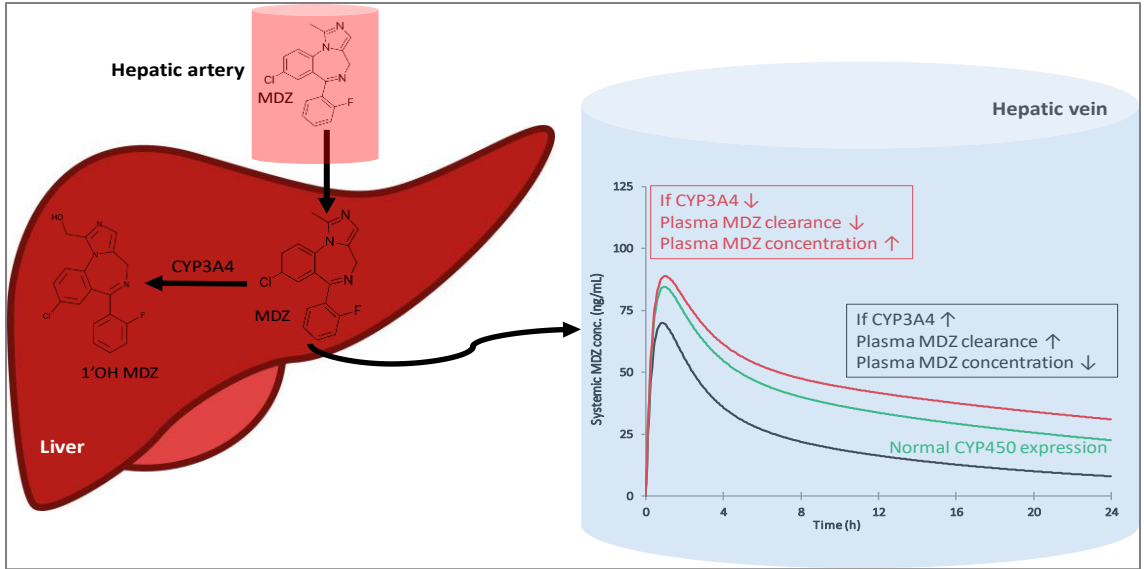


Figure 2: Effect of altered CYP3A4 on systemic midazolam exposure. The systemic exposure of a substrate may increase if the CYP450 responsible for its metabolism and clearance is reduced. The opposite is true when the expression is increased. The illustration shown here for CYP3A4 mediated midazolam (MDZ) in normal and altered states. 1'OH-MDZ: 1-hydroxy midazolam.

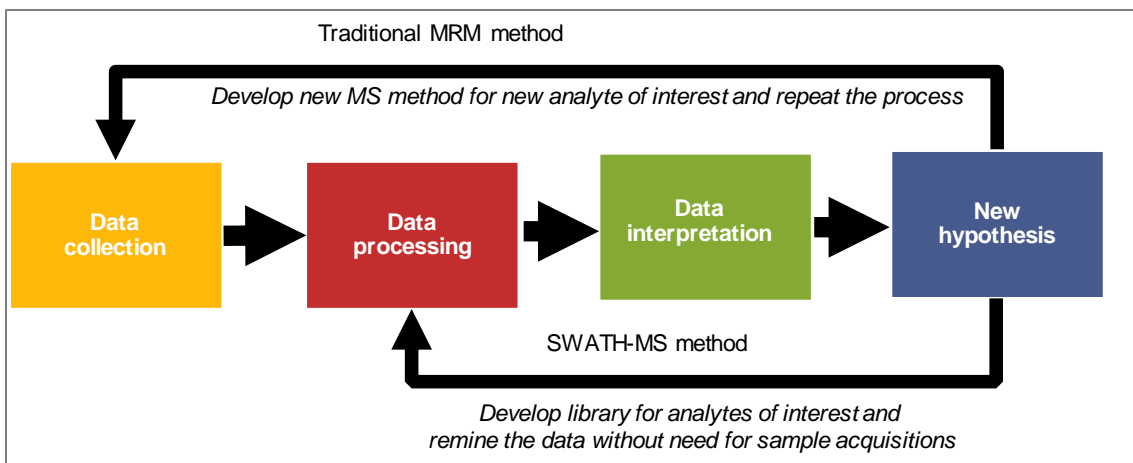


Figure 3: Graphical illustration of the advantage of SWATH-MS over traditional MRM based quantification method. MRM, Multiple reaction monitoring; SWATH-MS, Sequential windowed analysis of all the theoretical mass spectra.

Therapeutic candidate	Company	Mechanism of action	Target	Ref.
GFT505	Genfit Pharmaceuticals	PPAR α/δ agonist	Lipid metabolism	(Ratzu et al. 2016)
Obeticholic acid	Intercept Pharmaceuticals	FXR agonist	Lipid metabolism	(Neuschwander-Tetri et al. 2015)
BMS-986036	Bristol-Myers Squibb	FGF21 analog	Lipid metabolism	(Sanyal et al. 2017)
GS-0976	Gilead Sciences Inc.	ACC inhibitor	Lipid metabolism	(Lawitz et al. 2018)
PF-05221304	Pfizer Inc.	ACC inhibitor	Lipid metabolism	(Bergman et al. 2018)
Selonsertib	Gilead Sciences Inc.	ASK1 inhibitor	Lipid metabolism	(Loomba et al. 2017)
GR-MD-02	Galectin Therapeutics	Galectin inhibitor	Fibrosis	(Harrison et al. 2016)
Aramchol	Galmed Pharmaceuticals	SCD1 inhibitor	Lipid metabolism	(Hashmonai et al. 1974)
Cenicriviroc	Allergan plc	CCR2/5 antagonist	Inflammation/ cell death	(Friedman et al. 2018)
NGM282	NGM Biopharmaceuticals Inc.	FGF19 analogue	Lipid metabolism	(Harrison SA et al. 2018)
Volixibat (SHP626)	Shire	ASBT inhibitor	Bile acid synthesis	(Tiessen et al. 2018)
LIK066	Novartis Pharmaceuticals	SGLT1/2 inhibitor	Glucose reabsorption	(HE et al. 2018)
LJN452	Novartis Pharmaceuticals	FXR agonist	Lipid metabolism	(Tully et al. 2017)
MSDC 0602k	Cirius Therapeutics	mTOT modulator	Insulin signaling	(Colca et al. 2018)
Liraglutide (NN2211)	Novo Nordisk	GLP-1 analogue	Insulin signaling	(Armstrong et al. 2016)
Emricasan	Conatus and Novartis Pharmaceuticals	Pan-caspase inhibitor	Apoptosis	(Shiffman et al. 2015)
MGL-3196	Madrigal Pharmaceuticals	THR β -selective agonist	Lipid metabolism	(Harrison S et al. 2018)

Table 1: Therapeutic agents currently being developed for treatment of NAFLD.

Enzyme	Disease stage	mRNA expression	Protein expression	Activity	Ref.
CYP2E1	NAFLD	↑			(Kohjima et al. 2007)
	NAFLD			↔	(Prompila et al. 2008)
	NAFLD			↓	(Nakamuta et al. 2005)
	NAFLD progression	↓	↓	↔	(Fisher et al. 2009)
	NASH	↑			(Baker et al. 2010)
	NASH			↑	(Chalasanani et al. 2003)
	NASH			↑	(Orellana et al. 2006)
	NASH			↑	(Orellana et al. 2006)
	NASH			↑	(Weltman et al. 1998)
	NASH			↑	(Niemela et al. 2000)
	NAFL			↔	(Donato et al. 2006)
	NAFL	↑			(Emery et al. 2003)
CYP3A4/5	NASH	↔	↓	↓	(Jamwal et al. 2018)
	NAFL	↔	↓	↓	(Jamwal et al. 2018)
	NAFLD progression	↔	↔	↔	(Fisher et al. 2009)
	NAFLD		↔		(Bell et al. 2010)
	Hepatocytes			↔	(Donato et al. 2006)
	Steatosis			↔	(Donato et al. 2007)
	NASH		↑		(Niemela et al. 2000)
	NASH		↓		(Weltman et al. 1998)
CYP1A2	NAFLD progression	↔	↓	↓	(Fisher et al. 2009)
	NAFL			↓	(Donato et al. 2006)
	NAFL	↓			(Greco et al. 2008)
CYP2A6	NAFLD progression	↑	↑	↑	(Fisher et al. 2009)
	NASH	↓			(Rubio et al. 2007)
	NASH		↑		(Niemela et al. 2000)
CYP2B6	NAFLD progression	↑	↔	↔	(Fisher et al. 2009)
	NASH	↓			(Stepanova et al. 2010)
	NASH	↓			(Yoneda et al. 2008)
CYP2C8	NAFLD progression	↔	↔	↔	(Fisher et al. 2009)
CYP2C9	NAFLD progression	↔	↔	↑	(Fisher et al. 2009)
CYP2C19	NAFLD progression	↔	↓	↓	(Fisher et al. 2009)

Table 2: Altered expression and activity levels of CYP450 enzymes in NAFLD.

ml/min/100 g	Normal	NAFL	Early NASH	Advanced NASH
THBF	94.0±17.8	66.4±10.6	52.4±12.3	47.1±13.2
PVBF	72.4±16.2	41.6±5.6	33.6±7.0	28.4±6.3
HABF	21.2±7.4	24.8±8.5	18.7±7.0	18.7±8.4
	(Carlisle et al. 1992)	(Shigefuku et al. 2012)		

Table 3: Changes in hepatic blood flow in different stages of nonalcoholic fatty liver disease.

MANUSCRIPT II

Published as a research article in Journal of Proteome Research, 2017 Nov 3;16(11):4134-4143. PMID 28944677

Multiplex and Label-Free Relative Quantification Approach for Studying Protein Abundance of Drug Metabolizing Enzymes in Human Liver Microsomes Using SWATH-MS

Rohitash Jamwal¹, Benjamin J. Barlock¹, Sravani Adusumalli¹, Ken Ogasawara¹, Brigitte L. Simons², Fatemeh Akhlaghi^{1*}

¹ Clinical Pharmacokinetics Research Laboratory, Department of Biomedical and Pharmaceutical Sciences, University of Rhode Island, Kingston, 02881, RI, USA

² SCIEX, 71 Four Valley Dr., Concord, Ontario, L4K4V8, Canada

Author for correspondence:

*Fatemeh Akhlaghi, Ph.D., PharmD

Clinical Pharmacokinetics Research Laboratory, Department of Biomedical and Pharmaceutical Sciences, University of Rhode Island, 495A College of Pharmacy,

7 Greenhouse Road, Kingston, RI 02881, United States.

Email address: fatemeh@uri.edu

Keywords: Proteomics, SWATH-MS, label-free quantification, human liver, cytochrome-P450, CYP3A4

List of nonstandard abbreviations

BHT: Butylated hydroxytoluene; CYP: Cytochrome P450; DMEs: Drug metabolizing enzymes; DDA: Data dependent analysis; FDR: False discovery rate; HLM: Human liver microsomes; LFQ: Label-free quantification; MRM: Multiple reaction monitoring; PCT: Pressure cycling technology; SRM: Single-reaction monitoring; SWATH-MS: Sequential windowed acquisition of all theoretical fragment ion mass spectra; TPCK: Tosyl phenylalanyl chloromethyl ketone; UGT: UDP-glucuronosyltransferase; UHPLC: Ultra high performance liquid chromatography.

ABSTRACT

We describe a sequential windowed acquisition of all theoretical fragment ion mass spectra (SWATH-MS) based method for label-free, simultaneous, relative quantification of drug metabolism enzymes in human liver microsomes (HLM; n=78). In-solution tryptic digestion was aided by a pressure cycling method which allowed a 90-min incubation time, a significant reduction over classical protocols (12-18 h). Digested peptides were separated on an Acquity UHPLC Peptide BEH C18 column using a 60-min gradient method at a flow rate of 0.100 mL/min. The quadrupole-time-of-flight mass spectrometer (ESI-QTOFMS) was operated in positive electrospray ionization mode and data was acquired by Data-Dependent Acquisition (DDA) and SWATH-MS^{ALL} mode. A pooled HLM sample was used as quality control to evaluate variability in digestion and quantification among different batches, and inter-batch %CV for various proteins was between 3.1-7.8%. Spectral library generated from the DDA data identified 1,855 distinct proteins and 25,601 distinct peptides at a 1% global false discovery rate (FDR). SWATH data were queried and analyzed for 10 major cytochrome P450 (CYP) enzymes using Skyline, a targeted data extraction software. Further, correlation analysis was performed between functional activity, protein and mRNA expression for ten CYP enzymes. Pearson correlation coefficient (r) between protein and activity for CYPs ranged from 0.314 (CYP2C19) to 0.767 (CYP2A6). A strong correlation was found between CYP3A4 and CYP3A5 abundance and activity determined using midazolam and testosterone ($r > 0.600$, $p < 0.001$). A moderate protein-to-activity correlation ($r > 0.500$, $p < 0.01$) was also observed for CYP2A6, CYP1A2, CYP2C9, CYP2B6 and CYP2E1. The correlation for CYP2C8, CYP2D6 and CYP2C19 was significant but poor ($r < 0.400$, $p < 0.05$). The findings suggest

the suitability of SWATH-MS based method as a valuable and relatively fast analytical technique for relative quantification of proteins in complex biological samples. We also show that protein abundance is a better surrogate than mRNA to predict the activity of CYP activity.

INTRODUCTION

Hepatic drug metabolizing enzymes (DMEs) are responsible for the clearance of pharmacological agents and xenobiotics. The abundance of these enzymes in liver tissue determines the rate and extent to which drugs are metabolized and cleared from systemic circulation. Cytochrome P450s (CYPs) and uridine diphosphate glucuronyltransferases (UGTs) constitute the majority of phase I and phase II DMEs, respectively (1). CYPs are primarily involved in the oxidation of endogenous steroids, xenobiotics, and drugs (2, 3). Expression of CYPs thus impacts drug disposition, pharmacokinetics and adverse drug reactions (1). Characterization of expression and activity of DMEs in human liver microsomes and hepatocytes is a pivotal part of drug development. Moreover, induction potential of new chemical entities is typically screened using primary or cryopreserved hepatocyte culture (4).

It is important to understand how the level of different DMEs changes from one individual to another or how different disease states influence the abundance of these enzymes. Classical methods for protein quantification include Western blotting and ELISA (5). Western blotting is semi-quantitative, low throughput, labor intensive, and require the use of expensive antibodies (6). ELISA methods can be higher throughput and more quantitative than Western analysis, but this approach is also labor intensive, suffers from limited concentration range and can lack specificity (6). In the recent years, protein mass spectrometry has proved to be a powerful technique in different areas of biomedical research including in drug development (7). “Targeted” or “absolute” protein quantification methods use liquid chromatography coupled with a triple quadrupole mass spectrometer (LC-MS/MS) and consist of quantification of one or more signature peptides

per protein (8). These peptides are custom synthesized and are often paired with an isotope-labeled peptide as an internal standard. Several groups have used high-resolution mass spectrometry methods to analyze the expression of drug-metabolizing enzymes and transporters in human tissue (3, 9). Traditionally, in the drug metabolism field, multiple-reaction monitoring (MRM) method has been used for absolute quantification of clinically relevant CYPs and UGTs in human liver tissue (10-12). Others have measured the concentration of drug transporters using quantitative targeted proteomics (13). However, significant upfront assay development with 1-2 synthetic peptides for each protein is often required for targeted MRM methods developed to ensure detection of multiple transitions.

Label-free quantification (LFQ) techniques are now becoming common for analysis of proteins using mass spectrometry. Neilson et al. published a comprehensive review on LFQ approaches and compared it with other labeling based techniques (14). Sequential windowed acquisition of all theoretical fragment ion mass spectra (SWATH-MS) is a cost efficient, LFQ method that combines data-independent acquisition (DIA) and multiple reaction monitoring-like data processing for accurate peptide quantitation. It provides an advantage when compared to traditional mass spectrometry-based proteomics methods like shotgun (high throughput) and SRM (high reproducibility and consistency). The technique enables a complete and permanent recording of all fragment ions of the detectable peptide precursors present in a digested biological sample that can be interrogated retrospectively for peptide features for SRM-like quantitative information, time-consuming design of acquisition method (15). Data are acquired on the high-resolution time of flight mass spectrometer (TOF/MS) in consecutive continuous cycles through precursor isolation windows which collect fragment ion spectra for all analytes in a sample. The collected

data contain the spectra of fragment ions for all precursor ions that appear within the defined precursor retention time and m/z space. The combination of all the high-resolution spectra collected at $\geq 25,000$ resolution (FWHM) generates a fragment ion map which generates extracted ion chromatogram (XIC) measurements with high specificity derived by low mass error (15). This provides an unbiased quantification method which is reproducibly collected across all samples for relative quantitation and does not require a protein or sample specific method development. Peptide spectral library can be used for extraction of peptides of interest from the SWATH data and further statistical analysis.

The purpose of this work was to develop a SWATH-MS method for relative quantification of proteins in the microsomal fraction of 78 human liver tissue samples. Enzyme activities of DMEs as provided by the vendor were correlated with protein level determined in the human liver microsomes by using the current method. Additionally, we performed correlation analysis between protein and mRNA expression with enzyme activity of 10 major CYPs.

MATERIALS AND METHODS

Chemical and Reagents

Trypsin digested β -galactosidase (*E. coli*), protein preparation kit and TPCK-treated trypsin were procured from AB Sciex, Framingham, MA. Mass spectrometry grade acetonitrile and formic acid were from ThermoFisher Scientific, Waltham, MA. Acquity UHPLC Peptide BEH C18 analytical column and VanGuard pre-columns were from Waters Corp., Waltham, MA. RNeasy Mini Kit was purchased from Qiagen Inc., Valencia, CA.

Human liver microsomes

Human liver tissues retrieved from brain dead individuals by Sekisui Xenotech were used in this study. A brief overview of the donor demographics was given in **table 1**. Human liver microsomes (HLM) were prepared as described previously, with modifications (16).

Briefly, human liver samples were carefully thawed on ice and weighed. Tissue was immediately transferred to a pre-cooled 7 mL homogenization bead-mill tube containing 50 mM Tris-HCl (pH 7.4) buffer having 0.5 mM EDTA, 0.25 M sucrose and 20 μ M BHT (3 mL/g wet liver weight) and homogenized using a bead homogenizer (Bead Ruptor 24, Omni International, Kennesaw, GA). Homogenate was centrifuged at 10,000 *g* for 20 min at 4°C (Eppendorf 5810R, Eppendorf AG, Hamburg, Germany). The pellet containing cell debris was discarded, and supernatant (S9 fraction) was ultra-centrifuged at 100,000 *g* for 1 hour at 4°C (Beckman Coulter, Brea, CA). Further, the supernatant was separated and stored as a cytosolic fraction for future use. The pellet on the walls of the tubes was washed (50 nM sodium pyrophosphate, pH 7.4) and re-suspended in

homogenization buffer containing 20% glycerol (pH 7.4, 0.66 mL/g of tissue). The contents were carefully transferred to a 1 mL Dounce homogenizer for fine homogenization. The resulting microsomal fraction was stored at -80°C until analysis. Microsomal protein concentration was estimated using a bicinchoninic acid method (Pierce-Fisher, Rockford, IL) with bovine serum albumin as a standard. The samples were diluted to 2.5 mg/mL in phosphate-buffered saline (pH 7.4) before protein digestion as described below. XTreme 200 pool HLM was purchased from Sekisui XenoTech, LLC, Kansas City, KS.

Pressure cycling technology (PCT) based protein digestion

In-solution trypsin digestion was performed on each biological sample in duplicates according to a published method with modifications (17). Denaturation, reduction, and alkylation were performed in centrifuge tubes while digestion was carried out in MicroTubes (Pressure BioSciences Inc., South Easton, MA) under oscillating high-pressure cycles in a Barocycler NEP2320-45k (Pressure BioSciences Inc.). Briefly, 150 µg of microsomal protein was denatured and reduced for 1 h at 60°C in a shaking water bath (75 rpm). Reduced samples were alkylated for 10 min at room temperature to prevent free cysteine residues from the reformation of peptide bonds. Subsequently, samples were diluted with equal volume of 100 mM Tris buffer (pH 8) containing 4 mM MgCl₂ and digested with TPCK-treated trypsin (protease: protein, 1: 20) in the barocycler. PCT-aided digestion was performed at 50 °C for 90 cycles, 50 s at 35 kpsi and 10 s at ambient pressure for every cycle. Further, samples were transferred to a centrifuge tube, and digestion was stopped by addition of formic acid at a final

concentration of 0.1%. The mixture was vortex-mixed for 10 s before centrifugation at 5,000 rpm for 1 min at 10°C. The supernatant was collected and transferred to a clean micro-insert for further analysis. Two technical replicates for each HLM sample were digested and analyzed by mass spectrometry. XTreme 200 pool sample was used as digestion control to monitor the batch-to-batch variation of protein digestion carried out in 6 batches. Approximately 12 samples and one digestion control sample were digested and run in every batch along.

LC-QTOF/MS analysis

All experiments were performed on a Sciex 5600 TripleTOF[®] mass spectrometer equipped with a DuoSpray[™] ion source (AB Sciex, Concord, Canada) coupled to Acquity UHPLC HClass system (Waters Corp., Milford, MA, USA). The mass spectrometer was operated in positive electrospray ionization mode for the analysis. The peptides were separated on Acquity UHPLC Peptide BEH C18 (2.1 X 150 mm, 300 Å, 1.7 µm) equipped with Acquity VanGuard pre-column (2.1 X 5 mm, 300 Å, 1.7 µm). Digested samples were maintained at 10°C in the autosampler and the analytical column temperature was kept at 40°C. The amount of protein per injection on the column was 10 µg. The chromatographic separation was achieved with a runtime of 60 min at 100 µL/min with a gradient method using mobile phase A (98% water, 2% acetonitrile, 0.1% formic acid) and mobile phase B (98% acetonitrile, 2% water, 0.1% formic acid). A linear gradient scheme was used with solvent composition as follows; 98% A from 0-3 min: 60% to 90% A from 3-48 min: 20% A held from 49-52 min to flush the column, 98% A at 53 min. The column was allowed to equilibrate at 98% A from 53 to 60 min

before the start of next run. In each batch, trypsin-digested β -galactosidase peptides were injected (~30 pmol/injection) every 10 samples during the analysis to monitor mass calibration of the TOF detector and normalization of intensity during relative quantification. The average intensity of all the β -galactosidase peptide samples in a batch was used for data normalization of the respective batch of samples.

Standard DDA and SWATH-MS data acquisition

Mass spectrometry analysis was performed according to a previously described method with modifications (18). Analyst[®] TF 1.7 was used to acquire data during the study (AB Sciex, Framingham, MA). DDA was used to acquire data for generation of peptide ion library, and SWATH-MS^{ALL} mode for relative quantification of the proteins. Positive ionization monitoring was utilized for all the experiments during the study. DDA experiments were performed over a mass range of m/z 350-950 and all ions exceeding 350 cps, with a charge state 2 to 4, and quadrupole resolution of 0.7 AMU was used for automated MS/MS analysis. The mass tolerance was set at 50 mDa during the initial 250-milliseconds (ms) survey scan, and 8 ions were selected for product scan per cycle (total cycle time: 900-ms). A DuoSpray[™] ion source was used for all the experiments. Source specific parameters settings for the analysis were ion source gas 1 (GS1): 55 psi, ion source gas 2 (GS2): 60 psi, curtain gas (CUR):25 psi, source temperature (TEM): 500°C, and ionspray voltage floating (ISVF):5500 V. Compound-specific parameters for acquisition were declustering potential (DP): 120, and collision energy (CE): 10 (product ion experiments were carried out using rolling collision energy). SWATH-MS based spectra were acquired for mass range m/z 400-900 Da with

SWATH window width of 25 m/z resulting in 20 overlapping mass windows per cycle. Accumulation time of 109 ms per window was used which resulted in a total cycle time of 2.29 s. Rolling collision energy for +2 and +3 charges with collision energy spread of 15 V was applied to each SWATH window upon automatic calculation of the collision energy center value, dependent on the m/z range according to this rolling collision energy equation; $CE = 0.044*(m/z)+9$ (19).

Generation of spectral library

Protein database searching was performed against reference UniProt human proteome library (July 2015) by ProteinPilot 5.0 (AB Sciex; Framingham, MA, USA) using Paragon™ algorithm (5.0). A comprehensive spectral library of protein and peptides from DDA runs of the HLM samples was prepared. Data were uploaded to ProteinPilot Software to carry out protein identification against a Human Uniprot FASTA database. Search parameters in ProteinPilot were as follows: Cys alkylation-MMTS; digestion-Trypsin; instrument, TripleTOF® 5600; ID focus-Biological modifications, search effort-Thorough ID, detected protein threshold-0.05 (10%), and false discovery rate analysis - yes. The resulting library file (*.group) was uploaded to Skyline and label-free analyses of data was performed as described below. The spectral library is available on PeptideAtlas (Identified number PASS01078).

Data processing using Skyline

Skyline is an open source, Windows-based software for creating and analyzing data from proteomic experiments (20). Reviewed protein sequence of DMEs of interest was

retrieved from Uniprot and uploaded onto Skyline. Detailed Skyline and data processing settings are given in *supplementary information I*.

Briefly, spectral library generated from DDA files was uploaded in Skyline, and SWATH-MS data files were processed using the full scan MS/MS filtering at a resolution of 10,000. Unique, non-repetitive peptides were refined and curated for reproducible fragment ions, and peak boundaries for each selected peptide were manually supervised and when necessary, adjusted. The reproducibility and reliability of selected peptide and transitions were verified visually by looking at the peak area ratio of the ion across the samples. We used 2 peptides per protein and 3 fragment ions per peptide for every protein. Selected peptides for each protein for the relative quantification of the CYPs described in this study were also correlated (protein specific) to validate the selection of peptides (*supplementary figure 1*).

The total area of representative peptides for a protein was summed, and resulting intensity was normalized by total intensity of tryptic peptide of β -galactosidase. MultiQuant v 3.0 (AB Sciex, Framingham, MA) was used to retrieve intensity for APLDNDIGVSEATR peptide [(M+2H)²⁺: 729.365] and was subsequently used for normalization among different batches as described above (*supplementary information II*) (21). Percent coefficient of variation (CV%) of the proteins of interest (CYPs) between 6 batches was calculated and plotted using Prism 6.0 (GraphPad Inc., La Jolla, CA). Peptides used for relative quantification and the transitions for precursor and product ions are given in *supplementary information II*.

Quantification of hepatic mRNA expression

Total cellular RNA was isolated from the samples using RNeasy Mini Kit (QIAGEN Inc., Valencia, CA). The total RNA was reverse-transcribed, and the single-stranded DNA was used for real-time PCR. The mRNA expression of hepatic CYP was quantified in duplicates by real-time PCR using an Applied Biosystems 7500 real-time PCR system (Applied Biosystems) according to the manufacturer's instructions. 18S ribosomal RNA (rRNA) was also quantified as an internal control. The primers used for CYPs are given in *supplementary information III*.

Correlation and statistical analysis: Enzyme activity, protein, and mRNA expression

Enzymatic activity for 10 CYPs provided by Xenotech was used for correlation with the relative protein abundance estimated in HLM using the current method. The correlation analysis was also performed with mRNA levels determined from liver samples using method as described above. The incubation conditions, probe substrates and other details of the enzymatic assays performed by Xenotech on the livers are given in *supplementary information IV*. Information on mRNA probes is provided in *supplementary information III*. A three-way correlation analysis was conducted between enzyme activity, protein levels, and mRNA (described below).

Normality tests were performed before statistical analysis and to address the skewness, the data were natural log transformed (ln) before correlation analysis. Pearson correlation coefficient was used to determine the relationship between activity, protein and mRNA level. Correlation coefficient (r) >0.600 was considered strong while between 0.400 - 0.600 was considered moderate. Additionally, any correlation with $r<0.400$ was considered poor in this work. Statistical values ($p<0.05$) were considered significant for the analysis. All

statistical analysis was performed with SPSS 24 (IBM Corp., Armonk, NY) and graphs were plotted on Prism 6.0 (GraphPad Inc., La Jolla, CA).

RESULTS

Targeted data extraction using Skyline

At a critical FDR of 1.0%, we detected 1855 distinct proteins and 25,681 distinct peptides from global FDR fit (**Figure 1 (a-b)**). The in-house generated spectral library was imported into Skyline, and data extraction was performed. The list of peptides and their transitions along with charge state is provided in *supplementary information II*. The correlation analysis of two peptides for a protein is given in *supplementary figure 1*. Out of the 15 hepatic CYPs reported for xenobiotic metabolism, we were able to find 12 CYPs in this study (22). Inter-batch %CV for all the DMEs evaluated from quality control sample ranged from 3.1 to 7.8% (*supplementary figure 2*).

Correlation between protein expression and enzyme activity

Pearson correlation coefficient (r) for CYPs ranged from 0.314 (CYP219) to 0.767 (CYP2A6). All the major CYP enzymes showed a significant ($p < 0.05$) correlation between enzyme activity and protein levels (**Figure 2 (a-l)**). CYP3A4 and CYP3A5 abundance, and activity determined using midazolam and testosterone showed a significant association ($r > 0.650$, $p < 0.001$). A moderate protein-to-activity correlation ($r = 0.400-0.600$, $p < 0.001$) was also observed for CYP2A6, CYP1A2, CYP2C9, CYP2B6 and CYP2E1. The correlation for CYP2C8, CYP2D6 and CYP2C19 was significant but poor ($r < 0.400$, $p < 0.05$). A detailed correlation between activity and protein is provided in **Table 2**.

Correlation between mRNA expression and enzyme activity

The correlation coefficient for mRNA and activity ranged from -0.067 to 0.729 (**Figure 3 (a-l)**). CYP2C19 and CYP2E1 showed a slightly negative correlation but were not

significant. The correlation between mRNA expression and activity for CYP3A4, CYP1A2, CYP2A6, CYP2C8, and CYP2B6 showed a significant and moderate correlation ($r=0.400-0.600$, $p<0.01$). CYP3A5 mRNA correlated significantly only with midazolam hydroxylation activity. CYP2D6 exhibited a poor but significant correlation ($r=0.306$, $p<0.05$). The correlation was poor and insignificant for other CYP isoforms. A detailed correlation table is provided in **Table 2**.

Correlation between mRNA and protein expression

We found that only CYP2A6 ($r=0.395$), CYP1A2 ($r=0.271$), CYP3A4 ($r=0.577$) and CYP2B6 mRNA ($r=0.431$) levels showed a correlation which was statistically significant (**Figure 4 (a-j)**). There was some correlation ($r<0.200$) between CYP2C9 and CYP2C19 mRNA and protein level but did not reach statistical significance. All other isoforms showed a poor correlation between mRNA and protein which was again not significant ($p>0.1$). A detailed correlation table is provided in **Table 2**.

DISCUSSION

Studies involving drug metabolizing enzymes (DMEs) are critical for evaluating drug efficacy and safety. Thus, an understanding of the biological variation of these DMEs could provide useful insight into pharmacokinetics or drug interaction potential of new chemical entities. Conventional targeted methods for protein quantification rely on the use of 1 or 2 unique peptides per protein. The data are further acquired using MRM, and a ratio of unlabeled (light) to labeled peptide (heavy) is used to determine the level of that peptide present in a digested sample (23). However, a researcher would require a separate isotope-labeled peptide for each target peptide, and this leads to a significant cost. These high-purity isotope-labeled synthetic heavy peptides cost anywhere from \$700 to \$1,000 for ~1 mg of peptides with concentration certification by amino acid analysis. For the development of small numbers of assays, this is a reasonable investment. However, the cost can be prohibitive when the numbers of proteins of interest exceed a limited number or for experiments intended for biomarker discovery. In drug metabolism, usually only high abundance CYPs are measured using targeted approach and the low abundance CYPs or other microsomal enzymes are neglected.

SWATH-MS has found an important application is the discovery of novel biomarkers (24, 25). Drawbacks of traditional MRM based approaches of protein quantification make it unsuitable for the research area (26). Ortea and colleagues used SWATH-MS for mining potential protein biomarkers of lung adenocarcinoma (27). Quantitative mapping of ErbB2, a receptor tyrosine kinase biomarker was recently demonstrated using SWATH-MS approach and highlights the application of technique (28).

Pressure cycling technology (PCT) based digestion along with SWATH-MS acquisition (PCT-SWATH) was used to reduce the sample preparation time (17). The typical incubation time for digestion with trypsin is time-consuming and range from 12-18 h (usually overnight). PCT enhances proteolytic action by inducing denaturation of proteins, therefore allowing better access to trypsin for cleavage sites (29). This also significantly reduces the digestion and overall sample preparation time.

Skyline is a popular tool used for targeted data analyses of mass spectrometry data. It supports spectral library generation as well as data analyses of SWATH-MS files (20). Like other LFQ approaches, it relies on retention time (RT) alignment between the data files and the spectral library. A commonly used method for retention time normalization relies on the use of synthetic iRT peptides which are spiked to every sample before analysis and has few drawbacks (30). Complex and widely different matrix might significantly affect the ionization and retention time reproducibility of these peptides within their LC retention time space and would compromise the evaluation of peptide peak area and FDR calculation in the case of a low signal within background noise. After thorough literature review and taking into consideration the costs associated with insertion of standards for RT normalization, we used the method suggested by Parker et al. (2016) and Nakamura et al. (2016) in recent articles (21, 30). A retention time predictor was created from endogenous peptides present in our sample using Skyline allowing integration of fragment intensity over different batches.

Correlation between mRNA expression, protein abundance, and functional activity are not always tight due to complex regulation mechanisms involving pre and post-transcriptional events, translational modifications and subsequent protein localization

events (31). Among other mechanisms, stability and half-life of protein and mRNA in their *in vitro* conditions also contribute to poor correlation (31). Similar mechanisms also dictate the correlation between protein and activity. Further, a poor selection of peptides for quantification can also affect the outcome of correlation analysis.

In this work, we found that protein levels are better surrogates for estimating the activity of major xenobiotic CYP isoforms than mRNA. Additionally, we observed that both protein, as well as mRNA, can be used to access the functional activity of CYP2A6, CYP1A2, CYP2B6, CYP2C8 and CYP3A4. Interestingly, apart from CYP3A4, CYP1A2, CYP2B6 and CYP2A6, protein expression of none of the other six CYP isoforms showed a significant correlation with the mRNA expression. Pre-translational regulation of CYP1A2, CYP3A4 and CYP2B6 expression has already been reported to be responsible for good correlation between mRNA expression and enzyme activity (32).

Al Koudsi et al. found that CYP2A6 protein determined by Western blotting significantly correlate with nicotine C-oxidation activity in human livers (33). We also observed a significant correlation between protein, activity, and mRNA for CYP2A6. The correlation was in general stronger between activity and protein expression, followed by activity and mRNA. Similar correlations have been published previously for microsomal CYP2A6 (33).

CYP3A activity for testosterone and midazolam hydroxylation correlated strongly with mRNA as well as protein. There was a good correlation between CYP3A4 mRNA, protein, and activity suggesting that both protein, as well as mRNA could be used to estimate the functional activity of this enzyme. Similar results on the correlation of CYP3A4 activity with mRNA and protein has been previously published (34). CYP3A5 protein expression

correlated strongly with midazolam and as well as testosterone hydroxylation ($r > 0.600$, $p < 0.05$). In contrast, the correlation between CYP3A5 mRNA and activity was poor for testosterone activity ($r < 0.188$, $p > 0.10$) while it was significant for midazolam activity ($r = 0.330$, $p < 0.01$). There was no relationship observed between protein levels and mRNA ($r < 0.100$, $p > 0.10$).

As previously reported, CYP2E1 activity correlated strongly with protein level but not with the mRNA expression (34, 35). This again highlights the role of post-translational modifications of protein on the enzyme activity. Conversely, a pharmacogenomics study of CYP1A2 in human liver samples ($n = 150$) found that mRNA and protein correlated with the functional activity of this enzyme (36). The results are in line with the significant correlation observed for CYP1A2 in our studies also.

CYP2C9 metabolic activity was shown to have a higher correlation with protein than mRNA (32). This agrees with our findings for strong CYP2C9 protein and activity correlation ($r = 0.620$, $p < 0.001$). However, we insignificant correlation for mRNA with CYP2C9 activity and protein levels. Interestingly, CYP2B6 and CYP2C8 activity showed a better correlation with mRNA than protein levels. It was not unexpected as Ohtsuki and colleagues have earlier reported that mRNA is a better surrogate than protein level for prediction of CYP2B6 activity (3). For CYP2B6, our data agree with finding as we also found a strong correlation ($r = 0.729$, $p < 0.001$) between mRNA and activity while there was a moderate correlation ($r = 0.533$, $p < 0.001$) between activity and protein. The correlation between CYP2B6 protein and mRNA was also moderate ($r = 0.431$, $p < 0.001$). Genetic polymorphisms were previously suggested to be responsible for such correlation (Spearman $r = 0.44$) between CYP2B6 mRNA and protein expression (37). Studies have

also reported that the genetic polymorphism in CYP2C8, CYP2C19, and CYP2D6 account for major variability in the activity of these enzymes (38). Protein stability in isolated microsomes could also be attributed to poor correlation with mRNA.

Rodríguez-Antona et al. observed a moderate correlation between CYP2C8 protein abundance and enzyme activity (39). CYP2C8 activity correlated moderately with protein ($r=0.331$, $p<0.01$) but a strong correlation was observed with mRNA ($r=0.524$, $p<0.01$) suggesting the role of post-translational modifications. A significant correlation between mRNA and activity for CYP2C8 and CYP2D6 suggests the utility of mRNA for studying the functional activity of these CYP isoforms. Poor correlation of CYP2C19 mRNA and activity suggest towards major post-translational changes influencing its activity in human and makes a case for use of protein levels to predict the activity for this enzyme.

CONCLUSIONS

SWATH-MS exemplify a powerful LFQ technique, which addresses the limitations of the shotgun and targeted proteomics to provide a permanent digital repository of all peptides present in a sample. This method can serve as a valuable post hoc tool for studying new hypothesis and ideas without the need to re-acquire data. To the best of our knowledge, this is the first report demonstrating the use of SWATH-MS and pressure-cycling based digestion for relative quantification of drug metabolizing enzymes in human liver microsomes and the correlation with their functional activity and mRNA expression. The studies also highlight the importance of protein levels for prediction of the functional activity of CYP enzymes.

Financial support

This work was partly supported by National Institutes of Health grants to Fatemeh Akhlaghi [grant numbers R15-GM101599, UH3-TR000963]. Authors also acknowledge the use of equipment and services available through the RI-INBRE Centralized Research Core Facility which is supported by the Institutional Development Award (IDeA) Network for Biomedical Research Excellence from the National Institute of General Medical Sciences of the National Institutes of Health [grant number P20GM103430].

Acknowledgements

The authors would like to thank Prof. Ruedi Aebersold and Dr. Tiannan Guo at Institute of Molecular Systems Biology, ETH Zurich, Switzerland for their insightful guidance during the work. The suggestions from Dr. Vera Gross at Pressure Biosciences Inc., South Easton MA are also acknowledged. We sincerely thank Dr. Hui Zhang from Pfizer Groton Central Research (Groton, CT) for his helpful suggestions about this project. We also thank Prof. Bhagwat Prasad and Dr. Deepak Kumar Bhatt at University of Washington for their valuable comments to improve this work.

Conflict of Interest/Disclosure

Brigitte L. Simons was actively employed by SCIEX, Canada at the time when this work was conducted as well at the date of submission of this manuscript.

The authors would also like to highlight that this research was presented at 47th Gordon Research Conference for Drug Metabolism at Holderness, New Hampshire in July 2017.

References

1. Wienkers, L. C.; Heath, T. G., Predicting in vivo drug interactions from in vitro drug discovery data. *Nat Rev Drug Discov* **2005**, 4, (10), 825-33.
2. Sadler, N. C.; Nandhikonda, P.; Webb-Robertson, B. J.; Ansong, C.; Anderson, L. N.; Smith, J. N.; Corley, R. A.; Wright, A. T., Hepatic Cytochrome P450 Activity, Abundance, and Expression Throughout Human Development. *Drug Metab Dispos* **2016**, 44, (7), 984-91.
3. Ohtsuki, S.; Schaefer, O.; Kawakami, H.; Inoue, T.; Liehner, S.; Saito, A.; Ishiguro, N.; Kishimoto, W.; Ludwig-Schwellinger, E.; Ebner, T.; Terasaki, T., Simultaneous absolute protein quantification of transporters, cytochromes P450, and UDP-glucuronosyltransferases as a novel approach for the characterization of individual human liver: comparison with mRNA levels and activities. *Drug Metab Dispos* **2012**, 40, (1), 83-92.
4. Roymans, D.; Annaert, P.; Van Houdt, J.; Weygers, A.; Noukens, J.; Sensenhauser, C.; Silva, J.; Van Looveren, C.; Hendrickx, J.; Mannens, G.; Meuldermans, W., Expression and induction potential of cytochromes P450 in human cryopreserved hepatocytes. *Drug Metab Dispos* **2005**, 33, (7), 1004-16.
5. Aebersold, R.; Burlingame, A. L.; Bradshaw, R. A., Western blots versus selected reaction monitoring assays: time to turn the tables? *Mol Cell Proteomics* **2013**, 12, (9), 2381-2.
6. Murphy, R. M.; Lamb, G. D., Important considerations for protein analyses using antibody based techniques: down-sizing Western blotting up-sizes outcomes. *J Physiol* **2013**, 591, (23), 5823-31.

7. Qiu, X.; Zhang, H.; Lai, Y., Quantitative targeted proteomics for membrane transporter proteins: method and application. *AAPS J* **2014**, 16, (4), 714-26.
8. Burgess, M. W.; Keshishian, H.; Mani, D. R.; Gillette, M. A.; Carr, S. A., Simplified and efficient quantification of low-abundance proteins at very high multiplex via targeted mass spectrometry. *Mol Cell Proteomics* **2014**, 13, (4), 1137-49.
9. Yan, T.; Gao, S.; Peng, X.; Shi, J.; Xie, C.; Li, Q.; Lu, L.; Wang, Y.; Zhou, F.; Liu, Z.; Hu, M., Significantly decreased and more variable expression of major CYPs and UGTs in liver microsomes prepared from HBV-positive human hepatocellular carcinoma and matched pericarcinomatous tissues determined using an isotope label-free UPLC-MS/MS method. *Pharm Res* **2015**, 32, (3), 1141-57.
10. Achour, B.; Russell, M. R.; Barber, J.; Rostami-Hodjegan, A., Simultaneous quantification of the abundance of several cytochrome P450 and uridine 5'-diphosphoglucuronosyltransferase enzymes in human liver microsomes using multiplexed targeted proteomics. *Drug Metab Dispos* **2014**, 42, (4), 500-10.
11. Fallon, J. K.; Neubert, H.; Hyland, R.; Goosen, T. C.; Smith, P. C., Targeted quantitative proteomics for the analysis of 14 UGT1As and -2Bs in human liver using NanoUPLC-MS/MS with selected reaction monitoring. *J Proteome Res* **2013**, 12, (10), 4402-13.
12. Groer, C.; Busch, D.; Patrzyk, M.; Beyer, K.; Busemann, A.; Heidecke, C. D.; Drozdik, M.; Siegmund, W.; Oswald, S., Absolute protein quantification of clinically relevant cytochrome P450 enzymes and UDP-glucuronosyltransferases by mass spectrometry-based targeted proteomics. *J Pharm Biomed Anal* **2014**, 100, 393-401.

13. Wang, L.; Collins, C.; Kelly, E. J.; Chu, X.; Ray, A. S.; Salphati, L.; Xiao, G.; Lee, C.; Lai, Y.; Liao, M.; Mathias, A.; Evers, R.; Humphreys, W.; Hop, C. E.; Kumer, S. C.; Unadkat, J. D., Transporter Expression in Liver Tissue from Subjects with Alcoholic or Hepatitis C Cirrhosis Quantified by Targeted Quantitative Proteomics. *Drug Metab Dispos* **2016**, 44, (11), 1752-1758.
14. Neilson, K. A.; Ali, N. A.; Muralidharan, S.; Mirzaei, M.; Mariani, M.; Assadourian, G.; Lee, A.; van Sluyter, S. C.; Haynes, P. A., Less label, more free: approaches in label-free quantitative mass spectrometry. *Proteomics* **2011**, 11, (4), 535-53.
15. Rosenberger, G.; Koh, C. C.; Guo, T.; Rost, H. L.; Kouvonen, P.; Collins, B. C.; Heusel, M.; Liu, Y.; Caron, E.; Vichalkovski, A.; Faini, M.; Schubert, O. T.; Faridi, P.; Ebhardt, H. A.; Matondo, M.; Lam, H.; Bader, S. L.; Campbell, D. S.; Deutsch, E. W.; Moritz, R. L.; Tate, S.; Aebersold, R., A repository of assays to quantify 10,000 human proteins by SWATH-MS. *Sci Data* **2014**, 1, 140031.
16. Yalcin, E. B.; More, V.; Neira, K. L.; Lu, Z. J.; Cherrington, N. J.; Slitt, A. L.; King, R. S., Downregulation of sulfotransferase expression and activity in diseased human livers. *Drug Metab Dispos* **2013**, 41, (9), 1642-50.
17. Guo, T.; Kouvonen, P.; Koh, C. C.; Gillet, L. C.; Wolski, W. E.; Rost, H. L.; Rosenberger, G.; Collins, B. C.; Blum, L. C.; Gillessen, S.; Joerger, M.; Jochum, W.; Aebersold, R., Rapid mass spectrometric conversion of tissue biopsy samples into permanent quantitative digital proteome maps. *Nat Med* **2015**, 21, (4), 407-13.
18. Gillet, L. C.; Navarro, P.; Tate, S.; Rost, H.; Selevsek, N.; Reiter, L.; Bonner, R.; Aebersold, R., Targeted data extraction of the MS/MS spectra generated by data-

independent acquisition: a new concept for consistent and accurate proteome analysis. *Mol Cell Proteomics* **2012**, 11, (6), O111 016717.

19. Lange, V.; Picotti, P.; Domon, B.; Aebersold, R., Selected reaction monitoring for quantitative proteomics: a tutorial. *Mol Syst Biol* **2008**, 4, 222.

20. MacLean, B.; Tomazela, D. M.; Shulman, N.; Chambers, M.; Finney, G. L.; Frewen, B.; Kern, R.; Tabb, D. L.; Liebler, D. C.; MacCoss, M. J., Skyline: an open source document editor for creating and analyzing targeted proteomics experiments. *Bioinformatics* **2010**, 26, (7), 966-8.

21. Nakamura, K.; Hirayama-Kurogi, M.; Ito, S.; Kuno, T.; Yoneyama, T.; Obuchi, W.; Terasaki, T.; Ohtsuki, S., Large-scale multiplex absolute protein quantification of drug-metabolizing enzymes and transporters in human intestine, liver, and kidney microsomes by SWATH-MS: Comparison with MRM/SRM and HR-MRM/PRM. *Proteomics* **2016**, 16, (15-16), 2106-17.

22. Guengerich, F. P., Cytochrome P450s and other enzymes in drug metabolism and toxicity. *AAPS J* **2006**, 8, (1), E101-11.

23. Gillette, M. A.; Carr, S. A., Quantitative analysis of peptides and proteins in biomedicine by targeted mass spectrometry. *Nat Methods* **2013**, 10, (1), 28-34.

24. Liu, Y.; Huttenhain, R.; Collins, B.; Aebersold, R., Mass spectrometric protein maps for biomarker discovery and clinical research. *Expert Rev Mol Diagn* **2013**, 13, (8), 811-25.

25. Sajic, T.; Liu, Y.; Aebersold, R., Using data-independent, high-resolution mass spectrometry in protein biomarker research: perspectives and clinical applications. *Proteomics Clin Appl* **2015**, 9, (3-4), 307-21.

26. Doerr, A., DIA mass spectrometry. *Nat Meth* **2015**, 12, (1), 35-35.
27. Ortea, I.; Rodriguez-Ariza, A.; Chicano-Galvez, E.; Arenas Vacas, M. S.; Jurado Gamez, B., Discovery of potential protein biomarkers of lung adenocarcinoma in bronchoalveolar lavage fluid by SWATH MS data-independent acquisition and targeted data extraction. *J Proteomics* **2016**, 138, 106-14.
28. Held, J. M.; Schilling, B.; D'Souza, A. K.; Srinivasan, T.; Behring, J. B.; Sorensen, D. J.; Benz, C. C.; Gibson, B. W., Label-Free Quantitation and Mapping of the ErbB2 Tumor Receptor by Multiple Protease Digestion with Data-Dependent (MS1) and Data-Independent (MS2) Acquisitions. *Int J Proteomics* **2013**, 2013, 791985.
29. Freeman, E.; Ivanov, A. R., Proteomics under pressure: development of essential sample preparation techniques in proteomics using ultrahigh hydrostatic pressure. *J Proteome Res* **2011**, 10, (12), 5536-46.
30. Parker, S. J.; Rost, H.; Rosenberger, G.; Collins, B. C.; Malmstrom, L.; Amodei, D.; Venkatraman, V.; Raedschelders, K.; Van Eyk, J. E.; Aebersold, R., Identification of a Set of Conserved Eukaryotic Internal Retention Time Standards for Data-independent Acquisition Mass Spectrometry. *Mol Cell Proteomics* **2015**, 14, (10), 2800-13.
31. Maier, T.; Guell, M.; Serrano, L., Correlation of mRNA and protein in complex biological samples. *FEBS Lett* **2009**, 583, (24), 3966-73.
32. Rodriguez-Antona, C.; Donato, M. T.; Pareja, E.; Gomez-Lechon, M. J.; Castell, J. V., Cytochrome P-450 mRNA expression in human liver and its relationship with enzyme activity. *Arch Biochem Biophys* **2001**, 393, (2), 308-15.

33. Al Koudsi, N.; Hoffmann, E. B.; Assadzadeh, A.; Tyndale, R. F., Hepatic CYP2A6 levels and nicotine metabolism: impact of genetic, physiological, environmental, and epigenetic factors. *Eur J Clin Pharmacol* **2010**, 66, (3), 239-51.
34. Sumida, A.; Kinoshita, K.; Fukuda, T.; Matsuda, H.; Yamamoto, I.; Inaba, T.; Azuma, J., Relationship between mRNA levels quantified by reverse transcription-competitive PCR and metabolic activity of CYP3A4 and CYP2E1 in human liver. *Biochem Biophys Res Commun* **1999**, 262, (2), 499-503.
35. Powell, H.; Kitteringham, N. R.; Pirmohamed, M.; Smith, D. A.; Park, B. K., Expression of cytochrome P4502E1 in human liver: assessment by mRNA, genotype and phenotype. *Pharmacogenetics* **1998**, 8, (5), 411-21.
36. Klein, K.; Winter, S.; Turpeinen, M.; Schwab, M.; Zanger, U. M., Pathway-Targeted Pharmacogenomics of CYP1A2 in Human Liver. *Front Pharmacol* **2010**, 1, 129.
37. Hesse, L. M.; He, P.; Krishnaswamy, S.; Hao, Q.; Hogan, K.; von Moltke, L. L.; Greenblatt, D. J.; Court, M. H., Pharmacogenetic determinants of interindividual variability in bupropion hydroxylation by cytochrome P450 2B6 in human liver microsomes. *Pharmacogenetics* **2004**, 14, (4), 225-38.
38. Zhou, S. F.; Liu, J. P.; Chowbay, B., Polymorphism of human cytochrome P450 enzymes and its clinical impact. *Drug Metab Rev* **2009**, 41, (2), 89-295.
39. Rodriguez-Antona, C.; Niemi, M.; Backman, J. T.; Kajosaari, L. I.; Neuvonen, P. J.; Robledo, M.; Ingelman-Sundberg, M., Characterization of novel CYP2C8 haplotypes and their contribution to paclitaxel and repaglinide metabolism. *Pharmacogenomics J* **2008**, 8, (4), 268-77.

Tables

Table 1: Brief demographic summary of donors

Total number of donors (Male/Female)	78 (41, 37)
Ethnicity (C/AA/H)	66, 9, 3
	Mean \pm SD
Age (years)	51.5 \pm 12.9
Weight (kg)	90.6 \pm 27.2
Height (cm)	169.6 \pm 10.9

C: Caucasian, AA: African-American, H: Hispanic

Table 2: Correlation* between protein levels and activity, mRNA and activity, mRNA and protein

	Protein and activity			mRNA and activity			mRNA and protein		
	Sample size	Pearson Correlation Coefficient (r)	p-value	Sample size	Pearson Correlation Coefficient (r)	p-value	Sample size	Pearson Correlation Coefficient (r)	p-value
CYP1A2	69	0.720	<0.001	67	0.426	<0.001	76	0.271	<0.05
CYP2A6	67	0.767	<0.001	67	0.461	<0.001	78	0.395	<0.001
CYP3A4							78	0.577	<0.001
CYP3A4-M	67	0.652	<0.001	67	0.647	<0.001			
CYP3A4-T	69	0.725	<0.001	69	0.652	<0.001			
CYP3A5							78	0.058	0.616
CYP3A5-M	67	0.670	<0.001	67	0.330	0.006			
CYP3A5-T	69	0.734	<0.001	69	0.188	0.122			
CYP2B6	67	0.533	<0.001	63	0.729	<0.001	73	0.431	<0.001
CYP2C8	62	0.331	<0.01	66	0.524	<0.001	77	0.121	0.295
CYP2C9	67	0.620	<0.001	66	0.043	0.728	77	0.185	0.106
CYP2C19	65	0.314	<0.05	69	-0.067	0.584	78	0.197	0.084
CYP2D6	67	0.346	<0.01	67	0.306	0.012	78	0.110	0.341
CYP2E1	67	0.704	<0.001	67	-0.032	0.800	78	0.111	0.334

*All values were natural logarithm (ln) transformed before the correlation analysis. M: Midazolam 1-hydroxylation, T- Testosterone 6 β -hydroxylation

Figure legends

Figure 1 : Identified proteins and peptides at 1% false discovery rate (FDR). The graph depicts identification of 1855 proteins and 25681 peptides in the spectral library at 1% FDR.

Figure 2 (a-l): Correlation plots for relative protein expression and enzyme activity. Protein abundance values were expressed relative to APLDNDIGVSEATR peptide from *E. coli* β -galactosidase. The enzyme activity was represented as CYP-specific product formation/min/mg protein. All values are natural logarithm (ln) transformed and Pearson correlation analysis was performed.

Figure 3 (a-l): Correlation plots for mRNA and enzyme activity. Messenger RNA (mRNA) was expressed relative to β -actin. Protein abundance values were expressed relative to APLDNDIGVSEATR peptide from *E. coli* β -galactosidase. The enzyme activity was represented as CYP-specific product formation/min/mg protein. All values were natural logarithm (ln) transformed and Pearson correlation analysis was performed.

Figure 4 (a-j): Correlation plots for mRNA and protein expression. Messenger RNA (mRNA) was expressed relative to β -actin. Protein abundance values were expressed relative to APLDNDIGVSEATR peptide from *E. coli* β -galactosidase. All values are natural logarithm (ln) transformed and Pearson correlation analysis was performed.

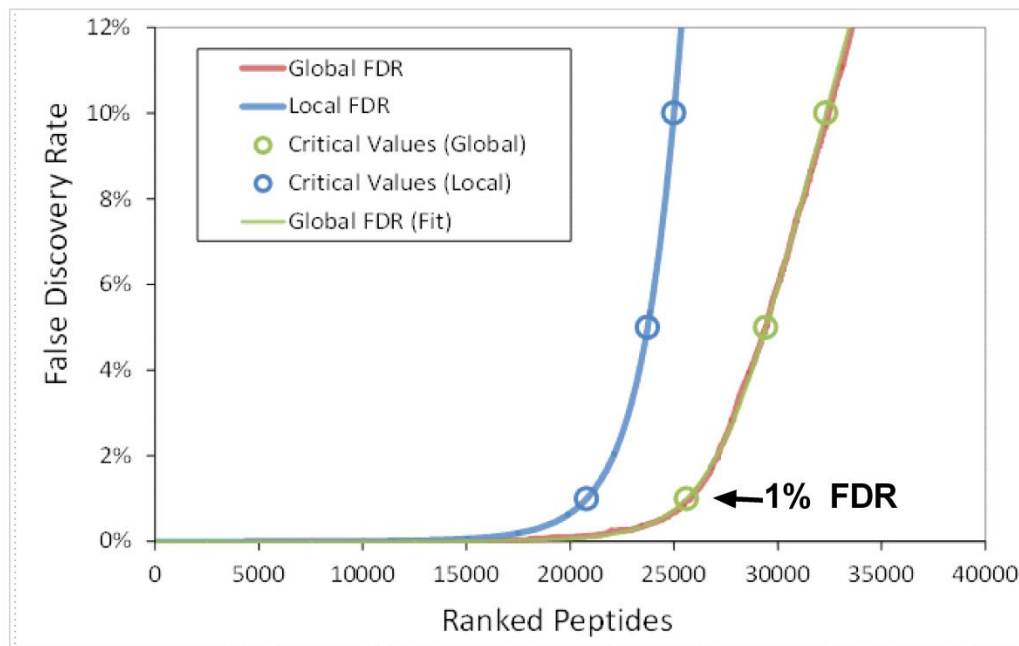


Figure 1: Identified proteins and peptides at 1% false discovery rate (FDR). The graph depicts identification of 1855 proteins and 25681 peptides in the spectral library at 1% FDR.

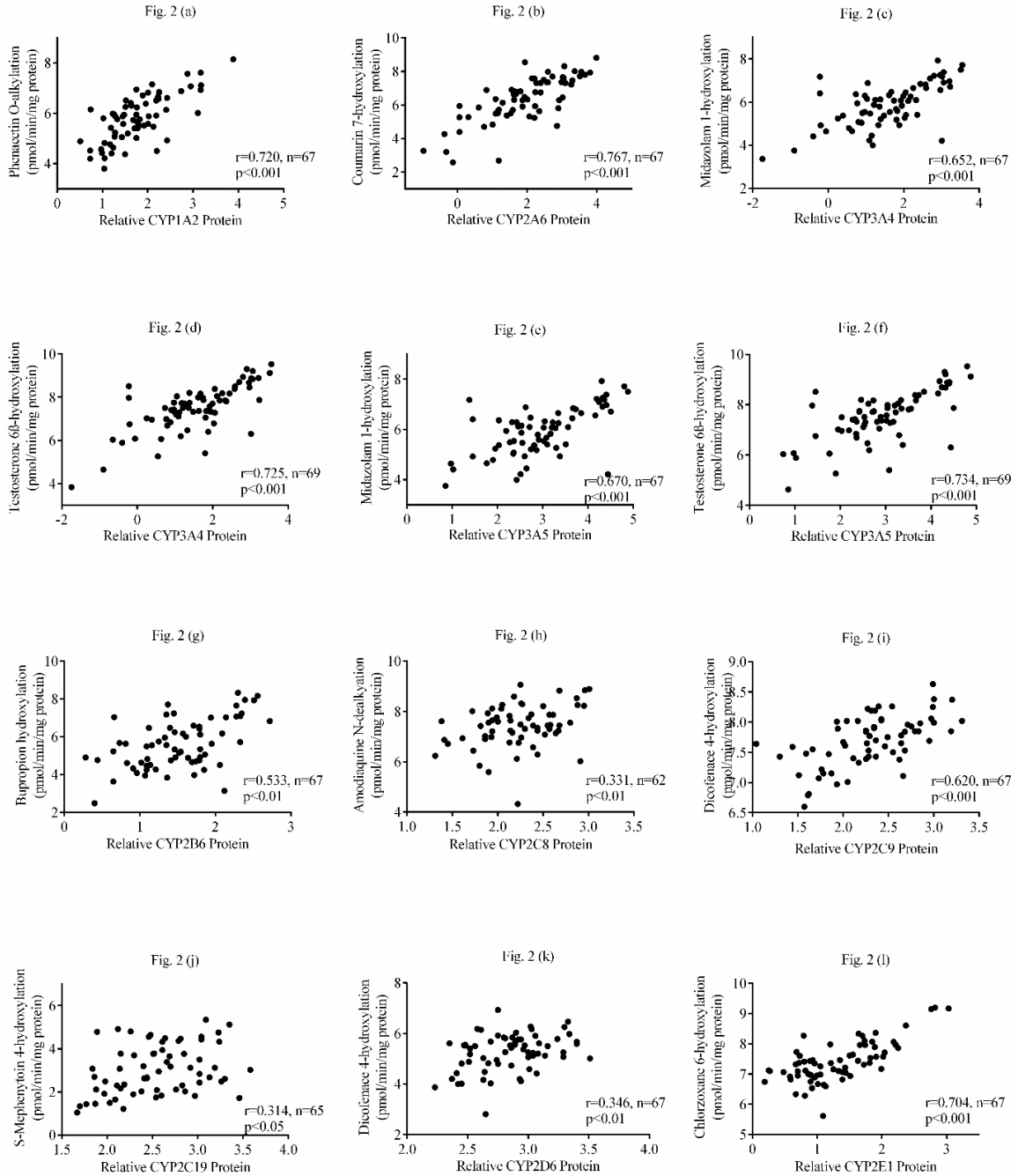


Figure 2 (a-l): Correlation plots for relative protein expression and enzyme activity. Protein abundance values were expressed relative to APLDNDIGVSEATR peptide from *E. coli* β -galactosidase. The enzyme activity was represented as CYP-specific product formation/min/mg protein. All values were natural logarithm (ln) transformed before Pearson correlation analysis.

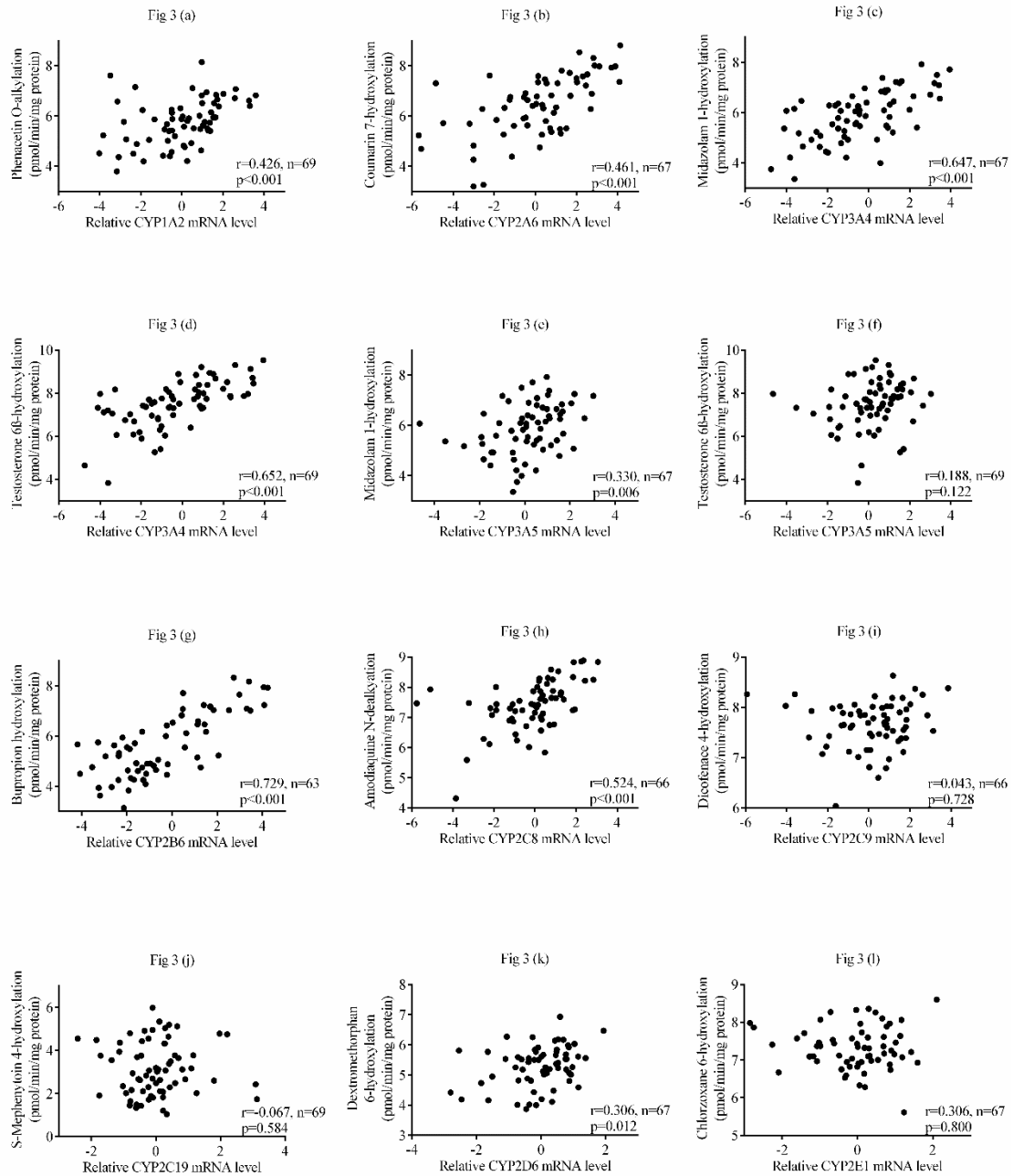


Figure 3 (a-l): Correlation plots for mRNA and enzyme activity. Messenger RNA (mRNA) was expressed relative to GAPDH and β -actin. Protein abundance values were expressed relative to APLDNDIGVSEATR peptide from *E. coli* β -galactosidase. The enzyme activity was represented as CYP-specific product formation/min/mg protein. All values were natural logarithm (ln) transformed before Pearson correlation analysis.

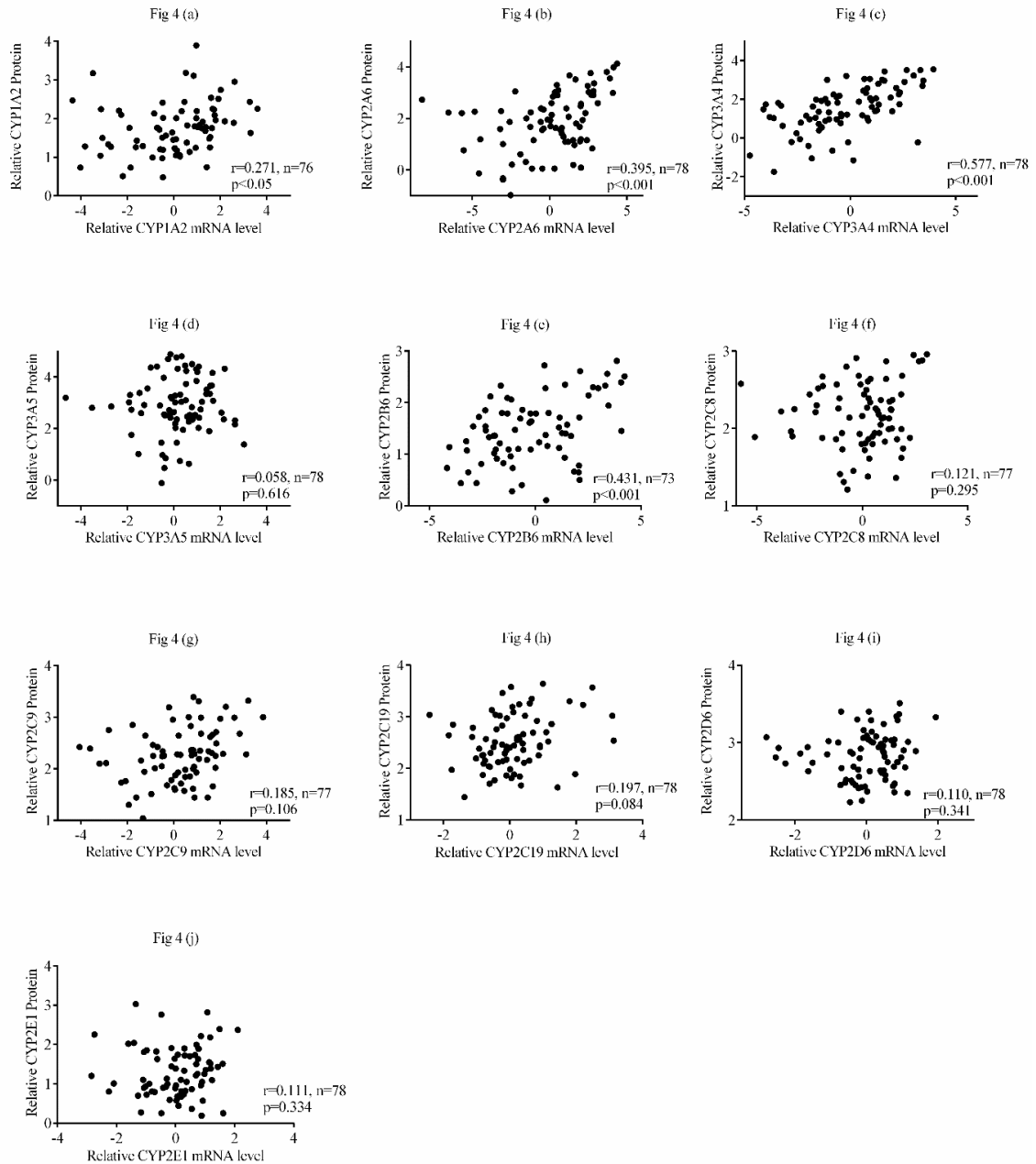
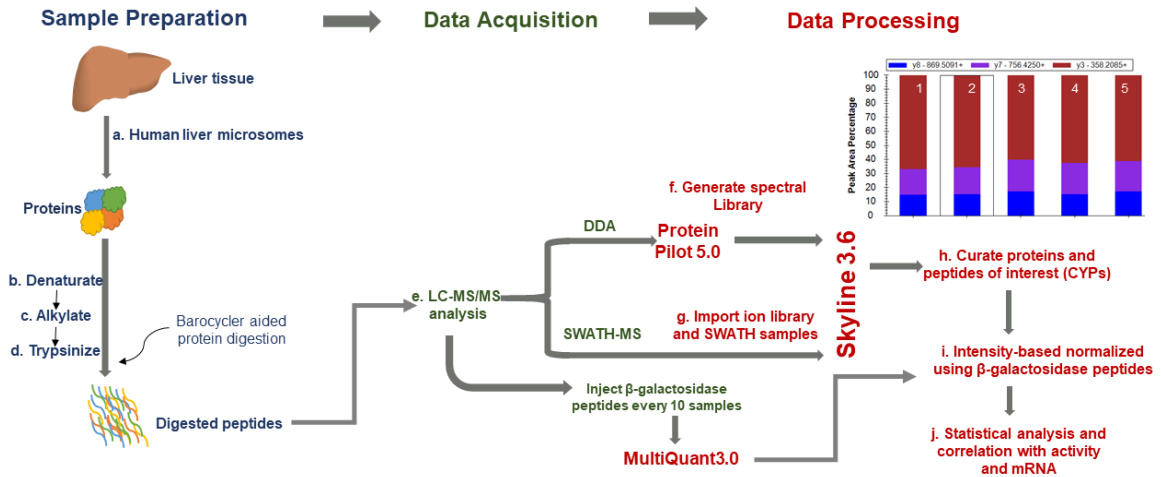


Figure 4 (a-j): Correlation plots for mRNA and protein expression. Messenger RNA (mRNA) was expressed relative to β -actin. Protein abundance values were expressed relative to APLDNDIGVSEATR peptide from *E. coli* β -galactosidase. All values are natural logarithm (ln) transformed before Pearson correlation analysis.



Abstract graphic. Liver microsomes were prepared from human liver samples and trypsin-based digestion was carried out on samples after denaturation and alkylation. Furthermore, tryptic peptides were analyzed using LC-MS/MS in data dependent and SWATH-MS mode. The in-house spectral library was prepared from the using Protein Pilot and targeted data extraction for CYPs was performed in SWATH files using Skyline. Total intensity of CYPs in each batch was normalized using average intensity of β -galactosidase for that batch. Subsequently, the relative protein abundance protein values were correlated with enzymatic activity and mRNA.

Supporting Information

Multiplex and Label-Free Relative Quantification Approach for Studying Protein Abundance of Drug Metabolizing Enzymes in Human Liver Microsomes Using SWATH-MS

Rohitash Jamwal¹, Benjamin J. Barlock¹, Sravani Adusumalli¹, Ken Ogasawara¹, Brigitte L. Simons², Fatemeh Akhlaghi^{1*}

¹ Clinical Pharmacokinetics Research Laboratory, Department of Biomedical and Pharmaceutical Sciences, University of Rhode Island, Kingston, 02881, RI, USA

² SCIEX, 71 Four Valley Dr., Concord, Ontario, L4K4V8, Canada

Author for correspondence:

*Fatemeh Akhlaghi, Ph.D., PharmD

Clinical Pharmacokinetics Research Laboratory, Department of Biomedical and Pharmaceutical Sciences, University of Rhode Island, 495A College of Pharmacy, 7 Greenhouse Road, Kingston, RI 02881, United States.

Email address: fatemeh@uri.edu

Table of Contents:

S-2: Supporting Information I: Skyline peptide and transition settings, peak scoring model

S-13: Supplementary information II: List of precursor and product ions for major drug metabolism enzymes quantified using the current method

S-17: Supplementary information III: Quantification of hepatic CYP mRNA expression

S-19: Supplementary information IV: Enzyme assay conditions as provided by Seksui Xenotech LLC, Kansas City, MO

Supplementary information I:

Skyline peptide and transition setting, peak scoring model.

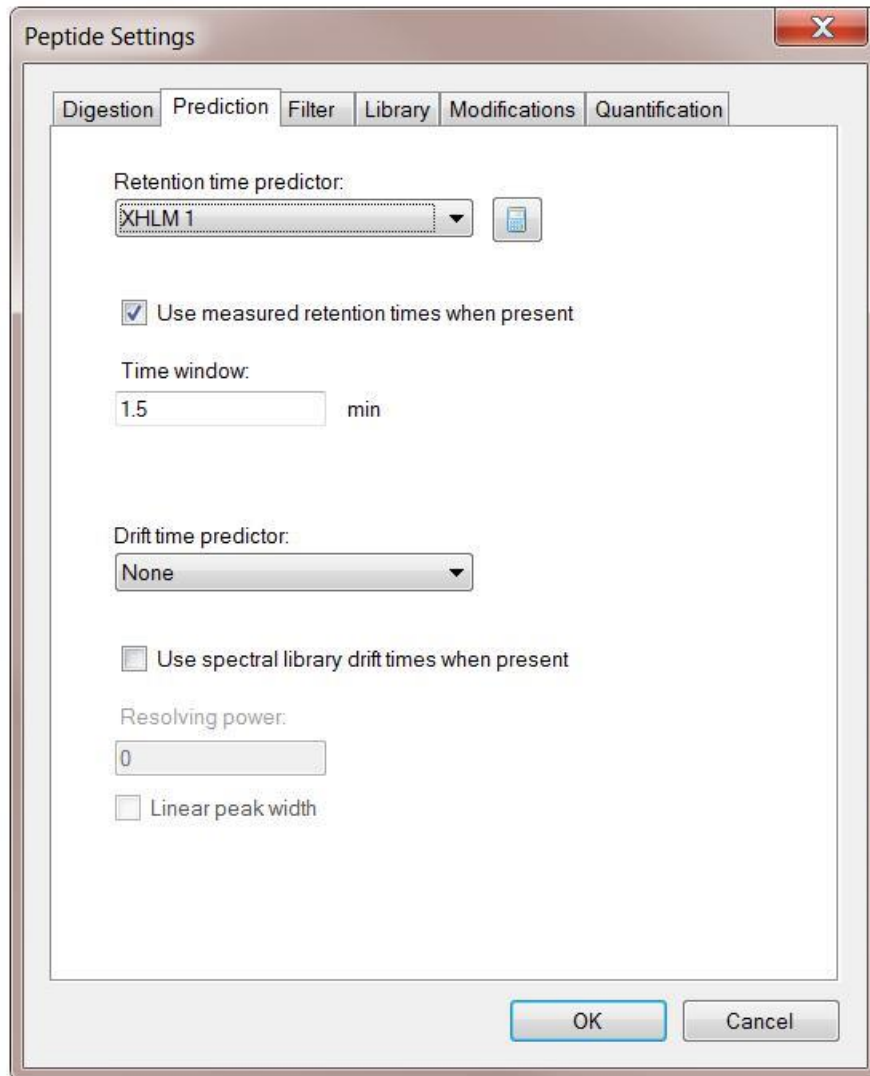
The image shows a software dialog box titled "Peptide Settings". At the top, there are five tabs: "Digestion", "Prediction", "Filter", "Library", "Modifications", and "Quantification". The "Digestion" tab is currently selected. Below the tabs, there are four settings, each with a dropdown menu:

- Enzyme: Trypsin [KR | P]
- Max missed cleavages: 0
- Background proteome: Human
- Enforce peptide uniqueness by: Proteins

At the bottom right of the dialog box, there are two buttons: "OK" and "Cancel".

Supplementary information I:

Skyline peptide and transition setting, peak scoring model.



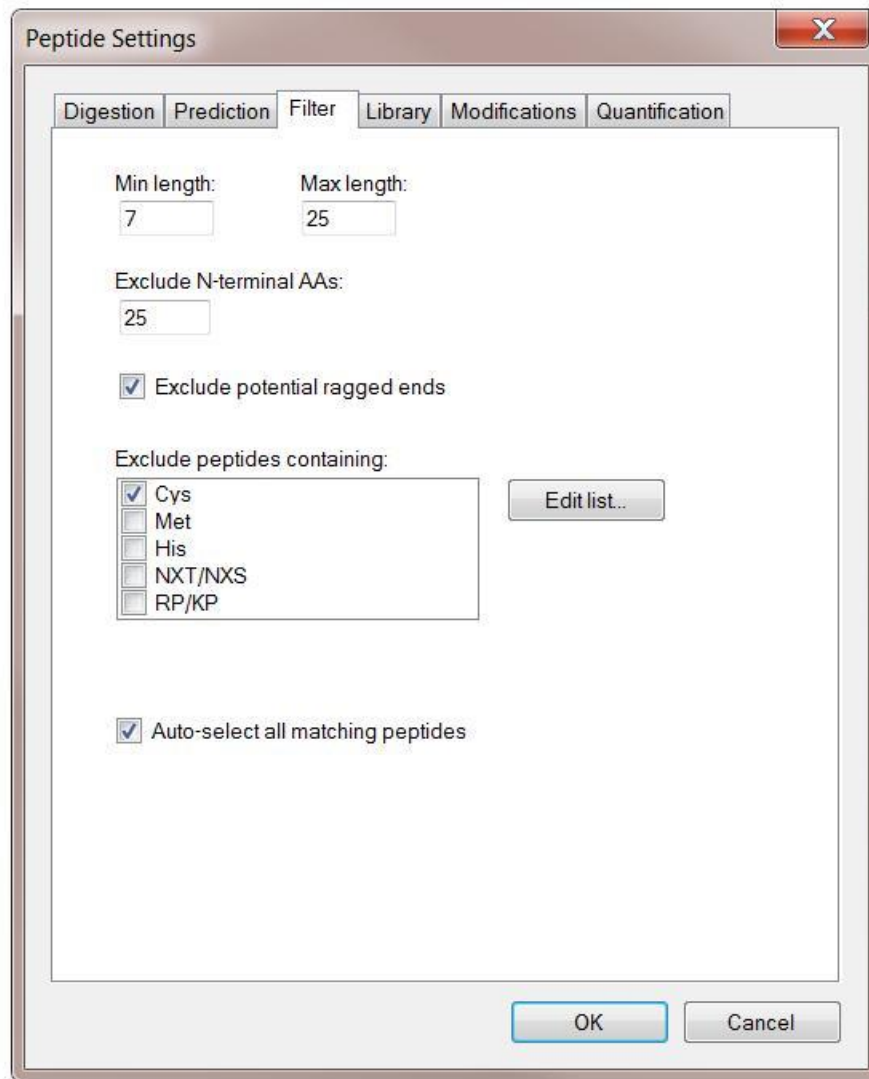
The image shows a software dialog box titled "Peptide Settings" with a close button (X) in the top right corner. The dialog has several tabs: "Digestion", "Prediction", "Filter", "Library", "Modifications", and "Quantification". The "Prediction" tab is currently selected. The settings within this tab are as follows:

- Retention time predictor:** A dropdown menu is set to "XHLM 1". To its right is a small icon of a document with a blue arrow pointing to it.
- Use measured retention times when present**
- Time window:** A text input field contains "1.5" followed by the unit "min".
- Drift time predictor:** A dropdown menu is set to "None".
- Use spectral library drift times when present**
- Resolving power:** A text input field contains "0".
- Linear peak width**

At the bottom right of the dialog, there are two buttons: "OK" and "Cancel".

Supplementary information I:

Skyline peptide and transition setting, peak scoring model.



The image shows a software dialog box titled "Peptide Settings" with a close button (X) in the top right corner. The dialog has five tabs: "Digestion", "Prediction", "Filter" (which is selected), "Library", and "Quantification".

Under the "Filter" tab, the following settings are visible:

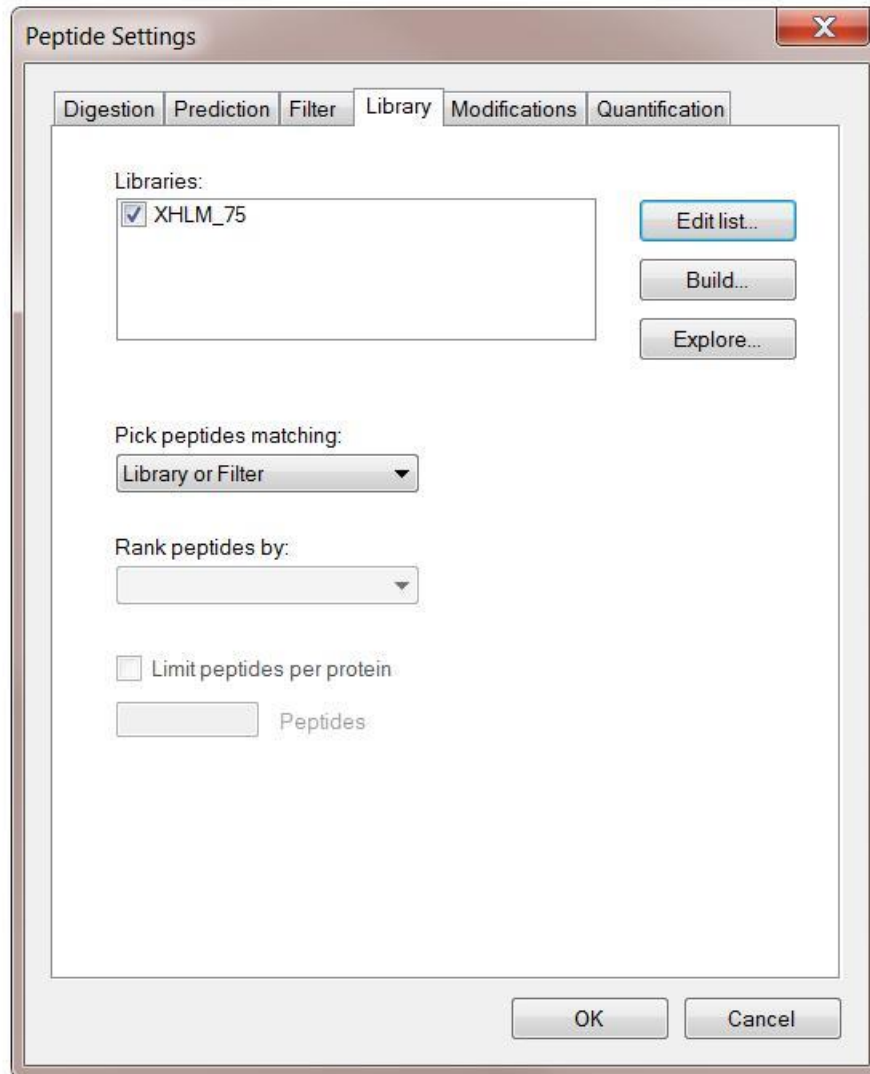
- Min length:
- Max length:
- Exclude N-terminal AAs:
- Exclude potential ragged ends
- Exclude peptides containing:
 - Cys
 - Met
 - His
 - NXT/NXS
 - RP/KP
- Auto-select all matching peptides

An "Edit list.." button is located to the right of the "Exclude peptides containing:" list.

At the bottom of the dialog are "OK" and "Cancel" buttons.

Supplementary information I:

Skyline peptide and transition setting, peak scoring model.



Supplementary information I:

Skyline peptide and transition setting, peak scoring model.

Peptide Settings

Digestion Prediction Filter Library Modifications Quantification

Structural modifications:

- Carbamidomethyl (C)
- Oxidation (M)
- Acetyl (N-term)
- Glu->pyro-Glu (N-term E)
- Gln->pyro-Glu (N-term Q)

Max variable mods: 3

Max neutral losses: 1

Isotope label type: heavy

Isotope modifications:

- Label:13C(6)15N(2) (C-term K)
- Label:13C(6)15N(4) (C-term R)

Internal standard type: none

OK Cancel

Supplementary information I:

Skyline peptide and transition setting, peak scoring model.

Transition Settings

Prediction Filter Library Instrument Full-Scan

Precursor mass: Monoisotopic

Product ion mass: Monoisotopic

Collision energy: ABI 5600

Declustering potential: ABI

Optimization library: None

Compensation voltage: ABI

Use optimization values when present

OK Cancel

Supplementary information I:

Skyline peptide and transition setting, peak scoring model.

Transition Settings

Prediction Filter Library Instrument Full-Scan

Precursor charges: 2, 3 Ion charges: 1, 2 Ion types: y

Productions

From: ion 4 To: last ion - 1

Special ions:

- N-terminal to Proline
- C-terminal to Glu or Asp
- iTRAQ-114
- iTRAQ-115
- iTRAQ-116
- iTRAQ-117
- TMT-126
- TMT-127L

Edit List..

Use DIA precursor window for exclusion

Auto-select all matching transitions

OK Cancel

Supplementary information I:

Skyline peptide and transition setting, peak scoring model.

Transition Settings

Prediction Filter **Library** Instrument Full-Scan

Ion match tolerance:
0.7 *m/z*

If a library spectrum is available, pick its most intense ions

Pick:
6 product ions

From filtered ion charges and types

From filtered ion charges and types plus filtered product ions

From filtered product ions

OK Cancel

Supplementary information I:

Skyline peptide and transition setting, peak scoring model.

Transition Settings

Prediction Filter Library Instrument Full-Scan

Min m/z: 50 m/z

Max m/z: 1500 m/z

Dynamic min product m/z

Method match tolerance m/z: 0.055 m/z

Firmware transition limit:

Firmware inclusion limit:

Min time: min

Max time: min

OK Cancel

Supplementary information I:

Skyline peptide and transition setting, peak scoring model.

Transition Settings

Prediction Filter Library Instrument Full-Scan

MS1 filtering

Isotope peaks included: Count
Precursor mass analyzer: TOF

Peaks: 3
Resolving power: 10,000

Isotope labeling enrichment: Default

MS/MS filtering

Acquisition method: DIA
Product mass analyzer: TOF

Isolation scheme: SWATH (25 m/z)
Resolving power: 10,000

Use high-selectivity extraction

Retention time filtering

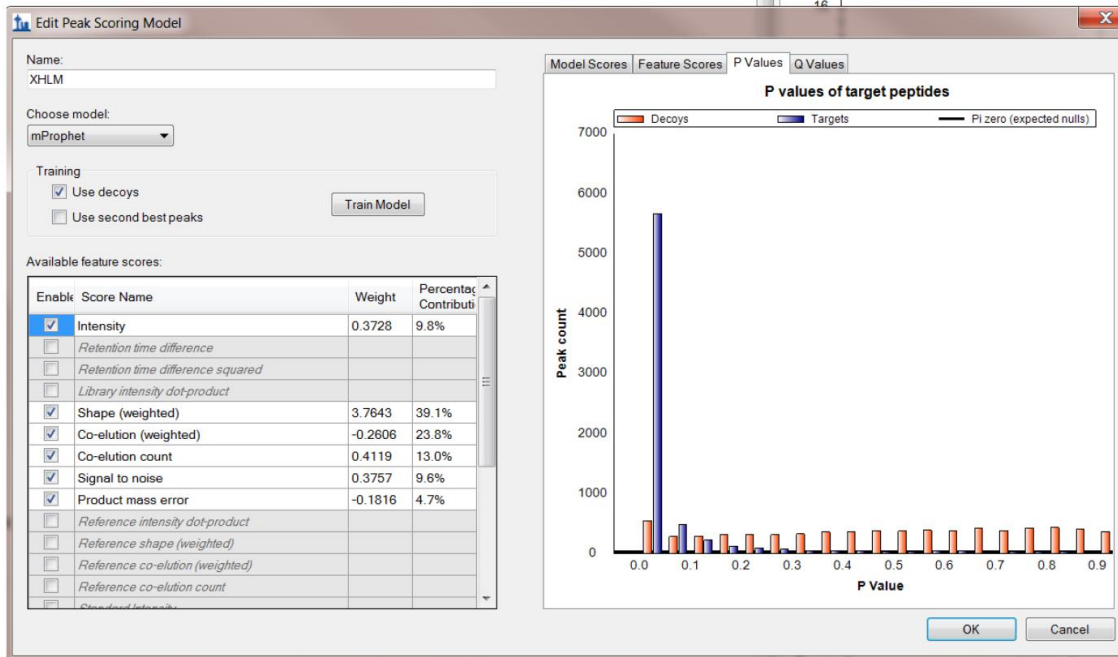
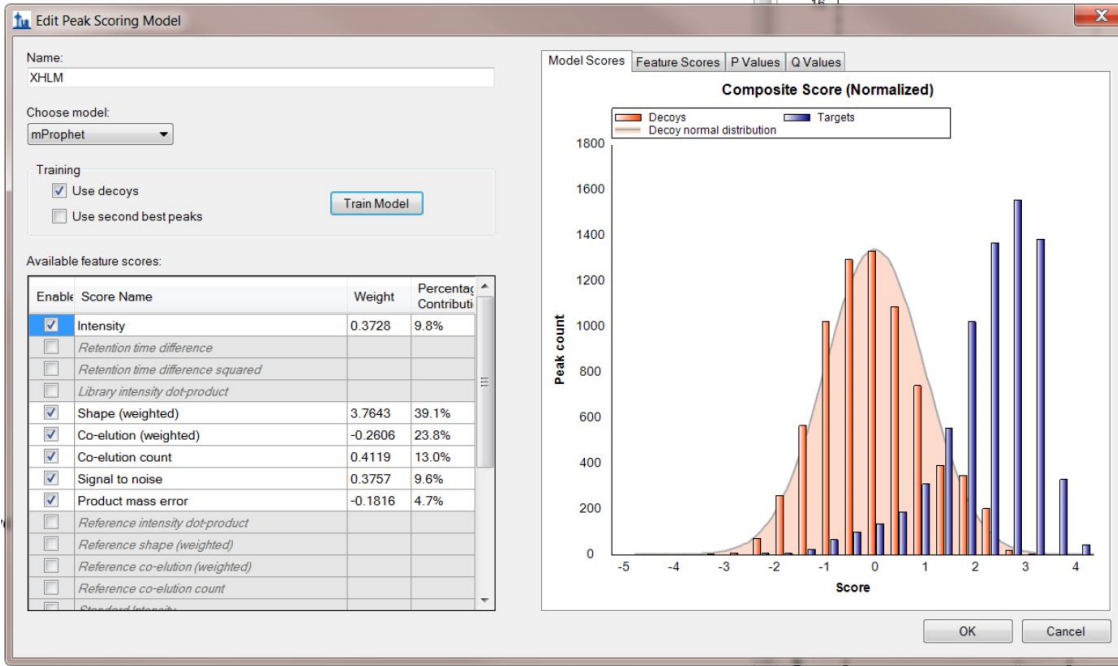
Use only scans within 5 minutes of MS/MS IDs

Use only scans within 5 minutes of predicted RT

Include all matching scans

OK Cancel

**Supplementary information I:
Skyline peptide and transition setting, peak scoring model.**



Supplementary information II: List of precursor and product ions for major drug metabolism enzymes quantified using the current method

Sr. No.	Enzyme	Peptide Sequence	Charge	Precursor m/z	Product m/z (transition) charge		
1	CYP1A2	YLPNPALQR	2	536.300915	795.44716 (y7)+	698.394398 (y6)+	584.351471 (y5)+
		ELDTVIGR	2	451.750724	660.36752 (y6)+	545.340572 (y5)+	444.292893 (y4)+ 345.22448 (y3)+
2	CYP2A6	IQEEAGFLDALR	2	737.898648	975.56219 (y9)+	904.525078 (y8)+	700.435201 (y6)+
		DFIDSLIR	3	563.300581	863.49853 (y7)+	750.414465 (y6)+	635.387522 (y5)+
3	CYP3A4	VWGFYDGGQPVLAITDPDMIK	3	798.399716	932.47575 (y8)+	819.391681 (y7)+	603.317059 (y5)+
		LSLGGLLQPEKPVVLK	3	564.353707	909.57678 (y8)+	789.484891 (y15)+	745.968876 (y14)+ 689.426844 (y13)+
4	CYP3A5	EMFPIAQYGDVLR	2	875.963465	1343.7682 (y12)+	1133.63133 (y10)+	1020.54727 (y9)+ 949.510157 (y8)+
		LDFLQLMIDSQNSK	2	826.42163	1035.5139 (y9)+	922.429857 (y8)+	791.389373 (y7)+ 678.305309 (y6)+
5	CYP2B6	IAMVDPFFR	2	548.286419	780.4039 (y6)+	681.335487 (y5)+	
		YGFLLMLK	2	492.782981	821.49536 (y7)+	764.473894 (y6)+	617.40548 (y5)+
6	CYP2C8	EALIDNGEEFSGR	2	718.836245	1010.4174 (y9)+	895.390435 (y8)+	781.347508 (y7)+
		GTTIMALLTSVLHDDK	2	857.955837	1027.5419 (y9)+	914.457787 (y8)+	813.410108 (y7)+
7	CYP2C9	LPPGPTLPVIGNLQIGIK	3	679.753871	898.57203 (y8)+	784.529101 (y7)+	558.360973 (y5)+
		GIFPLAER	3	451.758352	732.4039 (y6)+	585.335487 (y5)+	488.282723 (y4)+
8	CYP2C19	EALIDLGEFSGR	2	718.356813	1009.4585 (y9)+	894.431572 (y8)+	781.347508 (y7)+
		GTTILTSVSLHNDK	3	567.312348	1113.5899 (y10)+	725.394064 (y6)+	626.32565 (y5)+ 513.241586 (y4)+
9	CYP2D6	FGDIVPLGVTHMTR	3	543.952097	831.41415 (y7)+	631.298055 (y5)+	
		DEAVWEKPFRR	3	426.215538	961.52541 (y7)+	516.784901 (y8)+	
10	CYP2E1	YGLLILMK	2	475.790806	787.51101 (y7)+	730.489544 (y6)+	617.40548 (y5)+ 504.321416 (y4)+
		QEMPYMDAVVHEIQR	3	615.958922	781.43151 (y6)+	682.363098 (y5)+	545.304186 (y4)+
11	CYP2C18	GTTIITSLVSLHNDK	3	567.312348	1113.5899 (y10)+	1026.55784 (y9)+	725.394064 (y6)+
12	CYP2J2	LFVSHMIDK	2	545.291702	829.42365 (y7)+	730.355236 (y6)+	643.323207 (y5)+
		TELIFFFTSLMQK	2	802.923277	631.33611 (y10)+	354.191456 (y6)+	
13	CYP2S1	GTVAMLEGTFDGHGVVFFSNGER	3	776.695303	709.32638 (y6)+	562.257965 (y5)+	475.225936 (y4)+
		LPYTDVAVLHEAQR	3	504.93169	852.46863 (y7)+	753.400212 (y6)+	640.316148 (y5)+
14	CYP2U1	VPLISIVTK	2	485.320785	660.42905 (y6)+	547.344989 (y5)+	
		DPAIWEKPEDFYPNR	3	626.300331	647.80676 (y10)+	519.237981 (y8)+	
15	CYP3A7	RPFQVGFQFMK	2	568.307686	979.50699 (y9)+	735.385808 (y7)+	
		APPTYDTVLQLEYLDMVVNETLR	3	894.122799	961.51353 (y8)+	830.473043 (y7)+	731.404629 (y6)+ 632.336215 (y5)+
16	CYP3A43	ETQIPLK	2	414.74491	598.39227 (y5)+	470.333696 (y4)+	357.249632 (y3)+
17	CYP4A11	AVQLYLHR	2	500.290351	701.40932 (y5)+	588.325256 (y4)+	
		VQLYDPDYMK	2	636.302464	1044.4707 (y8)+	931.386596 (y7)+	653.296324 (y5)+
		FELLPDPTK	2	544.292756	811.46723 (y7)+	698.383165 (y6)+	
18	CYP4F8	VVLALLLR	2	499.342052	799.54 (y7)+	686.455936 (y6)+	
19	CYP4F12	TLDFIDVLLSK	3	459.606032	787.49238 (y7)+	672.465438 (y6)+	573.397024 (y5)+
		QEVQELLK	2	493.779482	729.45052 (y6)+	630.382102 (y5)+	502.323525 (y4)+
20	CYP4V2	AYPLVGHALLMKPDGR	3	579.987141	929.5237 (y8)+	816.439634 (y7)+	
		HPYAYVPFSAGPR	2	731.367318	830.45191 (y8)+	487.262322 (y5)+	
21	CYP7A1	YVHFITNPLSYHK	2	809.922457	959.49451 (y8)+	858.446828 (y7)+	744.403901 (y6)+
		AHILNLDNFK	2	649.846218	1090.5891 (y9)+	977.505071 (y8)+	
22	CYP20A1	TSDPFETMLK	2	584.781364	980.47575 (y8)+	768.396038 (y6)+	
23	CYP51A1	SGLNIAHFK	2	493.774534	729.40424 (y6)+	615.361307 (y5)+	
		FAVVPFGAGR	2	542.782359	866.45191 (y8)+	703.388585 (y7)+	

Supplementary information II: List of precursor and product ions for major drug metabolism enzymes quantified using the current method

Cytochrome P450 reductase	VYMGEMGR	2	471.71223	843.34877 (y7)+	680.285442 (y6)+	549.244957 (y5)+	
	YESGDHVAVYPANDSALVNQLGK	3	816.39943	929.54146 (y9)+	842.509428 (y8)+	771.472314 (y7)+	658.38825 (y6)+
	ATTPVIMVPGTGVAPFIGFIQER	3	820.110277	1106.5993 (y9)+	862.478128 (y7)+	749.394064 (y6)+	
UGT1A1	ESFVSLGHNVFENDSFLQR	3	742.358908	1155.5429 (y9)+	1008.4745 (y8)+	879.431906 (y7)+	650.362036 (y5)+
UGT1A3	VLVVPIDGSHWLSMR	3	570.311625	748.88756 (y13)++	699.353353 (y12)++		
	SMAMLNNMSLVYHR	2	833.896745	1377.6766 (y11)+	1246.6361 (y10)+	905.466183 (y7)+	574.309606 (y4)+
UGT1A4	LLTNSDHTMFLQR	3	559.619006	795.41817 (y6)+	664.377686 (y5)+		
UGT1A5	EVSVDLVSHASVWLFR	3	648.351025	1201.6477 (y10)+	1015.54721 (y8)+	807.451185 (y6)+	
	IPQTVLWR	2	506.800551	899.50976 (y7)+	802.456999 (y6)+	674.398421 (y5)+	573.350743(y4)+
	WLPQNDLLGHPMTR	3	559.955841	811.42432 (y7)+	698.340254 (y6)+	504.259879 (y4)+	
UGT1A6	GHEIVVVVPEVNLLK	3	586.688978	828.51893 (y7)+	699.476337 (y6)+	512.823692 (y9)++	
	SFLTAPQTEYR	2	656.830234	965.46869 (y8)+	864.421007 (y7)+	793.383893 (y6)++	
UGT1A9	TYSTSYLEDLDR	2	782.362292	1212.5743 (y10)+	861.431238 (y7)+		
UGT2A3	ANIASALAIQIPQK	2	719.424833	1026.5942	797.487965	485.308209	
UGT2B4	TILDELVQR	2	543.811313	872.48361 (y7)+	759.399543 (y6)+	644.3726 (y5)+	515.330007 (y4)+
	FSPGYAIEK	2	506.260925	777.41413 (y7)+	680.361367 (y6)+	389.239461 (y3)+	
	TVINDPLYK	2	531.795132	862.4669 (y7)+	749.382831 (y6)+	520.31296 (y4)+	
UGT2B7	TILDELIQR	2	550.819138	886.49926 (y7)+	773.415194 (y6)+	658.38825 (y5)+	529.345657 (y4)+
	IEIYPTSLTK	2	582.829171	1051.567 (y9)+	922.52441 (y8)+	809.440346 (y7)+	646.377017 (y6)+
	ANVIASALAIQIPQK	2	475.280431	797.48797 (y7)+	684.403901 (y6)+	613.366787 (y5)+	372.224145 (y3)+
UGT2B10	LEVYPTSLTK	2	575.821346	908.50876 (y8)+	809.440346 (y7)+	646.377017 (y6)+	
UGT2B15	VDFNTMSSDILLNALK	3	590.29771	1061.5837 (y10)+	786.47198 (y7)+	671.445037 (y6)+	558.360973 (y5)+
UGT2B17	SVINDPVIK	2	517.779482	848.45125 (y7)+	735.367181 (y6)+	621.324253 (y5)+	
UGT3A1	NDLEDFFMK	2	579.760432	929.44372 (y7)+	816.359652 (y6)+		
	SVINDPIYK	2	524.787307	862.4669 (y7)+	749.382831 (y6)+	635.339903 (y5)+	520.31296 (y4)+
FMO3	LNQVADTLTLTMK	2	774.918723	1193.6446 (y11)+	706.416773 (y6)+	593.332709 (y5)+	
	TAEQVMISSR	2	561.284605	949.47714 (y8)+	593.307557 (y5)+	462.267073 (y4)+	
	NNLPATASDWLYVK	2	817.432855	1195.6358 (y10)+	1023.55096 (y8)+	910.466895 (y7)+	
	NNEIILFK	2	495.784567	762.476 (y6)+	633.43341 (y5)+	520.349346 (y4)+	
	GVFPPLLEK	2	500.29731	843.49747 (y7)+	696.429053 (y6)+	599.376289 (y5)+	
FMO5	STIAVIGFVQSLGAAIPTVDLQSR	3	815.123351	1227.6692 (y12)+	1099.6106 (y10)+	1028.57349 (y9)+	
MAOA	FQENPEEGR	2	553.249077	830.36389 (y7)+	701.321293 (y6)+	587.278366 (y5)+	
	SVIINTSK	2	431.255642	675.40357 (y6)+	562.319502 (y5)+	449.235438 (y4)+	
	ALSQHPTLNDDLPIR	3	564.288425	1154.58 (y10)+	614.32565 (y5)+	499.298707 (y4)+	
MAOB	IMDLLGDQVK	2	566.307549	1018.5238 (y9)+	887.483273 (y8)+	772.45633 (y7)+	659.372266 (y6)+
	IFFAGTETATK	2	593.311146	925.46254 (y9)+	707.35701 (y7)+	650.335546 (y6)+	
	WSGYMEGAVEAGER	2	771.338097	1268.5576 (y12)+	917.4323 (y9)+	788.389707 (y8)+	
	DIWVQEPESK	2	615.803685	717.34136 (y6)+	589.282782 (y5)+	460.240189 (y4)+	
EPXH1	YVDLGGSYVGPQTQR	2	813.399543	1078.5276 (y10)+	934.474105 (y8)+	771.410777 (y7)+	672.342363 (y6)+
	TMDDMGR	2	413.165113	724.27527 (y6)+	478.207843 (y4)+	363.1809 (y3)+	
	IMDLLGDR	2	466.747127	819.40291 (y7)+	688.36243 (y6)+	347.167359 (y3)+	
	VPLGSVIK	2	406.765646	713.4556 (y7)+	616.402838 (y6)+	503.318774 (y5)+	
	VLSLEALEPVHYEEK	3	604.98412	1214.6052 (y10)+	1143.56807 (y9)+	705.32023 (y5)+	568.261319 (y4)+
EPXH2	IPLLTDPK	2	505.318243	783.46108 (y7)+	686.408317 (y6)+	573.324253 (y5)+	
	FLGLTER	2	418.237253	688.39882 (y6)+	575.314751 (y5)+	518.293287 (y4)+	
	DVELLYPVK	2	538.305332	732.46544 (y6)+	619.381374 (y5)+	506.29731 (y4)+	
	VYVPTGFSAFPFELLHTPEK	3	760.396412	1210.6467 (y10)+	611.314751 (y5)+	474.255839 (y4)+	
Beta galactosidase	FLDLTLK	2	425.257654	702.43962 (y6)+	589.355553 (y5)+	476.271489 (y4)+	
	DLGMVTILVQDITDALK	3	611.660648	1103.5943 (y10)+	802.931831 (y15)++	659.366649 (y12)++	

Supplementary information III: Quantification of hepatic CYP mRNA expression

Total cellular RNA was isolated from the samples using RNeasy Mini Kit (QIAGEN Inc., Valencia, CA). The total RNA was reverse-transcribed, and the single stranded DNA was used for real-time PCR. The mRNA expression of hepatic CYP was quantified by real-time PCR using an Applied Biosystems 7500 Real-Time PCR system (Applied Biosystems) at least two times according to the manufacturer's instructions. The primers for CYP were shown in table below. 18S ribosomal RNA (rRNA) was also quantified as an internal control.

References

- Busi F, Cresteil T. Phenotyping-genotyping of alternatively spliced genes in one step: study of CYP3A5*3 polymorphism. *Pharmacogenet Genomics*. 2005; 15: 433-9.
- He P, Court MH, Greenblatt DJ, von Moltke LL. Factors influencing midazolam hydroxylation activity in human liver microsomes. *Drug Metab Dispos*. 2006; 34:1198-207.
- Jigorel E, Le Vee M, Boursier-Neyret C, Parmentier Y, Fardel O. Differential regulation of sinusoidal and canalicular hepatic drug transporter expression by xenobiotics activating drug-sensing receptors in primary human hepatocytes. *Drug Metab Dispos*. 2006 Oct;34(10):1756-63.
- Katoh M, Matsui T, Nakajima M, Tateno C, Kataoka M, Soeno Y, Horie T, Iwasaki K, Yoshizato K, Yokoi T. Expression of human cytochromes P450 in chimeric mice with humanized liver. *Drug Metab Dispos*. 2004; 32:1402-10.
- Wilkening S, Stahl F, Bader A. Comparison of primary human hepatocytes and hepatoma cell line Hepg2 with regard to their biotransformation properties. *Drug Metab Dispos*. 2003; 31:1035-42.

	Sequence	Position	Accession number	Ref.
CYP1A2			NM000761	Katoh et al., 2004
Forward primer	GCTTCTACATCCCCAAGAAAT	1257-1277		
Reverse primer	TCCCACTTGGCCAGGACT	1464-1447		Katoh et al., 2004
CYP2A6			NM000762	
Forward primer	AGCAACAGGCCTTTCAGTT	722-740		
Reverse primer	CCCAATGAAGAGGTTCAAC	924-906		
CYP2B6			NM000767	Wilkening et al., 2004
Forward primer	ATGGGGCACTGAAAAAGACT GA	1257-1278		
Reverse primer	AGAGGCGGGGACACTGAATG AC	1539-1518		Katoh et al., 2004
CYP2C8			NM000770	
Forward primer	AGATCAGAATTTTCTCACCC	665-684		
Reverse primer	AACTTCGTGTAAGAGCAACA	822-803		Katoh et al., 2004
CYP2C9			NM000771	
Forward primer	CAGATCTGCAATAATTTTCTC	665-686		
Reverse primer	CTTTC AATAGTAAATTCAGAT G	882-861		Katoh et al., 2004
CYP2C19			NM000769	
Forward primer	ATTGAATGAAAACATCAGGAT TG	600-622		
Reverse primer	GAGGGTTGTTGATGTCCATC	781-762		Katoh et al., 2004
CYP2D6			NM000106	
Forward primer	GGTGTGACCCATATGACATC	1207-1226		
Reverse primer	CTCCCCGAGGCATGCACG	1428-1411		
CYP2E1			NM000773	Wilkening et al., 2004
Forward primer	GACTGTGGCCGACCTGTT	906-923		
Reverse primer	ACTACGACTGTGCCCTTGG	1202-1184		
CYP3A4			NM000940	He et al., 2006
Forward primer	CTTTTATGATGGTCAACAGCC TGTG	326-350		
Reverse primer	CTTTTCATAAATCCCACTGGA CCA	454-431		
CYP3A5			NM000777	Busi et al., 2005
Forward primer	CCCACACCTCTGCCTTTG	223-240		
Reverse primer	CAGGGAGTTGACCTTCATACG	343-323		Jigorel et al., 2006
18S rRNA			NM003286	
Forward primer	CGCCGCTAGAGGTGAAATTC	948-967		
Reverse primer	TTGGCAAATGCTTTCGCTC	1009-991		

Supplementary information IV: Enzyme assay conditions as provided by Seksui Xenotech LLC, Kansas City, MO

Enzymatic assay conditions

- HLM protein concentration: 50 µg/mL
- Incubation temp: 37°C
- Reaction time: 10 min
- Potassium phosphate buffer (50 mM, pH 7.4) containing 3.0 mM MgCl₂, EDTA (1.0 mM), NADP (1.0 mM), glucose-6-phosphate (5.0 mM), glucose-6-phosphate dehydrogenase (1 Unit/mL)
- Probe substrates were incubated at a final concentration mentioned in the table below.

	Probe substrate	Probe reaction	Substrate conc. (µM)
CYP1A2	Phenacetin	Phenacetin <i>O</i> -alkylation	80
CYP2A6	Coumarin	Coumarin 7-hydroxylation	50
CYP3A4/3A5	Midazolam	Midazolam 1-hydroxylation	30
CYP3A4/3A5	Testosterone	Testosterone 6β-hydroxylation	250
CYP2B6	Bupropion	Bupropion hydroxylation	500
CYP2C8	Amodiaquine	Amodiaquine <i>N</i> -dealkylation	20
CYP2C9	Diclofenac	Diclofenac 4-hydroxylation	100
CYP2C19	S-Mephenytoin	S-Mephenytoin 4-hydroxylation	400
CYP2D6	Dextromethorphan	Dextromethorphan 6-hydroxylation	80
CYP2E1	Chlorzoxane	Chlorzoxane 6-hydroxylation	500

Reference: Pearce et al., Effects of freezing, thawing, and storing human liver microsomes on cytochrome P450 activity. Arch Biochem Biophys. 1996, 15;331(2):145-69.

MANUSCRIPT III

This manuscript was prepared and published as a research article in *Molecular Pharmaceutics*, 2018 Jul 2;15(7):2621-2632

Nonalcoholic fatty liver disease and diabetes is associated with decreased CYP3A4 protein expression and activity in human liver

Rohitash Jamwal ¹, Suzanne M. de la Monte ², Ken Ogasawara ¹, Sravani Adusumalli ¹, Benjamin B Barlock ¹, Fatemeh Akhlaghi ¹

¹ Biomedical and Pharmaceutical Sciences, College of Pharmacy, University of Rhode Island, Kingston, RI, 02881, USA

² Departments of Medicine, Pathology, Neurology, and Neurosurgery, Rhode Island Hospital and the Warren Alpert Medical School of Brown University, Providence, RI 02903, USA.

Corresponding author at:

Fatemeh Akhlaghi, Ph.D.

Clinical Pharmacokinetics Research Laboratory, Department of Biomedical and Pharmaceutical Sciences, The University of Rhode Island, 495A College of Pharmacy, 7 Greenhouse Road, Kingston, RI 02881, United States.

Email address: fatemeh@uri.edu

The number of words in the abstract: 276

The number of words in the introduction: 751

The number of words in the discussion: 1599

The number of figures: 6

The number of tables: 4

The number of references: 66

The number of supplemental tables: 5

The number of supplemental figures: 5

List of abbreviations in the order of appearance:

BMI: Body mass index; CAR: Constitutive androstane receptor; CPR: NADPH-cytochrome P450 reductase, Cyb5: Cytochrome b5; CYP3A: Cytochrome P450 3A; CYP3A4: Cytochrome P450 3A4; CYP3A5: Cytochrome P450 3A5; CYP3A43: Cytochrome P450 3A43; CYP3A7: Cytochrome P450 3A7; GAPDH: Glyceraldehyde 3-phosphate dehydrogenase; HCC: hepatocellular carcinoma; HNF4 α : Hepatocyte nuclear factor 4 α ; HLM: Human liver microsomes; NAFLD: Non-alcoholic fatty liver disease; NAFL: Non-alcoholic fatty liver; NASH: Non-alcoholic steatohepatitis; NADPH: Nicotinamide adenine dinucleotide phosphate; PCR: Polymerase chain reaction; PXR: Pregnane X receptor; TBARS: Thiobarbituric acid reactive substances; TOF: Time of flight; UPLC-MS: Ultra performance liquid chromatography-mass spectrometer.

ABSTRACT

Nonalcoholic fatty liver disease (NAFLD) is a major cause of chronic liver disease in the Western population. We investigated the association of nonalcoholic fatty liver disease (NAFLD) and diabetes mellitus on CYP3A4 activity in human liver tissue from brain dead donors (N=74). Histopathologically graded livers were grouped into normal (n=24), nonalcoholic fatty liver (NAFL, n=26) and nonalcoholic steatohepatitis (NASH, n=24) categories. The rate of conversion of midazolam to its 1-hydroxy metabolite was used to assess *in vitro* CYP3A4 activity in human liver microsomes (HLM). A proteomics approach was utilized to quantify the protein expression of CYP3A4 and related enzymes. Moreover, a physiologically based pharmacokinetic (PBPK) model was developed to allow prediction of midazolam concentration in NAFL and NASH patients. CYP3A4 activity in NAFL and NASH was 1.9 and 3.1-fold ($p<0.05$) lower than normal donors, respectively. Intrinsic clearance (CL_{int}) was 2.7 ($p<0.05$) and 4.1 ($p<0.01$) fold lower in donors with NAFL and NASH, respectively. CYP3A4 protein expression was significantly lower in NAFL and NASH donors ($p<0.05$) and accounted for midazolam hydroxylation variability in a multiple linear regression analysis ($\beta=0.869$, $r^2=0.762$, $P<0.01$). Diabetes was also associated with decreased CYP3A4 activity and protein. Both midazolam CL_{int} and CYP3A4 protein abundance decreased significantly with increase in hepatic fat accumulation. Age and gender did not exhibit any significant association with the observed alterations. Predicted midazolam exposure was 1.7 and 2.3-fold higher for NAFL and NASH, respectively, which may result in a longer period of sedation in these patients. Data suggests that NAFLD and diabetes are associated with the decreased hepatic CYP3A4

activity. Thus, further evaluation of clinical consequences of these findings on the efficacy and safety of CYP3A4 substrates is warranted.

Keywords:

CYP3A4, diabetes, drug metabolism, midazolam, nonalcoholic fatty liver disease, nonalcoholic steatohepatitis, PBPK, pharmacokinetics, proteomics

INTRODUCTION

The prevalence of nonalcoholic fatty liver disease (NAFLD) is rising at an alarming rate in populations with diabetes and obesity. The clinical diagnosis of NAFLD is based on limited or no consumption of alcohol, evidence of hepatic steatosis based on either biopsy or imaging, and the exclusion of other causes of liver disease. NAFLD is sub-categorized histopathologically as non-alcoholic fatty liver (NAFL), which is characterized by lipid accumulation in hepatocytes, or non-alcoholic steatohepatitis (NASH), which is associated with hepatic steatosis with inflammation and ongoing inflammatory or degenerative injury to hepatocytes^{1,2}. Significant lobular inflammation, hepatic fibrosis, and hepatocyte necrosis present in NASH can progress to life-threatening liver cirrhosis and hepatocellular carcinoma (HCC).³

Over 64 million people in the United States are projected to have NAFLD, with an estimated economic burden of about \$103 billion, and these costs are highest among patients aged 45-65 year.⁴ Presence of NAFLD is highly correlated with insulin resistance and diabetes.⁵ Diabetes and NAFLD share common underlying pathophysiological processes including insulin resistance, hyperglycemia, dyslipidemia, inflammation and other cardiovascular conditions.⁶ A retrospective analysis of the hospital admission of patients with type 2 diabetes showed that the relative risk of NAFLD among these patients was 3-times higher in men and 5-times higher in women than those without diabetes.⁷

Despite the widespread prevalence of NAFLD, no specific pharmacological therapies are available for its treatment; however, management of associated conditions including obesity, diabetes, and hyperlipidemia are often achieved pharmacologically or through lifestyle intervention.⁸⁻¹⁰ CYP3A enzymes metabolize most of the drugs prescribed

for these comorbidities.¹¹ Moreover, CYP3A enzymes are also responsible for the metabolism of 30-50% of all drugs available in the market.^{11, 12} CYP3A4 and CYP3A5 proteins of this superfamily of enzymes are expressed in human liver as well as extrahepatic tissues including intestine.¹³ Moreover, CYP3A4 plays a significant role in the catabolism of carcinogens (aflatoxin B1), and various endogenous steroids (progesterone, testosterone, cortisol and bile acids).¹⁴⁻¹⁷ Additionally, the enzyme is involved in the biotransformation of cholesterol, and the plasma concentration of cholesterol 4 β -hydroxy has been used as an endogenous marker of CYP3A4 activity.¹⁸ CAR, PXR, HNF α , and PPAR α are some of the transcription factors which has been reported to modulate the expression of CYP3A4.^{19, 20}

A perturbation in CYP3A4 activity associated with diabetes, NAFLD or both is likely to alter the clearance of some drugs thereby changing the efficacy or safety of CYP3A substrates. Current studies in rodent models of the disease are conflicting as it has been widely known that most models fail to recapitulate the complex pathophysiology of human NAFLD fully.²¹⁻²³ In rat models, reduced or elevated expression and activity of Cyp3a in steatosis and NASH has been reported²⁴⁻²⁸. Similarly, studies in mice models are inconsistent, and results vary with diet and species²⁹⁻³¹.

Genome-wide studies (GWAS) in human NAFLD patients found no significant changes in drug metabolism genes between normal and steatotic livers at mRNA expression level.^{32, 33} However, these results don't capture the post-transcriptional and post-translational changes which may alter protein expression or activity. The results of studies in human liver examining the impact of NAFLD on CYP3A4 activity are heterogeneous and lacks agreement.³⁴⁻³⁷ Fisher et al. found a trend of decreasing CYP3A4

protein expression with severity of NAFLD, but no change in enzyme activity was observed.³⁴ However this study was done in a small sample size (steatosis =10, NASH=10) and no information on the ethnicity was provided. In contrast, Woolsey et al. found significantly lower activity CYP3A4 activity in human NASH subjects.³⁷ Diabetes was found to be associated with significant reduced CYP3A4 activity in human livers.³⁸ However, the sample size in this study investigation was small, and presence of NAFL or NASH status was unknown.

Therefore, using a large human liver tissue repository (N=74), well-characterized with respect to the presence of diabetes and NAFLD, we aimed to verify which disease condition influence the expression and activity of CYP3A4. The goal of studies using microsomes it to determine the intrinsic clearance and in vitro in vivo extrapolation (IVIVE). CYP3A4 functional activity and intrinsic clearance of midazolam was evaluated in HLM. As protein expression is an important factor for IVIVE, we determined the expression of CYP3A4 and related proteins in HLM using mass spectrometry. Furthermore, we developed a physiologically based pharmacokinetic (PBPK) model and predicted midazolam exposure in virtual populations of NAFL and NASH patients.

EXPERIMENTAL SECTION

Materials and reagents. Midazolam (MDZ), 1-hydroxy midazolam (1'-OH MDZ), and 1-hydroxy midazolam-D₄ (1'-OH MDZ-D₄) were purchased from Cerilliant Corporation (Round Rock, TX). MS-grade formic acid, acetonitrile, and methanol were obtained from ThermoFisher Scientific (Waltham, MA). NADPH tetrasodium salt was from Calbiochem (EMD Millipore, Billerica, MA). OxiSelect TBARS assay kit (Malondialdehyde quantification) was purchased from Cell Biolabs, Inc., San Diego, CA and Amplex[®] Red Cholesterol Assay Kit was from ThermoFisher Scientific, Waltham MA. All other reagents and solvents used in the study were of analytical grade.

Human liver bank. A novel human liver tissue repository (N=106) was created in our laboratory from hepatic tissue purchased from Sekisui XenoTech LLC (Kansas City, KS). The identity of donors was not known thereby the study was designated as Institutional Review Board (IRB) exempt category 4. Age, gender, ethnicity, the cause of death, cold ischemia time, liver and body weight was available for $\geq 95\%$ of the samples. While being accessible, smoking and alcohol consumption was not assessed for effect on CYP3A4 activity due to reasons discussed later in the text. Detailed donor demographics are given in **Table 1**. The primary objective of the work was to study the effect of NAFLD and diabetes on CYP3A4 activity and protein levels. Therefore, only samples that were homozygous for *CYP3A5**3/*3 (n=74) were included in this study. The results and findings of this study are thus limited to Caucasian male and female population. Moreover, five donors were identified with *CYP3A4**22 variant and one possessed *CYP3A4**1B (**Table 1**).

Histological grading and study grouping. Liver tissue was graded for steatosis, lobular inflammation, hepatocyte ballooning, and fibrosis by a physician specializing in histopathology (Suzanne Delamonte, MD). The standardized scoring protocol assessed the presence and severity of hepatocellular steatosis, lobular inflammation, ballooning degeneration, and fibrosis.³⁹ Formalin-fixed paraffin-embedded histological sections (5 μm thick) of the liver, stained with hematoxylin and eosin dyes, were used to grade the severity of the disease. In brief, the slides were coded and scored concerning the abundance and distribution of hepatic steatosis, lobular inflammation, hepatocellular ballooning degeneration, and fibrosis. Steatosis was graded as 0 (<5%), 1 (5-33%), 2 (34-66%), or 3 (>66%), reflecting the cross-sectional areas of the section showing hepatocytes with steatosis. Lobular inflammation was graded as 0 (absent), 1 (<2 foci/200x microscopic field), 2 (between 2 and 4 foci/200x microscopic field), or 3 (>4 foci/200x microscopic field). Hepatocyte ballooning degeneration was graded as 0 (absent), 1 (rare, scattered cells) or 2 (readily detected). Fibrosis grading was simplified relative to the original report and graded as 0 (absent), 1 (mild and delicate in the perisinusoidal regions), 2 (conspicuously present in perisinusoidal and periportal regions), 3 (bridging fibrosis), or 4 (cirrhosis, which requires bridging fibrosis and regenerative nodules). The final scores represent the summed sub-scores. Steatosis was confirmed by Oil Red O staining of cryostat sections (10 microns) of the same liver samples, and fibrosis was confirmed by Sirius red staining of adjacent formalin fixed paraffin-embedded tissue sections.⁴⁰ A composite of different histological sections of representative liver samples from different groups is given in **Fig. 1**.

Subsequently, livers were categorized as normal, NAFL, and NASH based on the scoring algorithm described in **supplemental figure I**.⁴¹ Detailed histological characteristics of donors are given in **supplemental table I**.

Malondialdehyde and cholesterol estimation. Quantification of malondialdehyde (MDA) in donor liver homogenate was determined using OxiSelect TBARS assay kit according to manufacturer instructions (Cell Biolabs, Inc., San Diego, CA). Total liver cholesterol was estimated using Amplex[®] Red cholesterol assay kit according to manufacturer's instruction (ThermoFisher Scientific, Waltham, MA).

Quantification of mRNA. Total RNA from liver tissues was isolated using the RNeasy mini kit (Qiagen Inc., Valencia, CA). Subsequently, the total cellular RNA was reverse-transcribed, and the cDNA was used for real-time PCR analysis. The mRNA expression of hepatic CYP3A4 and the relevant transcription factors were quantified by real-time PCR using SYBR Green Master Mix on 7500 Real-Time PCR system (Applied Biosystems, ThermoFisher Scientific, MA). Human 18S ribosomal RNA (rRNA) was used as an internal control for relative expression of data. The information on PCR primers used is available in **supplemental table II**.

CYP3A4 activity assay. Microsomes were prepared from liver samples as described previously in detail.⁴² CYP3A4 activity was assessed by formation of 1-hydroxy midazolam in HLM using midazolam as probe substrate.⁴³ Enzymatic incubations were carried out in 100 mM potassium phosphate buffer containing 3 mM MgCl₂ (pH 7.4).

Microsomal protein concentration used was 50 $\mu\text{g/mL}$ and concentrations of midazolam were 0, 0.2, 1, 2.5, 5, 10, 25 μM . The addition of NADPH initiated the reaction, and the incubations were carried out in a shaking water bath (75 rpm) kept at 37°C. After 20 min, the reaction was terminated by addition of ice-cold acetonitrile containing 0.5% formic acid and internal standard (1-hydroxymidazolam-D₄, 50 ng/mL). Subsequently, samples were centrifuged at 2000 g for 5 min at 4°C. The supernatant was collected, and 5 μL was injected for quantification of 1-hydroxy midazolam using the UPLC-MS method described below. CYP3A4 activity (V_{max} ; maximum rate of reaction) was expressed as pmol/mg microsomal protein.

Quantification of 1-hydroxy midazolam. Samples were analyzed using a previously published method with some modifications to chromatography method as described below⁴³. Chromatographic separation was performed using a gradient elution mode using 10 mM ammonium acetate and 10% methanol (A) and acetonitrile (B) at the flow rate of 400 $\mu\text{L}/\text{min}$. The linear gradient started with 25% B until 0.5 min, 60% B at 1.5 min, 90% B at 3 min before returning to 25% B at 4 min. All other mass spectrometer parameters were same as previously described.⁴³

Quantification of proteins using mass spectrometry. Protein levels of CYP3A4, NADPH-cytochrome P450 reductase (CPR), and Cytochrome b5 (Cyb5) in human liver microsomes were determined using mass spectrometry and “Total Protein Approach”.⁴⁴ Microsomal fractions were digested with trypsin and analyzed in Data-Dependent Acquisition (DDA) mode on SCIEX TripleTOF 5600+ mass spectrometer (SCIEX,

Concord, CA). The raw data files from one of our previous study were analyzed using MaxQuant (ver 1.5.2.10).⁴² The specifics of protein digestion and mass spectrometry analysis were previously described in the literature.^{42, 44} The proteins were searched on Andromeda search engine against UniProt human protein database (updated Oct 2016) at 1% false discovery rate (FDR).⁴⁵ Cysteine carbamidomethylation was selected as fixed modifications for the search. Label-free quantification (LFQ) was performed with a ratio count of 1 and maximum of two missed cleavages were allowed. All the other MaxQuant settings were kept as default values. The absolute protein levels were calculated using “Total Protein Approach” from LFQ intensities obtained from MaxQuant using the equations given below⁴⁴.

$$Total\ protein\ (p) = \frac{MS\ signal\ (p)}{Total\ MS\ signal}$$

$$Protein\ concentration\ (p) = \frac{MS\ signal\ (p)}{Total\ MS\ signal \times MW(p)} \text{ [mol/gram total protein]}$$

where MS signal (p) refers to total LFQ signal intensity for CYP3A4, CPR or Cyb5. Total MS signal refers to the total LFQ intensity of all the proteins and MW represents the molecular weight of respective protein.

Modeling of enzyme kinetics data. *In vitro* CYP3A4 kinetics data were fitted using Prism[®] version 6 (GraphPad Software Inc., La Jolla, CA) into a nonlinear least-squares regression equation given below ⁴⁶.

$$v = \frac{V_{max} \times S}{K_m + S \times \left(1 + \frac{S}{K_s}\right)}$$

Where S represents the concentration of substrate, v is the velocity of 1-OH midazolam formation; K_m is Michaelis-Menten constant (substrate concentration required for an enzyme to reach one-half its maximum velocity), and K_s is inhibition constant. V_{max} (maximum rate of product formation) and K_m were estimated from the equation, and apparent *in vitro* intrinsic clearance ($CL_{int, app}$) was calculated as V_{max}/K_m . Intrinsic clearance for whole liver ($CL_{int, whole liver}$) was calculated using the equations given below and was expressed as L/min. MPPGL denotes the yield of membrane proteins per gram of liver.

$$CL_{int} (whole liver) = CL_{int, app} \times MPPGL \times Liver\ weight$$

SimCYP based PBPK simulation. A physiologically based pharmacokinetic (PBPK) model was developed in SimCYP population-based simulator (ver 15, Certara LP, Sheffield, UK) using CYP3A4 protein and midazolam enzyme kinetic parameters. A virtual Caucasian population (Sim-NEurcaucasian) with an equal proportion of males and females, 20-65 year old, was selected for simulations. A minimal PBPK model was utilized for estimating plasma concentration-time profiles. Portal and arterial blood flow were the same for all the populations given a lack of data on hepatic blood flows in NAFL and NASH. An intravenous bolus dose of 5 mg midazolam was given, and default SimCYP compound file was used. In vitro V_{max} and K_m values were substituted for a respective study group in the “whole organ metabolic clearance” tab implemented in SimCYP. Default CYP3A4 phenotype values for the Caucasian population was replaced with protein concentrations determined in this study. Five virtual trials with 50 subjects per study were used for prediction of systemic midazolam concentration. All other parameters were kept as the default values.

Statistical analysis. Statistical analysis was performed with SPSS version 24 (IBM Analytics, Armonk, NY), and Prism[®] version 6 (GraphPad Software Inc., La Jolla, CA) was used for graphs, V_{\max} and K_m calculations. Descriptive statistical values in tables are reported as mean \pm standard error (SE) unless otherwise stated. Mann-Whitney U test (2-tailed) was used to compare the effect of gender. Non-parametric Kruskal-Wallis test (2-tailed) without multiple corrections was used when studying three or more groups. The correlation was analyzed using nonparametric Spearman correlation analysis. Linear and multiple regression analysis were used to determine the contribution of predictors toward explaining variability in CYP3A4 activity. $P < 0.05$ was considered significant for all the statistical tests and correlation analysis.

RESULTS

CYP3A4 activity and protein expression are decreased in NAFLD. Significantly lower CYP3A4 activity (V_{max} expressed as pmol/min/mg protein) was observed in microsomes from NAFLD donors (**Fig. 2**). HLM from NASH donors exhibited 3.1-fold lower midazolam V_{max} as compared with normal donors (**Table 2**). Midazolam V_{max} was 1.9-fold lower in HLM from NAFL donors, but the effect was not statistically significant ($P>0.05$). CL_{int} (L/min) was significantly lower intrinsic clearance in NAFL (2.7 ± 0.9 , $P<0.05$) and NASH (1.8 ± 0.6 , $P<0.01$) as compared to normal (7.3 ± 1.8 , **Fig. 3**). Michaelis-Menten constant (K_m) was comparable in different study groups and ranged from 1.6 to 2.3 μM (**Table 2**).

Mean protein levels of CYP3A4 decreased with progression of disease ($P<0.05$, **Fig. 3**). CPR and Cyb5 protein levels were significantly lower ($P<0.05$) in HLM from NAFLD donors (**Table 3**). The progression of disease from NAFL to NASH reduced the CYP3A4 mRNA expression (**Fig. 4**). However, the decrease was not significant. The levels of transcription factors, PXR, CAR, HNF4 α and PPAR α mRNA, decreased with disease progression (**Fig. 4**). The reduction in CAR mRNA level was significantly different between normal and NASH donors ($P<0.05$).

CYP3A4 activity and protein expression are decreased in diabetes and NAFLD. Given the high prevalence of NAFLD in patients with diabetes, we further studied the combined effect of the insulin resistance and fatty liver on CYP3A4 protein and activity. The levels of CYP3A4 activity, protein and mRNA expression and relevant transcription factors are summarized in **Table 4**. We observed that the effect of NAFLD was more prominent and

statistically significant in HLM from diabetic donors. For non-diabetic donors, the study parameters showed a trend of reduction in disease state but were not statistically significant except CPR. In contrast, CYP3A4 activity and Clint was significantly lower in HLM from diabetic NAFL and NASH donors. Similarly, a significant decrease in CYP3A4, CPR, and Cyb5 was also observed in diabetic donors with NAFLD. Interestingly, while mRNA expression decreased in both disease states, the mean differences failed to achieve statistical significance.

CYP3A4 activity and protein expression decrease with increase in liver fat. The impact of varying grades of steatosis on CYP3A4 activity, protein and mRNA levels was also evaluated. When the donors were categorized based on the severity of steatosis, a significant reduction in CLint was observed (**Fig. 5**). CYP3A4 activity decreased with increase in liver fat content, but the decline was not significant due to extensive variability. CYP3A4, CPR, and Cyb5 protein levels also reduced with an increase in the severity of steatosis (**Fig. 5, supplemental figure III**).

Effect of age. The average age of normal donors was similar in NAFL and NASH donors (**Table 1**). Donor age showed no significant correlation with CYP3A4 activity ($r=-0.143$, $P > 0.1$), CYP3A4 protein ($r=-0.101$, $P > 0.1$), and CLint ($r=-0.228$, $P > 0.1$, **Supplemental figure IV**). The association with age was also insignificant for CYP3A4 mRNA.

Effect of gender. Almost equal number of male and female donors were included in this study (males=36, females=38, **Supplemental table III**). In general, males exhibited

marginally higher CYP3A4 activity, CL_{int}, protein and mRNA levels than female donors. However, no significant association ($P > 0.1$) was observed between gender and CYP3A4 activity, CL_{int} as well as CYP3A4, CPR and Cyb5 protein abundance. The relationship between gender and CYP3A4 and related proteins was also examined, and no significant correlations were found (**Supplemental table III**).

Correlation between activity, mRNA and protein levels. The rate of 1-hydroxymidazolam formation showed a significantly positive correlation with CYP3A4 protein and mRNA levels. Similarly, CYP3A4 protein and mRNA expression levels exhibited significant positive correlation (**supplemental figure V**). A significant but moderate correlation was found between CPR protein and CYP3A4 activity ($r=0.446$, $P < 0.01$), and CYP3A4 protein ($r=0.547$, $P < 0.01$). The correlation between Cyb5 protein and CYP3A4 activity ($r=0.463$, $P < 0.01$), and CYP3A4 protein ($r=0.592$, $P < 0.01$) was moderate and significant. The association between two CPR and Cyb5 was significant as well ($r=0.607$, $P < 0.01$). Correlation plots can be found in **supplemental figure V**.

Linear regression analysis of protein and activity. Univariate linear regression analysis was used to determine how much of the variability in CYP3A4 activity was accounted by CYP3A4, CPR, and Cyb5 protein levels. We found that CYP3A4 ($r^2=0.761$, $P < 0.01$), CPR ($r^2=0.331$, $P < 0.01$) and Cyb5 ($r^2=0.197$, $P < 0.01$) protein levels were significant predictors of the CYP3A4 activity in HLM. However, multiple linear regression analysis returned a regression coefficient ($r^2=0.762$, $P < 0.01$) which was marginally better than the coefficient returned by univariate linear regression between CYP3A4 protein and activity ($r^2=0.761$).

Standardized beta coefficients of multiple regression models for CYP3A4 protein ($\beta=0.869$, $P<0.01$) explained most of the variability in midazolam hydroxylation activity, whereas CPR protein ($\beta =0.062$, $P>0.1$) and Cyb5 protein ($\beta =-0.069$, $P>0.1$) revealed the minimal contribution of each predictor to the model.

SimCYP based PBPK model. The simulated plasma profile of midazolam was in good agreement with the observed profiles previously reported in the literature so as the values of area under the concentration-time curve (AUC₀₋₂₄), maximum midazolam concentration (C_{max}) and clearance (CL).⁴⁷ A 1.8 and 2.3-fold increase in exposure (based on AUC) was found for NAFL and NASH populations, respectively (**supplemental table IV**). Predicted plasma concentration of midazolam in a Caucasian population with CYP3A4 phenotype and enzyme kinetic parameters is shown in **Fig. 6**. . The predicted intravenous clearance (CL) of midazolam in normal, NAFL and NASH group was 16.6, 9.4 and 8.6 L/h, respectively (**supplemental table IV**). The pharmacokinetic parameters when accounting for insulin resistance (diabetes) and fatty liver (NAFLD) are given in **supplemental table V**.

DISCUSSION

Our studies suggest downregulation of CYP3A4 protein and activity in NAFLD. While some findings were not statistically significant for NAFL, a trend of reduction was observed. This pattern achieved significance for HLM from NASH donors suggesting that the decrease in CYP3A4 activity and CYP3A4 protein continues with the severity of disease as it progresses from benign stage to NAFL and NASH. We also found that insulin resistance along with steatosis appears to provide a double-blow leading to decreased CYP3A4 protein and activity. Similar substrate affinity (K_m) among the groups indicate that the differences seen in the velocity of the reaction (1-hydroxy midazolam formation) were in fact due to an altered enzyme level rather than its affinity for the substrate. Multiple linear regression modeling showed that the variability in midazolam hydroxylation was accounted mainly by CYP3A4 protein in HLM. SimCYP based PBPK model was in good agreement for the healthy population when *in vitro* parameters from this study were used.

Woolsey and colleagues found that midazolam concentrations in human subjects with NASH were significantly higher as compared to control subjects (indicating reduced CYP3A activity).³⁷ Fisher and colleagues suggested a decrease in CYP3A4 expression and functional activity with the progression of NAFLD, but this difference was not statistically significant.³⁴ The same study reported that the mRNA expression was not different between NAFLD groups. We found that the mRNA expression of CYP3A4 and its transcription factors (CAR, PXR, HNF4 α , and PPAR α) was reduced in livers from NAFLD donors, but the effect was statistically insignificant except for CAR mRNA. In contrast, the level of protein expression was significantly lower in such donors possibly indicating the

involvement of transcriptional and translational mechanisms in down-regulation of CYP3A4 activity.

Two primary inducible nuclear transcription regulators of CYP3A4 mRNA expression in human, PXR and CAR, are widely affected by dietary, genetic, environmental and pathological factors.⁴⁸ Similar PXR mRNA levels between fatty and normal human liver microsomes were previously reported.³⁵ HNF4 α was identified as a critical constitutive regulator of PXR and CAR-mediated transcriptional induction of CYP3A4.⁴⁹ Conversely, we found a decrease in HNF4 α levels, but the alteration was statistically insignificant between the three groups. Interestingly, a study on PXR-knockout rat model indicated that down-regulation of hepatic CYP450s via a PXR-independent mechanism.⁵⁰ It could partially explain why the PXR mRNA levels were not significantly different in our study despite a discernible decrease in the disease state. Recently, Woolsey et al. reported that CYP3A4 down-regulation might be due induced fibroblast growth factor 21 (FGF21) leading to reduced PXR localization and binding to the CYP3A4 proximal promoter.⁵¹ While some have reported elevated CAR in the pathogenesis of NASH in mice, other studies suggest a downregulation of CAR.^{52, 53} We also found that CAR mRNA expressed was decreased with progression of NAFLD. PPAR α governs transport and β -oxidation of fatty acid in the liver in addition to regulation of inflammatory response. We found different levels of PPAR α in our groups, but the effect was insignificant. Due to lack of data, we speculate that tandem decrease in levels of transcription factors may result in significant downregulation of some target proteins.

Diabetes and insulin resistance are associated with NAFLD with up to 70% patients having been reported to share both these comorbidities.^{54, 55} Our lab has reported the effect

of diabetes on CYP3A4 expression and activity in human liver, but the impact of NAFLD was not studied.³⁸ In this study, we found that while there was a decrease in CYP3A4 activity and protein, the effect was statistically insignificant in HLM from non-diabetic donors. In contrast, NAFL and NASH donors with diabetes showed a statistically significant decrease in activity, protein expression, and midazolam clearance. Interestingly, we found that diabetic, normal donors exhibited marginally higher CYP3A4 activity and Clint as compared to non-diabetic normal donors. We speculate that this anomaly could be possibly attributed to pharmacological agents that these diabetic donors might be receiving. Our lab is currently pursuing a challenging project to find out the exposure to different drugs at the time of death in our liver bank. Based on the data, we speculate that the heightened reduction of activity and midazolam Clint in diabetic subjects may be due to the double-punch which insulin resistance appears to trigger in steatotic livers. It is also supported in part by lack of statistically significant decrease in CYP3A4 activity in non-diabetic livers.

Kolwankar and colleagues found an independent association between hepatic steatosis and reduced CYP3A activity which decreased with the severity of steatosis.³⁵ Another study in human hepatocytes isolated from macrosteatosis livers found a significant reduction in CYP3A4 activity without any alteration in CPR levels in microsomes from steatotic and nonsteatotic livers.⁵⁶ We also found that livers with >5% hepatic fat were associated with the low CYP3A4 activity and intrinsic clearance of midazolam in HLM.

Previous studies have reported a higher amount of protein, mRNA and CYP3A4 activity in female livers.¹³ In contrast, we found that males exhibited slightly higher CYP3A4 level than females. A few clinical studies have reported that women have higher

CYP3A4 activity than men based on pharmacokinetic studies with cyclosporine, erythromycin, and midazolam.^{57, 58} Conversely, studies with cyclosporine and midazolam suggest an insignificant gender difference in metabolism of these drugs. As CYP3A4 and P-glycoprotein 1 (Pgp) share a large number of common substrates; increased metabolism in females may in part be due to lower Pgp activity in canalicular membrane rather than the CYP3A4 activity in the endoplasmic reticulum.⁵⁹ Schuetz reported that Pgp in women was almost half the levels of that in men.⁶⁰ Moreover, another study in HLM found that median CYP3A4 content was 2-fold higher in women than men with the *CYP3A5**3/*3 livers ($P < 0.05$).⁶¹

Reports on the effect of NAFLD on NADPH-cytochrome P450 reductase (CPR) are lacking. The expression of CPR reduced significantly with progression of disease from NAFL to NASH. Multiple linear regression analysis with CYP3A activity as the dependent variable revealed that CPR protein content does not account for additional variability when CYP3A4 protein is present as a predictor variable. These results are in line with a previous report which found that CYP3A variability was independent of CPR protein level.⁶²

Oxidative stress has been found to be a critical factor associated independently with NAFLD.^{63, 64} We found that livers from NAFLD donors had higher malondialdehyde levels compared to normal donors suggesting increased oxidative stress (**Table 1**). Additionally, liver samples from NAFLD donors exhibited a significantly higher amount of cholesterol as compared to normal donors (**Table 1**). Increased liver cholesterol leads to activation of Kupffer and stellate cells in the liver, thereby promoting inflammation and fibrogenesis.⁶⁵ Production of reactive oxygen species during NAFLD may lead to lipid peroxidation which stimulates subsequent activation of stellate cells resulting in fibrogenesis^{66, 67}.

Studies in the last decade have suggested a strong relationship between metabolic diseases like NAFLD and microRNA expression in human liver.^{68, 69} These miRs can regulate expression and mRNA stability function, in addition to the regulation of lipid metabolism, inflammation, and apoptosis.^{70, 71} Significantly, upregulated miR-155 levels in cirrhotic livers showed a strong negative correlation with CYP3A activity.⁷² Moreover, miR-27b was found to suppress the translation of CYP3A4 protein without affecting the mRNA levels of the enzyme.⁷³ We speculate elevated miR species to be one of the factors responsible for a contrast of mRNA and protein expression levels in NAFLD.

The information on any other underlying disease or drug use by donors at the time of their death was not available. The data on prior drug usage, alcohol consumption, and smoking can be challenging to interpret, and it is naïve to assume that such information provided by the vendor is accurate.⁷⁴ Contrary to this, data on age and gender can be considered reliable. Therefore, we did not evaluate the effect of smoking and alcohol consumption on the CYP3A activity and clearance of midazolam.

The performance of PBPK model in the normal population was used to estimate the accuracy of predictions made in the normal population.⁴⁷ Compared to normal population, a 2.3 fold higher midazolam exposure was predicted by the model for NASH population (**supplemental table IV**), which is consistent with 2.4-fold higher systemic midazolam concentration reported in a clinical study with subjects with NASH.³⁷ PBPK model also suggested prolonged sedation in NAFLD patients with compromised liver function. An average midazolam effective concentration (EC₅₀) of 68.7 ng/mL (10.9-165.0, 95% CI) for a Ramsay score between 3-5 was recently reported in a population-based pharmacodynamic model in Caucasians.⁷⁵ Considering this, PBPK simulation in

NAFLD population showed that the midazolam concentration would remain over EC₅₀ for extended time compared to the normal population (**Fig. 6**). It was reported that subjects with alcoholic cirrhosis had a significantly higher elimination half-life of midazolam compared to healthy subjects.⁷⁶ Indeed, Li et al. have reported that patients with the severe liver disease were more sensitive to midazolam and achieved loss of consciousness at much lower systemic concentration compared to subjects with normal hepatic function.⁷⁷ Therefore, we can speculate that NAFL and NASH patients may also be more sensitive to midazolam than non-NAFLD patients.

Further studies with different probes and population cohorts are warranted to corroborate these findings and understand the underlying mechanism/s responsible for perturbations in CYP3A4 expression. A well-planned in vivo trial would be an ideal study to address the discrepancies in literature but has its limitations. For instance, obtaining a biopsy sample from healthy individuals remains an ethical challenge for researchers. Given these results are largely limited to Caucasian population, care should be taken for interpolation of the results. Efforts are currently underway in our lab to study different pathways involved in regulation of CYP3A4 expression at protein level.

Acknowledgment

Authors would like to acknowledge insights and comments about the work by Drs. Scott Obach and David Rodriguez from Pfizer, Groton, CT. This work was partially presented as a poster at 21st North American ISSX Meeting at Providence, RI, USA, September 24 - 28, 2017.

Conflict of interest

None of the authors have any conflict of interest to declare.

Statement of financial support

Financial support for this study was provided by National Institutes of Health grants to Fatemeh Akhlaghi [grant numbers R15-GM101599, UH3-TR000963]. Some instrumental support for the work was provided by RI-INBRE Centralized Research Core Facility supported by the Institutional Development Award (IDeA) Network for Biomedical Research Excellence from the National Institute of General Medical Sciences of the National Institutes of Health [grant number P20GM103430].

Supporting information

Supplemental table I: Histological characteristics of the donors.

Supplemental table II: PCR primers used in the study.

Supplemental table III: Effect of gender on CYP3A4 activity, protein and mRNA expression.

Supplemental table IV: Predicted pharmacokinetic parameters (Geometric mean, 95% CI) after 5 mg intravenous dose in populations accounting for fatty liver.

Supplemental table V: Predicted pharmacokinetic parameters (Geometric mean, 95% CI) after 5 mg intravenous dose in populations accounting for fatty liver and insulin resistance.

Supplemental figure I. Scheme of the histological scoring system used for group formation in the study.

Supplemental figure II. Correlation of CYP3A4 activity with (A) CYP3A4 mRNA and (B) CYP3A4 protein. (C) Correlation between CYP3A4 mRNA and protein expression.

Supplemental figure III. Effect of different grades of steatosis (A) NADPH cytochrome P450 reductase protein, and (B) Cytochrome b5 protein.

Supplemental figure IV: Spearman correlation analysis of age with (A) CYP3A4 activity (pmol/min/mg protein), (B) CL_{int} (L/min), (C) CYP3A4 protein (pmol/mg protein) and (D) CYP3A4 mRNA.

Supplemental figure V. Association of NADPH-cytochrome P450 reductase with (A) CYP3A4 activity (pmol/min/mg protein) and (B) CYP3A4 protein (pmol/mg protein). Correlation of cytochrome b5 with (C) CYP3A4 activity (pmol/min/mg protein) and (D) CYP3A4 protein (pmol/mg protein). (E) Correlation between NADPH-cytochrome P450 reductase and cytochrome b5 proteins.

REFERENCES

1. Chalasani, N.; Younossi, Z.; Lavine, J. E.; Charlton, M.; Cusi, K.; Rinella, M.; Harrison, S. A.; Brunt, E. M.; Sanyal, A. J. The diagnosis and management of nonalcoholic fatty liver disease: Practice guidance from the American Association for the Study of Liver Diseases. *Hepatology* **2018**, *67*, (1), 328-357.
2. Hashimoto, E.; Tokushige, K.; Ludwig, J. Diagnosis and classification of non-alcoholic fatty liver disease and non-alcoholic steatohepatitis: Current concepts and remaining challenges. *Hepatol Res* **2015**, *45*, (1), 20-8.
3. Farrell, G. C.; Larter, C. Z. Nonalcoholic fatty liver disease: from steatosis to cirrhosis. *Hepatology* **2006**, *43*, (2 Suppl 1), S99-S112.
4. Younossi, Z. M.; Koenig, A. B.; Abdelatif, D.; Fazel, Y.; Henry, L.; Wymer, M. Global epidemiology of nonalcoholic fatty liver disease-Meta-analytic assessment of prevalence, incidence, and outcomes. *Hepatology* **2016**, *64*, (1), 73-84.
5. Bugianesi, E.; Moscatiello, S.; Ciaravella, M. F.; Marchesini, G. Insulin resistance in nonalcoholic fatty liver disease. *Curr Pharm Des* **2010**, *16*, (17), 1941-51.
6. Mikolasevic, I.; Milic, S.; Turk Wensveen, T.; Grgic, I.; Jakopic, I.; Stimac, D.; Wensveen, F.; Orlic, L. Nonalcoholic fatty liver disease - A multisystem disease? *World J Gastroenterol* **2016**, *22*, (43), 9488-9505.
7. Wild, S. H.; Morling, J. R.; McAllister, D. A.; Kerssens, J.; Fischbacher, C.; Parkes, J.; Roderick, P. J.; Sattar, N.; Byrne, C. D.; Scottish; Southampton, D.; Liver Disease, G.; Scottish Diabetes Research Network Epidemiology, G. Type 2 diabetes and risk of hospital admission or death for chronic liver diseases. *J Hepatol* **2016**.

8. Barb, D.; Portillo-Sanchez, P.; Cusi, K. Pharmacological management of nonalcoholic fatty liver disease. *Metabolism* **2016**, *65*, (8), 1183-95.
9. Sumida, Y.; Seko, Y.; Yoneda, M.; Japan Study Group of, N. Novel antidiabetic medications for non-alcoholic fatty liver disease with type 2 diabetes mellitus. *Hepatol Res* **2017**, *47*, (4), 266-280.
10. Takaki, A.; Kawai, D.; Yamamoto, K. Molecular mechanisms and new treatment strategies for non-alcoholic steatohepatitis (NASH). *Int J Mol Sci* **2014**, *15*, (5), 7352-79.
11. Guengerich, F. P. Cytochrome P-450 3A4: regulation and role in drug metabolism. *Annu Rev Pharmacol Toxicol* **1999**, *39*, 1-17.
12. Zanger, U. M.; Schwab, M. Cytochrome P450 enzymes in drug metabolism: regulation of gene expression, enzyme activities, and impact of genetic variation. *Pharmacol Ther* **2013**, *138*, (1), 103-41.
13. Lamba, V.; Panetta, J. C.; Strom, S.; Schuetz, E. G. Genetic predictors of interindividual variability in hepatic CYP3A4 expression. *J Pharmacol Exp Ther* **2010**, *332*, (3), 1088-99.
14. Ueng, Y. F.; Shimada, T.; Yamazaki, H.; Guengerich, F. P. Oxidation of aflatoxin B1 by bacterial recombinant human cytochrome P450 enzymes. *Chem Res Toxicol* **1995**, *8*, (2), 218-25.
15. Waxman, D. J.; Attisano, C.; Guengerich, F. P.; Lapenson, D. P. Human liver microsomal steroid metabolism: identification of the major microsomal steroid hormone 6 beta-hydroxylase cytochrome P-450 enzyme. *Arch Biochem Biophys* **1988**, *263*, (2), 424-36.

16. Abel, S. M.; Back, D. J. Cortisol metabolism in vitro--III. Inhibition of microsomal 6 beta-hydroxylase and cytosolic 4-ene-reductase. *J Steroid Biochem Mol Biol* **1993**, *46*, (6), 827-32.
17. Yamazaki, H.; Shimada, T. Progesterone and testosterone hydroxylation by cytochromes P450 2C19, 2C9, and 3A4 in human liver microsomes. *Arch Biochem Biophys* **1997**, *346*, (1), 161-9.
18. Diczfalusy, U.; Nylen, H.; Elander, P.; Bertilsson, L. 4beta-Hydroxycholesterol, an endogenous marker of CYP3A4/5 activity in humans. *Br J Clin Pharmacol* **2011**, *71*, (2), 183-9.
19. Martinez-Jimenez, C. P.; Jover, R.; Donato, M. T.; Castell, J. V.; Gomez-Lechon, M. J. Transcriptional regulation and expression of CYP3A4 in hepatocytes. *Curr Drug Metab* **2007**, *8*, (2), 185-94.
20. Thomas, M.; Burk, O.; Klumpp, B.; Kandel, B. A.; Damm, G.; Weiss, T. S.; Klein, K.; Schwab, M.; Zanger, U. M. Direct transcriptional regulation of human hepatic cytochrome P450 3A4 (CYP3A4) by peroxisome proliferator-activated receptor alpha (PPARalpha). *Mol Pharmacol* **2013**, *83*, (3), 709-18.
21. Lau, J. K.; Zhang, X.; Yu, J. Animal models of non-alcoholic fatty liver disease: current perspectives and recent advances. *J Pathol* **2017**, *241*, (1), 36-44.
22. Dietrich, C. G.; Rau, M.; Jahn, D.; Geier, A. Changes in drug transport and metabolism and their clinical implications in non-alcoholic fatty liver disease. *Expert opinion on drug metabolism & toxicology* **2017**, *13*, (6), 625-640.
23. Machado, M. V.; Michelotti, G. A.; Xie, G.; Almeida Pereira, T.; Boursier, J.; Bohnic, B.; Guy, C. D.; Diehl, A. M. Mouse models of diet-induced nonalcoholic

steatohepatitis reproduce the heterogeneity of the human disease. *PLoS One* **2015**, *10*, (5), e0127991.

24. Baumgardner, J. N.; Shankar, K.; Hennings, L.; Badger, T. M.; Ronis, M. J. A new model for nonalcoholic steatohepatitis in the rat utilizing total enteral nutrition to overfeed a high-polyunsaturated fat diet. *Am J Physiol Gastrointest Liver Physiol* **2008**, *294*, (1), G27-38.

25. Li, P.; Robertson, T. A.; Thorling, C. A.; Zhang, Q.; Fletcher, L. M.; Crawford, D. H.; Roberts, M. S. Hepatic pharmacokinetics of cationic drugs in a high-fat emulsion-induced rat model of nonalcoholic steatohepatitis. *Drug Metab Dispos* **2011**, *39*, (4), 571-9.

26. Weltman, M. D.; Farrell, G. C.; Liddle, C. Increased hepatocyte CYP2E1 expression in a rat nutritional model of hepatic steatosis with inflammation. *Gastroenterology* **1996**, *111*, (6), 1645-53.

27. Zhang, Y. K.; Yeager, R. L.; Tanaka, Y.; Klaassen, C. D. Enhanced expression of Nrf2 in mice attenuates the fatty liver produced by a methionine- and choline-deficient diet. *Toxicol Appl Pharmacol* **2010**, *245*, (3), 326-34.

28. Li, H.; Clarke, J. D.; Dzierlenga, A. L.; Bear, J.; Goedken, M. J.; Cherrington, N. J. In vivo cytochrome P450 activity alterations in diabetic nonalcoholic steatohepatitis mice. *Journal of biochemical and molecular toxicology* **2017**, *31*, (2).

29. Fisher, C. D.; Jackson, J. P.; Lickteig, A. J.; Augustine, L. M.; Cherrington, N. J. Drug metabolizing enzyme induction pathways in experimental non-alcoholic steatohepatitis. *Arch Toxicol* **2008**, *82*, (12), 959-64.

30. Kim, S.; Sohn, I.; Ahn, J. I.; Lee, K. H.; Lee, Y. S.; Lee, Y. S. Hepatic gene expression profiles in a long-term high-fat diet-induced obesity mouse model. *Gene* **2004**, *340*, (1), 99-109.
31. Yoshinari, K.; Takagi, S.; Sugatani, J.; Miwa, M. Changes in the expression of cytochromes P450 and nuclear receptors in the liver of genetically diabetic db/db mice. *Biol Pharm Bull* **2006**, *29*, (8), 1634-8.
32. Greco, D.; Kotronen, A.; Westerbacka, J.; Puig, O.; Arkkila, P.; Kiviluoto, T.; Laitinen, S.; Kolak, M.; Fisher, R. M.; Hamsten, A.; Auvinen, P.; Yki-Jarvinen, H. Gene expression in human NAFLD. *Am J Physiol Gastrointest Liver Physiol* **2008**, *294*, (5), G1281-7.
33. Lake, A. D.; Novak, P.; Fisher, C. D.; Jackson, J. P.; Hardwick, R. N.; Billheimer, D. D.; Klimecki, W. T.; Cherrington, N. J. Analysis of global and absorption, distribution, metabolism, and elimination gene expression in the progressive stages of human nonalcoholic fatty liver disease. *Drug Metab Dispos* **2011**, *39*, (10), 1954-60.
34. Fisher, C. D.; Lickteig, A. J.; Augustine, L. M.; Ranger-Moore, J.; Jackson, J. P.; Ferguson, S. S.; Cherrington, N. J. Hepatic cytochrome P450 enzyme alterations in humans with progressive stages of nonalcoholic fatty liver disease. *Drug Metab Dispos* **2009**, *37*, (10), 2087-94.
35. Kolwankar, D.; Vuppalanchi, R.; Ethell, B.; Jones, D. R.; Wrighton, S. A.; Hall, S. D.; Chalasani, N. Association between nonalcoholic hepatic steatosis and hepatic cytochrome P-450 3A activity. *Clin Gastroenterol Hepatol* **2007**, *5*, (3), 388-93.
36. Niemela, O.; Parkkila, S.; Juvonen, R. O.; Viitala, K.; Gelboin, H. V.; Pasanen, M. Cytochromes P450 2A6, 2E1, and 3A and production of protein-aldehyde adducts in the

liver of patients with alcoholic and non-alcoholic liver diseases. *J Hepatol* **2000**, *33*, (6), 893-901.

37. Woolsey, S. J.; Mansell, S. E.; Kim, R. B.; Tirona, R. G.; Beaton, M. D. CYP3A Activity and Expression in Nonalcoholic Fatty Liver Disease. *Drug Metab Dispos* **2015**, *43*, (10), 1484-90.

38. Dostalek, M.; Court, M. H.; Yan, B.; Akhlaghi, F. Significantly reduced cytochrome P450 3A4 expression and activity in liver from humans with diabetes mellitus. *Br J Pharmacol* **2011**, *163*, (5), 937-47.

39. Kleiner, D. E.; Brunt, E. M.; Van Natta, M.; Behling, C.; Contos, M. J.; Cummings, O. W.; Ferrell, L. D.; Liu, Y. C.; Torbenson, M. S.; Unalp-Arida, A.; Yeh, M.; McCullough, A. J.; Sanyal, A. J.; Nonalcoholic Steatohepatitis Clinical Research, N. Design and validation of a histological scoring system for nonalcoholic fatty liver disease. *Hepatology* **2005**, *41*, (6), 1313-21.

40. Caldwell, S.; Ikura, Y.; Dias, D.; Isomoto, K.; Yabu, A.; Moskaluk, C.; Pramoonjago, P.; Simmons, W.; Scruggs, H.; Rosenbaum, N.; Wilkinson, T.; Toms, P.; Argo, C. K.; Al-Osaimi, A. M.; Redick, J. A. Hepatocellular ballooning in NASH. *J Hepatol* **2010**, *53*, (4), 719-23.

41. Bedossa, P.; Poitou, C.; Veyrie, N.; Bouillot, J. L.; Basdevant, A.; Paradis, V.; Tordjman, J.; Clement, K. Histopathological algorithm and scoring system for evaluation of liver lesions in morbidly obese patients. *Hepatology* **2012**, *56*, (5), 1751-9.

42. Jamwal, R.; Barlock, B. J.; Adusumalli, S.; Ogasawara, K.; Simons, B. L.; Akhlaghi, F. Multiplex and Label-Free Relative Quantification Approach for Studying

Protein Abundance of Drug Metabolizing Enzymes in Human Liver Microsomes Using SWATH-MS. *J Proteome Res* **2017**, *16*, (11), 4134-4143.

43. Dostalek, M.; Macwan, J. S.; Chitnis, S. D.; Ionita, I. A.; Akhlaghi, F. Development and validation of a rapid and sensitive assay for simultaneous quantification of midazolam, 1'-hydroxymidazolam, and 4-hydroxymidazolam by liquid chromatography coupled to tandem mass-spectrometry. *J Chromatogr B Analyt Technol Biomed Life Sci* **2010**, *878*, (19), 1629-33.

44. Wisniewski, J. R.; Rakus, D. Multi-enzyme digestion FASP and the 'Total Protein Approach'-based absolute quantification of the Escherichia coli proteome. *J Proteomics* **2014**, *109*, 322-31.

45. Cox, J.; Mann, M. MaxQuant enables high peptide identification rates, individualized p.p.b.-range mass accuracies and proteome-wide protein quantification. *Nat Biotechnol* **2008**, *26*, (12), 1367-72.

46. Dostalek, M.; Sam, W. J.; Paryani, K. R.; Macwan, J. S.; Gohh, R. Y.; Akhlaghi, F. Diabetes mellitus reduces the clearance of atorvastatin lactone: results of a population pharmacokinetic analysis in renal transplant recipients and in vitro studies using human liver microsomes. *Clin Pharmacokinet* **2012**, *51*, (9), 591-606.

47. Schwagmeier, R.; Alincic, S.; Striebel, H. W. Midazolam pharmacokinetics following intravenous and buccal administration. *Br J Clin Pharmacol* **1998**, *46*, (3), 203-6.

48. Tolson, A. H.; Wang, H. Regulation of drug-metabolizing enzymes by xenobiotic receptors: PXR and CAR. *Adv Drug Deliv Rev* **2010**, *62*, (13), 1238-49.

49. Tirona, R. G.; Lee, W.; Leake, B. F.; Lan, L. B.; Cline, C. B.; Lamba, V.; Parviz, F.; Duncan, S. A.; Inoue, Y.; Gonzalez, F. J.; Schuetz, E. G.; Kim, R. B. The orphan nuclear receptor HNF4 α determines PXR- and CAR-mediated xenobiotic induction of CYP3A4. *Nat Med* **2003**, *9*, (2), 220-4.
50. Richardson, T. A.; Morgan, E. T. Hepatic cytochrome P450 gene regulation during endotoxin-induced inflammation in nuclear receptor knockout mice. *J Pharmacol Exp Ther* **2005**, *314*, (2), 703-9.
51. Woolsey, S. J.; Beaton, M. D.; Mansell, S. E.; Leon-Ponte, M.; Yu, J.; Pin, C. L.; Adams, P. C.; Kim, R. B.; Tirona, R. G. A Fibroblast Growth Factor 21-Pregnane X Receptor Pathway Downregulates Hepatic CYP3A4 in Nonalcoholic Fatty Liver Disease. *Mol Pharmacol* **2016**, *90*, (4), 437-46.
52. Dong, B.; Saha, P. K.; Huang, W.; Chen, W.; Abu-Elheiga, L. A.; Wakil, S. J.; Stevens, R. D.; Ilkayeva, O.; Newgard, C. B.; Chan, L.; Moore, D. D. Activation of nuclear receptor CAR ameliorates diabetes and fatty liver disease. *Proc Natl Acad Sci U S A* **2009**, *106*, (44), 18831-6.
53. Yamazaki, Y.; Kakizaki, S.; Horiguchi, N.; Sohara, N.; Sato, K.; Takagi, H.; Mori, M.; Negishi, M. The role of the nuclear receptor constitutive androstane receptor in the pathogenesis of non-alcoholic steatohepatitis. *Gut* **2007**, *56*, (4), 565-74.
54. Hazlehurst, J. M.; Woods, C.; Marjot, T.; Cobbold, J. F.; Tomlinson, J. W. Non-alcoholic fatty liver disease and diabetes. *Metabolism* **2016**, *65*, (8), 1096-108.
55. Williamson, R. M.; Price, J. F.; Glancy, S.; Perry, E.; Nee, L. D.; Hayes, P. C.; Frier, B. M.; Van Look, L. A.; Johnston, G. I.; Reynolds, R. M.; Strachan, M. W.; Edinburgh Type 2 Diabetes Study, I. Prevalence of and risk factors for hepatic steatosis

and nonalcoholic Fatty liver disease in people with type 2 diabetes: the Edinburgh Type 2 Diabetes Study. *Diabetes Care* **2011**, *34*, (5), 1139-44.

56. Donato, M. T.; Lahoz, A.; Jimenez, N.; Perez, G.; Serralta, A.; Mir, J.; Castell, J. V.; Gomez-Lechon, M. J. Potential impact of steatosis on cytochrome P450 enzymes of human hepatocytes isolated from fatty liver grafts. *Drug Metab Dispos* **2006**, *34*, (9), 1556-62.

57. Meibohm, B.; Beierle, I.; Derendorf, H. How important are gender differences in pharmacokinetics? *Clin Pharmacokinet* **2002**, *41*, (5), 329-42.

58. Tanaka, E. Gender-related differences in pharmacokinetics and their clinical significance. *J Clin Pharm Ther* **1999**, *24*, (5), 339-46.

59. Cummins, C. L.; Jacobsen, W.; Benet, L. Z. Unmasking the dynamic interplay between intestinal P-glycoprotein and CYP3A4. *J Pharmacol Exp Ther* **2002**, *300*, (3), 1036-45.

60. Schuetz, E. G.; Furuya, K. N.; Schuetz, J. D. Interindividual variation in expression of P-glycoprotein in normal human liver and secondary hepatic neoplasms. *J Pharmacol Exp Ther* **1995**, *275*, (2), 1011-8.

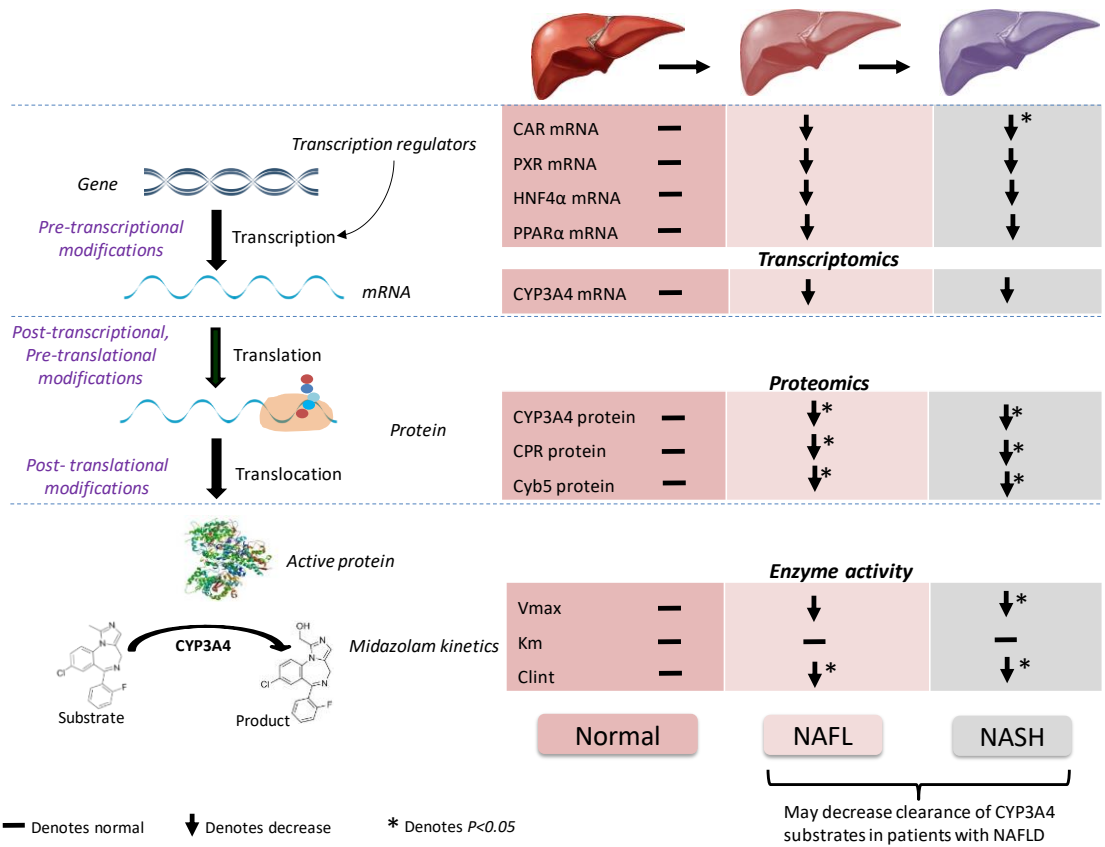
61. Lin, Y. S.; Dowling, A. L.; Quigley, S. D.; Farin, F. M.; Zhang, J.; Lamba, J.; Schuetz, E. G.; Thummel, K. E. Co-regulation of CYP3A4 and CYP3A5 and contribution to hepatic and intestinal midazolam metabolism. *Mol Pharmacol* **2002**, *62*, (1), 162-72.

62. Gan, L.; von Moltke, L. L.; Trepanier, L. A.; Harmatz, J. S.; Greenblatt, D. J.; Court, M. H. Role of NADPH-cytochrome P450 reductase and cytochrome-b5/NADH-b5 reductase in variability of CYP3A activity in human liver microsomes. *Drug Metab Dispos* **2009**, *37*, (1), 90-6.

63. Narasimhan, S.; Gokulakrishnan, K.; Sampathkumar, R.; Farooq, S.; Ravikumar, R.; Mohan, V.; Balasubramanyam, M. Oxidative stress is independently associated with non-alcoholic fatty liver disease (NAFLD) in subjects with and without type 2 diabetes. *Clin Biochem* **2010**, *43*, (10-11), 815-21.
64. Spahis, S.; Delvin, E.; Borys, J. M.; Levy, E. Oxidative Stress as a Critical Factor in Nonalcoholic Fatty Liver Disease Pathogenesis. *Antioxid Redox Signal* **2016**.
65. Arguello, G.; Balboa, E.; Arrese, M.; Zanlungo, S. Recent insights on the role of cholesterol in non-alcoholic fatty liver disease. *Biochim Biophys Acta* **2015**, *1852*, (9), 1765-78.
66. Angulo, P. Nonalcoholic fatty liver disease. *N Engl J Med* **2002**, *346*, (16), 1221-31.
67. Polimeni, L.; Del Ben, M.; Baratta, F.; Perri, L.; Albanese, F.; Pastori, D.; Violi, F.; Angelico, F. Oxidative stress: New insights on the association of non-alcoholic fatty liver disease and atherosclerosis. *World J Hepatol* **2015**, *7*, (10), 1325-36.
68. Cheung, O.; Puri, P.; Eicken, C.; Contos, M. J.; Mirshahi, F.; Maher, J. W.; Kellum, J. M.; Min, H.; Luketic, V. A.; Sanyal, A. J. Nonalcoholic steatohepatitis is associated with altered hepatic MicroRNA expression. *Hepatology* **2008**, *48*, (6), 1810-20.
69. Willeit, P.; Skroblin, P.; Kiechl, S.; Fernandez-Hernando, C.; Mayr, M. Liver microRNAs: potential mediators and biomarkers for metabolic and cardiovascular disease? *Eur Heart J* **2016**, *37*, (43), 3260-3266.
70. Pirola, C. J.; Fernandez Gianotti, T.; Castano, G. O.; Mallardi, P.; San Martino, J.; Mora Gonzalez Lopez Ledesma, M.; Flichman, D.; Mirshahi, F.; Sanyal, A. J.; Sookoian,

- S. Circulating microRNA signature in non-alcoholic fatty liver disease: from serum non-coding RNAs to liver histology and disease pathogenesis. *Gut* **2015**, *64*, (5), 800-12.
71. Szabo, G.; Csak, T. Role of MicroRNAs in NAFLD/NASH. *Dig Dis Sci* **2016**, *61*, (5), 1314-24.
72. Vuppalanchi, R.; Liang, T.; Goswami, C. P.; Nalamasu, R.; Li, L.; Jones, D.; Wei, R.; Liu, W.; Sarasani, V.; Janga, S. C.; Chalasani, N. Relationship between differential hepatic microRNA expression and decreased hepatic cytochrome P450 3A activity in cirrhosis. *PLoS One* **2013**, *8*, (9), e74471.
73. Ekstrom, L.; Skilving, I.; Ovesjo, M. L.; Aklillu, E.; Nylen, H.; Rane, A.; Diczfalusy, U.; Bjorkhem-Bergman, L. miRNA-27b levels are associated with CYP3A activity in vitro and in vivo. *Pharmacol Res Perspect* **2015**, *3*, (6), e00192.
74. Parkinson, A.; Mudra, D. R.; Johnson, C.; Dwyer, A.; Carroll, K. M. The effects of gender, age, ethnicity, and liver cirrhosis on cytochrome P450 enzyme activity in human liver microsomes and inducibility in cultured human hepatocytes. *Toxicol Appl Pharmacol* **2004**, *199*, (3), 193-209.
75. Franken, L. G.; de Winter, B. C. M.; Masman, A. D.; van Dijk, M.; Baar, F. P. M.; Tibboel, D.; Koch, B. C. P.; van Gelder, T.; Mathot, R. A. A. Population pharmacodynamic modelling of midazolam induced sedation in terminally ill adult patients. *Br J Clin Pharmacol* **2017**.
76. MacGilchrist, A. J.; Birnie, G. G.; Cook, A.; Scobie, G.; Murray, T.; Watkinson, G.; Brodie, M. J. Pharmacokinetics and pharmacodynamics of intravenous midazolam in patients with severe alcoholic cirrhosis. *Gut* **1986**, *27*, (2), 190-5.

77. Li, Y. H.; He, R.; Ruan, J. G. Effect of hepatic function on the EC50 of midazolam and the BIS50 at the time of loss of consciousness. *J Zhejiang Univ Sci B* **2014**, *15*, (8), 743-9.



Graphical abstract

Table 1: Overview of Caucasian donor demographics

	Normal	NAFL	NASH
n (Male, Female)	24 (13, 11)	26 (10, 16)	24 (11, 13)
Ethnicity[#] (n) C, AA, H	24, 0, 0	26, 0, 0	22, 1, 1
Age¹ (years)	50.2±3.0	52.4± 2.1	53.1±2.1
Body-mass index¹ (kg/m²)	31.4±3.0	33.9±2.5	32.5±1.6
Diabetes mellitus (no, yes)	11, 13	14, 12	11, 13
Liver weight¹ (kg)	1.6±0.1	2.0±0.2	1.9±0.1
Body weight¹ (kg)	88.7±7.2	97.1±6.6	94.0±4.7
Malondialdehyde¹ (nmol/mg protein)	0.7±0.1	1.2±0.2**	1.5±0.2**
Cholesterol¹ (µg/mg liver)	16.3±1.3	21.0±1.7*	22.6±1.9**
CYP3A5*3/*3 (n)	24	26	24
CYP3A4*22 (n) *1/*1, *1/*22	23, 1	23, 3	23, 1
CYP3A4*1B (n) *1/*1, *1/*1B	24, 0	26, 0	23, 1

[#]C-Caucasian, AA-Afro-American, H-Hispanic; ¹All descriptive statistics values represent mean ± SE. **P* < 0.05, ***P* < 0.01 as compared to normal. *P*-values reported from non-parametric Kruskal-Wallis test (2-sided) without adjustment for multiple comparisons.

Table 2: Effect of nonalcoholic fatty liver disease on midazolam hydroxylation parameters

	Normal	NAFL	NASH
V_{max} (pmol/min/mg protein)	553.8±134.9	281.2±80.9	176.2±40.4*
K_m (μM)	1.6±0.1	2.0±0.2	2.3±0.4
CL_{int}, whole liver (L/min)	7.3±1.8	2.7±0.9*	1.8±0.6**

All descriptive statistics values represent mean±SE. * $P < 0.05$, ** $P < 0.01$ as compared to normal. P -values reported from non-parametric Kruskal-Wallis test (2-sided) without adjustment for multiple comparisons.

Table 3: Effect of nonalcoholic fatty liver disease on protein abundance

	Normal	NAFL	NASH
CYP3A4 (pmol/mg protein)	131.8±20.4	68.0±18.0*	59.9±7.3*
CPR (pmol/mg protein)	51.1±2.3	39.3±2.4**	36.6±1.9**
Cyb5 (pmol/mg protein)	654.5±41.2	506.5±26.3*	515.3±24.6*

All descriptive statistics values represent mean±SE. * $P < 0.05$, ** $P < 0.01$ as compared to normal. P -values reported from nonparametric Kruskal-Wallis test (2-sided) without adjustment for multiple comparisons.

Table 4: Effect of diabetes and NAFLD on CYP3A4 activity, protein and mRNA expression, and relevant proteins and transcription factors

	Non-diabetic			Diabetic		
	Normal (n=11)	NAFL (n=14)	NASH (n=11)	Normal (n=13)	NAFL (n=12)	NASH (n=13)
V _{max} pmol/min/mg protein	528.4±243.7	411.6±140.2	264.2±79.4	575.3±149.8	129.2±34.7**	101.7±17.6**
K _m (μM)	1.8±0.2	2.2±0.4	2.6±0.7	1.4±0.1	1.7±0.2	2.0±0.4
CL _{int} (L/min)	5.1±2.6	3.5±1.6	2.8±1.3	9.2±2.6	1.6±0.7**	1.0±0.2**
CYP3A4 (pmol/mg protein)	125.7±30.2	95.1±28.9	75.3±12.2	137.4±28.6	32.8±11.7**	48.1±7.7*
CPR (pmol/mg protein)	48.2±3.16	40.6±3.4	34.0±2.9*	53.5±3.3	37.5±3.4*	38.5±2.4*
Cyb5 (pmol/mg protein)	580.4±42.9	498.6±30.5	495.9±47.7	716.2±62.7	516.6±47.5**	527.3±27.9*
CYP3A4 mRNA	9.5±3.9	8.7±4.7	6.6±3.3	4.8±1.4	1.7±0.9	2.1±0.7
PXR mRNA	2.7±0.5	2.0±0.4	1.7±0.5	3.9±1.8	2.4±0.7	1.3±0.4
CAR mRNA	2.1±0.4	2.2±0.6	1.7±0.4	2.3±0.5	1.7±0.3	1.6±0.3
HNF4α mRNA	1.6±0.5	2.2±0.6	1.9±0.6	2.1±0.4	1.0±0.2*	1.4±0.4
PPARα mRNA	1.6±0.5	1.3±0.3	1.1±0.3	1.5±0.2	0.9±0.2	1.2±0.3

All descriptive statistics value represent mean±SE. * $P < 0.05$, ** $P < 0.01$ as compared to normal. P -values reported from nonparametric Kruskal-Wallis test (2-sided) without adjustment for multiple comparisons. Messenger RNA data expressed relative to 18S rRNA.

Table 4: Effect of diabetes and NAFLD on CYP3A4 activity, protein and mRNA expression, and relevant proteins and transcription factors

Figure legends

Figure 1. Histological staining of liver sections. (A, D) normal controls, (B, E) patients with diabetes mellitus and hepatic steatosis, i.e. non-alcoholic fatty liver (NAFL), and (C, F) patients with diabetes mellitus and non-alcoholic fatty liver disease with inflammation, i.e. non-alcoholic steatohepatitis (NASH) were stained with (A-C) Hematoxylin and Eosin or (D-F) Sirius Red. (A) Control livers exhibited uniform chord-like arrangements of hepatocytes, (A-Inset) homogeneous cytoplasm, and (D and D-inset) minimal delicate Sirius red staining of sinusoidal collagen. (B) In diabetes, NAFL was associated with (B, B-inset) macrovesicular (large vacuoles filling cytoplasm) and microvesicular (clusters of small cytoplasmic vacuoles) lipid droplets (clear circumscribed structures in cytoplasm) and (E, E-inset) predominantly delicate but focally moderate Sirius red labeling of sinusoidal and pericellular collagen. (C) In patients with diabetes and NASH, the livers showed abundant (C, C-inset) macrovesicular and microvesicular lipid vacuoles in hepatocytes, conspicuous lymphomononuclear inflammatory cell infiltrates among hepatocytes, and (F) prominent Sirius red staining of bridging fibrosis and (F-inset) peri-hepatocyte collagen. (Original magnifications x625)

Figure 2. Effect of nonalcoholic fatty liver disease on CYP3A4 activity. (A) CYP3A4 activity, (B) CLint (whole liver). Column and error bars represent mean \pm SE. * P <0.05 as compared to normal. P -values reported from nonparametric Kruskal-Wallis test (2-sided) without adjustment for multiple comparisons.

Figure 3. Effect of nonalcoholic fatty liver disease on protein expression. (A) CYP3A4, (B) cytochrome P450 reductase and (C) Cytochrome b5 protein. Column and error bars

represent mean±SE. * P <0.05 as compared to normal. P -values reported from nonparametric Kruskal-Wallis test (2-sided) without adjustment for multiple comparisons.

Figure 4. Effect of nonalcoholic fatty liver disease on relative mRNA expression. (A) CYP3A4 mRNA, (B) CAR mRNA, (C) PXR mRNA and (D) HNF4 α mRNA. Column and error bars represent mean±SE. * P <0.05 as compared to normal. P -values reported from nonparametric Kruskal-Wallis test (2-sided) without adjustment for multiple comparisons. Messenger RNA data expressed relative to 18S rRNA

Figure 5. Effect of different grades of steatosis. (A) CYP3A4 activity, (B) CLint (whole liver), (C) CYP3A4 protein. Column and error bars represent mean±SE. * P <0.05 as compared to <5% liver fat. P -values reported from nonparametric Kruskal-Wallis test (2-sided) without adjustment for multiple comparisons.

Figure 6. SimCYP predicted plasma concentration of midazolam in virtual Caucasian population indicating a higher concentration and longer sedation time with respect to disease state (A) in a virtual population of normal, NAFL or NASH patients irrespective of diabetes status (B) without diabetes normal versus NAFL or NASH (C) with diabetes normal versus NAFL or NASH.

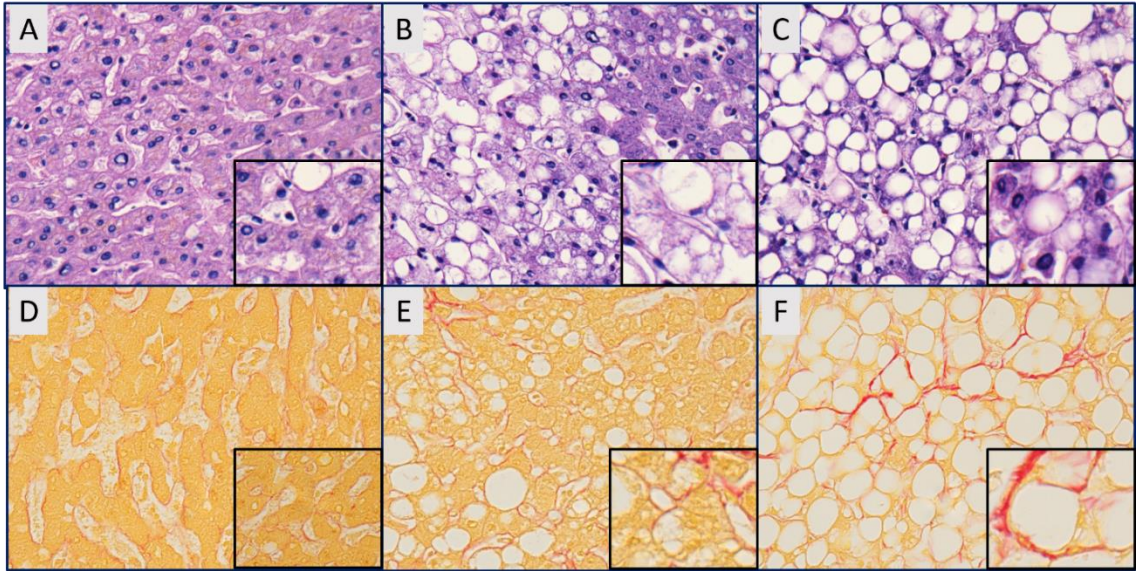


Figure 1.

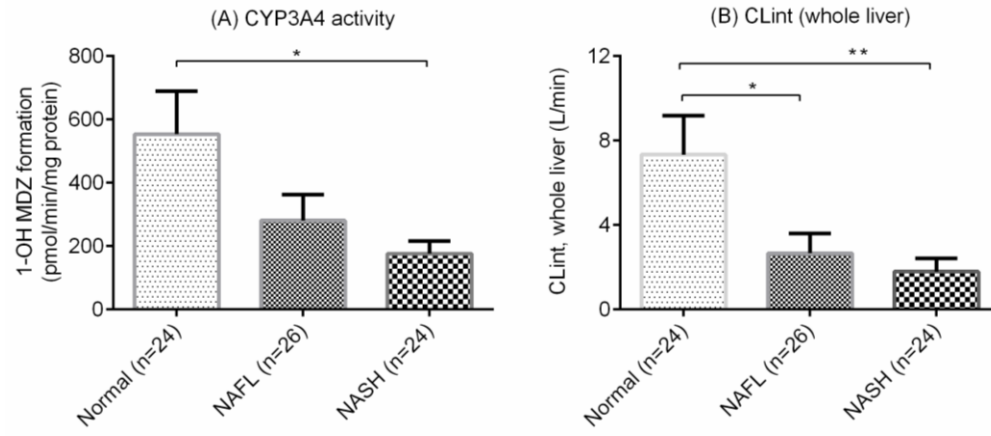


Figure 2.

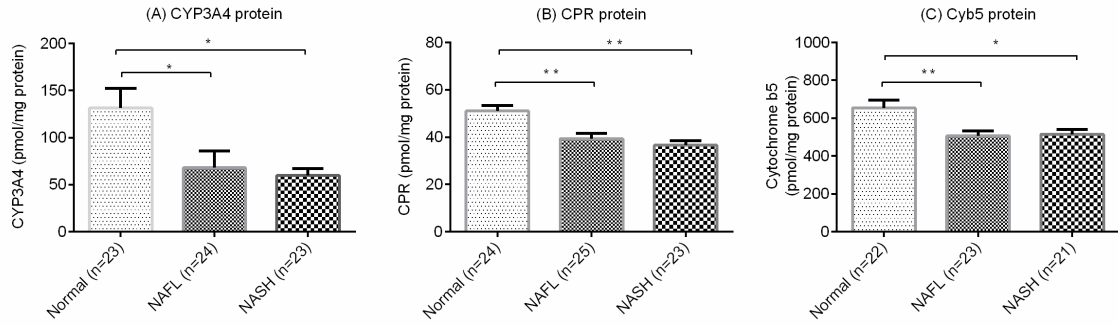


Figure 3.

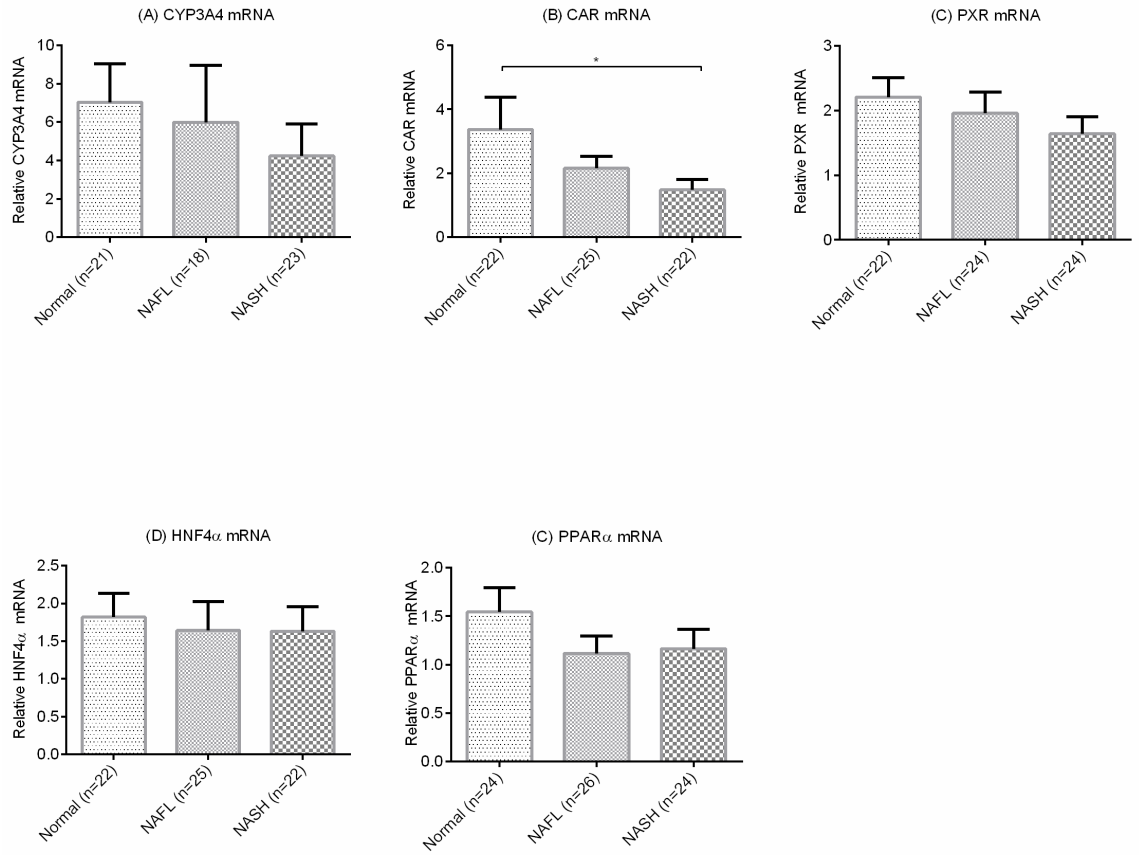


Figure 4.

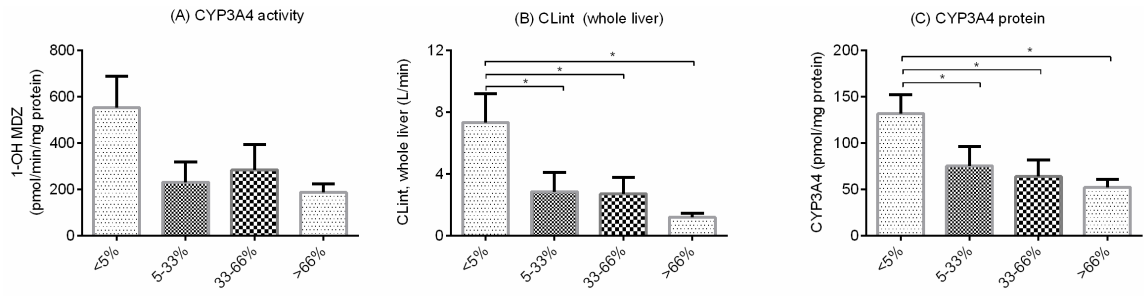


Figure 5.

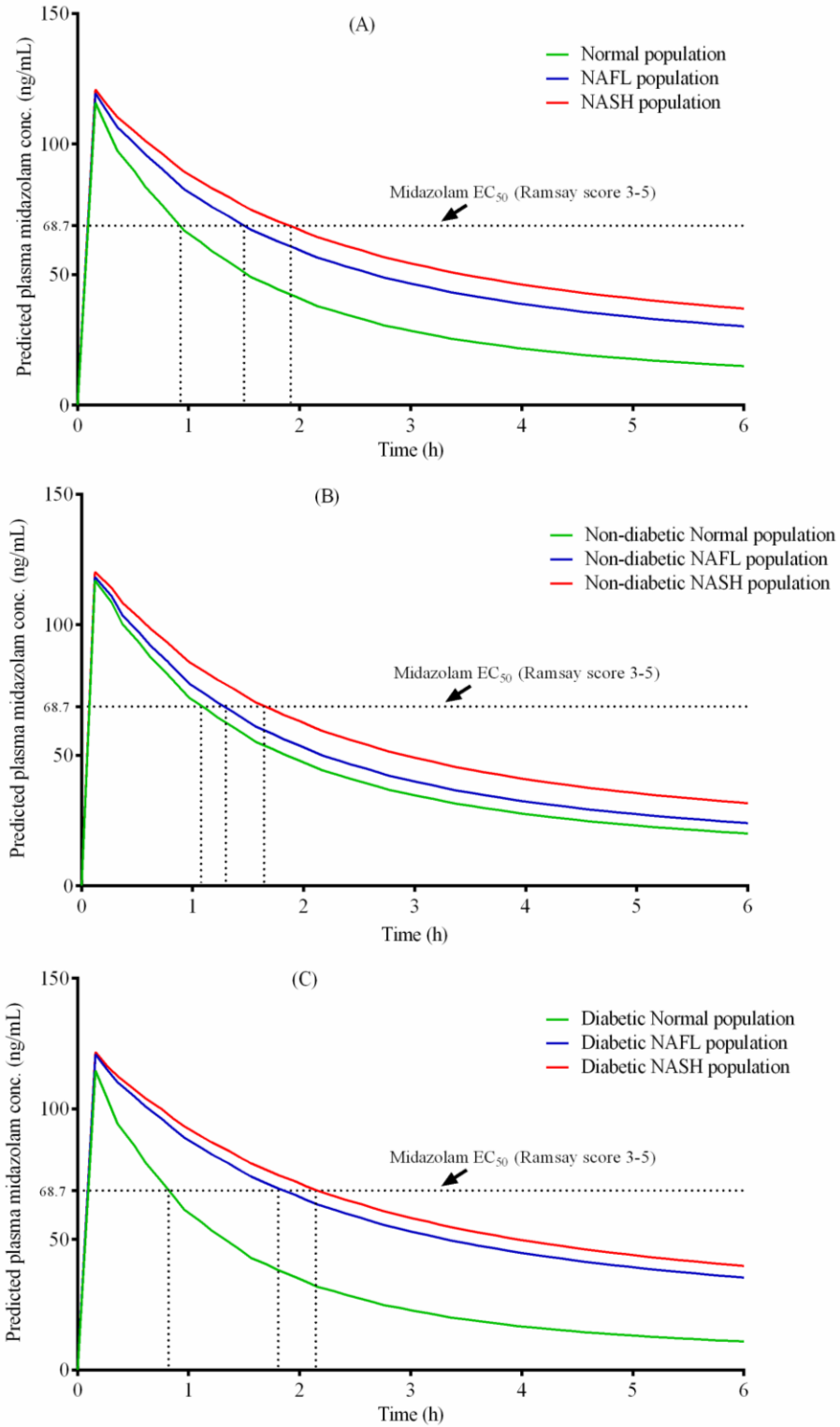


Figure 6.

Supplemental table files

Supplemental table 1: Histological characteristics of the donors.

Supplemental table II: PCR primers used in the study.

Supplemental table III: Effect of gender on CYP3A4 activity, protein and mRNA expression.

Supplemental table IV: Predicted pharmacokinetic parameters (Geometric mean, 95% CI) after 5 mg intravenous dose in populations accounting for fatty liver.

Supplemental table V: Predicted pharmacokinetic parameters (Geometric mean, 95% CI) after 5 mg intravenous dose in populations accounting for fatty liver and insulin resistance.

Supplemental figure files

Supplemental figure I. Scheme of the histological scoring system used for group formation in the study.

Supplemental figure II. Correlation of CYP3A4 activity with (A) CYP3A4 mRNA and (B) CYP3A4 protein. (C) Correlation between CYP3A4 mRNA and protein expression. $P < 0.05$ were considered significant. Correlation coefficient represents Spearman r . Messenger RNA data expressed relative to 18S rRNA. Some parameters were \log_{10} transformed for graphical representation.

Supplemental figure III. Effect of different grades of steatosis (A) NADPH cytochrome P450 reductase protein, and (B) Cytochrome b5 protein. Column and error bars represent

mean \pm SE. * $P < 0.05$ as compared to $< 5\%$ liver fat. * P -values reported from nonparametric Kruskal-Wallis test (2-sided) without adjustment for multiple comparisons.

Supplemental figure IV: Spearman correlation analysis of age with (A) CYP3A4 activity (pmol/min/mg protein), (B) CL_{int} (L/min), (C) CYP3A4 protein (pmol/mg protein) and (D) CYP3A4 mRNA. $P < 0.05$ was considered significant. Correlation coefficient represents Spearman r . Messenger RNA data expressed relative to 18S rRNA. Closed circles represent normal, open circles represent NAFL and triangles represent NASH samples.

Supplemental figure V. Association of NADPH-cytochrome P450 reductase with (A) CYP3A4 activity (pmol/min/mg protein) and (B) CYP3A4 protein (pmol/mg protein). Correlation of cytochrome b5 with (C) CYP3A4 activity (pmol/min/mg protein) and (D) CYP3A4 protein (pmol/mg protein). (E) Correlation between NADPH-cytochrome P450 reductase and cytochrome b5 proteins. $P < 0.05$ was considered significant. Correlation coefficient represents Spearman r . Messenger RNA data expressed relative to 18S rRNA. Some parameters were \log_{10} transformed for graphical representation.

Supplemental tables

Supplemental table 1: Histological characteristics of donors			
Histological score	Normal n=24	NAFL n=26	NASH n=24
Steatosis			
0	24	0	0
1	0	12	7
2	0	7	7
3	0	7	10
Hepatocyte ballooning			
0	23	19	0
1	1	6	18
2	0	1	6
Lobular inflammation			
0	9	9	0
1	12	13	18
2	3	4	6
Fibrosis			
0	12	10	8
1	9	11	12
2	2	4	3
3	1	1	1
Diabetic	11	14	11
Non-diabetic	13	12	13

Supplemental table II: PCR primers used in the study

Gene	Primer type	Primer Sequence	Length	GC number	GC %	Tm
CYP3A4	Forward	CTTTTATGATGGTCAACAGCCTGTG	25	11	44	58.8
	Reverse	CTTTTCATAAATCCCCTGGACCA	24	10	42	57.1
CYP3A5	Forward	CCCACACCTCTGCCTTTG	18	11	61	58.1
	Reverse	CAGGGAGTTGACCTTCATACG	21	11	52	58.5
PXR	Forward	GCTGACAGAGGAGCAGCGGATGA	23	14	61	64.0
	Reverse	CCCTGGCAGCCGGAAATCTT	21	12	57	60.4
CAR	Reverse	AGATGGAGCCCGTGTGGG	18	12	67	60.4
	Forward	GGTAACTCCAGGTCGGTCAGG	21	13	62	62.4
HNF4α	Reverse	CTGCTCGGAGCCACCAAGAGATCCATG	27	16	59	66.6
	Forward	ATCATCTGCCAGGTGATGCTCTGCA	25	13	52	62.1
PPARα	Reverse	CCAGTATTTAGGAAGCTGTCCTG	23	11	48	58.7
	Forward	CGTTGTGTGACATCCCGACAG	21	12	57	60.4
18S rRNA	Reverse	CGCCGCTAGAGGTGAAATTC	20	11	55	58.4
	Forward	TTGGCAAATGCTTTTCGCTC	19	9	47	53.9

Supplemental table III: Effect of gender on activity, protein and mRNA expression		
Gender	Female	Male
Sample size (n)	38	36
Vmax (pmol/min/mg protein)	303.95±84.21	368.95±74.42
Km (µM)	1.96±0.18	1.96±0.25
Clint, whole liver (L/min)	3.03±0.96	4.79±1.17
CYP3A4 (pmol/mg protein)	73.71±13.54	100.66±14.71
CPR (pmol/mg protein)	40.60±2.01	44.15±2.12
Cyb5 (pmol/mg protein)	505.66±19.32	618.40±33.41
CYP3A4 mRNA¹	5.41±1.88	6.03±1.62
CAR mRNA¹	1.94±0.24	2.76±0.73
PXR mRNA¹	1.98±0.25	1.87±0.24
HNF4α mRNA¹	1.81±0.31	1.56±0.24
PPARα mRNA¹	1.33±0.20	1.21±0.24

All descriptive statistics value represent mean±SE. * $P < 0.05$ as compared to normal liver. P-values reported from non-parametric Mann-Whitney U test (2-sided). ¹Messenger RNA data expressed relative to 18S rRNA

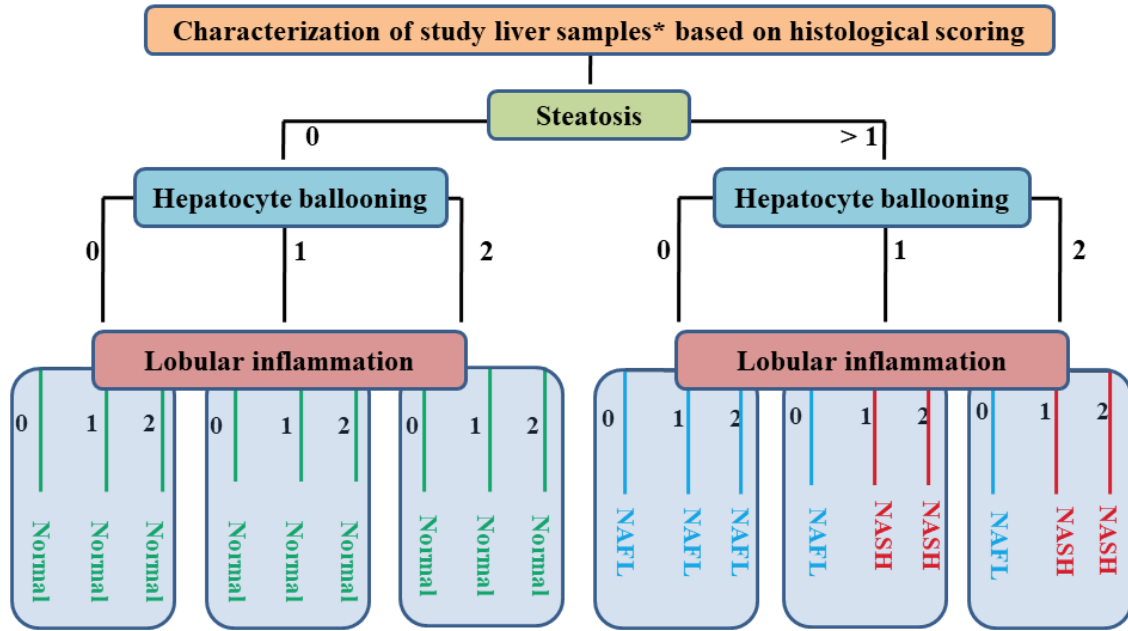
Supplemental table IV: Predicted pharmacokinetic parameters (Geometric mean, 95% CI) after 5 mg intravenous dose in virtual populations (n=250 in each group) accounting for fatty liver.

	Normal	NAFL	NASH
C_{max} (ng/mL)	114.8 (107.7-122.4)	114.8 (107.7-122.4)	114.8 (107.7-122.4)
AUC₀₋₂₄ (ng/mL.h)	301.3 (280.3-323.9)	533.5 (492.2-578.3)	680.7 (634.9-729.7)
CL (L/h)	16.6 (15.4-17.8)	9.4 (8.6-10.2)	8.6 (6.8-7.9)

Supplemental table V: Predicted pharmacokinetic parameters (Geometric mean, 95% CI) after 5 mg intravenous dose in virtual populations (n=250 in each group) accounting for fatty liver and diabetes.

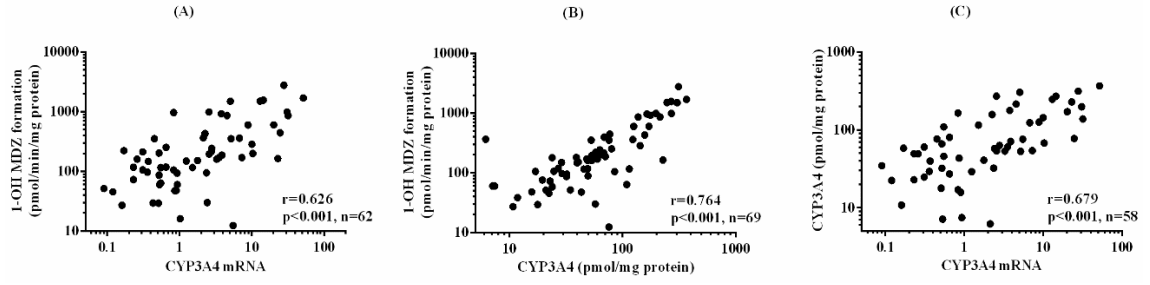
	Non-diabetic			Diabetic		
	Normal	NAFL	NASH	Normal	NAFL	NASH
C_{max} (ng/mL)	114.8 (107.7-122.4)	114.8 (107.7-122.4)	114.8 (107.7-122.4)	114.8 (107.7-122.4)	114.8 (107.7-122.4)	114.8 (107.7-122.4)
AUC₀₋₂₄ (ng/mL.h)	363.1 (334.5-394.2)	436.4 (404.0-471.5)	584.8 (546.3-626.0)	252.7 (237.6-268.7)	660.1 (618.8-704.3)	769.0 (729.3-810.9)
CL (L/h)	13.8 (12.7-14.9)	11.5 (10.6-12.4)	8.6 (8.0-9.2)	19.8 (18.6-21.0)	7.6 (7.1-8.1)	6.5 (6.2-6.9)

Supplemental figures

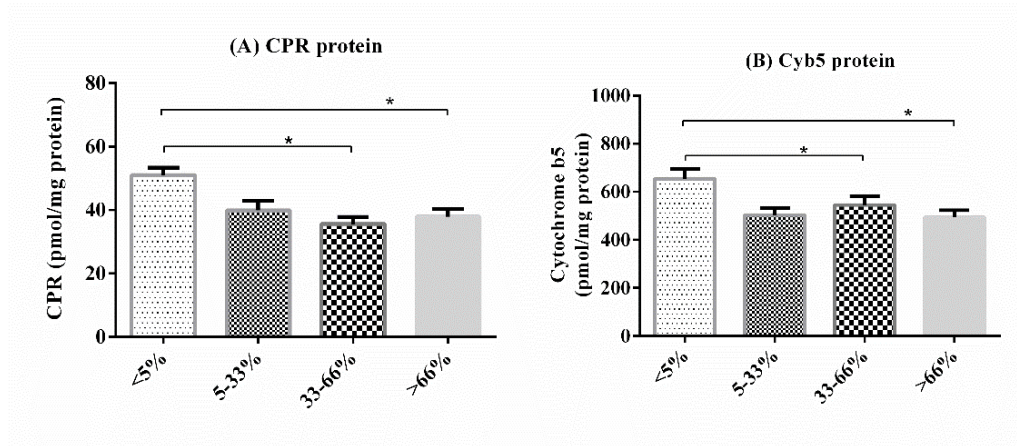


*(n): Normal=24, NAFL=26, NASH=24

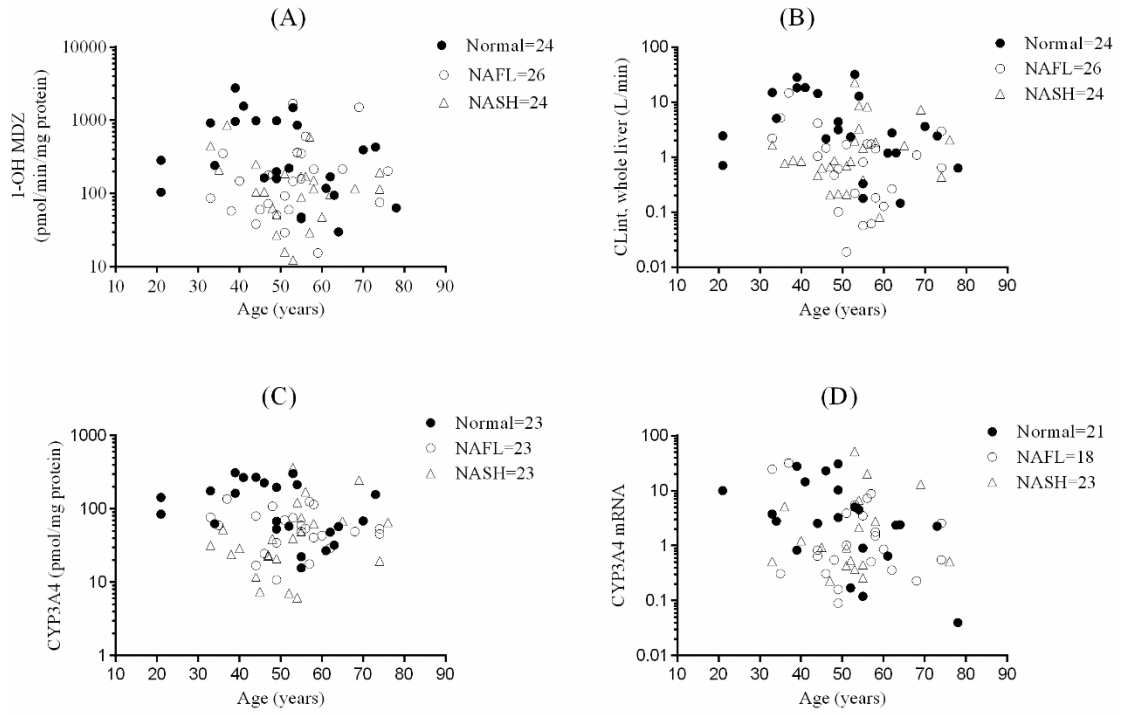
Supplemental figure I



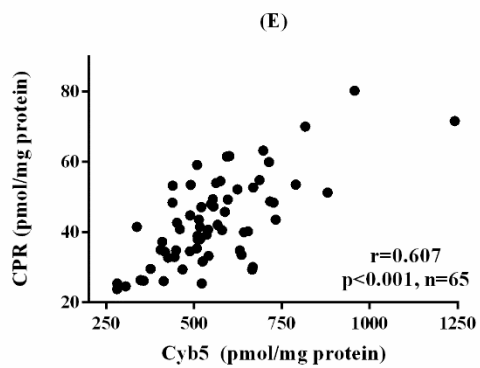
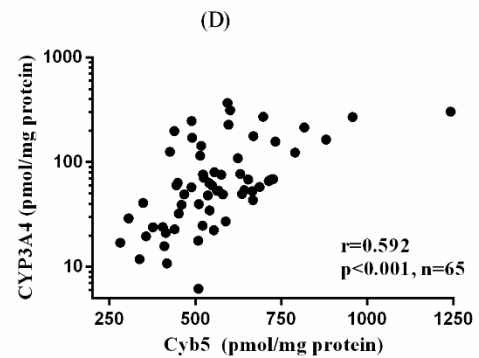
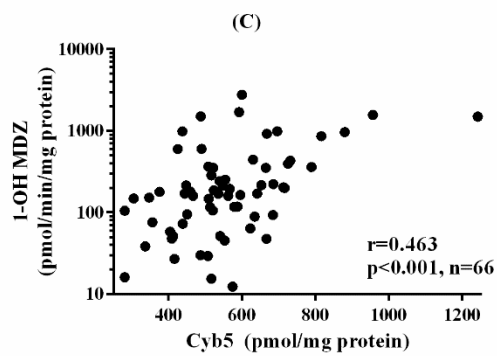
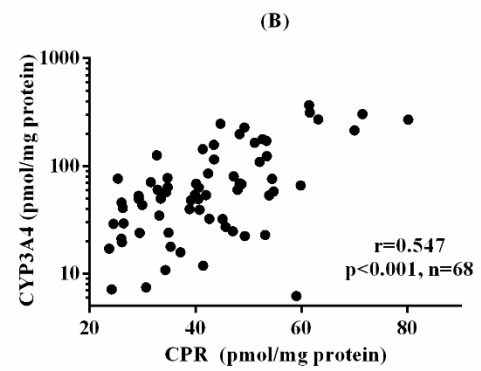
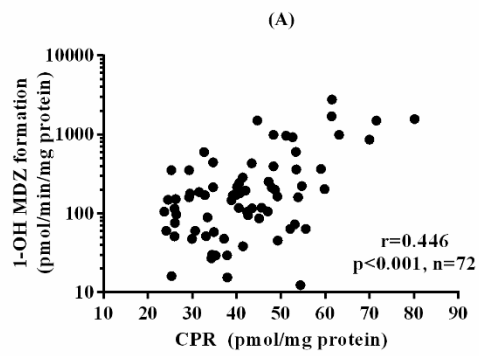
Supplemental figure II.



Supplemental figure III.



Supplemental figure IV.



Supplemental figure V.

MANUSCRIPT IV

This manuscript has been prepared as a research article for submission to the Journal of Pharmacology and Experimental Therapeutics, ASPET Publications

Effect of non-alcoholic fatty liver disease (NAFLD) on the protein abundance and activity of hepatic drug metabolizing enzymes in human

Rohitash Jamwal, Benjamin B Barlock, Fatemeh Akhlaghi*

Biomedical and Pharmaceutical Sciences, College of Pharmacy, University of Rhode Island, Kingston, RI,

Running title: NAFLD is associated with altered CYP activity and protein

Corresponding author at:

Fatemeh Akhlaghi, Ph.D.

Department of Biomedical and Pharmaceutical Sciences, University of Rhode Island,
495A College of Pharmacy, 7 Greenhouse Road, Kingston, RI 02881, United States.

Email address: fatemeh@uri.edu

The number of words in the abstract: 231

The number of words in the introduction: 782

The number of words in the discussion: 1517

The number of figures: 6

The number of tables: 3

The number of references: 62

Conflict of interest:

None of the authors have any conflict of interest to declare.

Abstract

Differential basal expression of drug disposition proteins (DDP) in the disease state can contribute to significant changes in systemic exposure to xenobiotics. The changes in abundance of drug-metabolizing enzymes (DME) is vital for accurate *in vivo* extrapolation and prediction of hepatic clearance from *in vitro* data. To gain insight into the alterations of phase-I and phase-II DDPs during non-alcoholic fatty liver disease (NAFLD), we compared the protein abundance and activity in 106 human liver samples (control=42, nonalcoholic fatty liver; NAFL=34 and nonalcoholic steatohepatitis; NASH=30). In-solution trypsin digestion of proteins in whole tissue lysate was carried out using pressure-cycling technology. Data were acquired in data-dependent acquisition (DDA) mode on a triple-time of flight (TOF) mass spectrometer, and absolute protein levels were determined using total protein approach. Functional activity data from the tissue vendor were used to evaluate the effect of disease on activity and further correlated with protein abundance. CYP1A2 and CYP3A4/5 protein abundance and activity were downregulated in the NAFLD whereas minor changes were observed for other CYPs. UGT and SULT-regulation were mostly similar between the different groups except for SULT1A1 and SULT1A2. Mitochondrial proteins (ACADSB, ACSM3/5) involved in lipid metabolism were also dysregulated in NAFLD. Levels of CPS1 were significantly lower in the disease state. Here, we provide a quantitative protein abundance data which would allow development of PBPK models for prediction of drug disposition in the NAFLD population.

Introduction

Human liver, facilitated by several drug metabolizing enzymes (DMEs) and transporters, is the primary organ responsible for the elimination of xenobiotics and endogenous compounds. Nonalcoholic fatty liver disease (NAFLD), a chronic liver condition is defined as the presence of >5% of macrovascular steatosis in individuals without high alcohol intake (<20 g per day for women, <30 g per day for men) and ranges from the benign fatty liver to severe nonalcoholic steatosis (NASH) (Vuppalanchi and Chalasani, 2009). A recent meta-analytic report estimated higher prevalence in the Middle East and South America with a global NAFLD prevalence of 25.24% (95%CI 22.1-28.7) (Younossi et al., 2016b). The prevalence of NAFLD in the United States was found to be 30% with 10.3% of patients with advanced fibrosis (Le et al., 2017). In the USA, NAFLD is also associated with significant economic (~\$103 billion) and clinical burden (~64 million people projected to have NAFLD) (Younossi et al., 2016a). NAFLD is commonly associated with hepatic fat accumulation, lipotoxicity, insulin resistance, obesity and cardiovascular diseases (Brunt and Tiniakos, 2010). The disease is characterized by the presence of significant hepatic steatosis in patients without the considerable intake of alcohol (Chalasani et al., 2012)., NAFLD is associated with the histopathological features including steatosis, hepatocyte ballooning and lobular inflammation (Younossi and Henry, 2016). Recent studies have shown significant dysregulation of hepatic DMEs in S9 fractions from cirrhotic liver samples (Prasad et al., 2017). NAFLD was associated with substantial downregulation of CYP3A4 protein and activity in liver from CYP3A5*3/*3 expressers (Jamwal et al., 2018). However, the information on the expression of other DMEs in NAFLD is limited, and wherever available, lacks consensus (Cobbina and

Akhlaghi, 2017). The current literature suggests alteration in hepatic cytochrome P450 (CYP) expression, activity or both, however, the directionality of change lacks agreement (Niemela et al., 2000; Kolwankar et al., 2007; Fisher et al., 2009; Woolsey et al., 2015). One potential explanation for such a wide discrepancy in literature can be attributed to the interindividual variability, and sample size used to derive the inferences. Misuse of classification systems and incorrect characterization of study samples may have also lead to different conclusions (Brunt et al., 2011).

The last decade has seen a rise in the use of mass spectrometry (MS) based techniques for quantification of the protein expression (Prasad and Unadkat, 2014; Fallon et al., 2016). Despite being the gold standard, targeted methods of protein quantification are costly and need significant time for optimization of mass spectrometer conditions. Label-free quantification (LFQ) has emerged recently as an alternative approach for comparative analysis of protein expression across different samples (Wong and Cagney, 2010). Accurate and robust quantification with LFQ approaches is complex, and different strategies for extracting quantitative data has been developed (Wong and Cagney, 2010). A comprehensive cost comparison of different mass spectrometry-based techniques reported significant cost savings with label-free based quantitative proteomics (Al Feteisi et al., 2015).

Disease conditions have been known to impact the abundance of drug disposition proteins (DDPs) in the liver, hence leading to altered drug profiles and often to side-effects (Gandhi et al., 2012; Dietrich et al., 2017; Evers et al., 2018). However, it is not always practical to measure the impact of hepatic impairment on clinical outcomes in special population. Physiologically based pharmacokinetic (PBPK) models for prediction of

pharmacokinetic and drug metabolism in populations are gaining popularity for populations which represent clinical challenges (Sager et al., 2015; Jamei, 2016). The patients with metabolic syndrome are often on multiple medications and alterations in expression of DMEs carries a potential of significant drug-drug interactions (DDI). PBPK models can be used in such cases to predict DDI once representative clinical parameters are available (Marsousi et al., 2017). Along with physicochemical properties of a drug, physiological information is vital for accurate prediction of drug exposure. Quantification of DDPs is therefore important for development of simulation models. Due to the lack of clinical studies in NAFLD patients, PBPK models should be qualified for the normal population before using them for prediction in special population groups (Shebley et al., 2018). Availability of clinical study data in the future would help to validate these models.

Traditionally, the expression and activity of DMEs have been measured in a human liver microsomal fraction. However, the quantification of DMEs in subcellular fractions usually suffers from batch-to-batch variability in recovery and enrichment of proteins (Xu et al., 2018). Therefore, we developed a simple whole tissue lysate method for simultaneous quantification of hepatic drug metabolism enzymes in human liver using LC-MS/MS. The method was applied to study the effect of NAFLD on the expression of clinically important drug disposition proteins (phase-I and phase-II proteins). The effect of disease on the functional activity of 8 CYP enzymes was also studied.

Materials and Methods

Chemicals and Reagents

Protein preparation kit, TPCK-treated trypsin, trypsin digested β -galactosidase, and mass spectrometer tuning solution was from AB Sciex, Framingham, MA. Aquity UPLC Peptide BEH C18 analytical column and VanGuard pre-columns were procured from Waters Corp. (Waltham, MA). Calbiochem ProteoExtract Native Membrane Protein Extraction Kit was purchased from EMD Millipore (Billerica, MA). 1,4-Dithiothreitol (DTT) was obtained from Roche Diagnostics (Indianapolis, IN). Sodium deoxycholate and iodoacetamide (IAA) were procured from Sigma Aldrich (St. Louis, MO). MS grade acetonitrile and formic acid were purchased from ThermoFisher, Waltham, MA. Aquity UPLC Peptide BEH C18 analytical column and VanGuard pre-columns were procured from Waters Corp., Waltham, MA.

Human liver and homogenate preparation

Frozen human liver samples from brain dead donors were purchased from Sekisui XenoTech LLC, Kansas City, KS. The detailed demographics of the donors are given in table 1. Livers were graded by a histopathologist as previously described and were categorized as control, NAFL (steatosis) or NASH (Jamwal et al., 2018). Samples were randomly ordered, and the liver homogenate was prepared in homogenization buffer (8 M urea, 50 mM Triethylammonium bicarbonate, 10 mM DTT', v/v). Briefly, liver tissue (~50 mg) was weighed and homogenized in 1000 μ l of HB. Tissue was homogenized on an Omni bead homogenizer as described previously (Jamwal et al., 2017). Further, samples were spun at 1,000 g for 5 min, and the supernatant was collected. The total protein

concentration of the resulting sample was determined using Pierce BCA protein assay kit (ThermoFisher Scientific, Waltham, MA). Lipid peroxidation and total cholesterol were measured as described previously (Jamwal et al., 2017).

Pressure-cycling technology (PCT) aided trypsin digestion

Protein digestion was conducted as described previously, with few adaptations (Prasad et al., 2014; Jamwal et al., 2017). Protein samples (250 µg protein) were spiked with 2 µg BSA and denatured with 25 µL DTT (100 mM) at 35°C for 30 min in a shaking water bath (100 rpm). After denaturation, samples were alkylated in the dark with 25 µL IAA (200 mM) for 30 min at room temperature. Samples were subsequently concentrated using the cold water, methanol and chloroform (1:2:1) precipitation method (centrifugation at 10000 rpm, 5min at 10°C). The protein pellet was washed with ice-cold methanol and then suspended in 100 µL of 50 mM ammonium bicarbonate (pH ~8) containing 3% w/v sodium deoxycholate (DOC). Further, TPCK-treated trypsin (10 µg) was added to samples at a ratio of 1:25 (trypsin: protein) and samples were transferred into digestion tubes (PCT MicroTubes, Pressure Biosciences Inc., Easton, MA). The barocycler was run at 35°C, for 75 cycles with 60 sec per pressure-cycle (50-sec high pressure, 10-sec ambient pressure, 25 kpsi). Subsequently, 10 µg trypsin was again added to each sample and barocycler based digestion was repeated at the specifications mentioned above.

Further, to 110 µL of digested peptides sample, 10 µL of ACN/water (1:1, v/v containing 5% formic acid) was added to precipitate detergent (snow white pellet). Samples were spun to remove the pellet and 100 µL supernatant was collected (10,000 rpm for 5 min at 10°C). The collected supernatant was spiked with 5 µl trypsin-digested β-galactosidase peptides

(~15 pmol). Samples were spun (10,000 rpm for 5 min at 10°C) again to remove pellet if any. Subsequently, twenty-five microliters of the resulting peptide solution was injected on the analytical column and samples were analyzed using LC-MS/MS method described below.

LC-MS/MS Analysis

Data-dependent analysis (DDA) was performed in positive ionization mode using a DuoSpray™ ion source on a Sciex 5600 TripleTOF™ mass spectrometer (AB Sciex, Concord, Canada) equipped with an Acquity UPLC HClass system (Waters Corp., Milford, MA, USA). Gas 1 (GS1), gas 2 (GS2) and curtain gas (CUR) were maintained at 55, 60 and 25 psi, respectively. Ion spray voltage floating (ISVF) was kept at 5500 V while the source temperature (TEM) was 500°C. Declustering potential (DP), collision energy (CE) and collision energy spread (CES) were set at 120, 10 and 5 respectively. During the survey scan, all the ions with a charge state of 2 to 4, mass range of m/z 300-1250 and exceeding 25 cps were used for MS/MS analysis. Former target ions were excluded for 8 sec and the mass tolerance for TOF-MS was 50 mDa with a 100 milliseconds accumulation time. For product scan, data was acquired from 100 to 1250 m/z with an accumulation time of 75 millisecond with a total cycle time of 3.5 sec. Product ion analysis was done under dynamic accumulation and rolling collision energy dependent on the m/z of the ion.

Chromatographic separation was achieved over 180 min gradient method at 100 $\mu\text{L}/\text{min}$ on an Acquity UPLC Peptide BEH C18 (2.1 X 150 mm, 300 Å, 1.7 μm) preceded by an Acquity VanGuard pre-column (2.1 X 5 mm, 300 Å, 1.7 μm). Mobile phase A was 98% water, 2% acetonitrile, 0.1% formic acid and mobile phase B was 98%

acetonitrile, 2% water, 0.1% formic acid). Gradient conditions used were 98% A from 0 to 5 min, 98% to 70% A from 5 to 155 min, 70% to 50% A from 155 to 160 min, 50% to 5% A from 160 to 170 min, 5% to 98% A held from 170 to 175 min. The gradient was held at initial conditions from 175 min until the end of the run to equilibrate the column before the start of next run. The flow was diverted to waste for the first 8 minutes and last 20 minutes of the acquisition. Autosampler was maintained at 10°C, and the column was kept at 50°C. Trypsin-digested β -galactosidase peptides were injected to monitor TOF detector mass calibration every four sample.

Data processing

The absolute level of proteins was determined from DDA data using “Total Protein Approach”(Wisniewski and Rakus, 2014). Homogenate samples were analyzed as previously described using MaxQuant (ver 1.5.2.10) (Wisniewski and Rakus, 2014; Jamwal et al., 2017). The proteins were searched on Andromeda search engine against the Swiss-Prot human protein database (updated Apr 2018) at 1% false discovery rate (FDR)(Cox and Mann, 2008). Cysteine carbamidomethylation was selected as fixed modifications for the search. Oxidation (M) and acetyl (protein N-term) were used as a variable modification in protein quantification. Label-free quantification (LFQ) was performed with a ratio count of 1, and a maximum of two missed cleavages was allowed. Unique peptides were selected for protein quantification while all the other MaxQuant settings were kept as default values. The absolute protein levels were calculated using “Total Protein Approach” from raw intensities obtained from MaxQuant (Wisniewski and Rakus, 2014). The protein concentrations were expressed as picomoles of protein per gram liver tissue (pmol/g liver).

$$\text{Total protein (p)} = \frac{\text{MS signal (p)}}{\text{Total MS signal}}$$

$$\text{Protein conc. (p)} = \frac{\text{MS signal (p)} \times 10^6}{\text{Total MS signal} \times \text{MW(p)}} \text{ [pmol/mg homogenate protein]}$$

$$\text{Normalized Protein conc. (p)} = \text{Protein conc (p)} \times \text{PPGL} \times \text{NF} \text{ [pmol/g liver]}$$

where MS signal (p) refers to total LFQ signal intensity for a protein of interest. Total MS signal indicates to the total LFQ intensity of all the proteins in the sample and MW represents the molecular weight of respective protein. PPGL denotes the yield of milligrams of total protein per gram of liver tissue.

Statistical analysis

Q-Q plot was used to determine the normality of the protein samples. After determining that the protein samples violated the assumption of normal distribution, non-parametric tests were used for all the analyses. Non-parametric Mann-Whitney U test was used to compare the differences for two groups and Kruskal-Wallis for comparison of three or more groups. The vendor provided functional activity was used for correlation analysis with protein concentration. The details of the assay's conditions are described elsewhere (Jamwal et al., 2017). Spearman-correlation analysis was performed between the functional activity and protein levels. Correlation was expressed as strong ($r > 0.7$),

moderate ($r=0.5-0.7$) or weak ($r=0.3-0.5$). $P < 0.05$ was considered significant throughout the analysis. Data are reported as geometric mean and 95% confidence interval unless stated otherwise. Prism 6 (GraphPad Inc., La Jolla, CA) and SPSS 23 (IBM Corp., Armonk, NY) were used for graphing and statistical testing, respectively.

Results

NAFL and NASH liver samples exhibited significantly elevated levels of malondialdehyde and cholesterol (Table 1). The livers from NAFL and NASH donors were larger in weight than the control group. The total protein yield from samples with NAFLD was marginally lower as compared to the control. Donors with NAFLD also showed a trend of increased body weight and body mass index. The geometric mean of ????? for the control group was marginally lower than the NAFLD groups. The yield of protein per gram liver (mg/g) was slightly lower from NAFL and NASH groups as compared to control.

Effect of NAFLD on the expression and activity

The protein expression of CYP1A2 was significantly lower in NAFLD samples ($p < 0.05$). There was a discernible decrease in CYP3A4 and CYP3A5 levels in NAFL and NASH livers but the effect was not significant due to high interindividual variability (figure 1). We observed no change in the protein levels of CYP2E1, CYP2D6, CYP2C8, and CYP2C9 among different study groups (table 2). A trend of lower expression was observed for CYP2B6; however, the reduction was not significantly different from control samples. Cytochrome b5 was downregulated considerably as the severity of disease increased. There was no change observed for the amount of CPR between the different groups. The protein levels of CYP8B1, CYP27A1, and CYP51A1 were also similar among three study groups.

Similar to protein abundance, CYP1A2 phenacetin O-dealkylation activity was significantly lower in NAFL and NASH (figure 2). CYP3A4 mediated testosterone hydroxylation was moderately decreased in NAFLD group. The activity of other CYP450 enzymes remained mostly similar between control and disease state.

Furthermore, we did not see any significant differences in the protein expression of any of the UGTs included in the study (table 3, figure 3). Interestingly, SULT1A1 and SULT2A1 expression were lower in NAFL, but levels were similar for NASH and control livers (table 3). No significant alteration in SULT1C1 and SULT1A2 levels was observed (figure 4). A comprehensive list of other hepatic proteins studied, and the effect of NAFLD is given in supplementary table 1.

Correlation of CYP450 enzyme activity and protein expression

Non-parametric Spearman correlation analysis was performed between the determined protein levels and vendor provided enzyme activity (figure 5). A significant correlation with varying strength was observed for all the 9 CYP450 enzymes. CYP1A2, 2A6, 2B6, 3A4 exhibited strong correlation ($r > 0.7$) while it was moderate ($r = 0.5-0.7$) for CYP2C8, 2D6 and 3A5. Interestingly, the association between CYP2C9 protein and activity was weakest ($r = 0.48$) among all the proteins.

Biomarker proteins in NAFLD

Carbamoyl-phosphate synthase (CPS1), acyl-CoA dehydrogenase short/branched chain (ACADSB) and acyl-CoA synthetase medium-chain family member 5 (ACSM5) were significantly downregulated in NAFLD (table 3). In contrast, acyl-CoA synthetase medium-chain family member 3 (ACSM3) levels were significantly lower in NAFL but not NASH. The protein expression of fatty acid synthase (FASN) was unchanged in NAFL but was elevated in NASH (Fig 6). Hepatic glyoxalase 1 (GLO1) levels were moderately lower in NAFLD but the difference was statistically not significant.

Discussion

Variable effects were observed on the expression of most proteins suggesting involvement of complex transcriptional, translational, epigenetic and/or polymorphic regulatory events. Oxidative stress and lipid peroxidation play a significant role in the pathogenesis of NAFLD (Masarone et al., 2018). Studies in human have found elevated levels of malondialdehyde (MDA) and other markers of oxidative stress in NAFLD (Kumar et al., 2013). Higher cholesterol is also a significant risk factor for development and progression of the disease (Ioannou, 2016). The protein expression of CYP8B1 and CYP27A1 (bile acid synthesis) and CYP51A1 (cholesterol synthesis) was similar among three groups suggesting other mechanisms (uptake or efflux) for cholesterol accumulation may be at play in NAFLD. Suppressed cholesterol efflux capacity has been reported in NAFLD patients (Fadaei et al., 2018). No downregulation of CYP51A1 and CYP8B1 in NASH biopsy samples was reported in the Japanese population (Kakehashi et al., 2017). CYP4F2 level initially increased during acute lipid insult (hepatoprotective mechanism) but was found to be downregulated during chronic stimulation (hepatotoxicity) (Bartolini et al., 2017).

Studies in human liver microsomes have shown downregulation of CYP3A activity with the progression of disease and severity of steatosis (Kolwankar et al., 2007; Fisher et al., 2009). The plasma midazolam concentration in NASH patients was 2.4-fold higher than the control subjects (Woolsey et al., 2015). A recent study from our group found almost a 2-fold decrease of CYP3A4 protein expression and activity in liver microsomes from NAFLD donors (Jamwal et al., 2018). Studies in microsomal fractions from diabetic

livers found significant downregulation of CYP3A4 protein and activity but not mRNA (Dostalek et al., 2011).

Downregulation of CYP1A2 protein and activity has been reported in human liver microsomes and hepatocytes from fatty liver grafts (Donato et al., 2006; Fisher et al., 2009). Dysregulated cytokine and the chemokine-mediated inflammatory response is typical in NAFLD and plays a pivotal role in its pathophysiology (Braunersreuther et al., 2012). Elevated proinflammatory cytokines in NAFLD have been reported, and this may partially explain the downregulation of CYP1A2 and CYP3A4 activity and protein observed in our study (Liptrott et al., 2009). In contrast to other reports of significant up-regulation of CYP2A6 in NAFLD, we found a marginal decrease in the protein expression of the enzyme (Wang et al., 2018). The coumarin hydroxylation activity of the enzyme was similar between control and NAFLD livers. Donato et al. found significant downregulation of CYP2A6 mRNA and activity in a hepatocyte model of cellular steatosis (Donato et al., 2006).

CYP2E1 mediated biotransformation reactions in liver generate a significant amount of reactive oxygen species which further promote the oxidative stress in NAFLD (Aubert et al., 2011). In contrast to reports of elevated CYP2E1 in NAFL and NASH, we found that the protein expression and functional activity was similar among the three groups (Leung and Nieto, 2013). CYP2E1 mRNA and protein expression were found to be lower in another study in livers from NAFLD patients whereas activity was unaltered (Fisher et al., 2009). Fatty acid treatment in cultured HepG2 cells did not induce CYP2E1 expression (Aljomah et al., 2015). CHZ test (6-hydroxychlorzoxazone/chlorzoxazone

ratio) in patients with NAFLD was unable to distinguish NASH from NAFL (Chtioui et al., 2007).

CYP2C8 protein expression was downregulated in NASH-associated liver biopsy while CYP2C9 levels were unchanged compared to control (Takehashi et al., 2017). Other studies in human tissue also observed no changes in the expression of either isoforms (Chtioui et al., 2007). CYP2C8 activity was similar in different stages of NAFLD and control livers whereas CYP2C9 activity was reported to be higher (Fisher et al., 2009). A recent study in 3-dimensional hepatocyte culture model of NAFLD, CYP3A4 activity was found to be upregulated while CYP2C9 decreased (Kostrzewski et al., 2017). We could not determine the levels of CYP2C19 in our study and is one of the limitations of the homogenate-based method in which low abundance proteins are not measured due to a limited dynamic range of quantification.

CYP2B6 is one of most polymorphic enzymes which accounts for significant variability in its expression and activity (Zanger and Klein, 2013). Fisher et al. observed elevated CYP2B6 mRNA without any change in protein and activity during the progression of NAFLD (Fisher et al., 2009). Similar to CYP2B6, CYP2D6 is another highly polymorphic enzyme responsible with varying phenotypes and degree of metabolism of its substrates (Zhou, 2009). Current literature reports no significant alterations in CYP2D6 expression and activity in human liver (Fisher et al., 2009). A revisit to protein and activity data with information of polymorphism may help to ascertain the changes associated with these enzymes in NAFLD.

UDP glucuronosyltransferases (UGTs) are involved in phase-II metabolism (glucuronidation) of 40–70% of all clinical drugs in human and also detoxify endogenous compounds (Jancova et al., 2010; Rowland et al., 2013). While the effect of NAFL on CYP450 enzymes has been extensively studied, only limited information on the regulation of UGTs is available in human (Hardwick et al., 2013). Hardwick and colleagues identified significant alterations in mRNA of different UGT isoforms, but the acetaminophen glucuronidation activity was unchanged (Hardwick et al., 2013). UGT2B17 and UGT2B7 were identified to have similar protein levels between control and NASH biopsy samples (Kakehashi et al., 2017). Yalcin et al. also found that SULT1A1 protein expression and activity were significantly decreased in steatosis (Yalcin et al., 2013). Other have reported downregulation of human SULT1A2 in NAFLD (Younossi et al., 2005; Stepanova et al., 2010). In contrast, the elevated SULT1A1 protein was observed in steatosis, but it was found to be downregulated in NASH (Hardwick et al., 2013). Similar to reports for CYP450 enzymes, regulation of UGT and SULT is as heterogeneous; however, there is a scarcity of data for the later.

Mitochondrial distress and oxidative stress are common in NASH (Simoes et al., 2018). Studies have reported reduced anti-oxidant defense capacity in NASH (Koliaki et al., 2015). Significant suppression of numerous mitochondria associated proteins was observed in NAFLD samples. Differential expression of FASN has been reported in literature with common consensus on the increase in the levels of enzyme with the progression of steatosis (Dorn et al., 2010). Acyl-CoA dehydrogenase short/branched chain (ACADSB) is a mitochondrial enzyme involved in the metabolism of fatty acid and branched chain amino acids in mitochondria. Gene expression of ACADSB was almost 2-

fold lower in patients with NASH versus obese controls (Younossi et al., 2005). Concurrently, a decrease in the mitochondrial enzymes (ACSM3, ACSM5) involved in fatty acid oxidation was observed.

GLO1 is involved in metabolism of reactive glyoxal and methylglyoxal metabolites thereby preventing glycation of proteins. Decreased levels of GLO1 were recently identified in pediatric NAFLD biopsy samples (Spanos et al., 2018). A decrease in GLO1 (as observed in our study) may be responsible for elevated levels of methylglyoxal-derived advanced glycation end product observed in serum of NAFLD patients (Spanos et al., 2018). Downregulation of CPS1 and dysregulation of the urea cycle in NAFLD has been described in literature (De Chiara et al., 2018). Accumulation of urea leads to scar tissue development, one of the complications of NAFLD. The gradual decrease from control to NAFL and NASH samples in CPS1 expression was reported previously (Rodriguez-Suarez et al., 2010).

The sampling of human liver tissue is critical in the identification of the perturbations in the expression of DDPs. We speculate that the differences in the sampling may have presented some of the observed results in our study. Histopathological differences were found in liver biopsies from the right and left lobes of bariatric patients (Merriman et al., 2006). Given these results are primarily limited to Caucasian population, care should be taken for extrapolation of the results. The availability of human liver tissue for studying the hepatic xenobiotic transporters remains a challenge for researchers due to ethical consideration and the availability of tissue with adequate clinical information. Our knowledge of the drugs which the donors were taking at the time of death is limited only

to the information passed on by the vendor. Furthermore, there was no data available on the duration of hospitalization of donors before the organs were harvested.

NAFLD is often accompanied by other comorbidities (obesity, diabetes) which may confound the observations and could partially explain the wide discrepancy in the literature. While we accounted for the NAFLD with and without diabetes, small sample size deterred us from conducting statistical analysis of any sort (supplementary table 2-6). Therefore, the results and discussion of this work are mainly restricted to the effect of NAFLD on the expression of DMEs without any focus on underlying comorbidities.

To summarize, our research suggests that most drug metabolizing enzymes apart from CYP1A2 and CYP3A appears to be largely unaffected by NAFL and NASH. A lack of adverse clinical reports also indicates that most drugs appear to be well-tolerated by these patients despite the changes in the expression of drug metabolism enzymes. An understanding of metabolism, as well as transport protein, may provide a better picture of the clinical manifestations of the perturbed proteins in NAFLD. Multiple factors in NAFLD may affect the expression and activity of DDPs, and comprehensive study needs to be conducted to answer some of the questions around the discrepancies observed in the literature.

Statement of financial support

Financial support for this study was provided by National Institutes of Health grants to Fatemeh Akhlaghi [grant numbers R15-GM101599, UH3-TR000963].

References

- Al Feteisi H, Achour B, Barber J and Rostami-Hodjegan A (2015) Choice of LC-MS methods for the absolute quantification of drug-metabolizing enzymes and transporters in human tissue: a comparative cost analysis. *AAPS J* **17**:438-446.
- Aljomah G, Baker SS, Liu W, Kozielski R, Oluwole J, Lupu B, Baker RD and Zhu L (2015) Induction of CYP2E1 in non-alcoholic fatty liver diseases. *Exp Mol Pathol* **99**:677-681.
- Aubert J, Begriche K, Knockaert L, Robin MA and Fromenty B (2011) Increased expression of cytochrome P450 2E1 in nonalcoholic fatty liver disease: mechanisms and pathophysiological role. *Clin Res Hepatol Gastroenterol* **35**:630-637.
- Bartolini D, Torquato P, Barola C, Russo A, Rychlicki C, Giusepponi D, Bellezza G, Sidoni A, Galarini R, Svegliati-Baroni G and Galli F (2017) Nonalcoholic fatty liver disease impairs the cytochrome P-450-dependent metabolism of alpha-tocopherol (vitamin E). *J Nutr Biochem* **47**:120-131.
- Braunersreuther V, Viviani GL, Mach F and Montecucco F (2012) Role of cytokines and chemokines in non-alcoholic fatty liver disease. *World J Gastroenterol* **18**:727-735.
- Brunt EM, Kleiner DE, Behling C, Contos MJ, Cummings OW, Ferrell LD, Torbenson MS and Yeh M (2011) Misuse of scoring systems. *Hepatology* **54**:369-370; author reply 370-361.
- Brunt EM and Tiniakos DG (2010) Histopathology of nonalcoholic fatty liver disease. *World J Gastroenterol* **16**:5286-5296.

- Chalasani N, Younossi Z, Lavine JE, Diehl AM, Brunt EM, Cusi K, Charlton M and Sanyal AJ (2012) The diagnosis and management of non-alcoholic fatty liver disease: practice Guideline by the American Association for the Study of Liver Diseases, American College of Gastroenterology, and the American Gastroenterological Association. *Hepatology* **55**:2005-2023.
- Chtioui H, Semela D, Ledermann M, Zimmermann A and Dufour JF (2007) Expression and activity of the cytochrome P450 2E1 in patients with nonalcoholic steatosis and steatohepatitis. *Liver Int* **27**:764-771.
- Cobbina E and Akhlaghi F (2017) Non-alcoholic fatty liver disease (NAFLD) - pathogenesis, classification, and effect on drug metabolizing enzymes and transporters. *Drug Metab Rev* **49**:197-211.
- Cox J and Mann M (2008) MaxQuant enables high peptide identification rates, individualized p.p.b.-range mass accuracies and proteome-wide protein quantification. *Nat Biotechnol* **26**:1367-1372.
- De Chiara F, Heeboll S, Marrone G, Montoliu C, Hamilton-Dutoit S, Ferrandez A, Andreola F, Rombouts K, Gronbaek H, Felipe V, Gracia-Sancho J, Mookerjee RP, Vilstrup H, Jalan R and Thomsen KL (2018) Urea cycle dysregulation in non-alcoholic fatty liver disease. *J Hepatol* **69**:905-915.
- Dietrich CG, Rau M, Jahn D and Geier A (2017) Changes in drug transport and metabolism and their clinical implications in non-alcoholic fatty liver disease. *Expert Opin Drug Metab Toxicol* **13**:625-640.
- Donato MT, Lahoz A, Jimenez N, Perez G, Serralta A, Mir J, Castell JV and Gomez-Lechon MJ (2006) Potential impact of steatosis on cytochrome P450 enzymes of

- human hepatocytes isolated from fatty liver grafts. *Drug Metab Dispos* **34**:1556-1562.
- Dorn C, Riener MO, Kirovski G, Saugspier M, Steib K, Weiss TS, Gabele E, Kristiansen G, Hartmann A and Hellerbrand C (2010) Expression of fatty acid synthase in nonalcoholic fatty liver disease. *Int J Clin Exp Pathol* **3**:505-514.
- Dostalek M, Court MH, Yan B and Akhlaghi F (2011) Significantly reduced cytochrome P450 3A4 expression and activity in liver from humans with diabetes mellitus. *Br J Pharmacol* **163**:937-947.
- Evers R, Piquette-Miller M, Polli JW, Russel FGM, Sprowl JA, Tohyama K, Ware JA, de Wildt SN, Xie W, Brouwer KLR and International Transporter C (2018) Disease-Associated Changes in Drug Transporters May Impact the Pharmacokinetics and/or Toxicity of Drugs: A White Paper From the International Transporter Consortium. *Clin Pharmacol Ther.*
- Fadaei R, Poustchi H, Meshkani R, Moradi N, Golmohammadi T and Merat S (2018) Impaired HDL cholesterol efflux capacity in patients with non-alcoholic fatty liver disease is associated with subclinical atherosclerosis. *Sci Rep* **8**:11691.
- Fallon JK, Smith PC, Xia CQ and Kim MS (2016) Quantification of Four Efflux Drug Transporters in Liver and Kidney Across Species Using Targeted Quantitative Proteomics by Isotope Dilution NanoLC-MS/MS. *Pharm Res* **33**:2280-2288.
- Fisher CD, Lickteig AJ, Augustine LM, Ranger-Moore J, Jackson JP, Ferguson SS and Cherrington NJ (2009) Hepatic cytochrome P450 enzyme alterations in humans with progressive stages of nonalcoholic fatty liver disease. *Drug Metab Dispos* **37**:2087-2094.

- Gandhi A, Moorthy B and Ghose R (2012) Drug disposition in pathophysiological conditions. *Curr Drug Metab* **13**:1327-1344.
- Hardwick RN, Ferreira DW, More VR, Lake AD, Lu Z, Manautou JE, Slitt AL and Cherrington NJ (2013) Altered UDP-glucuronosyltransferase and sulfotransferase expression and function during progressive stages of human nonalcoholic fatty liver disease. *Drug Metab Dispos* **41**:554-561.
- Ioannou GN (2016) The Role of Cholesterol in the Pathogenesis of NASH. *Trends Endocrinol Metab* **27**:84-95.
- Jamei M (2016) Recent Advances in Development and Application of Physiologically-Based Pharmacokinetic (PBPK) Models: a Transition from Academic Curiosity to Regulatory Acceptance. *Current Pharmacology Reports* **2**:161-169.
- Jamwal R, Barlock BJ, Adusumalli S, Ogasawara K, Simons BL and Akhlaghi F (2017) Multiplex and Label-Free Relative Quantification Approach for Studying Protein Abundance of Drug Metabolizing Enzymes in Human Liver Microsomes Using SWATH-MS. *J Proteome Res* **16**:4134-4143.
- Jamwal R, de la Monte SM, Ogasawara K, Adusumalli S, Barlock BB and Akhlaghi F (2018) Nonalcoholic Fatty Liver Disease and Diabetes Are Associated with Decreased CYP3A4 Protein Expression and Activity in Human Liver. *Mol Pharm* **15**:2621-2632.
- Jancova P, Anzenbacher P and Anzenbacherova E (2010) Phase II drug metabolizing enzymes. *Biomed Pap Med Fac Univ Palacky Olomouc Czech Repub* **154**:103-116.

- Takehashi A, Stefanov VE, Ishii N, Okuno T, Fujii H, Kawai K, Kawada N and Wanibuchi H (2017) Proteome Characteristics of Non-Alcoholic Steatohepatitis Liver Tissue and Associated Hepatocellular Carcinomas. *Int J Mol Sci* **18**.
- Koliaki C, Szendroedi J, Kaul K, Jelenik T, Nowotny P, Jankowiak F, Herder C, Carstensen M, Krausch M, Knoefel WT, Schlensak M and Roden M (2015) Adaptation of hepatic mitochondrial function in humans with non-alcoholic fatty liver is lost in steatohepatitis. *Cell Metab* **21**:739-746.
- Kolwankar D, Vuppalanchi R, Ethell B, Jones DR, Wrighton SA, Hall SD and Chalasani N (2007) Association between nonalcoholic hepatic steatosis and hepatic cytochrome P-450 3A activity. *Clin Gastroenterol Hepatol* **5**:388-393.
- Kostrzewski T, Cornforth T, Snow SA, Ouro-Gnao L, Rowe C, Large EM and Hughes DJ (2017) Three-dimensional perfused human in vitro model of non-alcoholic fatty liver disease. *World J Gastroenterol* **23**:204-215.
- Kumar A, Sharma A, Duseja A, Das A, Dhiman RK, Chawla YK, Kohli KK and Bhansali A (2013) Patients with Nonalcoholic Fatty Liver Disease (NAFLD) have Higher Oxidative Stress in Comparison to Chronic Viral Hepatitis. *J Clin Exp Hepatol* **3**:12-18.
- Le MH, Devaki P, Ha NB, Jun DW, Te HS, Cheung RC and Nguyen MH (2017) Prevalence of non-alcoholic fatty liver disease and risk factors for advanced fibrosis and mortality in the United States. *PLoS One* **12**:e0173499.
- Leung TM and Nieto N (2013) CYP2E1 and oxidant stress in alcoholic and non-alcoholic fatty liver disease. *J Hepatol* **58**:395-398.

- Liptrott NJ, Penny M, Bray PG, Sathish J, Khoo SH, Back DJ and Owen A (2009) The impact of cytokines on the expression of drug transporters, cytochrome P450 enzymes and chemokine receptors in human PBMC. *Br J Pharmacol* **156**:497-508.
- Marsousi N, Desmeules JA, Rudaz S and Daali Y (2017) Usefulness of PBPK Modeling in Incorporation of Clinical Conditions in Personalized Medicine. *J Pharm Sci* **106**:2380-2391.
- Masarone M, Rosato V, Dallio M, Gravina AG, Aglitti A, Loguercio C, Federico A and Persico M (2018) Role of Oxidative Stress in Pathophysiology of Nonalcoholic Fatty Liver Disease. *Oxid Med Cell Longev* **2018**:9547613.
- Merriman RB, Ferrell LD, Patti MG, Weston SR, Pabst MS, Aouizerat BE and Bass NM (2006) Correlation of paired liver biopsies in morbidly obese patients with suspected nonalcoholic fatty liver disease. *Hepatology* **44**:874-880.
- Niemela O, Parkkila S, Juvonen RO, Viitala K, Gelboin HV and Pasanen M (2000) Cytochromes P450 2A6, 2E1, and 3A and production of protein-aldehyde adducts in the liver of patients with alcoholic and non-alcoholic liver diseases. *J Hepatol* **33**:893-901.
- Prasad B, Evers R, Gupta A, Hop CE, Salphati L, Shukla S, Ambudkar SV and Unadkat JD (2014) Interindividual variability in hepatic organic anion-transporting polypeptides and P-glycoprotein (ABCB1) protein expression: quantification by liquid chromatography tandem mass spectroscopy and influence of genotype, age, and sex. *Drug Metab Dispos* **42**:78-88.
- Prasad B, Johnson K, Xiao G, Lai Y, Lee C, Ray AS, Liao M, Chu X, Salphati L, Mathias A, Humphreys W, Hop CECA, Kumer S and Unadkat JD (2017) Protein

- Abundance of Phase I and II Drug Metabolizing Enzymes in Alcoholic and Hepatitis C Cirrhosis Livers. *The FASEB Journal* **31**:668.617.
- Prasad B and Unadkat JD (2014) Optimized approaches for quantification of drug transporters in tissues and cells by MRM proteomics. *AAPS J* **16**:634-648.
- Rodriguez-Suarez E, Duce AM, Caballeria J, Martinez Arrieta F, Fernandez E, Gomara C, Alkorta N, Ariz U, Martinez-Chantar ML, Lu SC, Elortza F and Mato JM (2010) Non-alcoholic fatty liver disease proteomics. *Proteomics Clin Appl* **4**:362-371.
- Rowland A, Miners JO and Mackenzie PI (2013) The UDP-glucuronosyltransferases: their role in drug metabolism and detoxification. *Int J Biochem Cell Biol* **45**:1121-1132.
- Sager JE, Yu J, Ragueneau-Majlessi I and Isoherranen N (2015) Physiologically Based Pharmacokinetic (PBPK) Modeling and Simulation Approaches: A Systematic Review of Published Models, Applications, and Model Verification. *Drug Metab Dispos* **43**:1823-1837.
- Shebley M, Sandhu P, Emami Riedmaier A, Jamei M, Narayanan R, Patel A, Peters SA, Reddy VP, Zheng M, de Zwart L, Beneton M, Bouzom F, Chen J, Chen Y, Cleary Y, Collins C, Dickinson GL, Djebli N, Einolf HJ, Gardner I, Huth F, Kazmi F, Khalil F, Lin J, Odinecs A, Patel C, Rong H, Schuck E, Sharma P, Wu SP, Xu Y, Yamazaki S, Yoshida K and Rowland M (2018) Physiologically Based Pharmacokinetic Model Qualification and Reporting Procedures for Regulatory Submissions: A Consortium Perspective. *Clin Pharmacol Ther* **104**:88-110.
- Simoes ICM, Fontes A, Pinton P, Zischka H and Wieckowski MR (2018) Mitochondria in non-alcoholic fatty liver disease. *Int J Biochem Cell Biol* **95**:93-99.

- Spanos C, Maldonado EM, Fisher CP, Leenutaphong P, Oviedo-Orta E, Windridge D, Salguero FJ, Bermudez-Fajardo A, Weeks ME, Evans C, Corfe BM, Rabbani N, Thornalley PJ, Miller MH, Wang H, Dillon JF, Quaglia A, Dhawan A, Fitzpatrick E and Bernadette Moore J (2018) Proteomic identification and characterization of hepatic glyoxalase 1 dysregulation in non-alcoholic fatty liver disease. *Proteome Sci* **16**:4.
- Stepanova M, Hossain N, Afendy A, Perry K, Goodman ZD, Baranova A and Younossi Z (2010) Hepatic gene expression of Caucasian and African-American patients with obesity-related non-alcoholic fatty liver disease. *Obes Surg* **20**:640-650.
- Vuppalanchi R and Chalasani N (2009) Nonalcoholic fatty liver disease and nonalcoholic steatohepatitis: Selected practical issues in their evaluation and management. *Hepatology* **49**:306-317.
- Wang K, Chen X, Ward SC, Liu Y, Ouedraogo Y, Xu C, Cederbaum AI and Lu Y (2018) CYP2A6 is associated with obesity: studies in human samples and a high fat diet mouse model. *Int J Obes (Lond)*.
- Wisniewski JR and Rakus D (2014) Multi-enzyme digestion FASP and the 'Total Protein Approach'-based absolute quantification of the Escherichia coli proteome. *J Proteomics* **109**:322-331.
- Wong JW and Cagney G (2010) An overview of label-free quantitation methods in proteomics by mass spectrometry. *Methods Mol Biol* **604**:273-283.
- Woolsey SJ, Mansell SE, Kim RB, Tirona RG and Beaton MD (2015) CYP3A Activity and Expression in Nonalcoholic Fatty Liver Disease. *Drug Metab Dispos* **43**:1484-1490.

- Xu M, Saxena N, Vrana M, Zhang H, Kumar V, Billington S, Khojasteh C, Heyward S, Unadkat JD and Prasad B (2018) A Targeted LC-MS/MS Proteomics-Based Strategy to Characterize In Vitro Models Used in Drug Metabolism and Transport Studies. *Anal Chem*.
- Yalcin EB, More V, Neira KL, Lu ZJ, Cherrington NJ, Slitt AL and King RS (2013) Downregulation of sulfotransferase expression and activity in diseased human livers. *Drug Metab Dispos* **41**:1642-1650.
- Younossi Z and Henry L (2016) Contribution of Alcoholic and Nonalcoholic Fatty Liver Disease to the Burden of Liver-Related Morbidity and Mortality. *Gastroenterology* **150**:1778-1785.
- Younossi ZM, Baranova A, Ziegler K, Del Giacco L, Schlauch K, Born TL, Elariny H, Gorreta F, VanMeter A, Younoszai A, Ong JP, Goodman Z and Chandhoke V (2005) A genomic and proteomic study of the spectrum of nonalcoholic fatty liver disease. *Hepatology* **42**:665-674.
- Younossi ZM, Blissett D, Blissett R, Henry L, Stepanova M, Younossi Y, Racila A, Hunt S and Beckerman R (2016a) The economic and clinical burden of nonalcoholic fatty liver disease in the United States and Europe. *Hepatology* **64**:1577-1586.
- Younossi ZM, Koenig AB, Abdelatif D, Fazel Y, Henry L and Wymer M (2016b) Global epidemiology of nonalcoholic fatty liver disease-Meta-analytic assessment of prevalence, incidence, and outcomes. *Hepatology* **64**:73-84.
- Zanger UM and Klein K (2013) Pharmacogenetics of cytochrome P450 2B6 (CYP2B6): advances on polymorphisms, mechanisms, and clinical relevance. *Front Genet* **4**:24.

Zhou SF (2009) Polymorphism of human cytochrome P450 2D6 and its clinical significance: Part I. *Clin Pharmacokinet* **48**:689-723.

Figures and tables

Figure 1: Effect of NAFLD on protein expression of various CYP450 proteins.

Figure 2: Effect of NAFLD on functional activity of various CYP450 proteins.

Figure 3: Effect of NAFLD on protein expression of UGT proteins.

Figure 4: Effect of NAFLD on protein expression of SULT proteins.

Figure 5: Correlation of protein expression and activity of CYP enzymes.

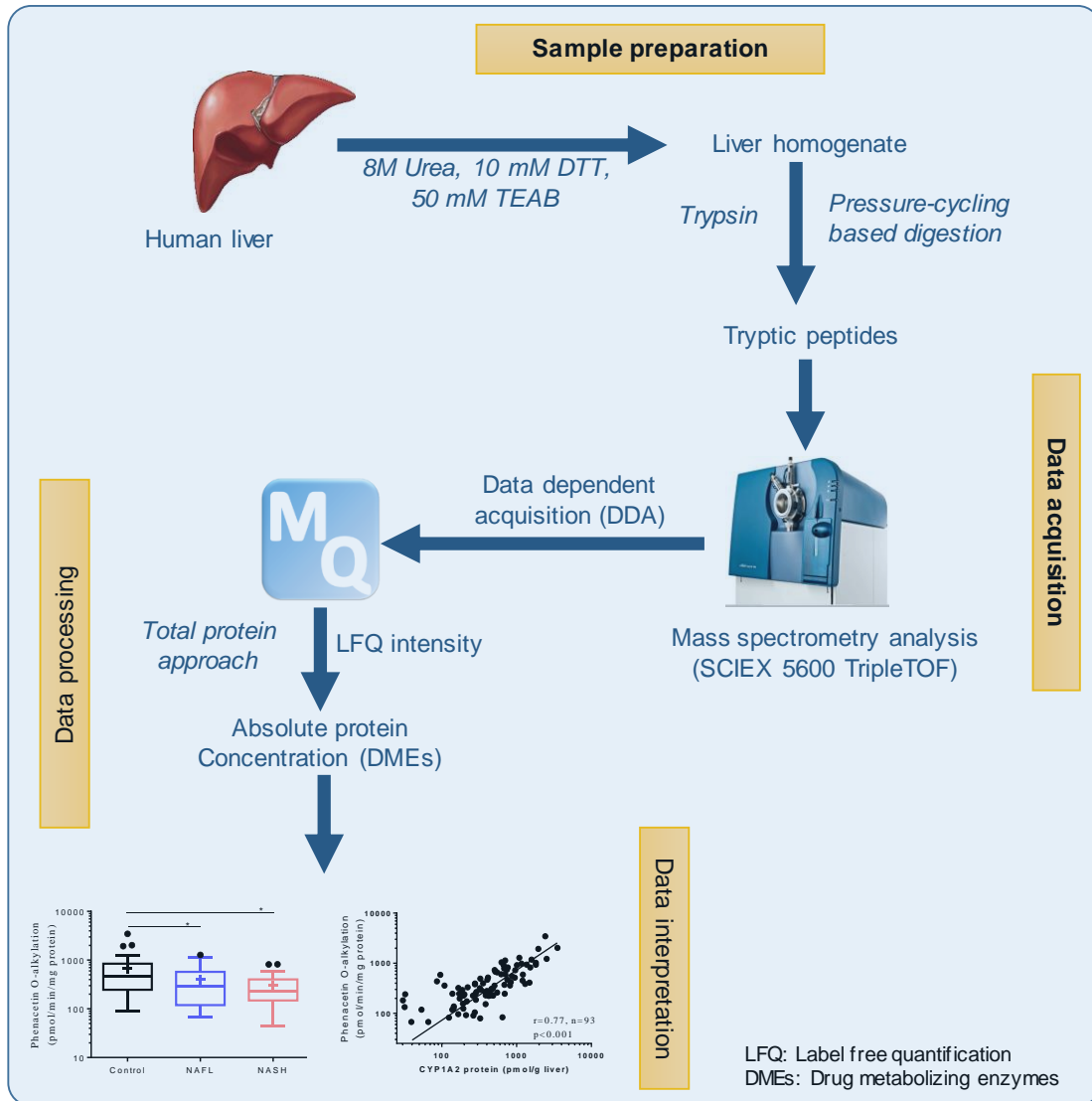
Figure 6: Effect of NAFLD on protein expression of some marker proteins in NAFLD.

Table 1: Demographic characteristics of study groups.

Table 2: Effect of NAFLD on the expression of major CYP450 enzymes and auxiliary proteins.

Table 3: Effect of NAFLD on the expression of major UGT enzymes.

Table 4: Effect of NAFLD on the expression of NAFLD specific marker proteins.



Graphical abstract

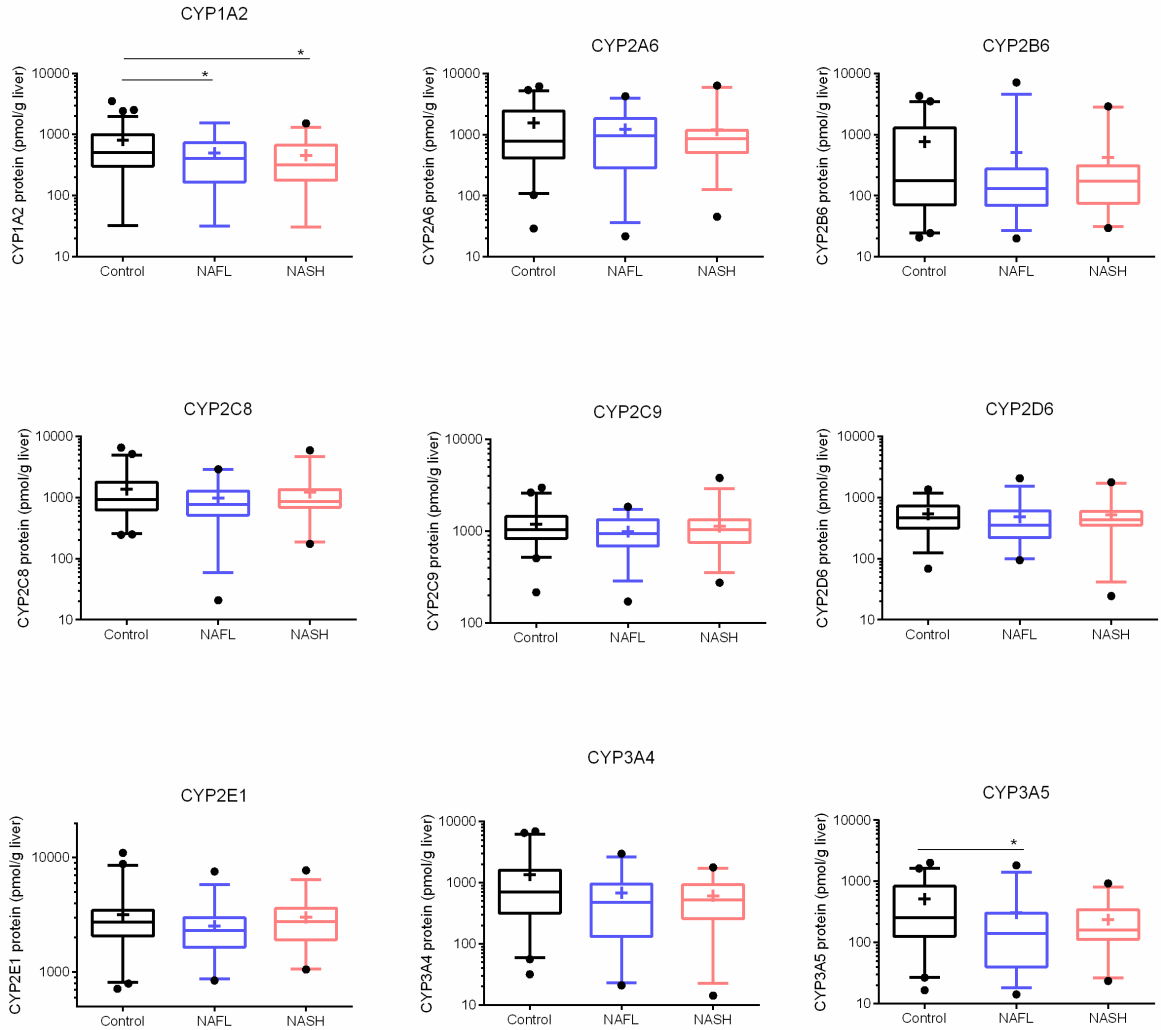


Figure 1: Effect of NAFLD on protein expression of various CYP450 proteins. Graphs represent Tukey box plots with median (horizontal line); + represent mean; P-value from non-parametric Kruskal-Wallis test with Dunn's multiple comparisons. * and ** represent p-value <0.05 and <0.01, respectively.

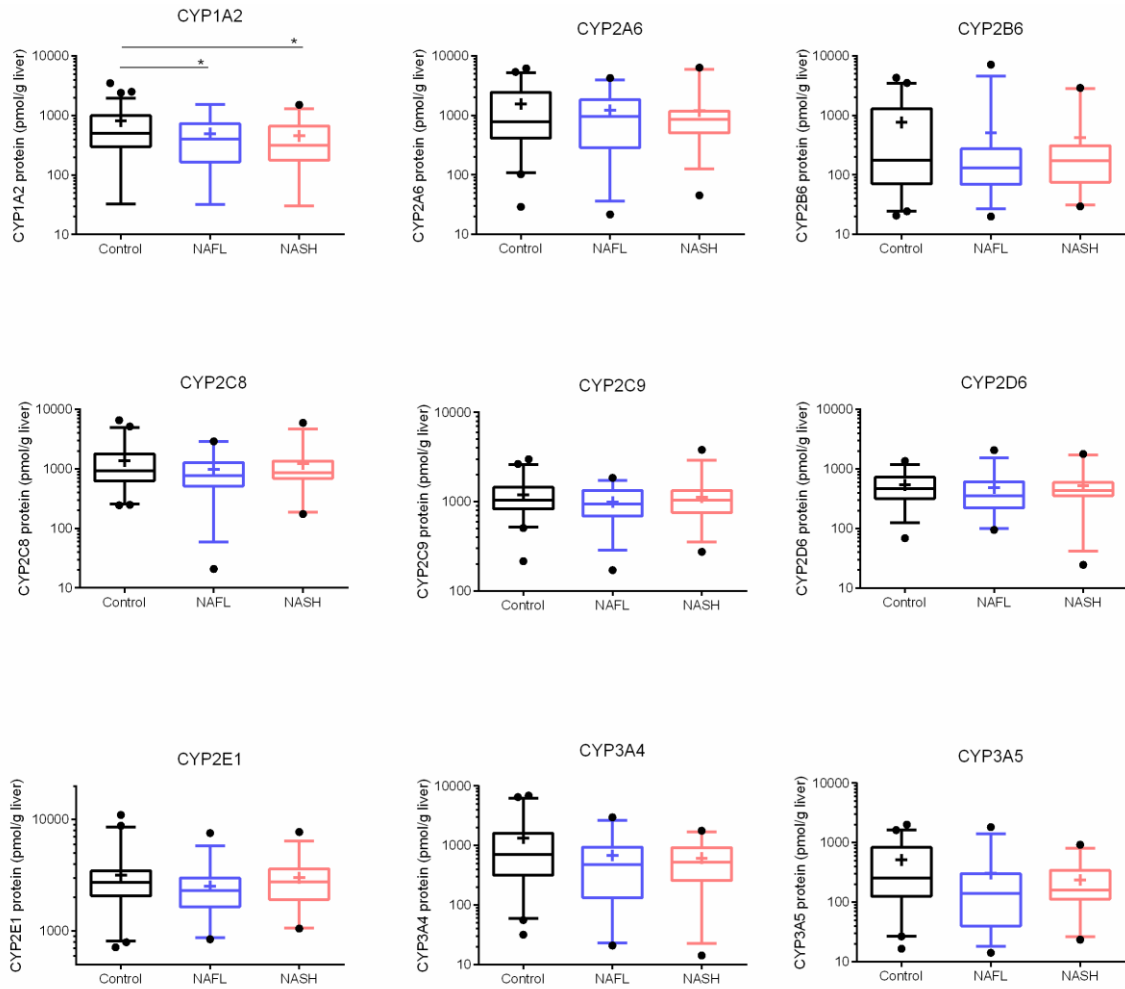


Figure 2: Effect of NAFLD on functional activity of various CYP450 proteins. Graphs represent Tukey box plots with median (horizontal line); + represent mean; P-value from non-parametric Kruskal-Wallis test with Dunn's multiple comparisons. * and ** represent p-value <0.05 and <0.01, respectively.

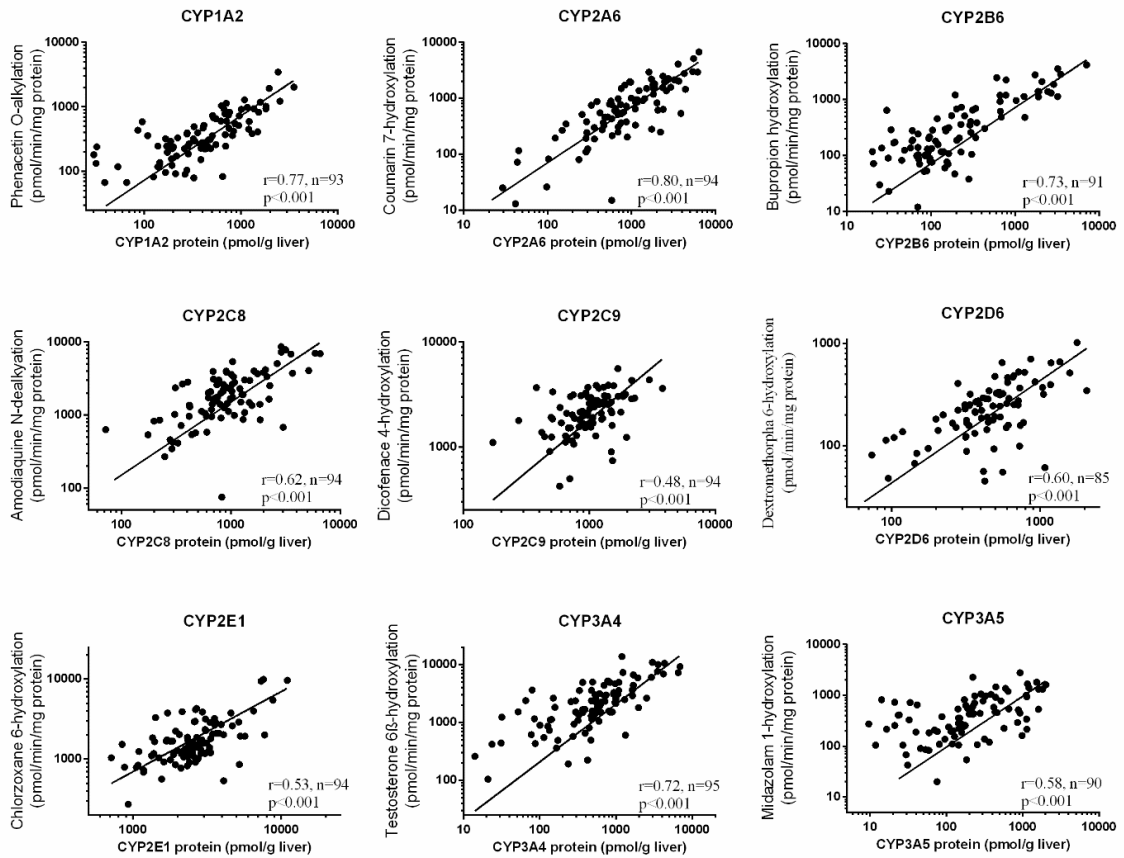


Figure 3: Correlation of protein expression and functional activity of CYP enzymes.
 Non-parametric Spearman correlation analysis.

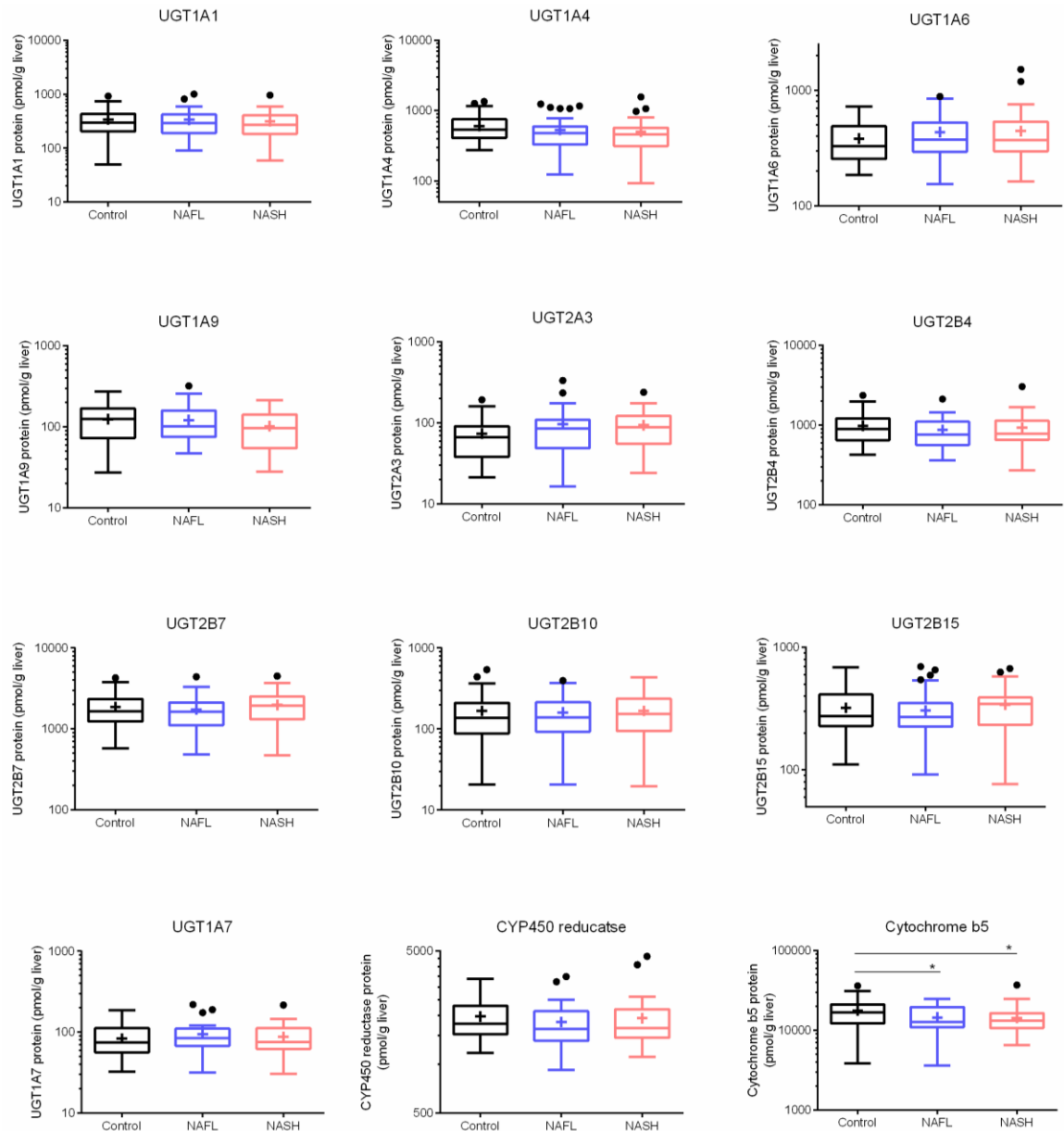


Figure 4: Effect of NAFLD on protein expression of UGT proteins. Graphs represent Tukey box plots with median (horizontal line); + represent mean; P-value from non-parametric Kruskal-Wallis test with Dunn's multiple comparisons. * and ** represent p-value <0.05 and <0.01, respectively.

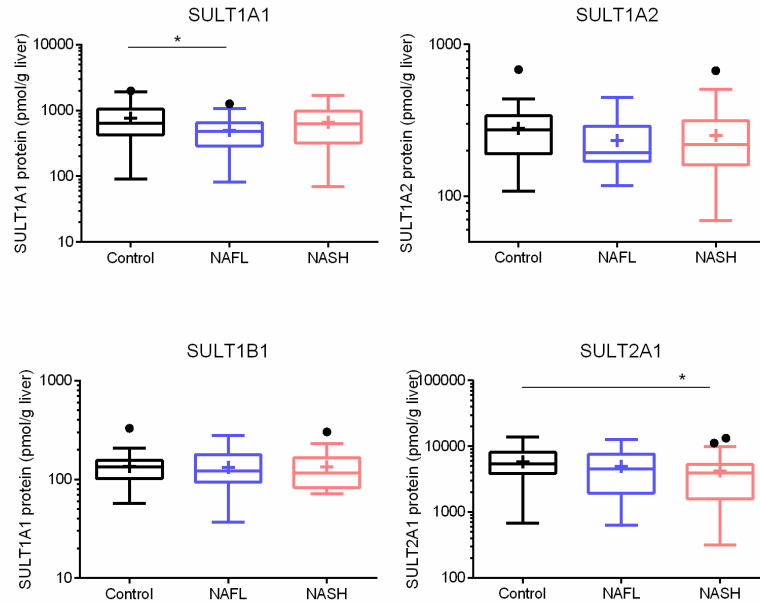


Figure 5: Effect of NAFLD on protein expression of SULT proteins. Graphs represent Tukey box plots with median (horizontal line); + represent mean; P-value from non-parametric Kruskal-Wallis test with Dunn's multiple comparisons. * and ** represent p-value <0.05 and <0.01, respectively.

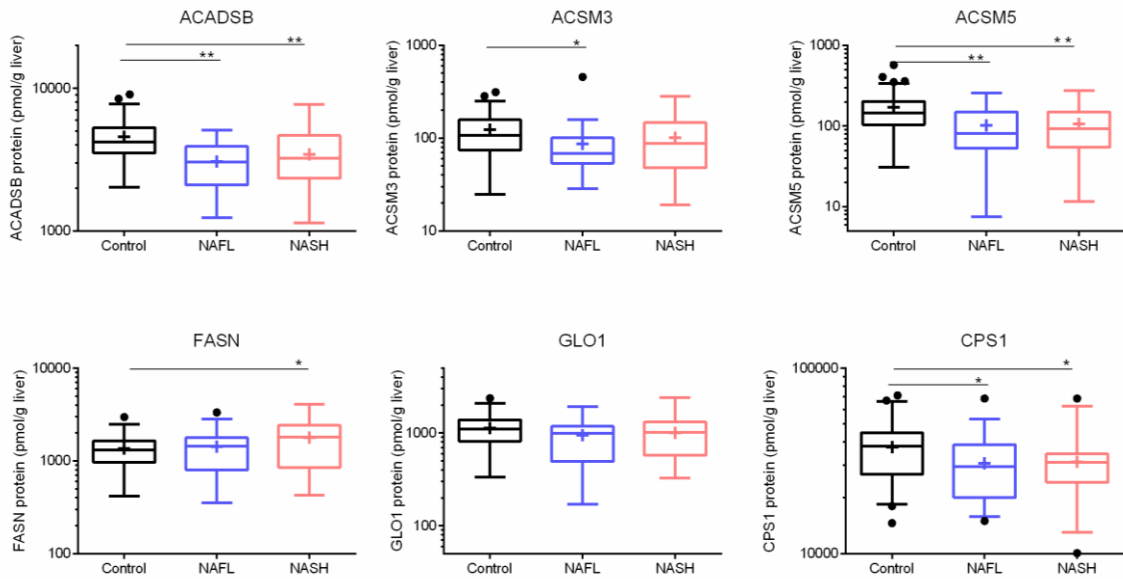


Figure 6: Effect of NAFLD on protein expression of some marker proteins in NAFLD.

Graphs represent Tukey box plots with median (horizontal line); + represent mean; P-value from non-parametric Kruskal-Wallis test with Dunn's multiple comparisons. * and ** represent p-value <0.05 and <0.01, respectively.

	Control	NAFL	NASH
N	42	34	30
Age (y)	46.5 (41.9 - 51.6)	52.8 (49.5 - 56.4)	50.8 (47.3 - 54.5)
Female	16	19	15
Male	26	15	15
Caucasian	33	20	28
Afro-American	8	1	1
Hispanic	1	3	1
Body weight (kg)	83.5 (76.2 - 91.5)	89.8 (80.6 - 100.1)	92.7 (86 - 99.9)
BMI (kg/m ²)	29.3 (26.5 - 32.3)	31.2 (28 - 34.8)	32.2 (29.9 - 34.7)
Liver weight (g)	1482.4 (1374.9 - 1598.3)	1798.5 (1603.2 - 2017.6) *	1839 (1678.4 - 2014.9) **
Malondialdehyde (nmol/mg protein)	0.6 (0.5 - 0.7)	0.9 (0.8 - 1.2) **	1.2 (1 - 1.6) **
Cholesterol (µg/g liver)	14.2 (12.4 - 16.2)	18.7 (16 - 21.9) **	20.8 (17.9 - 24.1) **
PPGL (mg/g)	83.1 (77.4 - 89.3)	78.9 (71.8 - 86.8)	79.8 (72.1 - 88.3)
Non-diabetic	21	19	13
Diabetic	21	15	17

Table 1: Demographic characteristics of control, NAFL and NASH groups. BMI: Body-mass index; PPGL: Protein per gram liver. P-value from non-parametric Kruskal-Wallis and Dunn's multiple comparison test. * and ** represent p-value <0.05 and <0.01, respectively.

	Control		NAFL	NASH
CYP1A2	549.4 (413.2 - 730.6)	294 (193.2 - 447.5) *	307.3 (213.9 - 441.3) *	
CYP2A6	893.8 (628.2 - 1271.7)	657.6 (417.1 - 1036.7)	787.7 (562.2 - 1103.6)	
CYP2B6	258.3 (159.3 - 418.9)	156.5 (99.9 - 245.2)	181.3 (116.3 - 282.7)	
CYP2C8	1001.3 (794.2 - 1262.4)	712.7 (513.7 - 988.7)	882.2 (664.8 - 1170.8)	
CYP2C9	1072.2 (924 - 1244.1)	888.9 (747.5 - 1057)	987.2 (817.9 - 1191.5)	
CYP2D6	459.6 (379.3 - 556.8)	370.4 (285 - 481.5)	397.5 (283 - 558.2)	
CYP2E1	2651.6 (2215.6 - 3173.4)	2264 (1937.2 - 2645.9)	2706.3 (2289.6 - 3198.9)	
CYP3A4	673.6 (459.4 - 987.7)	355 (227.1 - 554.9)	410.8 (273.7 - 616.4)	
CYP3A5	223.9 (142.8 - 351.1)	117.9 (70.6 - 196.7)	136.2 (86.7 - 213.9)	
POR	1893.8 (1738.5 - 2062.9)	1739.8 (1566 - 1932.8)	1814.5 (1611.8 - 2042.7)	
CYP5A	16130.3 (14038.3 - 18534)	13115.4 (11138.9 - 15442.6) *	13214.4 (11540 - 15131.7) *	
CYP51A1	43.8 (36.2 - 53.1)	34.4 (28.5 - 41.5)	39.8 (29.2 - 54.3)	
CYP8B1	394.5 (325.3 - 478.6)	362.2 (300.1 - 437)	371 (306.5 - 449)	
CYP27A1	304.3 (269 - 344.2)	288.2 (244.7 - 339.5)	314.7 (275.3 - 359.7)	
CYP4F11	84.3 (75 - 94.8)	80.9 (69.5 - 94.3)	83.9 (71.7 - 98.3)	
CYP4F2	215.9 (189.9 - 245.5)	160.2 (128.7 - 199.4)	190.9 (161.8 - 225.2)	
CYP4F3	50.2 (44.6 - 56.5)	51.3 (43.6 - 60.3)	51.2 (44.4 - 59.1)	

Table 2: Effect of NAFLD on the expression of major CYP450 enzymes and auxiliary proteins. P-value from non-parametric Kruskal-Wallis test and Dunn's multiple comparison test. * and ** represent p-value <0.05 and <0.01, respectively.

	Control	NAFLD	NASH
UGT1A1	295.1 (249.3 - 349.3)	283.3 (233.6 - 343.6)	271.2 (221.6 - 331.7)
UGT1A4	556.5 (491.7 - 629.8)	465.8 (390.5 - 555.6)	429.9 (350.2 - 527.8)
UGT1A6	355.6 (316.7 - 399.3)	395.2 (340.4 - 458.9)	387.8 (324.9 - 462.8)
UGT1A7	76 (65.9 - 87.5)	86.5 (74.1 - 101)	79.2 (67.4 - 93.2)
UGT1A9	110 (93.5 - 129.3)	109 (93.6 - 127.1)	89.8 (74.1 - 108.8)
UGT2A3	63.2 (52.6 - 76)	78.9 (62.6 - 99.5)	82.8 (68.4 - 100.2)
UGT2B10	132.6 (104.9 - 167.7)	124.2 (93.8 - 164.4)	141.1 (111.5 - 178.8)
UGT2B15	292 (255.7 - 333.5)	271.6 (229.8 - 320.9)	308.9 (260.3 - 366.6)
UGT2B4	901.3 (794.5 - 1022.4)	801.6 (698.9 - 919.4)	831.9 (704.8 - 981.8)
UGT2B7	1682.6 (1465 - 1932.5)	1543.2 (1300.2 - 1831.6)	1771.5 (1480.4 - 2119.8)
SULT1A1	609.5 (489.6 - 758.9)	396.3 (308.6 - 509) *	501.7 (369.8 - 680.7)
SULT1A2	260.2 (231 - 293)	207.3 (176.5 - 243.4)	223.6 (187.1 - 267.1)
SULT1B1	127 (111.9 - 144.2)	119 (99.5 - 142.4)	123 (105 - 144.1)
SULT2A1	5015.1 (4137.2 - 6079.2)	3654.7 (2720.7 - 4909.3) *	4000.4 (3026 - 5288.6)

Table 3: Effect of NAFLD on the expression of major UGT enzymes. P-value from non-parametric Kruskal-Wallis test with Dunn's multiple comparisons. * and ** represent p-value <0.05 and <0.01, respectively.

	Control	NAFL	NASH
ACADSB	4330.2 (3917.2 - 4786.8)	2835.3 (2477 - 3245.4) **	3119.4 (2646.1 - 3677.3) **
ACSM3	105.8 (89 - 125.9)	72.7 (59.8 - 88.3) *	81.3 (62.9 - 105.1)
ACSM5	142 (117 - 172.4)	76.7 (57.1 - 103) **	83.7 (63.3 - 110.8) **
GLO1	981.4 (819.3 - 1175.6)	816.8 (670.2 - 995.6)	894 (745.4 - 1072.3)
FASN	1238.1 (1081.7 - 1417.1)	1243.3 (1033.3 - 1496)	1538.5 (1249.7 - 1894.1)
CPS1	35368.4 (31705.4 - 39454.6)	28656.6 (25251.2 - 32521.1) *	29682.5 (25883.7 - 34038.9) *

Table 4: Effect of NAFLD on the expression of NAFLD specific marker proteins. P-value from non-parametric Kruskal-Wallis test without adjustment for multiple comparisons. * and ** represent p-value <0.05 and <0.01, respectively.

Supplementary information

Supplementary Table 1: Effect of NAFLD on protein expression of other drug disposition proteins.

Supplementary Table 2: Donor demographics for NAFL and diabetes

Supplementary Table 3: Effect of NAFLD and diabetes on the expression of CYP450 proteins.

Supplementary Table 4: Effect of NAFLD and diabetes on protein expression of phase-II proteins.

Supplementary Table 5: Effect of NAFLD and diabetes on protein expression of some marker proteins.

Supplementary Table 6 a,b: Effect of NAFLD and diabetes on protein expression of cytosolic and hepatic enzymes.

	Control			NAFL	NASH
AOX1	2884.5 (2614 - 3183)	2557 (2323.2 - 2814.4)	2451.3 (2118.8 - 2835.9)		
CES1	23945.2 (21599 - 26546.1)	23671 (20631.5 - 27158.3)	24813.4 (21638.2 - 28454.5)		
CES2	922.9 (849.2 - 1003.1)	755.1 (647.9 - 879.9)	790.2 (679.2 - 919.3)		
XDH	152.5 (135.2 - 171.9)	150.7 (123.8 - 183.3)	182.2 (152.6 - 217.6)		
ADH1A	3456.5 (2986.7 - 4000.2)	3112.8 (2549.7 - 3800.3)	3680 (2931.7 - 4619.3)		
ADH1B	18450.3 (16255.2 - 20941.9)	15631.4 (13337.9 - 18319.2)	16746.2 (13917.8 - 20149.4)		
ADH1C	4339.7 (3611.1 - 5215.3)	3645.1 (3070.5 - 4327.2)	3626.1 (2967.8 - 4430.3)		
ADH4	30365.9 (25686.6 - 35897.6)	23980.4 (19101.7 - 30105.1)	27478.9 (22360.6 - 33768.6)		
ADH5	2576.4 (2322.3 - 2858.2)	2246.3 (1920 - 2628)	2533.5 (2121.6 - 3025.4)		
ADH6	4474.9 (3971 - 5042.8)	3643.2 (3058.9 - 4339.2)	4185.1 (3443.2 - 5086.9)		
AKR1A1	3248.2 (2935.9 - 3593.6)	2780 (2300.2 - 3359.8)	3286.5 (2761.8 - 3910.7)		
AKR1C1	591.9 (486 - 720.9)	507.4 (409.5 - 628.6)	570.1 (449.4 - 723.2)		
AKR1C3	543.7 (473.7 - 624)	465.3 (380.4 - 569.1)	497.1 (414.8 - 595.6)		
AKR1C4	2173.3 (1879 - 2513.7)	1544.1 (1240.6 - 1921.9)	1887.3 (1530.6 - 2327.1)		
AKR1D1	1305 (1137.6 - 1497)	1081.1 (888 - 1316.3)	1380.6 (1083.9 - 1758.5)		
ALDH1A1	10299.4 (9044.8 - 11728.1)	8831.4 (7408.2 - 10528.2)	9554.2 (8098.5 - 11271.6)		
ALDH1B1	985.4 (775.9 - 1251.6)	1024.4 (785.6 - 1335.9)	1080.7 (817.9 - 1428.1)		
ALDH1L1	3166.9 (2748.8 - 3648.4)	2849.6 (2454.5 - 3308.2)	3063.1 (2586.1 - 3628.1)		
ALDH2	13875 (12500.5 - 15400.7)	11062.1 (9461.8 - 12933.1)	12769.6 (10662.5 - 15293.1)		
ALDH3A2	837.3 (773.3 - 906.6)	823.3 (736.2 - 920.6)	796.6 (707.6 - 896.9)		
ALDH4A1	5339 (4841.9 - 5887.2)	4911.9 (4336.6 - 5563.5)	4935.8 (4377.8 - 5564.9)		
ALDH5A1	1057.1 (959.3 - 1164.9)	866.1 (764.8 - 980.8)	997.7 (871.4 - 1142.3)		
ALDH6A1	5604.1 (4890.5 - 6421.8)	4526.1 (3965.8 - 5165.7)	4448.3 (3884.8 - 5093.5)		
ALDH8A1	911.3 (776.9 - 1069)	760.3 (649.7 - 889.8)	824.2 (630.4 - 1077.6)		
ALDH9A1	2173.8 (1972.9 - 2395.2)	1916.5 (1642 - 2236.8)	2003.2 (1721 - 2331.6)		
GSTA1	269.2 (227.7 - 318.3)	251.8 (187.4 - 338.3)	345.2 (255.9 - 465.6)		
GSTA2	1174.1 (873.1 - 1579)	1018.8 (701.2 - 1480.3)	1003.8 (673.9 - 1495.1)		
GSTK1	2034.3 (1656.1 - 2498.9)	1654.7 (1233.5 - 2219.8)	2108.1 (1706.2 - 2604.6)		
GSTO1	3466.7 (3053 - 3936.5)	2916.8 (2406.1 - 3535.8)	2819.5 (2318.2 - 3429.3)		
GSTP1	418.8 (372.2 - 471.2)	440.9 (362.7 - 535.9)	418 (354.4 - 492.9)		
GSTZ1	1294.1 (1141.2 - 1467.4)	956.2 (765.7 - 1194.1)	1079.5 (890.9 - 1308)		

Supplementary table 1

Supplementary table 2

	Control		NAFL		NASH	
	Non-diabetic	Diabetic	Non-diabetic	Diabetic	Non-diabetic	Diabetic
N	21	21	19	15	16	17
Age (y)	46.4 (39.3 - 54.8)	46.6 (40.9 - 53.2)	51.9 (47.3 - 56.8)	54.1 (49.3 - 59.3)	50.2 (43.9 - 57.3)	51.2 (47.5 - 55.2)
Female	9	7	10	9	9	9
Male	12	14	9	6	7	8
Caucasian	17	16	16	14	13	15
Afro-American	4	4	1	0	0	1
Hispanic	0	1	2	1	0	1
Body weight (kg)	78.5 (70.8 - 87.1)	89.1 (76.6 - 103.6)	85.7 (74.5 - 98.6)	95.3 (80.4 - 113)	86.6 (78.8 - 95.1)	97.6 (87.7 - 108.7)
BMI (kg/m ²)	27.5 (24.7 - 30.7)	31.2 (26.4 - 36.7)	28.6 (25.4 - 32.3)	34.7 (28.9 - 41.7)	29.3 (27 - 31.8)	34.6 (31.1 - 38.4)
Liver weight (g)	1372.5 (1245.1 - 1513)	1601 (1438.5 - 1781.9)	1682.1 (1470.1 - 1924.7)	1957.6 (1612.9 - 2376)**	1745 (1530 - 1990.3)	1914.2 (1687.6 - 2171.3)**
Malondialdehyde (nmol/mg protein)	0.5 (0.4 - 0.6)	0.7 (0.6 - 0.8)	0.9 (0.7 - 1.1)	1 (0.7 - 1.4)**	1.2 (0.8 - 1.9)**	1.2 (0.9 - 1.6)**
Cholesterol (µg/g liver)	14.3 (11.8 - 17.3)	14.1 (11.6 - 17)	20.1 (15.4 - 26.3)	17.8 (14.6 - 21.7)	22 (17.6 - 27.5)	20.1 (16.5 - 24.5)
PPGL (mg/g)	90.9 (84.1 - 98.3)	76 (68.2 - 84.6)	82.6 (73.4 - 93.1)	74.5 (64 - 86.7)	83.1 (72 - 96)	77.3 (67 - 89.2)

Protein	Control		NAFL		NASH	
	Non-diabetic	Diabetic	Non-diabetic	Diabetic	Non-diabetic	Diabetic
CYP1A2	618.9 (401.2 - 954.8)	484.9 (335.1 - 701.7)	318.1 (178.1 - 568.1)	267.5 (143 - 500.4)	396.9 (186.4 - 845.4)	260.4 (185.1 - 366.3)
CYP2A6	785.5 (453.9 - 1359.6)	1017 (648.4 - 1595.1)	816.1 (471.7 - 1412)	500.2 (233.4 - 1072.1)	903.1 (573.9 - 1421.1)	709.5 (434.8 - 1157.8)
CYP2B6	300 (151.3 - 594.7)	220.7 (110.3 - 441.7)	249.8 (133.3 - 468.4)	79 (52.8 - 118.3)	170.8 (93.2 - 313.1)	191 (98.7 - 369.4)
CYP2C8	1153.7 (834.3 - 1595.4)	869 (626.2 - 1205.9)	801.9 (486.7 - 1321.2)	613.8 (413.7 - 910.6)	820.2 (523.8 - 1284.4)	932.8 (642.5 - 1354.4)
CYP2C9	1140.4 (944 - 1377.6)	1008 (799.9 - 1270.3)	994.8 (843.1 - 1173.8)	770.7 (556.7 - 1067)	1031.2 (806.4 - 1318.7)	954.8 (722.3 - 1262.2)
CYP2D6	518.9 (402.4 - 668.9)	409.5 (308.6 - 543.5)	448.7 (307.7 - 654.2)	293.5 (210.9 - 408.6)	361.8 (183.8 - 712.1)	425.8 (304 - 596.5)
CYP2E1	3474.9 (2781 - 4341.9)	2023.4 (1601.8 - 2556)	2419.8 (2026.1 - 2889.9)	2081 (1582.4 - 2736.7)	2614.8 (2064.6 - 3311.5)	2778.5 (2188.2 - 3528)
CYP3A4	1019.2 (627.2 - 1656.1)	445.2 (257.7 - 769.2)	502.3 (259.1 - 974.1)	234.1 (138.3 - 396.1)	402 (208.1 - 776.7)	418 (247.4 - 706.5)
CYP3A5	308.5 (161.7 - 588.5)	162.5 (88.2 - 299.4)	191.7 (94.5 - 389)	67.9 (35.2 - 131.2)	189.2 (110.2 - 324.8)	104.7 (53.3 - 205.5)
POR	2058.4 (1803.3 - 2349.6)	1742.3 (1577.9 - 1923.9)	1858.7 (1650.9 - 2092.7)	1600 (1334.9 - 1917.8)	1680.8 (1398.4 - 2020.3)	1923.9 (1650 - 2243.2)
CYB5A	19217.9 (16842.7 - 21928.2)	13538.8 (10827.9 - 16928.4)	14203.7 (11596.3 - 17397.5)	11855.7 (9090.1 - 15462.6)	13482.2 (10814 - 16808.7)	13013.2 (10921.9 - 15504.9)
CYP51A1	50.1 (37.7 - 66.6)	38.3 (29.9 - 49.2)	41.8 (33.8 - 51.7)	25.6 (19.6 - 33.5)	33.2 (20.5 - 53.5)	45.6 (30.3 - 68.6)
CYP8B1	447.6 (372.5 - 537.9)	347.8 (248.5 - 486.7)	361.8 (268.9 - 486.9)	362.6 (293.3 - 448.3)	318.2 (231.9 - 436.8)	417.1 (332.4 - 523.3)
CYP27A1	345.8 (295.3 - 405)	267.7 (224.4 - 319.3)	318.9 (264 - 385.3)	253.5 (192.1 - 334.6)	316.3 (278.8 - 358.9)	313.5 (251.8 - 390.3)
CYP4F11	97.7 (84.1 - 113.6)	72.1 (61.6 - 84.4)	85.9 (70.7 - 104.3)	74.3 (57.9 - 95.2)	91 (71.9 - 115.1)	78.9 (63.8 - 97.7)
CYP4F2	258.9 (230.9 - 290.3)	178.4 (145.2 - 219.3)	164.9 (117.7 - 231)	154.5 (118.5 - 201.4)	222.7 (187.5 - 264.6)	168.4 (130.7 - 216.9)
CYP4F3	55.4 (47.1 - 65.1)	45.5 (38.6 - 53.6)	52.3 (42.3 - 64.7)	49.9 (38.6 - 64.6)	52 (41.7 - 64.7)	50.8 (41.8 - 61.7)

Supplementary table 3

Protein	Control		NAFL		NASH	
	Non-diabetic	Diabetic	Non-diabetic	Diabetic	Non-diabetic	Diabetic
UGT1A1	361.2 (286.8 - 454.9)	241.1 (193.7 - 300)	323.4 (248.1 - 421.6)	239.6 (183.7 - 312.4)	258.4 (178.1 - 374.8)	281.4 (225 - 351.9)
UGT1A4	566.7 (473.8 - 677.9)	546.4 (458.8 - 650.8)	585 (483.8 - 707.3)	349 (269.7 - 451.6)	437.6 (311.5 - 614.7)	424.2 (326.6 - 550.8)
UGT1A6	379.4 (325.5 - 442.1)	333.3 (280.3 - 396.4)	454.8 (377.8 - 547.5)	330.8 (265.9 - 411.5)	438.7 (349.3 - 551)	352.9 (273.2 - 455.7)
UGT1A7	87.7 (72.5 - 106)	66.8 (55.1 - 81.1)	105.7 (90.1 - 123.9)	68.8 (54.7 - 86.5)	80.1 (64.4 - 99.5)	78.6 (61.8 - 100)
UGT1A9	130 (107.8 - 156.8)	93 (72.5 - 119.3)	125 (102.6 - 152.2)	91.8 (73.9 - 113.9)	98.2 (74.7 - 129)	83.8 (64 - 109.8)
UGT2A3	70.7 (52.6 - 95.1)	57.2 (45.7 - 71.5)	80.7 (57.7 - 112.8)	76.5 (55.9 - 104.7)	85 (62.6 - 115.6)	80.9 (63.1 - 103.9)
UGT2B10	166.8 (127.7 - 217.9)	101.5 (70 - 147.2)	151.9 (107.2 - 215.1)	100.2 (65.1 - 154.2)	126.9 (84.2 - 191.2)	153.9 (117 - 202.5)
UGT2B15	326 (274.6 - 387)	261.6 (215.1 - 318)	270.5 (212.8 - 343.9)	272.9 (215.9 - 345.1)	266.7 (200.6 - 354.5)	345.6 (282.8 - 422.4)
UGT2B4	977.2 (806.8 - 1183.6)	831.3 (707.5 - 976.7)	871.1 (720.9 - 1052.6)	721.5 (595.7 - 873.8)	827 (638 - 1072.1)	835.6 (669.4 - 1043.1)
UGT2B7	1823.6 (1469.8 - 2262.6)	1552.5 (1307.1 - 1844.1)	1631.2 (1300.7 - 2045.7)	1438.5 (1102.1 - 1877.5)	1699.7 (1266.4 - 2281.3)	1828.4 (1452.9 - 2300.9)
SULT1A1	740.3 (575.4 - 952.4)	501.9 (355.5 - 708.7)	427.8 (312.1 - 586.6)	359.7 (238.8 - 541.8)	587.5 (377 - 915.7)	441.3 (289.5 - 672.6)
SULT1A2	279 (238.9 - 326)	240.8 (201 - 288.3)	215 (163.5 - 282.7)	198.3 (173 - 227.3)	253.3 (180.6 - 355.2)	204.8 (170 - 246.6)
SULT1B1	140.4 (120.1 - 164.1)	114.2 (94.1 - 138.6)	123.2 (94.7 - 160.3)	113.2 (90 - 142.3)	126.1 (97.2 - 163.7)	120.1 (98.7 - 146.2)
SULT2A1	6072.1 (5071.9 - 7269.5)	4142.1 (2994 - 5730.5)	3794.3 (2522.3 - 5707.8)	3485.2 (2246.8 - 5406.1)	5568.8 (4164.7 - 7446.3)	3106.4 (2068.4 - 4665.2)

Supplementary table 4

Protein	Control		NAFL		NASH	
	Non-diabetic	Diabetic	Non-diabetic	Diabetic	Non-diabetic	Diabetic
ACADSB	4695.5 (4041.4 - 5455.5)	3993.3 (3516.4 - 4535)	2959.2 (2507.4 - 3492.5)	2685.8 (2141.2 - 3368.9)	3686.2 (3022.4 - 4495.7)	2745.5 (2171.8 - 3470.8)
ACSM3	137.2 (115.8 - 162.6)	81.6 (62.8 - 106.1)	80.8 (59.4 - 109.9)	62.7 (52.8 - 74.5)	85.8 (56.2 - 131.1)	77.8 (56.3 - 107.5)
ACSM5	166.1 (128.6 - 214.7)	121.4 (91.7 - 160.8)	81 (53.2 - 123.2)	71.1 (47.1 - 107.4)	68.2 (42.1 - 110.6)	100 (74.2 - 134.9)
GLO1	1184.7 (1039.7 - 1350)	813 (589.8 - 1120.5)	871.3 (692.1 - 1097)	752.7 (532.6 - 1063.6)	983.1 (742.8 - 1301.3)	831.4 (653.8 - 1057.2)
FASN	1461.9 (1281.7 - 1667.3)	1048.6 (844.4 - 1302.1)	1302.7 (994.4 - 1706.7)	1171.9 (913 - 1504.3)	1946.1 (1469.7 - 2577)	1285.5 (977.2 - 1690.9)
CPS1	39339.9 (34682.6 - 44622.5)	31797.9 (26836 - 37677.2)	30621.2 (26007.8 - 36053)	26347.9 (21647.2 - 32069.3)	32715.6 (27470.5 - 38962.1)	27554.3 (22593.2 - 33604.9)

Supplementary table 5

Proteins	Control		NAFL		NASH	
	Non-diabetic	Diabetic	Non-diabetic	Diabetic	Non-diabetic	Diabetic
ALDH1A1	11702.2 (9834.4 - 13924.7)	9064.8 (7565.7 - 10861)	9319.6 (7593.6 - 11437.9)	8249.6 (6067.3 - 11217)	10799.9 (8264.2 - 14113.7)	8699.5 (7096.8 - 10664.1)
ALDH1B1	1361.3 (1080.2 - 1715.4)	713.4 (490.2 - 1038.2)	1141.1 (796.4 - 1635.1)	893.6 (601.6 - 1327.4)	1527.1 (1150.2 - 2027.5)	829.7 (553.6 - 1243.4)
ALDH1L1	3598.2 (2992.3 - 4326.6)	2787.2 (2271.3 - 3420.4)	3136.6 (2510.2 - 3919.4)	2523.4 (2116.5 - 3008.4)	3375 (2548.9 - 4469)	2844.2 (2309.3 - 3503)
ALDH2	15840.9 (14025.1 - 17891.9)	12153.1 (10441.2 - 14145.7)	11977.4 (10017.9 - 14320.3)	10002.4 (7627 - 13117.5)	14404.4 (11412.5 - 18180.6)	11645.8 (8968.7 - 15121.9)
ALDH3A2	888.7 (795.6 - 992.7)	788.8 (706 - 881.4)	887.1 (776.9 - 1013)	749 (623.4 - 899.8)	747.9 (645.7 - 866.2)	836 (700.6 - 997.7)
ALDH4A1	5957.7 (5204.7 - 6819.7)	4784.6 (4211.4 - 5435.8)	5143.6 (4393.9 - 6021.4)	4633.2 (3785.7 - 5670.4)	5221.8 (4438.2 - 6143.8)	4727.7 (3977.6 - 5619.2)
ALDH5A1	1187.2 (1044.4 - 1349.4)	941.3 (826 - 1072.7)	914.5 (769.7 - 1086.6)	808.5 (676.1 - 966.7)	1087.8 (906.4 - 1305.5)	933.9 (770.3 - 1132.1)
ALDH6A1	5981.3 (5107.5 - 7004.6)	5250.6 (4203.4 - 6558.7)	4563.8 (3879.4 - 5369)	4478.8 (3579.2 - 5604.6)	4724.4 (3869.8 - 5767.6)	4248.1 (3526.3 - 5117.7)
ALDH8A1	1123.8 (992.3 - 1272.6)	739 (565.1 - 966.5)	810.5 (650.5 - 1009.8)	701.2 (560.5 - 877.4)	933.7 (613.6 - 1420.7)	749.2 (527.1 - 1065.1)
ALDH9A1	2438.8 (2182.2 - 2725.6)	1937.7 (1675.6 - 2240.7)	2012.7 (1670.3 - 2425.3)	1801.2 (1384.8 - 2342.7)	2181.9 (1679.1 - 2835.2)	1876.5 (1569 - 2244.2)
GSTA1	301.3 (241.4 - 376.2)	241.8 (189 - 309.3)	212.6 (148 - 305.5)	316.8 (195.6 - 513)	448.7 (290.8 - 692.2)	282.4 (190.2 - 419.3)
GSTA2	1418.4 (969.3 - 2075.6)	971.9 (620.6 - 1522.1)	1050 (604.4 - 1824.1)	982.5 (591.9 - 1631)	1845.9 (1048.2 - 3250.7)	653 (412.4 - 1033.9)
GSTK1	2632 (2417 - 2866.1)	1572.4 (1080.5 - 2288)	1918.6 (1387.2 - 2653.7)	1371.9 (814 - 2312.3)	2556 (2166 - 3016.2)	1819.3 (1295.3 - 2555.1)
GSTO1	3740.6 (3291.4 - 4251.1)	3212.8 (2582.9 - 3996.4)	3059.7 (2427.4 - 3856.7)	2745.3 (1973.9 - 3818.1)	3297 (2518.7 - 4315.8)	2501.7 (1909.1 - 3278.2)
GSTP1	433.6 (381.6 - 492.7)	404.5 (331 - 494.2)	459.7 (342.8 - 616.6)	418.1 (326.1 - 536)	403.6 (315.5 - 516.3)	429.3 (341.9 - 539)
GSTZ1	1500.1 (1313.6 - 1713.1)	1116.3 (916.8 - 1359.3)	1104.2 (849.1 - 1435.9)	796.9 (551.8 - 1150.9)	1253.9 (952.7 - 1650.3)	962.7 (742.7 - 1247.9)

Supplementary table 6a

Proteins	Control		NAFL		NASH	
	Non-diabetic	Diabetic	Non-diabetic	Diabetic	Non-diabetic	Diabetic
AOX1	3111.6 (2714.7 - 3566.5)	2674.1 (2330.4 - 3068.5)	2798 (2522.4 - 3103.6)	2281.3 (1946.2 - 2674.2)	2496.2 (1914.3 - 3255)	2417.4 (2048.5 - 2852.9)
CES1	26713.2 (23114.9 - 30871.8)	21463.9 (18764.5 - 24551.7)	26430.5 (22727.6 - 30736.7)	20585.3 (16308.8 - 25983.4)	24607.1 (20650.5 - 29321.8)	24972.2 (20329 - 30676.1)
CES2	970.6 (864.4 - 1090)	877.5 (779.5 - 987.9)	799.2 (702.9 - 908.7)	702.6 (515.6 - 957.5)	816.9 (708.5 - 942)	770.4 (601.4 - 986.8)
XDH	181.9 (161.6 - 204.8)	127.8 (106.5 - 153.3)	147.7 (111.9 - 195.1)	154.5 (116.6 - 204.6)	177.1 (125.9 - 249.1)	186.2 (154.9 - 223.8)
ADH1A	4120.9 (3375.1 - 5031.6)	2899.2 (2399.7 - 3502.7)	3075.6 (2337.5 - 4046.7)	3160.7 (2341.5 - 4266.4)	3373.9 (2125.3 - 5356)	3932.7 (3216.8 - 4807.9)
ADH1B	21513.4 (18374.8 - 25188.2)	15823.4 (13236.9 - 18915.3)	16002.6 (12849.9 - 19928.8)	15173.5 (11984.2 - 19211.6)	17298.5 (12266.7 - 24394.3)	16335.8 (13329.3 - 20020.5)
ADH1C	5734.5 (4736.7 - 6942.5)	3284.1 (2510.7 - 4295.8)	3719.6 (2849.9 - 4854.5)	3552.9 (2898.9 - 4354.6)	4148.4 (2902.6 - 5929.1)	3271.4 (2619.9 - 4085)
ADH4	37716 (31392.3 - 45313.5)	24448.2 (19017.8 - 31429.2)	25236.1 (18488.2 - 34446.8)	22479.1 (15973.7 - 31633.7)	30823.9 (21137.4 - 44949.5)	25168 (20125.7 - 31473.6)
ADH5	2811.4 (2453.2 - 3221.9)	2361 (2030.9 - 2744.7)	2312.4 (1899.1 - 2815.7)	2165.2 (1669 - 2809.1)	2780.6 (2095.4 - 3689.8)	2359.5 (1878.5 - 2963.7)
ADH6	5112 (4325.7 - 6041.2)	3917.3 (3357.1 - 4571)	3776.8 (2970.1 - 4802.5)	3480.8 (2680.6 - 4519.8)	4286.2 (2958.4 - 6210)	4109.4 (3341.7 - 5053.6)
AKR1A1	3588.7 (3210 - 4012)	2940 (2505.1 - 3450.5)	2894.6 (2270.5 - 3690.2)	2641.2 (1942.4 - 3591.5)	3542 (2607.5 - 4811.3)	3103.6 (2533.9 - 3801.3)
AKR1C1	768.3 (644.6 - 915.7)	456 (331.1 - 627.9)	560.7 (419.6 - 749.2)	447.1 (325.5 - 614)	811.7 (675.7 - 975.1)	435.1 (307.1 - 616.4)
AKR1C3	663 (568.8 - 772.7)	445.8 (365.7 - 543.6)	523.1 (398.9 - 686)	401.1 (299 - 538.1)	581.6 (468 - 722.6)	440.9 (338.6 - 574)
AKR1C4	2520.7 (2190.5 - 2900.6)	1873.8 (1470.7 - 2387.3)	1638.8 (1257.6 - 2135.6)	1432 (986.3 - 2079)	2222.9 (1652.4 - 2990.4)	1665.2 (1252.3 - 2214.3)
AKR1D1	1482.1 (1218.7 - 1802.5)	1149 (958.9 - 1376.8)	1129.7 (842.8 - 1514.3)	1022.6 (791.5 - 1321.1)	1644.9 (1073.7 - 2520.2)	1207.5 (921.8 - 1581.8)

Supplementary table 6b

MANUSCRIPT V

This manuscript has been prepared as a research article for submission to the Journal of Proteomics

SWATH-MS based method for simultaneous relative quantification of 25 clinically important drug transporters in human liver

Rohitash Jamwal, Benjamin J. Barlock, Sravani Adusumalli, Fatemeh Akhlaghi

Biomedical and Pharmaceutical Sciences, College of Pharmacy, University of Rhode Island, Kingston, RI, 02881, USA

Corresponding author:

Fatemeh Akhlaghi, Ph.D.

Clinical Pharmacokinetics Research Laboratory, Department of Biomedical and Pharmaceutical Sciences, The University of Rhode Island, 495A Avedisian Hall, 7 Greenhouse Road, Kingston, RI 02881, United States.

Email address: fatemeh@uri.edu

Keywords: gender differences, hepatic drug transporters, label-free quantification, membrane proteins, proteomics, SWATH-MS

Number of words:

Abstract: 200

Introduction: 778

Discussion: 1619

References: 66

Tables: 4

Figures: 3

Supplementary files: 4

Abstract

Hepatic xenobiotic transporters in human liver play an important role in the elimination of drugs or toxins and significantly contribute to variability in drug response. We developed a label-free mass spectrometry-based method to study the protein expression of 25 clinically relevant transporter proteins (12 ABC and 13 SLC) in liver tissue from 22 donors (9 female, 12 male). Membrane fractions were extracted from the tissue using ProteoExtract membrane extraction kit and in-solution trypsin digestion was performed using pressure-cycling technology. Data was acquired in data-dependent and sequential window acquisition of all theoretical mass spectra (SWATH-MS) mode. Chromatographic separation was achieved over a 90-min gradient on Acquity UPLC BEH C18 peptide column, and mass spectrometer was operated in positive electrospray mode. Digested *E. coli* β -galactosidase peptides were spiked in each sample before LC-MS/MS analysis, and intensity was expressed relative to APLDNDIGVSEATR peptide. ProteinPilot (ver 5.0.1) was used for peptide identification and Skyline (ver 4.0) was used for targeted data extraction from SWATH files. Na⁺/K⁺ transporting subunit alpha 4 (ATP1A4), was quantified as a cell membrane marker and its coefficient of variation was 9.7% across different liver samples.

Significance: The work highlights the suitability of SWATH-MS for large-scale simultaneous quantification of several xenobiotic transporters important in drug disposition. We found that average differential expression of transporters proteins was similar and much smaller than the inter-individual variability observed between the genders

1. Introduction

Xenobiotic transporters play a crucial role in drug disposition by mediating drug uptake and efflux. These proteins govern the absorption, distribution, metabolism, and elimination of drugs, toxins and endogenous molecules across the cell membrane. Thus, transporters can govern the rate-limiting step in systemic and tissue exposure of drugs. Biologically, transporters are membrane-bound proteins which are ubiquitously expressed throughout the body. These proteins are mostly localized on the apical or basolateral membranes of various organs including intestine, liver, kidney, and brain and facilitate the efflux and uptake of xenobiotics [1]. The ATP-binding cassette (ABC) family and the solute carrier (SLC) family represent the two significant super families of membrane transporters in human [2-4]. ABC transporters utilize ATP for transport of substrates across the membrane, and most of efflux transporters belong to this family (*Supplementary table 1a*). In contrast, SLC transporters mainly facilitate uptake which can be active or facilitated (*Supplementary table 1b*). Some SLC transporters also mediate bidirectional movement of molecules. The altered systemic exposure and organ toxicity can be related to transporters mediated drug interactions [1, 5]. Therefore, the last decade has seen a significant amount of research focusing on quantification and de-orphanization of these transporters as well as elucidation of their functionality [6, 7]. Inter-individual variability in the expression and drug response of xenobiotic transporters may arise from non-genetic (age and gender), genetic (polymorphism), epigenetic and regulatory factors [8]. While more than 400 different transporters have been annotated in the human genome, the function of many of these remains unknown [2, 9].

Efflux transporters localized on the canalicular membrane (e.g., P-gp/MDR1, MRP2, BCRP, BSEP, MDR3, and MATE1) facilitate excretion of molecules from hepatocytes into bile [4, 6, 10]. Meanwhile, basolateral hepatic efflux transporters (e.g., MRP1, MRP3, MRP4, MRP5, and MRP6) return molecules to hepatic blood from the hepatocyte [4, 6, 11]. Prominent uptake transporters that are localized on the sinusoidal membrane of hepatocyte include NTCP, OATP1B1, OATP1B3, OATP2B1, OAT2, and OCT1 [12, 13]. These uptake transporters, facilitate uptake of drugs from the blood into hepatocyte thereby facilitating metabolic clearance of drugs. Moreover, OAT7 on the sinusoidal membrane and sterolin-1 and sterolin-2 on basolateral membrane mediate bidirectional (efflux and uptake) transport of various substrates [14, 15].

Traditionally, researchers have relied on quantification of mRNA expression of transporters as a surrogate to the functional activity in the tissue. However, a weak correlation was observed between mRNA and protein expression in human livers [16, 17]. Protein abundance levels of these transporters are usually estimated by cumbersome Western blot analyses that is semi-quantitative at best. Last decade has seen a rise in the use of mass-spectrometry (MS) based techniques for quantification of the protein expression [10, 18]. Available MS methods for quantification of liver transporters are based on targeted quantitative proteomics approaches [10, 16, 17, 19, 20]. A comprehensive cost comparison of different mass spectrometry-based techniques reported significant cost savings with label-free based quantitative proteomics [21]. Lfq approaches are relatively inexpensive as compared to targeted MRM methods as there is no need to synthesize unique peptides for each protein and isotopically labeled isoforms of these peptide as the internal standard.

Relative label-free quantification (LFQ) using the sequential window acquisition of all theoretical mass spectra (SWATH-MS) technique provides an alternative to targeted approaches for protein estimation [22]. SWATH is a data-independent acquisition (DIA) technique in which all the precursors within a predefined m/z are fragmented, and product ions of these precursors are recorded as a digital repository [23]. The data is further deconvoluted and extracted using software like OpenSWATH, SWATH 2.0 and Skyline [24]. A significant advantage of SWATH-MS over the other mass spectrometry methods is related to the ability to perform retrospective mining of the data. For instance, if the researcher comes up with a new hypothesis in the future, SWATH-MS data would allow interrogation of the existing data for additional protein/s of interest without the need for sample digestion or data reacquisition. Such a strategy offers a tremendous benefit concerning saving of sample, time and money. A high linear association between MRM based methods with SWATH-MS has been shown in the past making it a suitable and reliable technique for proteomics-based studies [25, 26]. Nakamura et al. also described a SWATH-MS for quantification of drug-related transporter proteins in human liver microsomes, however no gender specific differences were reported due to use of small sample size (n=4) [25].

In this work, we report the development of a SWATH-MS based method to study the gender-specific differential expression of important drug and xenobiotic transporters in human liver (12 ABC and 13 SLC family). The transporter proteins were shortlisted based on the recommendation made by the International Transporter Consortium (ITC), the US Food and Drug Administration (USFDA) and the European Medicines Agency (EMA), as human xenobiotic transporters that play a significant role in drug discovery [6, 7, 27].

2. Materials and methods

2.1 Chemicals and Reagents

Protein preparation kit, TPCK-treated trypsin, trypsin digested β -galactosidase, and MS tuning solution was obtained from SCIEX (Framingham, MA). Acquity UPLC Peptide BEH C18 analytical column and VanGuard pre-columns were procured from Waters Corp. (Waltham, MA). Calbiochem ProteoExtract Native Membrane Protein Extraction Kit was purchased from EMD Millipore (Billerica, MA). 1,4-Dithiothreitol (DTT) was obtained from Roche Diagnostics (Indianapolis, IN). Sodium deoxycholate and iodoacetamide (IAA) were procured from Sigma Aldrich (St. Louis, MO). MS grade acetonitrile and formic acid were purchased from ThermoFisher (Waltham, MA).

2.2 Human Liver Bank

Frozen human liver samples from brain dead donors were purchased from Sekisui XenoTech LLC, Kansas City, KS. All the livers are from organ donors involved in automobile accidents and therefore are IRB-exempt. The age of liver donors ranged from 21 to 64 years, with 13 males and 9 females. Most livers were from organ donors involved in automobile accidents. The detailed demographics of the donors is given in **table 1**.

2.3 Human Liver Tissue Preparation

Membrane extraction from human tissue was performed as described in the ProteoExtract kit protocol with slight modifications. Briefly, liver tissue (~100 mg) was placed in a Dounce homogenizer with 1000 μ l of extraction buffer-I (EBI) and five μ l of the protease inhibitor cocktail. All the subsequent steps were carried out at 4°C unless specified

otherwise. Tissue was homogenized on ice with 10-15 strokes and incubated for 10 min with gentle agitation. Samples were spun at 16,000 x *g* for 15 min, and the supernatant was stored for future analysis of soluble proteins. The remaining pellet was gently resuspended in 500 μ l of extraction buffer-II (EBII) and 2.5 μ l of the protease inhibitor cocktail. Following 30 min incubation with gentle agitation, samples were centrifuged at 16,000 x *g* for 15 min, and the supernatant containing the membrane-bound and associated proteins was collected for further analysis. Total protein concentration was estimated using Pierce BCA protein assay kit (ThermoFisher Scientific, Waltham, MA).

2.4 Pressure-Cycling Technology (PCT) aided trypsin digestion

Protein digestion was performed as described by Prasad et al. with modifications [28]. Membrane fractions (250 μ g protein) were denatured with 25 μ L DTT (20 mM) at 95°C for 15 min in a shaking water bath (100 rpm). After denaturation, samples were alkylated in the dark with 25 μ L IAA (33 mM) for 30 min at room temperature. Samples were subsequently concentrated using the cold methanol, chloroform, and water (2:1:1) precipitation method. Samples were washed with ice-cold methanol and then resuspended in 75 μ L of 50 mM ammonium bicarbonate (pH 7.8) containing 3% w/v sodium deoxycholate (DOC). Further, TPCCK-treated trypsin was added to samples at a ratio of 1:20 (trypsin: protein) and samples were transferred into digestion tubes (PCT MicroTubes, Pressure Biosciences Inc., Easton, MA). The barocycler was run as described previously by our group [29]. Post tryptic digestion, 20 μ L of 2.5% formic acid in 50:50 water: acetonitrile was added to 80 μ L of digested protein samples to precipitate DOC and any undigested proteins as well as quench the trypsin digestion. Samples were spun at 5000 *g* at 10°C for 5 min, and the supernatant was collected for further analysis. Each sample was

spiked with trypsin-digested β -galactosidase peptides (15 pmol) before mass spectrometry analysis and 15 μ L was injected.

2.5 LC-MS/MS Analysis

Mass spectrometry analysis was performed as described previously with modifications [29]. All experiments were performed on a SCIEX 5600 TripleTOF® mass spectrometer equipped with a DuoSpray™ ion source (SCIEX, Concord, Canada) coupled to Acquity UHPLC HClass system (Waters Corp., Milford, MA, USA). Sample separation was achieved on an Acquity UPLC Peptide BEH C18 (2.1 X 150 mm², 300 Å, 1.7 μ m) attached to an Acquity VanGuard pre-column (2.1 X 5 mm², 300 Å, 1.7 μ m). Autosampler and analytical column were maintained at 10°C and 40°C, respectively. The chromatographic separation was achieved over a 90-min gradient at 100 μ L/min. A linear gradient was used for chromatographic separation using mobile phase A (98% water, 2% acetonitrile, 0.1% formic acid) and mobile phase B (98% acetonitrile, 2% water, 0.1% formic acid). The solvent composition was 98% A from 0 to 5 min, 98% to 75% A from 5 to 55 min, 75% to 50% A from 55 to 60 min, 50% to 20% from 60 to 70 min, 20% A held from 70 to 75 min to flush the column back to 98% A at 80 min. The gradient was held at initial conditions from 80 min until the end of the run to equilibrate the column before the start of next run. Mass calibration of the QTOF detector was monitored by injecting trypsin-digested β -galactosidase peptides every ten samples during the analysis.

2.6 Data-dependent and SWATH acquisition parameters

Data-dependent, as well as data independent (SWATH) analysis, was performed in positive ionization mode. The method specific parameters were as follows: gas 1 (GS1) 60 psi, gas 2 (GS2) 60 psi, curtain gas (CUR) 25 psi. The source-specific parameters were: temperature (TEM) 450°C, ion spray voltage floating (ISVF) 5500 V, declustering potential (DP): 120, collision energy (CE) 10, collision energy spread (CES) 5.

A maximum of 50 candidate ions with a charge state 2 to 4 was monitored every survey scan cycle. All the ions between m/z 300-1250 which exceeded 25 cps were subjected to MS/MS analysis. Rolling collision energy dependent on the m/z of the ion and dynamic accumulation were used. The mass tolerance was set at 50 mDa during the initial 0.25 sec survey scan (total cycle time: 3.90 sec).

All the parameters for SWATH acquisition were similar as described above except the following: Source temperature (TEM) was 400°C, GS 1 was 55 psi, and TOF masses were collected from m/z 300 to 1500. The total cycle time for SWATH acquisition was 3.95 sec. SWATH data was acquired (m/z 400-1100) over 70 SWATH windows per cycles with a window size of m/z 10.

2.7 Data processing and extraction

DDA samples were searched against reviewed Swiss-Prot identifiers (October 2016) using ProteinPilot 5 (SCIEX, Concord, Canada). The search was performed using Paragon algorithm for identification of peptides and proteins from DDA data. Thorough ID search mode with digestion: trypsin, Cys alkylation: iodoacetamide with false discovery analysis (1.0%) was searched against UniProt human protein database. ID focus during the

processing was maintained on biological modifications only. Raw data files and search results are available at Japan Proteome Standard Repository (*jPOSTrepo* JPST000372, *ProteomeXchange* PXD008593), a publicly *available* data repository for proteomics data [30]. Spectral library and SWATH data were uploaded to Skyline for peptide and transition picking. Skyline is an opensource application for targeted extraction of peptide information from the SWATH data. Surrogate flyable peptides were selected as previously described [31]. For each protein, peptide correlation analysis was performed to choose surrogate peptides with a significant correlation coefficient (Spearman $r > 0.500$, $P < 0.05$). Only peptides between 6 to 25 amino acids, that were not embedded in the transmembrane domain were included. We also excluded peptides with known posttranslational modifications and polymorphic variations. Wherever possible, two peptides per protein were used to estimate the relative abundance of transporter proteins.

2.8 Data normalization

The raw peptide intensity data was expressed relative to the β -galactosidase peptide (APLDNDIGVSEATR [M + 2H]²⁺: 729.3652) intensity. Subsequently, these relative values were normalized with membrane protein yield to account for the differences in protein abundance among samples.

$$\text{Relative intensity} = \frac{\text{Raw intensity (protein)}}{\text{Raw intensity (APLDNDIGVSEATR)}}$$

$$\text{Normalized intensity} = \text{Relative intensity} * \text{membrane protein per mg tissue}$$

$$\text{Normalized intensity} = \text{Relative intensity} * \text{membrane protein per mg tissue} * \text{liver weight}$$

2.9 Statistical analysis

The correlation analysis for selection of surrogate peptides and statistical analysis was performed on Prism 6 (GraphPad Software Inc. La Jolla, Ca). Non-parametric Mann Whitney U test was used to compare the differences in demographic data and Chi-square test was used to compare the proportionality. Normalized intensity data were natural-logarithm transformed before statistical analysis [32]. The geometric mean was calculated from non-transformed data using SPSS v24 (IBM Analytics, Armonk, NY). Gender differences in the relative expression of major xenobiotic and drug transporters in human liver were carried out using a t-test on the natural logarithmic transformed data. Non-parametric Spearman analysis was used for correlation between different transporter proteins. $P < 0.05$ was considered significant throughout the analysis. Demographic data were reported as mean \pm SEM unless stated otherwise.

3. Results

SWATH-MS was used to estimate the protein expression of 25 hepatic drug transporters (12 ABC and 13 SLC family) in membrane fractions from 22 human liver donors. A complete list of surrogate peptides used for the relative estimation of transporters in liver samples is given in *supplementary table 2*. All transporters were quantified with two unique surrogate peptides except OATP1B1, OCT3, ENT1, NTCP, and sterolin-2 where only one unique surrogate peptide was qualified for inclusion based on the criteria described in 2.7.

3.1 Yield of membrane protein per gram of liver tissue

The average membrane yield (mg/g liver tissue) for all the livers was 20.33 ± 4.42 , $n=22$ (**fig 1a**). Membrane protein yield was marginally lower in females (19.05 ± 1.44 , $n=9$) as compared to males (21.21 ± 1.23 , $n=13$). However, the gender-difference in yield was statistically insignificant ($p > 0.46$). The variability in sodium/potassium-transporting ATPase subunit alpha-4 (ATP1A4, an integral membrane marker) levels was used to gauge the quality of the membrane fractions and % coefficient of variation among the 22 samples was 9.7% (**fig 1b**).

3.2 Effect of gender on drug efflux transporters

We found that none of the investigated efflux transporters was differentially expressed in males and females (**fig 2a**). BCRP was detected in membrane fractions from 7/9 female and 7/12 male donor livers. In females, BSEP was found in eight out of nine donors. Other efflux transporters studied in this work were found in all the liver samples. Six MRP

transporters quantified using this assay are given in **fig 2b**. No significant gender difference was seen in transporter proteins with efflux/uptake function as well (**fig 2c**). Sterolin-1 was detected in 8 and 9 membrane fractions from female and male donors, respectively. ENT2 was detectable in membrane fraction from 8 females and 9 male donors.

3.3 Effect of gender on drug uptake transporters

Gender was not found to influence the protein abundance of any of the uptake transporters in this study (**fig 3**). All the uptake transporters included in the study except OATP transporters were detectable in all the liver samples. In males, OATP1B3, and OATP2B1 were present in 12, and ten donor liver samples, respectively. In females, OATP1B3, and OATP2B1 were present in 7, and 8 donor liver samples, respectively. OAT1B1 was found in all the samples included in the study. Gender-specific expression level and male/female ratio of transporter proteins is available at **table 2-5**.

4. Discussion

Drug response, efficacy, and toxicity are dependent on the expression of drug metabolizing enzymes and transporters in the intestine and liver. Differences in the basal expression of these proteins in the human liver can contribute to significant changes in systemic exposure of a drug. Extensive research in human has shown the gender-related differences which partly explain the interindividual variability in drug disposition, toxicity and therapeutic response [33, 34]. Gender is an essential underlying biological factor for the development of personalized medicine. A study by the US General Accounting Office found that 80% of FDA-approved prescription drugs withdrawn from the market between 1997-2000 were due to higher adverse drug-related events in women [35]. While a considerable amount of data is available on the gender differences in transporter protein expression in rat and mice, studies are lacking in human [36, 37]. Also, limited data is available for the gender differences in expression of transporter proteins in human since most available information is based on gene expression [34]. Interestingly, growing body of research is suggesting that mRNA serves as a poorer surrogate than protein expression for prediction of transporter activity [17, 28, 38].

The availability of human liver tissue for studying the hepatic xenobiotic transporters remains a challenge for researchers due to ethical consideration and the availability of tissue with adequate clinical information. Most of the samples available from healthy people come from donors who have sadly passed away in automobile accidents. Therefore, when possible, a judicious and parsimonious use of such tissue is warranted to obtain maximum data. MRM-based methods of protein quantification rely on customization of processes for each target protein before quantification. Though such means can be adapted

to quantify more than one protein at a time, the cost and method complexity increases exponentially with an increase in the number of target proteins [21]. Despite the benefits offered by SWATH-MS, there are some limitations to the methodology. First, a few of the low abundance transporters were quantified using one surrogate peptide. As the window size in SWATH increases, the noise level increases drastically and impedes the quantification of low abundance proteins. Second, we assume that the total cellular membrane protein expression serves as a surrogate for purified plasma membrane. Nevertheless, the advantages of this technique outweigh its drawbacks.

We observed that the inter-individual variability seen in this study was much higher than the average differences between the two genders. While a study with a large sample set is desired to completely address the cofactors contributing to this variability, such studies are often limited due to lack of availability of the liver tissue. Most of the tissue that is available for commercial purchase is obtained from motor vehicle accidents or other brain-dead donors and a detailed medical history is often lacking. Therefore, the potential of conflicting effects from obesity, diabetes or any other undiagnosed disease cannot be ruled out. Interestingly, there are currently no reports for any significant alteration of transporter proteins in human liver. Our findings are also limited as we do not have a large enough sample size to separately study the effect of obesity (BMI>30) or diabetes in our sample set. Therefore, future studies with a larger sample size are currently being planned to address the high inter-individual variability and differential effect of obesity and diabetes. Few transporter proteins (OST, OCT3) were close to $p < 0.05$ but failed to reach statistical significance possibly due to sample size constraint. Based on means and standard deviations, we calculated that would have got significance difference between two genders

had we included a sample size of n=42. In contrast, for proteins with a very high p-value, significantly large and practically challenging cohort of sample would be required.

Permeability glycoprotein 1 (P-gp) and multidrug and toxin extrusion protein 1 (MATE-1) are predominantly responsible for efflux of cations from hepatocyte into the bile duct. Prasad et al. found no association between age and gender with an expression of P-gp in human livers (n=64) [28]. MATE-1 was reported to exhibit significant correlation with age but not gender [38]. Li et al. found that the protein expression of breast cancer resistance protein (BCRP) in human liver tissue was almost 10-fold lower than the bile salt export pump (BSEP) [39]. Low levels of BCRP, as compared to other canalicular-localized transporters, could explain why we were able to detect BCRP only 12 out of 20 samples. The hepatic expression of BCRP in previous studies in human was independent of sex and age [17]. Cheng et al. also found no significant gender-specific differences in human hepatic BSEP expression [37].

Multidrug resistance protein 3 (MDR3) is expressed in canalicular membrane of hepatocytes and plays an integral role in the transport of phospholipids into the bile [40]. Multidrug resistance-associated protein (MRP2) plays an important role in the efflux of lyophilic conjugates (glutathione, glucuronate, sulfate) [41]. MRP2 is localized on the apical membrane of polarized hepatocytes and expressed in kidney and intestine among other tissues [42].

Equilibrative nucleoside transporter 1 and 2 (ENT1 and ENT2) are ubiquitously expressed in tissues like human liver, heart, kidney, intestine, erythrocytes, and brain [43]. Higher levels of ENT1 compared to ENT2 were observed in orthotopic liver transplantation [44].

Organic anion transporting polypeptides (OATPs) facilitate uptake of large hydrophobic organic anions while smaller and hydrophilic organic anions are transported by the organic anion transporters (OATs) [45]. OATP1B1, OATP1B3, and OATP2B1 are most notable transporters for drug uptake in the liver. OATP1B1 and OATP1B2 are expressed predominantly in liver whereas OAT2B1 is ubiquitously expressed [46]. No gender-specific expression of hepatic OATPs was found in previous or the current studies [16, 28, 47].

OAT2 is highly expressed in the sinusoidal membrane of hepatocytes with lower expression also seen in the kidney [45]. OAT7 is exclusively expressed in the basolateral membrane of human hepatocytes in the liver and participate in the transport of anionic substances in exchange for butyrate [14]. Members of the OCT family transport organic cations down their electrochemical gradients [45]. OCT1 and OCT3 are predominantly expressed in human liver and are localized to the basolateral membrane of hepatocyte [48]. Prasad et al. also reported no gender differences in expression of OATPs, OATs and OCTs in human liver [49]. Even though OCT3 showed a trend towards higher expression in males in our study ($P=0.051$), it failed to reach significance possibly due to sample size constraint.

Sodium/taurocholate co-transporting polypeptide (NTCP) is expressed predominantly on the basolateral membrane of hepatocyte and facilitates the uptake of bile acids [50]. NTCP mRNA expression was found to be higher in women than men, but the differences in the expression were statistically insignificant [37]. Organic solute transporters, OST α /OST β form a heterometric transporter complex which is localized on the basolateral membrane of hepatocytes and transports bile acids, conjugated steroids and substrates with similar

molecular structure [15]. These transporters are expressed in higher abundance in human tissue (intestine, liver, kidney) involved in bile acid and steroid homeostasis [15].

5. Conclusion

We developed a SWATH-MS based method for label-free, relative quantitative proteomics analyses of drug and xenobiotic transporters in human liver. SWATH-MS based studies can be used for comparative global proteomics analysis and large-scale relative protein quantification, especially for studies that a limited quantity of tissue is available. We successfully showed that the current approach could be directly applied to estimate the protein expression of many target proteins at once and can be further applied to study the difference in expression in relation to demographic characteristics or disease state. Future studies with a larger sample size are in progress to address other factors (disease, alcohol consumption, and smoking) which may contribute to differential expression of these transporter proteins.

Supplementary material

Supplementary table 1a, b: List of hepatic ABCs and SLC transporters included in this study

Supplementary table 2: Surrogate peptide and transitions used for relative quantification of transporter proteins

Acknowledgements

Authors would like to acknowledge partial support for this work by National Institutes of Health grants [grant numbers R15-GM101599, UH3-TR000963]. Authors also acknowledge the use of equipment and services available through the RI-INBRE Centralized Research Core Facility that is supported by the Institutional Development Award (IDeA) Network for Biomedical Research Excellence from the National Institute of General Medical Sciences of the National Institutes of Health [grant number P20GM103430].

Conflict of interest

The authors have no conflict of interest to declare for this work.

List of nonstandard abbreviations

ABC: ATP-binding cassette transporters; BCRP: Breast cancer resistance protein; BSEP: Bile salt export pump; DDA: Data dependent acquisition; DIA: Data independent acquisition; ENT: Equilibrative nucleoside transporter; LFQ: Label-free quantification; MDR: Multidrug resistance protein; MRM: Multiple reaction monitoring; MRP: Multidrug resistance-associated protein; NTCP: Sodium/Taurocholate Co-transporting Polypeptide; OAT: Organic anion transporter; OATP: organic anion-transporting polypeptide; OCT: Organic cation transporter; OST: Organic solute transporter; PCT: Pressure cycling technology; SLC: Solute carrier; SRM: Single-reaction monitoring; SWATH-MS: Sequential windowed acquisition of all theoretical fragment ion mass spectra; UHPLC: Ultra high performance liquid chromatography

References

- [1] K.M. Hillgren, D. Keppler, A.A. Zur, K.M. Giacomini, B. Stieger, C.E. Cass, L. Zhang, C. International Transporter, Emerging transporters of clinical importance: an update from the International Transporter Consortium, *Clin Pharmacol Ther* 94(1) (2013) 52-63.
- [2] Y. Liang, S. Li, L. Chen, The physiological role of drug transporters, *Protein Cell* 6(5) (2015) 334-50.
- [3] L. Lin, S.W. Yee, R.B. Kim, K.M. Giacomini, SLC transporters as therapeutic targets: emerging opportunities, *Nat Rev Drug Discov* 14(8) (2015) 543-60.
- [4] N.D. Pfeifer, R.N. Hardwick, K.L. Brouwer, Role of hepatic efflux transporters in regulating systemic and hepatocyte exposure to xenobiotics, *Annu Rev Pharmacol Toxicol* 54 (2014) 509-35.
- [5] F. Muller, M.F. Fromm, Transporter-mediated drug-drug interactions, *Pharmacogenomics* 12(7) (2011) 1017-37.
- [6] C. International Transporter, K.M. Giacomini, S.M. Huang, D.J. Tweedie, L.Z. Benet, K.L. Brouwer, X. Chu, A. Dahlin, R. Evers, V. Fischer, K.M. Hillgren, K.A. Hoffmaster, T. Ishikawa, D. Keppler, R.B. Kim, C.A. Lee, M. Niemi, J.W. Polli, Y. Sugiyama, P.W. Swaan, J.A. Ware, S.H. Wright, S.W. Yee, M.J. Zamek-Gliszczynski, L. Zhang, Membrane transporters in drug development, *Nat Rev Drug Discov* 9(3) (2010) 215-36.
- [7] S.M. Huang, L. Zhang, K.M. Giacomini, The International Transporter Consortium: a collaborative group of scientists from academia, industry, and the FDA, *Clin Pharmacol Ther* 87(1) (2010) 32-6.

- [8] P. Fisel, A.T. Nies, E. Schaeffeler, M. Schwab, The importance of drug transporter characterization to precision medicine, *Expert Opin Drug Metab Toxicol* 13(4) (2017) 361-365.
- [9] B. Stieger, B. Hagenbuch, Recent advances in understanding hepatic drug transport, *F1000Res* 5 (2016) 2465.
- [10] J.K. Fallon, P.C. Smith, C.Q. Xia, M.S. Kim, Quantification of Four Efflux Drug Transporters in Liver and Kidney Across Species Using Targeted Quantitative Proteomics by Isotope Dilution NanoLC-MS/MS, *Pharm Res* 33(9) (2016) 2280-8.
- [11] J.P. Jackson, K.M. Freeman, W.W. Friley, R.L. St. Claire, C. Black, K.R. Brouwer, Basolateral Efflux Transporters: A Potentially Important Pathway for the Prevention of Cholestatic Hepatotoxicity, *Applied In Vitro Toxicology* 2(4) (2016) 207-216.
- [12] C. Fahrmayr, M.F. Fromm, J. König, Hepatic OATP and OCT uptake transporters: their role for drug-drug interactions and pharmacogenetic aspects, *Drug Metab Rev* 42(3) (2010) 380-401.
- [13] A. Kalliokoski, M. Niemi, Impact of OATP transporters on pharmacokinetics, *Br J Pharmacol* 158(3) (2009) 693-705.
- [14] H.J. Shin, N. Anzai, A. Enomoto, X. He, D.K. Kim, H. Endou, Y. Kanai, Novel liver-specific organic anion transporter OAT7 that operates the exchange of sulfate conjugates for short chain fatty acid butyrate, *Hepatology* 45(4) (2007) 1046-55.
- [15] N. Ballatori, N. Li, F. Fang, J.L. Boyer, W.V. Christian, C.L. Hammond, OST alpha-OST beta: a key membrane transporter of bile acids and conjugated steroids, *Front Biosci (Landmark Ed)* 14 (2009) 2829-44.

- [16] S. Ohtsuki, O. Schaefer, H. Kawakami, T. Inoue, S. Liehner, A. Saito, N. Ishiguro, W. Kishimoto, E. Ludwig-Schwellinger, T. Ebner, T. Terasaki, Simultaneous absolute protein quantification of transporters, cytochromes P450, and UDP-glucuronosyltransferases as a novel approach for the characterization of individual human liver: comparison with mRNA levels and activities, *Drug Metab Dispos* 40(1) (2012) 83-92.
- [17] B. Prasad, Y. Lai, Y. Lin, J.D. Unadkat, Interindividual variability in the hepatic expression of the human breast cancer resistance protein (BCRP/ABCG2): effect of age, sex, and genotype, *J Pharm Sci* 102(3) (2013) 787-93.
- [18] B. Prasad, J.D. Unadkat, Optimized approaches for quantification of drug transporters in tissues and cells by MRM proteomics, *AAPS J* 16(4) (2014) 634-48.
- [19] V. Kumar, B. Prasad, G. Patilea, A. Gupta, L. Salphati, R. Evers, C.E. Hop, J.D. Unadkat, Quantitative transporter proteomics by liquid chromatography with tandem mass spectrometry: addressing methodologic issues of plasma membrane isolation and expression-activity relationship, *Drug Metab Dispos* 43(2) (2015) 284-8.
- [20] A.K. Deo, B. Prasad, L. Balogh, Y. Lai, J.D. Unadkat, Interindividual variability in hepatic expression of the multidrug resistance-associated protein 2 (MRP2/ABCC2): quantification by liquid chromatography/tandem mass spectrometry, *Drug Metab Dispos* 40(5) (2012) 852-5.
- [21] H. Al Feteisi, B. Achour, J. Barber, A. Rostami-Hodjegan, Choice of LC-MS methods for the absolute quantification of drug-metabolizing enzymes and transporters in human tissue: a comparative cost analysis, *AAPS J* 17(2) (2015) 438-46.
- [22] L.C. Gillet, P. Navarro, S. Tate, H. Rost, N. Selevsek, L. Reiter, R. Bonner, R. Aebersold, Targeted data extraction of the MS/MS spectra generated by data-independent

acquisition: a new concept for consistent and accurate proteome analysis, *Mol Cell Proteomics* 11(6) (2012) O111 016717.

[23] G. Rosenberger, C.C. Koh, T. Guo, H.L. Rost, P. Kouvonen, B.C. Collins, M. Heusel, Y. Liu, E. Caron, A. Vichalkovski, M. Faini, O.T. Schubert, P. Faridi, H.A. Ebhardt, M. Matondo, H. Lam, S.L. Bader, D.S. Campbell, E.W. Deutsch, R.L. Moritz, S. Tate, R. Aebersold, A repository of assays to quantify 10,000 human proteins by SWATH-MS, *Sci Data* 1 (2014) 140031.

[24] P. Navarro, J. Kuharev, L.C. Gillet, O.M. Bernhardt, B. MacLean, H.L. Rost, S.A. Tate, C.C. Tsou, L. Reiter, U. Distler, G. Rosenberger, Y. Perez-Riverol, A.I. Nesvizhskii, R. Aebersold, S. Tenzer, A multicenter study benchmarks software tools for label-free proteome quantification, *Nat Biotechnol* 34(11) (2016) 1130-1136.

[25] Y. Liu, R. Huttenhain, S. Surinova, L.C. Gillet, J. Mouritsen, R. Brunner, P. Navarro, R. Aebersold, Quantitative measurements of N-linked glycoproteins in human plasma by SWATH-MS, *Proteomics* 13(8) (2013) 1247-56.

[26] K. Nakamura, M. Hirayama-Kurogi, S. Ito, T. Kuno, T. Yoneyama, W. Obuchi, T. Terasaki, S. Ohtsuki, Large-scale multiplex absolute protein quantification of drug-metabolizing enzymes and transporters in human intestine, liver, and kidney microsomes by SWATH-MS: Comparison with MRM/SRM and HR-MRM/PRM, *Proteomics* 16(15-16) (2016) 2106-17.

[27] T. Prueksaritanont, X. Chu, C. Gibson, D. Cui, K.L. Yee, J. Ballard, T. Cabalu, J. Hochman, Drug-drug interaction studies: regulatory guidance and an industry perspective, *AAPS J* 15(3) (2013) 629-45.

- [28] B. Prasad, R. Evers, A. Gupta, C.E. Hop, L. Salphati, S. Shukla, S.V. Ambudkar, J.D. Unadkat, Interindividual variability in hepatic organic anion-transporting polypeptides and P-glycoprotein (ABCB1) protein expression: quantification by liquid chromatography tandem mass spectroscopy and influence of genotype, age, and sex, *Drug Metab Dispos* 42(1) (2014) 78-88.
- [29] R. Jamwal, B.J. Barlock, S. Adusumalli, K. Ogasawara, B.L. Simons, F. Akhlaghi, Multiplex and Label-Free Relative Quantification Approach for Studying Protein Abundance of Drug Metabolizing Enzymes in Human Liver Microsomes Using SWATH-MS, *J Proteome Res* (2017).
- [30] S. Okuda, Y. Watanabe, Y. Moriya, S. Kawano, T. Yamamoto, M. Matsumoto, T. Takami, D. Kobayashi, N. Araki, A.C. Yoshizawa, T. Tabata, N. Sugiyama, S. Goto, Y. Ishihama, jPOSTrepo: an international standard data repository for proteomes, *Nucleic Acids Res* 45(D1) (2017) D1107-D1111.
- [31] D.K. Bhatt, B. Prasad, Critical Issues and Optimized Practices in Quantification of Protein Abundance Level to Determine Interindividual Variability in DMET Proteins by LC-MS/MS Proteomics, *Clin Pharmacol Ther* (2017).
- [32] J.M. Bland, D.G. Altman, Statistics Notes: Transforming data, *BMJ* 312(7033) (1996) 770.
- [33] D.J. Waxman, M.G. Holloway, Sex differences in the expression of hepatic drug metabolizing enzymes, *Mol Pharmacol* 76(2) (2009) 215-28.
- [34] L. Yang, E.T. Price, C.W. Chang, Y. Li, Y. Huang, L.W. Guo, Y. Guo, J. Kaput, L. Shi, B. Ning, Gene expression variability in human hepatic drug metabolizing enzymes and transporters, *PLoS One* 8(4) (2013) e60368.

- [35] M.T. Gahart, E.J. Rowe, L. Bradley, Most Drugs Withdrawn in Recent Years Had Greater Health Risks for Women, US Government Accountability Office, 2000, p. 8.
- [36] S.C. Buist, N.J. Cherrington, S. Choudhuri, D.P. Hartley, C.D. Klaassen, Gender-specific and developmental influences on the expression of rat organic anion transporters, *J Pharmacol Exp Ther* 301(1) (2002) 145-51.
- [37] X. Cheng, D. Buckley, C.D. Klaassen, Regulation of hepatic bile acid transporters Ntcp and Bsep expression, *Biochem Pharmacol* 74(11) (2007) 1665-76.
- [38] L. Wang, B. Prasad, L. Salphati, X. Chu, A. Gupta, C.E. Hop, R. Evers, J.D. Unadkat, Interspecies variability in expression of hepatobiliary transporters across human, dog, monkey, and rat as determined by quantitative proteomics, *Drug Metab Dispos* 43(3) (2015) 367-74.
- [39] N. Li, J. Palandra, O.V. Nemirovskiy, Y. Lai, LC-MS/MS mediated absolute quantification and comparison of bile salt export pump and breast cancer resistance protein in livers and hepatocytes across species, *Anal Chem* 81(6) (2009) 2251-9.
- [40] J.J. Smit, A.H. Schinkel, C.A. Mol, D. Majoor, W.J. Mooi, A.P. Jongsma, C.R. Lincke, P. Borst, Tissue distribution of the human MDR3 P-glycoprotein, *Lab Invest* 71(5) (1994) 638-49.
- [41] G. Jedlitschky, U. Hoffmann, H.K. Kroemer, Structure and function of the MRP2 (ABCC2) protein and its role in drug disposition, *Expert Opin Drug Metab Toxicol* 2(3) (2006) 351-66.
- [42] A.T. Nies, D. Keppler, The apical conjugate efflux pump ABCC2 (MRP2), *Pflugers Arch* 453(5) (2007) 643-59.

- [43] R.W. Li, C. Yang, A.S. Sit, S.Y. Lin, E.Y. Ho, G.P. Leung, Physiological and pharmacological roles of vascular nucleoside transporters, *J Cardiovasc Pharmacol* 59(1) (2012) 10-5.
- [44] M.A. Zimmerman, E. Tak, S.F. Ehrentraut, M. Kaplan, A. Giebler, T. Weng, D.S. Choi, M.R. Blackburn, I. Kam, H.K. Eltzhig, A. Grenz, Equilibrative nucleoside transporter (ENT)-1-dependent elevation of extracellular adenosine protects the liver during ischemia and reperfusion, *Hepatology* 58(5) (2013) 1766-78.
- [45] M. Roth, A. Obaidat, B. Hagenbuch, OATPs, OATs and OCTs: the organic anion and cation transporters of the SLCO and SLC22A gene superfamilies, *Br J Pharmacol* 165(5) (2012) 1260-87.
- [46] B. Hagenbuch, P.J. Meier, The superfamily of organic anion transporting polypeptides, *Biochim Biophys Acta* 1609(1) (2003) 1-18.
- [47] J. Badee, B. Achour, A. Rostami-Hodjegan, A. Galetin, Meta-analysis of expression of hepatic organic anion-transporting polypeptide (OATP) transporters in cellular systems relative to human liver tissue, *Drug Metab Dispos* 43(4) (2015) 424-32.
- [48] A.T. Nies, E. Herrmann, M. Brom, D. Keppler, Vectorial transport of the plant alkaloid berberine by double-transfected cells expressing the human organic cation transporter 1 (OCT1, SLC22A1) and the efflux pump MDR1 P-glycoprotein (ABCB1), *Naunyn Schmiedebergs Arch Pharmacol* 376(6) (2008) 449-61.
- [49] B. Prasad, A. Gaedigk, M. Vrana, R. Gaedigk, J.S. Leeder, L. Salphati, X. Chu, G. Xiao, C. Hop, R. Evers, L. Gan, J.D. Unadkat, Ontogeny of Hepatic Drug Transporters as Quantified by LC-MS/MS Proteomics, *Clin Pharmacol Ther* 100(4) (2016) 362-70.

[50] B. Hagenbuch, P.J. Meier, Molecular cloning, chromosomal localization, and functional characterization of a human liver Na⁺/bile acid cotransporter, *J Clin Invest* 93(3) (1994) 1326-31.

Tables and figure legends:

Tables

Table 1. Donor demographics data. *P value* represent the significance from Mann-Whitney U test. C: Caucasian, AA: Afro-American, H: Hispanic

Table 2. Gender-specific expression levels of hepatic efflux transporters. ¹Geometric mean (95% Confidence Interval), ²Mann-Whitney U test

Table 3. Gender-specific expression levels of hepatic efflux/uptake transporters. ¹Geometric mean (95% Confidence Interval), ²Mann-Whitney U test

Table 4. Gender-specific expression levels of hepatic uptake transporters. ¹Geometric mean (95% Confidence Interval), ²Mann-Whitney U test

Figures

Figure 1. Gender difference on membrane protein abundance and ATP1A4 (a membrane proteins marker). Normalized intensity expressed as natural logarithm transform relative to β -gal peptide intensity and further normalized to membrane protein yield. The line represents the arithmetic mean for the respective group and individual values are shown as aligned dots plot. Relative Intensity not be used for comparison between levels of different proteins.

Figure 2. Effect of gender on hepatic 2(a) efflux, 2(b) efflux (MRPs), and 2 (c) efflux/uptake transporters. Normalized intensity expressed as natural logarithm transform relative to β -gal peptide intensity and further normalized to membrane protein yield. The line represents the arithmetic mean for the respective group and individual

values are shown as aligned dots plot. Relative Intensity not be used for comparison between levels of different proteins.

Figure 3. Effect of gender on hepatic uptake transporters. Normalized intensity expressed as natural logarithm transform relative to β -gal peptide intensity and further normalized to membrane protein yield. The line represents the arithmetic mean for the respective group and individual values are shown as aligned dots plot. Relative Intensity not be used for comparison between levels of different proteins.

Table 1: Donor demographics data for transporter quantification. P-value represent the significance from Mann-Whitney U test and * represent $p < 0.05$; C: Caucasian, AA: Afro-American, H: Hispanic. #Significance from Chi-square test.

	Female	Male	p-value
N (%)	9 (40.9%)	13 (59.1%)	-
Age (years)	44.44 ± 5.76	45.69 ± 3.28	$p = 0.89$
Body weight (kg)	87.75 ± 9.06	78.15 ± 4.96	$p = 0.41$
Height (cm)	158.75 ± 2.76	175.27 ± 1.80	$p < 0.01^*$
Body mass index (kg/m ²)	34.63 ± 3.20	25.54 ± 1.64	$p < 0.05^*$
Liver weight (kg)	1.44 ± 0.18	1.53 ± 0.11	$p = 0.29$
Ethnicity (C, AA, H)	7, 2, 0	7, 5, 1	$p = 0.45^{\#}$
Cause of death			
Anoxia			
Cerebrovascular aneurysm	6	7	$p = 0.30^{\#}$
Head trauma	3	3	
Smoking status	0	3	
Smoking status			
Non-smoker	3	5	$p = 0.80^{\#}$
Smoker	6	8	
Alcohol consumption			
No	5	4	$p = 0.24^{\#}$
Yes	4	9	
Diabetic status			
Diabetic	5	7	$p = 0.94^{\#}$
Non-diabetic	4	6	
Hepatic Steatosis			
<5%	8	13	$p = 0.22^{\#}$
>5%	1	0	

Table 2: Gender-specific expression levels of hepatic efflux transporters. ¹Geometric mean (95% Confidence Interval), ²Mann-Whitney U test

Transporter protein	Normalized Intensity¹			p-value²
	Female	Male	Female/Male ratio	
MRP1	27.61 (20.68-36.87)	29.43 (22.43-38.97)	0.94	0.989
MRP2	63.50 (46.50-86.61)	79.60 (58.09-109.1)	0.80	0.230
MRP3	80.86 (60.34-108.30)	94.53 (73.48-121.60)	0.86	0.316
MRP4	43.17 (31.72-58.76)	36.76 (28.27-47.79)	1.17	0.355
MRP5	126.5 (75.07-213.2)	178.7 (120.3-265.5)	0.71	0.142
MRP6	29.36 (20.72-41.60)	27.55 (18.47-41.09)	1.07	0.937
MATE1	17.95 (10.40-30.98)	22.36 (18.19-27.49)	0.80	0.256
BSEP	15.82 (11.75-21.31)	14.10 (10.17-19.55)	1.12	0.851
BCRP	32.37 (23.41-44.49)	38.09 (24.00-60.47)	0.85	0.313
MDR1	200.10 (134.80-296.90)	166.90 (127.00-219.50)	1.20	0.322
MDR3	41.50 (23.85-72.20)	57.72 (35.43-94.04)	0.72	0.316
Sterolin-1	41.62 (29.64-58.44)	32.37 (21.21-49.41)	1.29	0.366
Sterolin-2	18.50 (13.72-24.94)	23.14 (16.30-32.84)	0.80	0.316

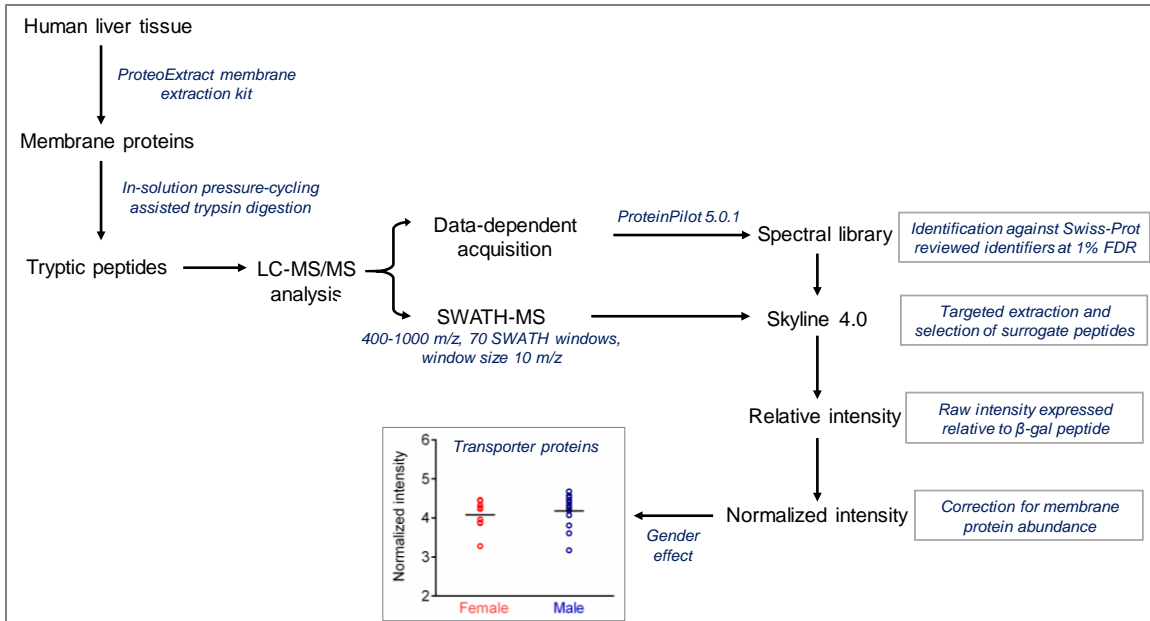
Table 3. Gender-specific expression levels of hepatic efflux/uptake transporters.

¹Geometric mean (95% Confidence Interval), ²Mann-Whitney U test

Transporter protein	Normalized Intensity ¹		Female/Male ratio	p-value ²
	Female	Male		
OSTα	3.76 (2.92-4.85)	5.42 (3.95-7.44)	0.69	0.081
OSTβ	39.50 (29.11-53.60)	37.25 (29.05-47.77)	1.06	0.886
ENT1	10.44 (7.49-14.56)	7.98 (5.88-10.84)	1.31	0.234
ENT2	24.01 (15.84-36.40)	21.42 (13.76-33.34)	1.12	0.814
OAT7	19.51 (14.02-27.15)	16.46 (11.73-23.10)	1.19	0.595

Table 4. Gender-specific expression levels of hepatic uptake transporters. ¹Geometric mean (95% Confidence Interval), ²Mann-Whitney U test

Transporter protein	Normalized Intensity ¹			p-value ²
	Female	Male	Female/Male ratio	
OATP1B1	5.35 (3.1-9.08)	3.34 (2.39-5.23)	1.60	0.182
OATP1B3	36.69 (31.21-43.14)	33.32 (25.03-44.37)	1.10	0.645
OATP2B1	14.74 (9.60-22.62)	15.80 (11.33-22.04)	0.93	0.915
OCT1	21.16 (13.46-33.21)	16.67 (11.82-23.51)	1.27	0.355
OCT3	10.50 (7.74-14.24)	14.10 (10.04-19.80)	0.74	0.051
OAT2	53.77 (31.60-91.48)	69.73 (48.43-100.4)	0.77	0.315
NTCP	74.44 (56.04-98.88)	96.09 (73.55-125.5)	0.77	0.142



Graphical abstract: Workflow for quantification of transporter proteins in human liver tissue using SWATH-MS

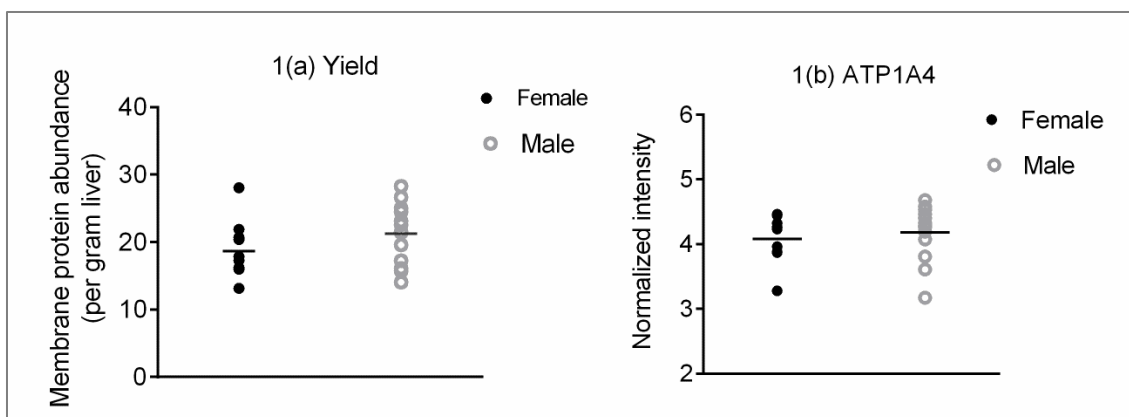


Figure 1: Gender difference on membrane protein abundance and ATP1A4 (a membrane proteins marker). Normalized intensity expressed as natural logarithm transform relative to β -gal peptide intensity and further normalized to membrane protein yield. The line represents the arithmetic mean for the respective group and individual values are shown as aligned dots plot.

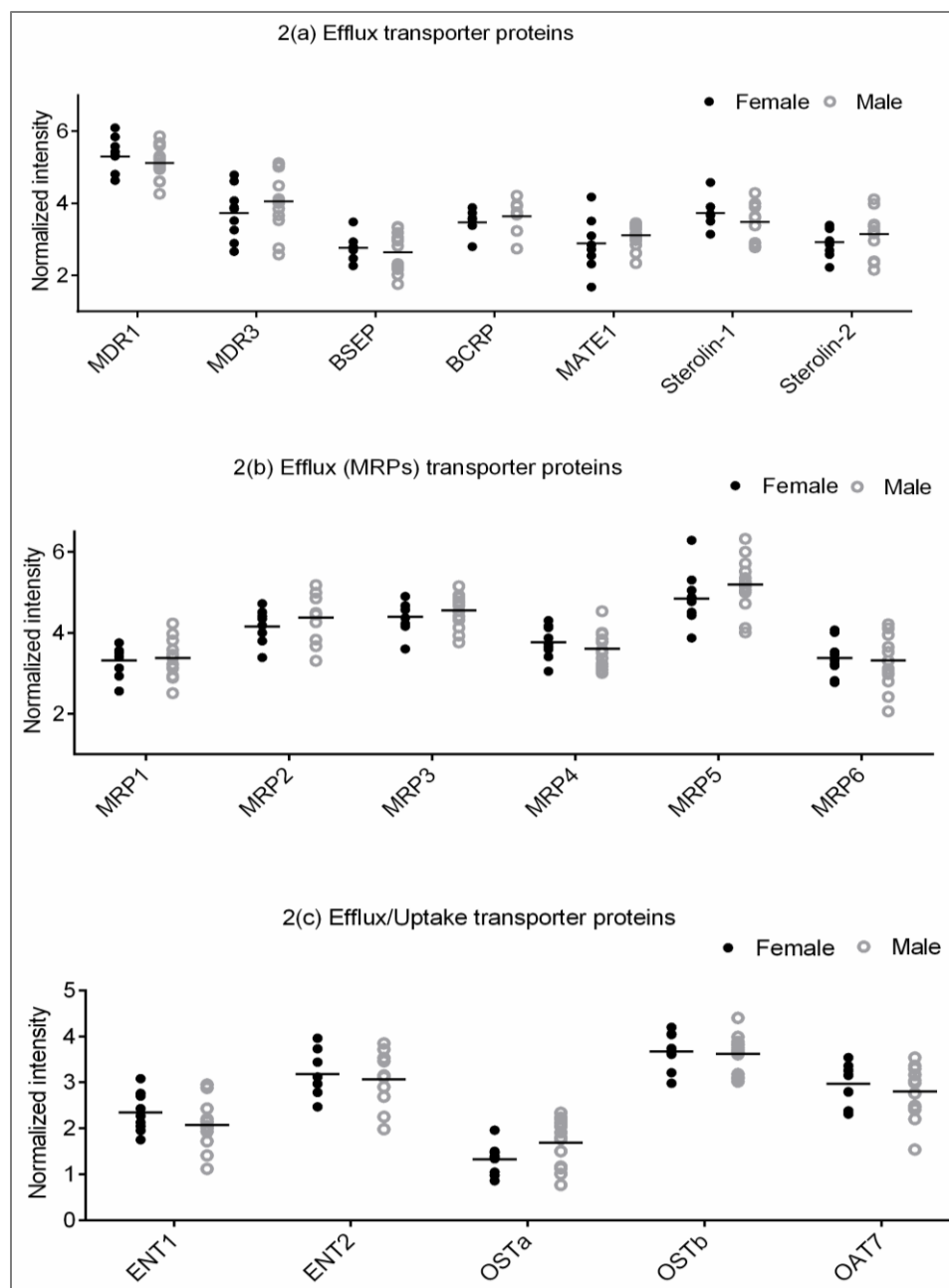


Figure 2: Effect of gender on hepatic (a) efflux, (b) efflux (MRPs), and (c) efflux/uptake transporters. Normalized intensity expressed as natural logarithm transform relative to β -gal peptide intensity and further normalized to membrane protein yield. The line represents the arithmetic mean for the respective group and individual values are shown as aligned dots plot. Relative Intensity not to be used for comparison between levels of different proteins.

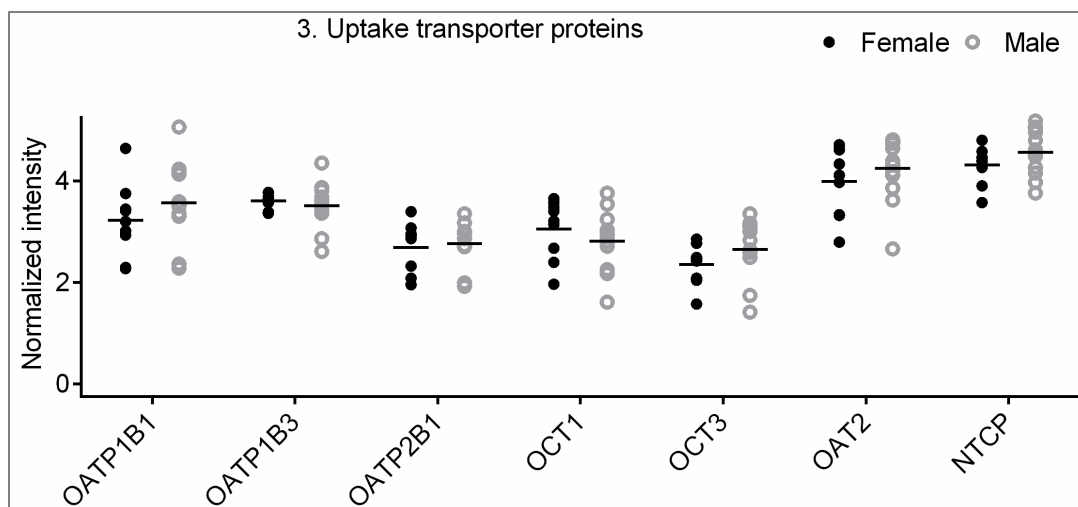


Figure 3: Effect of gender on hepatic uptake transporters. Normalized intensity expressed as natural logarithm transform relative to β -gal peptide intensity and further normalized to membrane protein yield. The line represents the arithmetic mean for the respective group and individual values are shown as aligned dots plot. Relative Intensity not to be used for comparison between levels of different proteins.

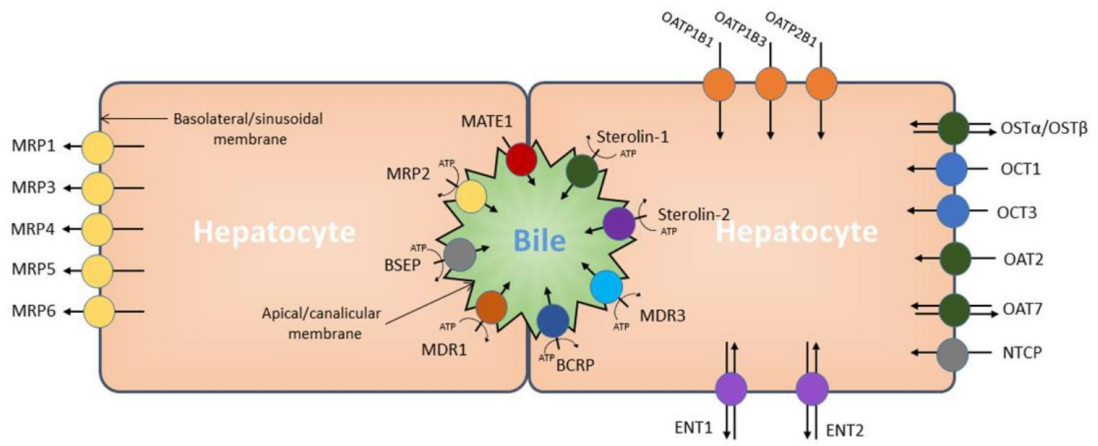
Supplementary information

Supplementary figure 1: Hepatic transporters quantified using SWATH-MS and their location and transport properties

Supplementary table 1a: Major hepatic transporters of ABC superfamily quantified in this study

Supplementary table 1b: Major hepatic transporters of ABC superfamily quantified in this study

Supplementary table 2: Surrogate peptide and transitions used for relative quantification of transporter proteins



Supplementary figure 1

Supplementary table 1a

Sr. no	Protein name	Gene name	Membrane localization in hepatocyte	Primary Function
1	MDR1/P-gp	<i>ABCB1</i>	Canalicular membrane	Efflux
2	MDR3	<i>ABCB4</i>	Canalicular membrane	Efflux
3	BCRP	<i>ABCG2</i>	Canalicular membrane	Efflux
4	BSEP	<i>ABCB11</i>	Canalicular membrane	Efflux
5	MRP1	<i>ABCC1</i>	Basolateral/Sinusoidal membrane	Efflux
6	MRP2	<i>ABCC2</i>	Canalicular membrane	Efflux
7	MRP3	<i>ABCC3</i>	Basolateral/Sinusoidal membrane	Efflux
8	MRP4	<i>ABCC3</i>	Basolateral/Sinusoidal membrane	Efflux
9	MRP5	<i>ABCC5</i>	Basolateral/Sinusoidal membrane	Efflux
10	MRP6	<i>ABCC6</i>	Basolateral/Sinusoidal membrane	Efflux
11	Sterolin -1	<i>ABCG5</i>	Canalicular membrane	Efflux
12	Sterolin -2	<i>ABCG8</i>	Canalicular membrane	Efflux

Supplementary table 1b

Sr. no	Protein name	Gene name	Membrane localization in hepatocyte	Primary Function
1	OCT1	<i>SLC22A1</i>	Basolateral/Sinusoidal membrane	Uptake
2	OCT3	<i>SLC22A3</i>	Basolateral/Sinusoidal membrane	Uptake
3	OAT2	<i>SLC22A7</i>	Basolateral/Sinusoidal membrane	Uptake
4	OAT7	<i>SLC22A9</i>	Basolateral/Sinusoidal membrane	Uptake/Efflux
5	OATP1B1	<i>SLCO1B1</i>	Basolateral/Sinusoidal membrane	Uptake
6	OATP1B3	<i>SLCO1B3</i>	Basolateral/Sinusoidal membrane	Uptake
7	OATP2B1	<i>SLCO2B1</i>	Basolateral/Sinusoidal membrane	Uptake
8	NTCP	<i>SLC10A1</i>	Basolateral/Sinusoidal membrane	Uptake
9	ENT1	<i>SLC29A1</i>	Basolateral/Sinusoidal membrane	Uptake/Efflux
10	ENT2	<i>SLC29A2</i>	Basolateral/Sinusoidal membrane	Uptake/Efflux
11	MATE1	<i>SLC47A1</i>	Canalicular membrane	Efflux
12	OST α	<i>SLC51A</i>	Basolateral/Sinusoidal membrane	Uptake/Efflux
13	OST β	<i>SLC51B</i>	Basolateral/Sinusoidal membrane	Uptake/Efflux

Supplementary table 2

Protein	Precursor (m/z)	Product (m/z)	Peptide, charge and transition (precursor charge, fragment, fragment charge)
AT1A4	643.0238	886.5244	MQINVQEVVLGDLVEIK, +3y8
AT1A4	643.0238	716.4189	MQINVQEVVLGDLVEIK, +3y6
AT1A4	643.0238	488.3079	MQINVQEVVLGDLVEIK, +3y4
AT1A4	429.2400	519.2773	AAVPDAVSK, +2y5
AT1A4	429.2400	404.2504	AAVPDAVSK, +2y4
AT1A4	429.2400	308.6687	AAVPDAVSK, +2y6+2
OATP1B3	487.9319	535.7977	MFLAALSFSYIAK, +3y10+2
OATP1B3	487.9319	500.2791	MFLAALSFSYIAK, +3y9+2
OATP1B3	487.9319	408.2185	MFLAALSFSYIAK, +3y7+2
OATP1B3	570.8060	826.4458	NVTGFFQSLK, +2y7
OATP1B3	570.8060	769.4243	NVTGFFQSLK, +2y6
OATP1B3	570.8060	622.3559	NVTGFFQSLK, +2y5
OATP1B1	587.7982	961.4778	NVTGFFQSFK, +2y8
OATP1B1	587.7982	860.4301	NVTGFFQSFK, +2y7
OATP2B1	953.9921	1439.7754	ASPDQDVRPSVFHNIK, +2y12
OATP2B1	953.9921	720.3913	ASPDQDVRPSVFHNIK, +2y12+2
OATP2B1	953.9921	471.2638	ASPDQDVRPSVFHNIK, +2y8+2
OATP2B1	532.9579	657.3930	SSPAVEQQLLVSGPGK, +3y7
OATP2B1	532.9579	544.3089	SSPAVEQQLLVSGPGK, +3y6
OATP2B1	532.9579	445.2405	SSPAVEQQLLVSGPGK, +3y5
OAT2	705.4122	1325.7787	LTYGGIALLAAGTALLPETR, +3y13
OAT2	705.4122	1212.6947	LTYGGIALLAAGTALLPETR, +3y12
OAT2	509.5985	1086.5426	QAQLPETIQDVER, +3y9
OAT2	509.5985	989.4898	QAQLPETIQDVER, +3y8
OAT2	509.5985	860.4472	QAQLPETIQDVER, +3y7
OCT1	647.3158	1049.4997	MLSLEEDVTEK, +2y9
OCT1	647.3158	962.4677	MLSLEEDVTEK, +2y8
OCT1	647.3158	849.3836	MLSLEEDVTEK, +2y7
OCT1	440.7424	637.3919	ENTIYLK, +2y5
OCT1	440.7424	536.3443	ENTIYLK, +2y4
OCT1	440.7424	423.2602	ENTIYLK, +2y3
MRP1	496.2561	962.4942	QPLEGSDLWLSLNK, +3y8
MRP1	496.2561	760.4352	QPLEGSDLWLSLNK, +3y6
MRP1	496.2561	647.3511	QPLEGSDLWLSLNK, +3y5
MRP1	602.6402	517.2584	SSTVGEIVNLMSVDAQR, +3y9+2
MRP1	602.6402	460.2369	SSTVGEIVNLMSVDAQR, +3y8+2
MRP1	602.6402	338.1747	SSTVGEIVNLMSVDAQR, +3y6+2
MRP3	682.3605	1076.5656	SSLVSALLGEMEK, +2y10
MRP3	682.3605	977.4972	SSLVSALLGEMEK, +2y9
MRP3	682.3605	890.4652	SSLVSALLGEMEK, +2y8
MRP3	531.2591	875.4469	ADGALTQEEK, +2y8
MRP3	531.2591	634.3042	ADGALTQEEK, +2y5
MRP3	531.2591	374.1978	ADGALTQEEK, +2y6+2
MRP4	767.4470	790.4417	IIVFVTFTTYVLLGSVITASR, +3y8

MRP4	767.4470	814.4563	IIVFVTFTTYVLLGSVITASR, +3y15+2
MRP4	767.4470	690.3983	IIVFVTFTTYVLLGSVITASR, +3y13+2
MRP4	538.2851	875.4833	AEAAALTETAK, +2y9
MRP4	538.2851	733.4090	AEAAALTETAK, +2y7
MRP4	538.2851	549.2879	AEAAALTETAK, +2y5
MRP5	738.8831	1276.6428	SLFLMEEVHMIK, +2y10
MRP5	738.8831	1129.5744	SLFLMEEVHMIK, +2y9
MRP5	738.8831	1016.4903	SLFLMEEVHMIK, +2y8
MRP5	443.7301	701.3729	GQEFLHR, +2y5
MRP5	443.7301	572.3303	GQEFLHR, +2y4
MRP6	452.2665	729.4618	SSLASGLLR, +2y7
MRP6	452.2665	616.3777	SSLASGLLR, +2y6
MRP6	452.2665	545.3406	SSLASGLLR, +2y5
MRP6	694.4008	1203.6732	ALVASLPGQLQYK, +2y11
MRP6	694.4008	1104.6048	ALVASLPGQLQYK, +2y10
MRP6	694.4008	1033.5677	ALVASLPGQLQYK, +2y9
BSEP	515.3062	841.5254	STALQLIQR, +2y7
BSEP	515.3062	657.4042	STALQLIQR, +2y5
BSEP	515.3062	529.3457	STALQLIQR, +2y4
BSEP	515.2956	829.4679	SLNIQWLR, +2y6
BSEP	515.2956	715.4250	SLNIQWLR, +2y5
BSEP	515.2956	602.3409	SLNIQWLR, +2y4
BCRP	573.2846	961.4408	LATTMTNHEK, +2y8
BCRP	573.2846	759.3454	LATTMTNHEK, +2y6
BCRP	573.2846	527.2572	LATTMTNHEK, +2y4
BCRP	478.5819	504.2453	LAEIYVNSSFYK, +3y8+2
BCRP	478.5819	316.1579	LAEIYVNSSFYK, +3y5+2
MATE1	514.7722	688.3988	GGPEATLEVR, +2y6
MATE1	514.7722	617.3617	GGPEATLEVR, +2y5
MATE1	514.7722	409.2243	GGPEATLEVR, +2y7+2
MATE1	641.1041	656.4454	GLLLGVFLILLVGILVR, +3y6
MATE1	641.1041	557.3770	GLLLGVFLILLVGILVR, +3y5
MATE1	641.1041	628.4287	GLLLGVFLILLVGILVR, +3y11+2
MDR1	438.2327	717.3890	GTQLSGGQK, +2y7
MDR1	438.2327	589.3304	GTQLSGGQK, +2y6
MDR1	438.2327	476.2463	GTQLSGGQK, +2y5
MDR1	944.5180	819.4472	LSTIQNADLIVVFQNGR, +2y7
MDR1	944.5180	720.3787	LSTIQNADLIVVFQNGR, +2y6
MDR1	944.5180	474.2419	LSTIQNADLIVVFQNGR, +2y4
MDR3	824.4250	1288.7260	FVDTAGNFSFPVNFSLLLNPGK, +3y12
MDR3	824.4250	969.5096	FVDTAGNFSFPVNFSLLLNPGK, +3y18+2
MDR3	824.4250	766.9272	FVDTAGNFSFPVNFSLLLNPGK, +3y14+2
MDR3	523.3037	857.5203	STTVQLIQR, +2y7
MDR3	523.3037	756.4726	STTVQLIQR, +2y6
MDR3	523.3037	329.2058	STTVQLIQR, +2y5+2
MRP2	777.0112	1330.6022	AMQFSEASFTWEHDSEATVR, +3y11
MRP2	777.0112	1043.4752	AMQFSEASFTWEHDSEATVR, +3y9

MRP2	777.0112	914.4326	AMQFSEASFTWEHDSEATVR, +3y8
MRP2	521.2536	747.3632	FFDTPPTGR, +2y7
MRP2	521.2536	632.3362	FFDTPPTGR, +2y6
MRP2	521.2536	430.2409	FFDTPPTGR, +2y4
Sterolin-1	532.7739	862.4451	TTLLDAMSGR, +2y8
Sterolin-1	532.7739	749.3610	TTLLDAMSGR, +2y7
Sterolin-1	532.7739	636.2770	TTLLDAMSGR, +2y6
Sterolin-1	588.3666	864.5050	IVVLTIHQPR, +2y7
Sterolin-1	588.3666	751.4209	IVVLTIHQPR, +2y6
Sterolin-1	588.3666	650.3733	IVVLTIHQPR, +2y5
Sterolin-2	588.3666	650.3733	LVLISLHQPR, +2y5
Sterolin-2	588.3666	482.2904	LVLISLHQPR, +2y8+2
Sterolin-2	588.3666	369.2063	LVLISLHQPR, +2y6+2
Sterolin-2	938.4416	813.3939	YSNPADFYVDLTSIDR, +2y14+2
Sterolin-2	938.4416	541.2798	YSNPADFYVDLTSIDR, +2y9+2
Sterolin-2	938.4416	410.2140	YSNPADFYVDLTSIDR, +2y7+2
OAT7	500.6011	1089.5357	ISIPLDSNMRPEK, +3y9
OAT7	500.6011	976.4517	ISIPLDSNMRPEK, +3y8
OAT7	500.6011	861.4247	ISIPLDSNMRPEK, +3y7
OAT7	523.3106	829.5393	DTLTLEILK, +2y7
OAT7	523.3106	716.4553	DTLTLEILK, +2y6
OAT7	523.3106	615.4076	DTLTLEILK, +2y5
OCT3	471.7538	559.3198	GPSAAALAER, +2y5
OCT3	471.7538	488.2827	GPSAAALAER, +2y4
OCT3	471.7538	375.1987	GPSAAALAER, +2y3
ENT1	488.9196	1079.5844	DAQASAAPAAPLPER, +3y11
ENT1	488.9196	850.4781	DAQASAAPAAPLPER, +3y8
ENT2	440.5528	818.4254	SSQAQAQELETK, +3y7
ENT2	440.5528	619.3297	SSQAQAQELETK, +3y5
ENT2	440.5528	490.2871	SSQAQAQELETK, +3y4
ENT2	858.3992	904.3795	SLTSYFLWPDEDSR, +2y7
ENT2	858.3992	621.2475	SLTSYFLWPDEDSR, +2y5
ENT2	858.3992	758.3412	SLTSYFLWPDEDSR, +2y12+2
NTCP	768.0472	1090.5891	MIYTAATTEETIPGALGNGTYK, +3y11
NTCP	768.0472	823.4308	MIYTAATTEETIPGALGNGTYK, +3y8
NTCP	768.0472	468.2453	MIYTAATTEETIPGALGNGTYK, +3y4